Investigation on the valorization of lignin: Base catalyzed lignin depolymerization to aromatic monomers and their further functionalization and defunctionalization using heterogeneous catalysts

Thesis Submitted to AcSIR For the Award of the Degree of

DOCTOR OF PHILOSOPHY In CHEMISTRY

AcSIR

By
Dheerendra Singh
(Enrollment No. 10CC15J26009)

Under the guidance of
Dr. Paresh Laxmikant Dhepe

Catalysis & Inorganic Chemistry Division
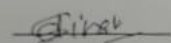CSIR-National Chemical Laboratory
Pune- 411 008, India
May 2020

Certificate

This is to Certified that the work incorporated in the Ph.D thesis entitled: *"Investigation on the valorization of lignin: Base catalyzed lignin depolymerization to aromatic monomers and their further functionalization and defunctionalization using heterogeneous catalysts* Submitted by Mr. Dheerendra Singh to Academy of Scientific and Innovative Research (AcSIR) in fulfillment of the requirement for the award of Degree of Doctor of Philosophy in Chemistry, was carried out by the candidate under my supervision at Catalysis and Inorganic Chemistry Division, National Chemical Laboratory, Pune-411008, India. I further certified that this work has not been submitted to any other University or Institution in part or full for the award of any degree or diploma. Research material obtained from other sources has been duly acknowledged in the thesis. Any text, illustration, table etc., used in the thesis from other sources, have been duly cited and acknowledged.

It is also certified that this work done by the student, under my supervision, is plagiarism free.
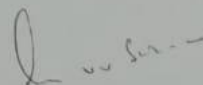
May, 2020

Ph.D. Student

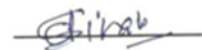**Dheerendra Singh**

(Research Guide)
Dr. Paresh L. Dhepe

(Research Co-Guide)
Dr. C.V.V Satyanarayana

DECLARATION BY RESEARCH SCHOLAR

I hereby declare that work reported in the thesis entitled **"*Investigation on the valorization of lignin: Base catalyzed lignin depolymerization to aromatic monomers and their further functionalization and defunctionalization using heterogeneous catalysts*"** submitted for the **Degree of Doctor of Philosophy** to Academy of Scientific and Innovative Research (AcSIR), has been carried out by me at Catalysis and Inorganic Chemistry Division, National Chemical Laboratory, Pune-411008, India, under the supervision of Dr. Paresh L. Dhepe. The work is original and has not been submitted in part or full by me for any other degree or diploma to this or any other University.

May 2020

Dheerendra Singh

(Enrollment No. 10CC15J26009)

Dedicated to…

My Family

Acknowledgments

At this very special juncture of my scientific career, this thesis not only represents my work but a milestone in many ways. I am indebted to many people for their continuous support and guidance. This journey has been a beautiful ride through lot of lifetime lessons, successes, failures, and most importantly the enjoyment I had working these years to reach to this destination. This thesis is also the result of many experiences I have from remarkable Individuals who I also wish to acknowledge.

Firstly, I would like to express my sincere and special appreciation to my supervisor, **Dr. Paresh L. Dhepe** for the patience, tremendous support, guidance and endless encouragement, he has given me throughout this journey which will continue to be felt for rest of my career. It was truly a pleasure to work under his guidance and therefore without his patience, advice, support, constructive suggestions, criticism, and continuous deliberation on the subject of my study, this thesis would not have been possible. His dedication to science is truly an inspiration and lessons I have learnt from him will guide me in my future endeavors as well. He has made research incredibly enjoyable and I simply could not have wished for a better supervisor.

I would like to thank my previous co-supervisor **Dr. Satyanarayana Chilukuri as well** for his support in boosting my confidence with my research work and helping me to find the way forward in difficult times. My sincere gratitude goes to **Dr. Nandini Devi** for extending her constant support and lab facilities. She has been very kind and helpful, without which none of this work would have been possible.

My sincere thanks to **Dr. Gopinath Chinnakonda, Head of the division** for providing overall support and extending all the facilities required for carrying out research work. This work was possible due to whole hearted support of the entire catalysis division.

I take this opportunity to sincerely thank my Doctoral Advisory Committee (DAC) members **Dr.Vilas Rane**, **Dr. B.L.V Prasad,** and **Dr. Nandini Devi** for continuously monitoring my progress through all course work, its critical evaluation, constructive and valuable inputs in all DAC meetings.

Table of contents

Chapter 1

Introduction and literature survey

Chapter 2A

Lignin Characterization

Chapter 2B

Catalyst characterization

Chapter 3

Base catalyzed depolymerization of lignin into low molecular weight compounds

Chapter 4A

Understanding the influence of alumina supported Ruthenium catalyst synthesis and reaction parameters on the hydrodeoxygenation of lignin derived monomers

Chapters 4B

Pathway for the transfer hydrogenation of lignin derived monomers: Mechanistic and kinetic study over the alumina supported Ruthenium catalyst

Chapter 5A

Catalytic defunctionalization of lignin-derived low molecular weight compound using AHF supported catalyst

Chapter 5B

Alumina Hollow Fiber (AHF) supported Co catalyzed continuous defunctionalization of guaiacol into cyclohexanol

Chapter 6

Functionalization of lignin derived monomers: Altering the O/C ratio of lignin derived monomers without sacrificing atom efficiency by alkylation

Chapter 7

Summary and Conclusion

List of Figures (Fig.)

List of Schemes

List of Tables

List of Abbreviations

BET	Braunauer-Emmett-Teller
BHT	Butylated hydroxyl toluene
CHNS	Carbon, Hydrogen, Nitrogen, Sulfur
DEE	Diethyl ether
EDAX	Energy Dispersive X-Ray Analysis
EtOAc	Ethyl acetate
FID	Flame ionization detector
FTIR	Fourier Transform Infrared
GC	Gas Chromatography
GC-MS	Gas Chromatography Mass Spectrometry
GPC	Gel Permeation Chromatography
HPLC	High Performance Liquid Chromatography
H-USY	Ultra Stable Zeolite Y (H-form)
HDO	Hydrodeoxygenation
ICP-OES	Inductively Coupled Plasma-Optical Emission
LC-MS	Liquid Chromatography Mass Spectrometry
MPa	Mega Pascal
NMR	Nuclear Magnetic Resonance
RT	Room Temperature
RI	Refractive Index

SEM	Scanning Electron Microscopy
TCD	Thermal Conductivity Detector
THF	Tetrahydrofuran
TPD	Temperature Programmed Desorption
TGA-DTA	Thermo Gravimetric Analysis-Differential Thermal Analysis
UV-Vis	Ultraviolet-Visible
XRD	X-Ray Diffraction

<u>Abstract of the Thesis</u>

Introduction

The high consumption rate of fossil feedstock throughout the world is responsible for decrease in its availability. Moreover, geo-political reasons and fluctuating prices are also playing crucial role in its utilization. At the same time, demand is increasing for the renewable, environment friendly resource for generating energy. Biomass, a sustainable and renewable resource has the potential to synthesize fuels and chemicals instead from fossil feedstock. Lignocellulosic biomass is readily available throughout the world at a lower cost.

Lignocellulosic biomass is made up of cellulose (40–50%), hemicelluloses (15–30%), lignin (10–25%) and many more smaller components such as protein, wax and nutrients [1, 2]. Value addition to cellulose and hemicellulose is well studied by researchers. However, valorization of lignin is still not done extensively because of its complex structure. Effective utilization of lignin has potential to replace the fossil based carbon resources partly. Lignin, a aromatic polymer is a good source of aromatic compounds and is made up of phenyl propane units, such as sinapyl alcohol, coumaryl alcohol, coniferyl alcohol linked together via various C-O-C and C-C linkages. Depolymerization of lignin will produce complex mixture of low molecular weight aromatic compounds and separation of formed monomers is very difficult due to their similar polarity. Hence, up-gradation of depolymerized products is an alternative pathway used to enhance the value of depolymerized products.

In this thesis, base-catalyzed depolymerization of lignin is discussed to obtain low molecular weight aromatic compounds and their further functionalization and defunctionalization is also discussed using solid acid catalysts and supported metal catalysts (Scheme 1 & 2).

Thesis work is divided into 7 chapters, excluding introduction chapter. Thesis discusses lignin characterization (Chapter 2), catalyst synthesis and characterization (Chapter 2), catalytic details, reaction results of lignin depolymerization (Chapter 3), and up-gradation strategy used for lignin model compounds (Chapters 4A, 4B, 5A, 5B, 6), and lastly overall summary and novelty of the work is also discussed (Chapter 7).

Base/H$_2$O/250°C/N$_2$
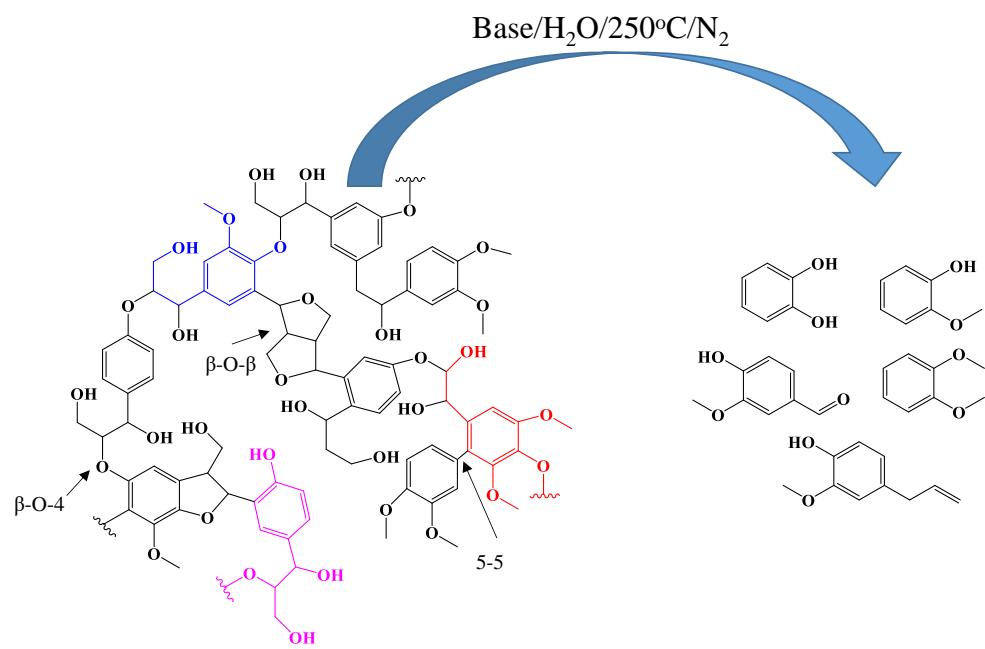
Lignin   Low molecular weight aromatic compounds

Scheme 1. Base catalyzed lignin depolymerization

Defunctionalization/HDO/Metal/Support

Functionalization/Alkylation/Solid acid
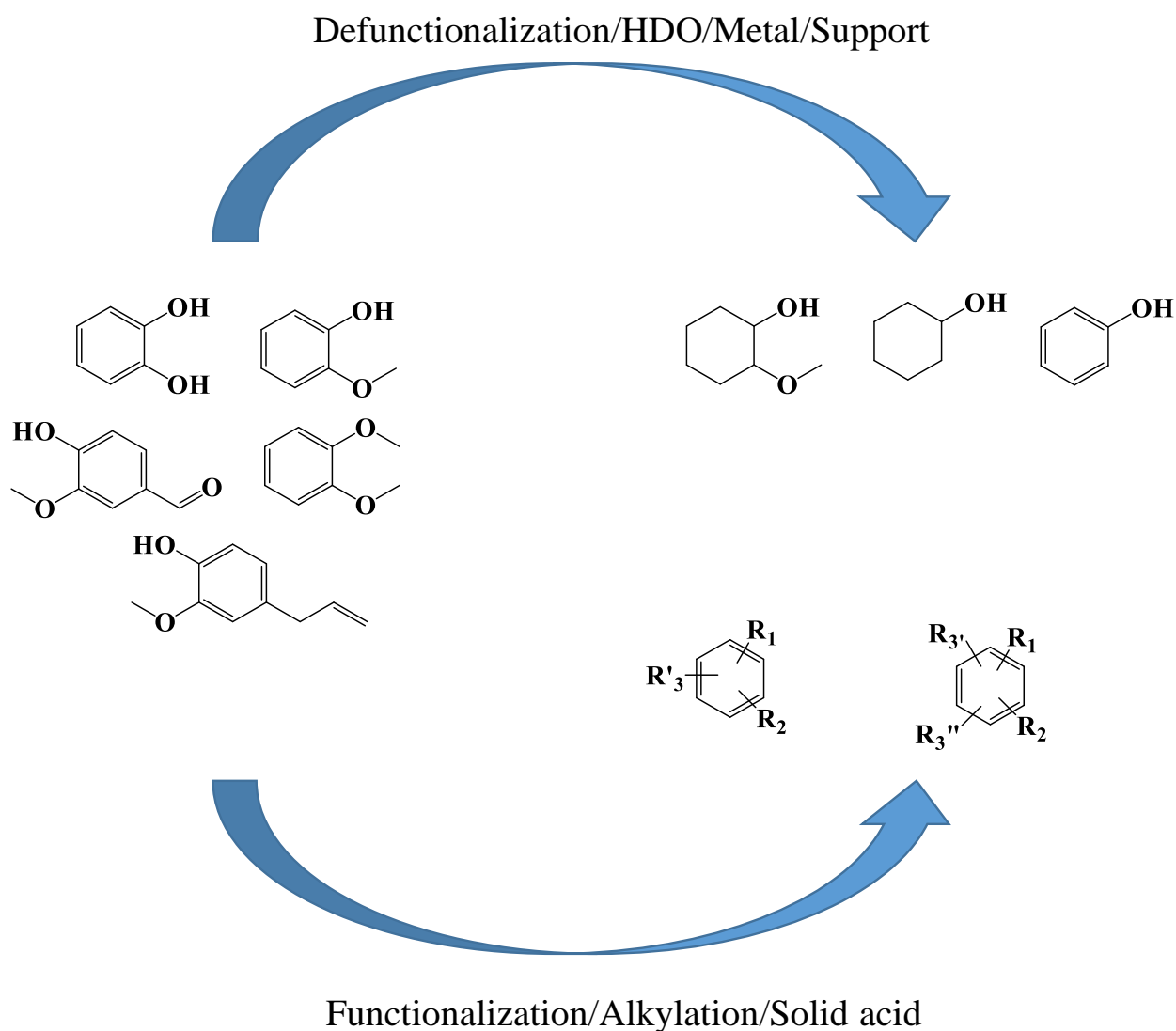
Scheme 2. Defunctionalization and functionalization of lignin derived low molecular weight aromatic compounds

Statement of problem

Lignin depolymerization is reported using homogeneous acids,[3, 4] solid acids,[5-7] ionic liquids,[8, 9] supported metal catalysts,[10-13] and supercritical fluids [13, 14] to produce low molecular weight compounds. However, problems associated with the reported literature are given below:

⚏ Due to complex chemistry of lignin (structure, properties etc.), most of the work is done with model compounds of lignin.

⫚ Low molecular weight aromatic compounds formed after depolymerization are useful, but their value-addition is must.

⫚ Catalyst stability and recyclability is a significant concern due to poisoning, coke formation.

Objective of the thesis work

Herein depolymerization of actual lignin is reported using homogeneous base catalysts to obtain low molecular weight aromatic compounds and further up-gradation of these products over solid acids and supported metal catalysts is reported to obtain value added products. The main objective was to develop novel methodologies with newer catalysts which are stable under reaction condition and are economical and will give better yields of desired products.

Methodology used

⫚ Employment of homogeneous bases in depolymerization of lignin.

⫚ Use of supported metal catalysts in up-gradation or defunctionalization of lignin-derived aromatic compounds into chemicals by destructive pathways.

⫚ Use of solid acid catalysts in up-gradation or functionalization of lignin-derived aromatic compounds into chemicals by the constructive pathway.

Synthesized catalysts were characterized using different physico-chemical techniques like XRD, TPD-NH$_3$/CO$_2$, N$_2$ sorption, ICP-OES, TEM and SEM to understand their morphologies and properties.

Catalytic experiments were carried out using Parr make batch mode autoclave and Hi-TECH engineering Make Fixed Bed Reactor (FBR). Reaction products analysis was done using GC, GC-MS, HPLC, LC-MS, Microanalysis, FT-IR, and MALDI-MS.

Reaction results of base-catalyzed lignin depolymerization

Effective depolymerization of lignin was possible in aqueous media using homogeneous base at 250 ºC for 1 h under 2 MPa N$_2$ @RT. Various type of lignins were possible to depolymerize using NaOH as a base under similar condition, however depending upon the properties of lignin, yields of depolymerized products soluble in diethyl ether (DEE) and ethyl acetate (EtOAc) were varying between 33-49% (Figure 1). Among all the used bases, NaOH was the

best catalyst to give low molecular weight aromatic compounds. Effects of the basic sites and pH of the reaction mixture were studied and it was observed that they exert high impact on depolymerization activity. Studies carried out with model compounds revealed that the yield of solid product formation was due to increased hydrophobicity of depolymerized products. Identifications and quantifications of low molecular weight aromatic compounds formed after depolymerization were done using GC, GC-MS, HPLC, LC-MS, Microanalysis, NMR and FT-IR.

Mw. (Da)	60,000	28000	60,000	52,000	-	-
pH of R.M.	12.65	12.53	12.30	12.48	12.35	12.38
(%) solubility in alkaline H_2O	100	100	100	100	100	100
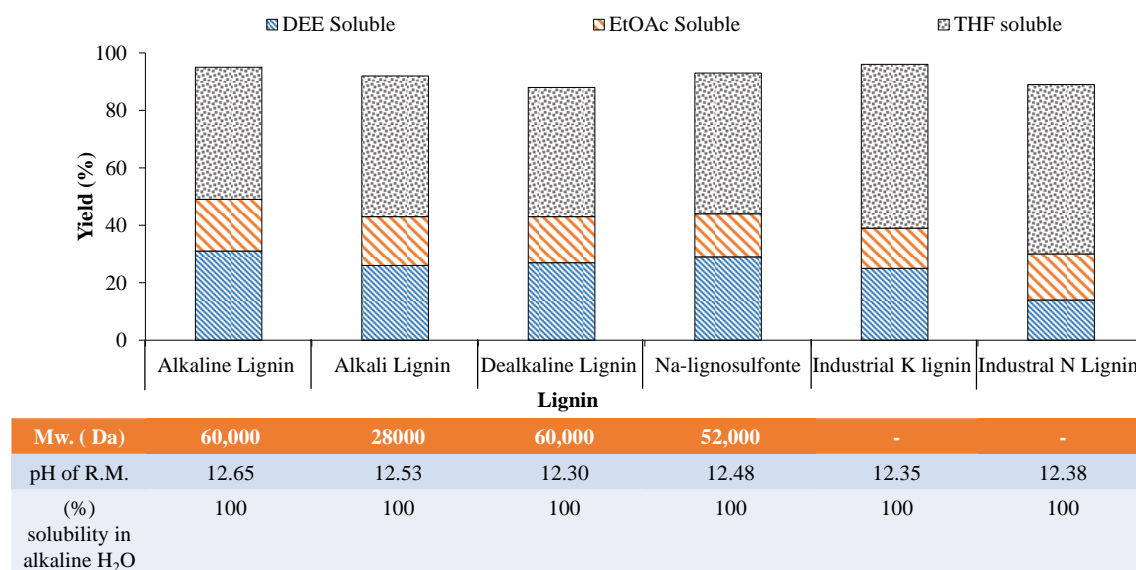
Figure 1. Lignin depolymerization using NaOH

Defunctionalization of lignin model compounds

Depolymerization of lignin prodcuces low molecular weight aromatic compounds, which have higher oxygen content and thus restricts their use as fuels. Defunctionalization of aromatic compounds via hydrodeoxygenation (HDO) process improves the fuel efficiency of compounds. Various oxygen-containing aromatic monomers such as guaiacol, veretrol, eugenol, phenol were studied using hydrodeoxygenation path because these monomers posses similar functional groups which are present in the lignin.

Precious metal (Ru), and Non-precious metals (Co, Ni) in combination with various supports such as Al_2O_3 (Acidic, Basic, Neutral), Alumina hollow fiber (AHF), SiO_2, and SiO_2-Al_2O_3 were employed for the hydrodeoxygenation of these compounds. Defunctionalization

experiments were carried out in both batch and flow mode reactors at temperature between 225-300 °C for 1- 4 h (batch reactor) in cyclohexane solvent either using molecular H_2 or in situ generated hydrogen from secondary alcohol (Figure 2).

It was found that the defunctionalization of aromatic monomers is heavily dependent on the nature of support. While it is possible to achieve 100% conversion of guaiacol with 72% yield of cyclohexanol using precious metal and molecular H_2, with catalytic transfer hydrogenation (CTH) of guaiacol again 100% conversion with 74% cyclohexanol yield was possible to achieve. Non-precious metal based catalyst was also used to carry out hydrodeoxygenation of guaiacol in both batch and continuous flow reactor and with this catalyst, 86% and 66% cyclohexanol yield, respectively were observed.
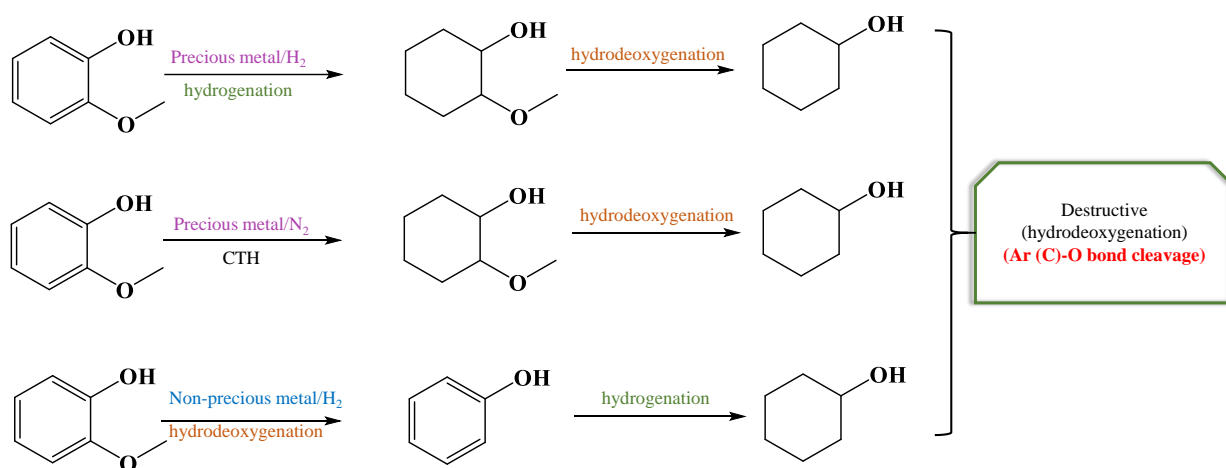
Figure 2. Defunctionalization/hydrodeoxygenation of lignin model compounds

Functionalization of lignin model compounds

Functionalization of aromatic monomers is another pathway used for the up-gradation of lignin-derived aromatic compounds by retaining their aromaticity and atom efficiency. Solid acid-catalyzed functionalization experiments were carried out in cyclohexane solvent in batch mode reactor at 250 °C for 1- 4 h under N_2 atmosphere. Products analysis was done using GC, GC-MS. It was seen from the obtained results that high functionalization activity is possible with electron rich aromatic compound (phenol, guaiacol,veretrol) as compared to electron-deficient (toluene). Functionalization activity also depends on polarity and steric of alkylating

agent (alcohols). The formation of mono and di-substituted alkyl functionalized products was seen and their yields were dependent on the catalyst used, either structured or amorphous. The MAP/DAP ratio was crucial to differentiate the activity of the catalysts.
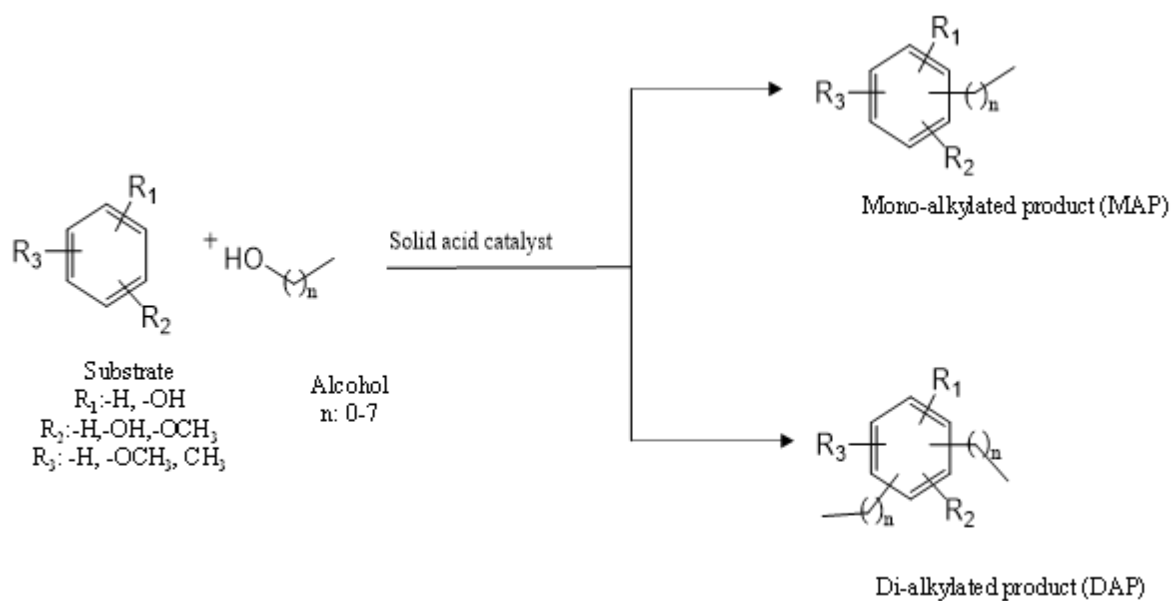
Figure 3. Functionalization of lignin model compounds

Summary

This thesis work is devoted to the overall development of lignin valorization. Lignin depolymerization was achieved using homogenous bases to obtain aromatic compounds and their defunctionalization and functionalization was carried out to reduce the oxygen content using solid acids and supported metal catalysts. Overall, a simple strategy was developed to increase the value of lignin and depolymerized products. Thesis covers the successive development of the lignin valorization process.

References:

1.   Luo, M. C. A. T. G., Green biomass pretreatment for biofuels production. *Springer* **2013**, 127-153.

2.   P. Maki-Arvela, T. S., B. Holmbom, S. Willfor, D. Y. Murzin, *Chemical reviews* **2011,** *111*, 5638-5666.

3.   Thring, R. W., *J. Chem. Eng.* **2000**.

4.   J. A. Onwudili, P. T. W., *Green Chem.* **2014,** *16*, 4740-4748.

5.   A. K. Deepa, P. L. D., *RSC Advances,* **2014,** *4*, 12625.

6.   A. K. Deepa, P. L. D., *ACS Catalysis* **2015,** *5*, 365-379.

7.   Bakhshi, N. N., *Energy & Fuels* **1992**.

8.   S. K. Singh, P. L. Dhepe., *Green Chem.* **2016, DOI: 10.1039/c6gc00771f**.

9.   K. Stark, N. T., A. Bosmann and P. Wasserscheid *ChemSusChem* **2010,** *3*, 719-723.

10.   W. Xu, S. J. M., P. K. Agrawal, C. W. Jones, *ChemSusChem* **2012,** *5*, 667-675.

11.   N. Yan, C. Z., P. J. Dyson, C. Wang, L. T. Liu, Y. Kou, *ChemSusChem* **2008,** *1*, 626-629.

12.   Q. Song, F. W., J. Cai, Y. Wang, J. Zhang, W. Yu, J. Xu, *Energy & Environmental Science,* **2013,** *6*, 994.

13.   Wahyudiono, T. K., M. Sasaki, M. Goto, *Chemical Engineering & Technology,* **2007,** *30*, 1113-1122.

14.   T. Furusawa, T. S., M. Saito, Y. Ishiyama, M. Sato, N. Itoh, N. Suzuki, *Applied Catalysis A: General,* **2007,** *327*, 300-310.

Chapter 1

Introduction and literature survey

1. Introduction

More than 95% of carbon-based chemicals currently manufactured by the chemical industry are derived from fossil reserves such as crude oil, coal, natural gas, etc.[1]. However, fossil reserves experience fluctuating costs and are not sustainable. Moreover, large consumption of fossil reserves is responsible for the greenhouse effect for increase in earth temperature. In view of these global and local factors, extensive research and development programs on biomass conversion by possible economical routes for making chemicals and fuels are globally undertaken in last two decades. In this context, many recent studies have evaluated the relative merits of applying different crop wastes for chemicals production [2]. Among numerous renewable resources (e.g., solar energy, tidal, wind, etc.), biomass is the only renewable organic carbon resource in nature, which allows its distinctive advantage in producing value-added products [3-5]. Historically, humans have been harnessing biomass as a source of energy since the time they knew to make a fire from woods. Even today, some countries depend on woods as a main source of energy. Biologically, biomass comprises C, H and O based matters those unify in a solid material and can be potentially converted in to fuels and chemicals.

1.1. Biomass: availability and composition

Biomass, a renewable source of carbon, is a material derived from plants and animals (Figure 1.1). It can be used in the production of chemicals and fuels after undergoing various conversions. Chemical composition of biomass includes a complex mixture of organic molecules containing approximately 47 to 53% of carbon, 5.9 to 6.1% hydrogen, and 41 to 45% of oxygen. Along with these, small amounts of nitrogen and sulfur, as well as traces of other elements, including metals, are also present [6].
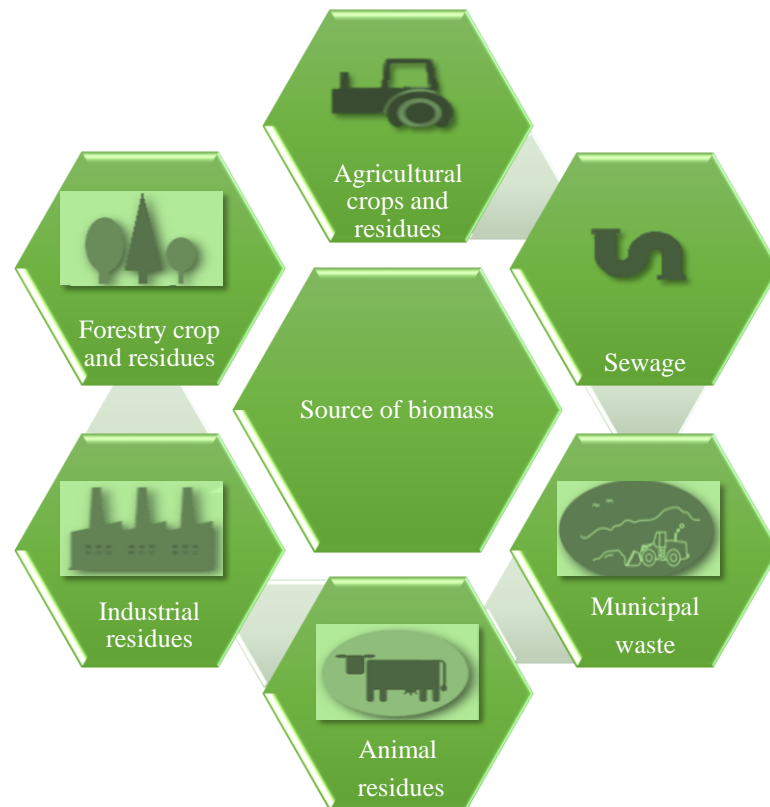
Figure 1.1. Significant biomass resources

Typically biomass is derived from either plants or animals. The main classification and subclassification of biomass is as follows:

1.1.1. Plant-derived biomass

Plant-derived biomass further can be categorized in the following parts

1.1.1.1. Edible biomass

- Crops (sugarcane, sugar-beet, and cassava)
- Starch crops (wheat, maize, potatoes)
- Oil crops (rapeseed, soy)

1.1.1.2. Non-edible biomass

- Forestry wood
- By-products agriculture (straw, corn stover)
- By-products industry (bagasse, paper-pulp)
- Algal crops from land and sea forming

1.1.1.3. Energy crops

- Short rotation coppice (SRC) (poplar, willow, eucalyptus)
- High-yield perennial grass (miscanthus, switchgrass)
- Non-edible oil plants (jatropha, camelina, sorghum)

1.1.2. Animal-derived biomass

Chitin can be considered as the most abundant source of animal-derived biomass. It can be extracted from the insect's crustaceans and microorganisms. The primary source of chitin biomass is the shell of shrimp and crab, lobster and krill, and commercially supplied by the shellfish processing industry.

Among all available resources of biomass, lignocellulosic biomass is considered as a more promising renewable feedstock due to its following properties:

- Non-edible to humans: use will not affect the food chain
- Inexpensive, locally available, and abundant

1.2. Lignocellulosic Biomass Composition

Lignocellulosic biomass contains three main components: cellulose, hemicellulose, and lignin linked to each other through various covalent and non-covalent linkages. Typically, lignocellulosic biomass has a composition of cellulose (30-50%), hemicellulose (15-40%), and lignin (10-30%) along with some macro and micronutrients [7, 8]. The composition of these biopolymers is dependent on its origin.

Cellulose is a linear high molecular weight polysaccharide made up of the D-glucose units linked to each other by β-1,4 glycosidic bonds (Figure 1.2) [9]. Degree of polymerization in cellulose ranges from few hundred up to several thousand units, depending on the origin of the material. Due to the presence of intramolecular and intermolecular hydrogen bonding in cellulose, highly ordered microfibrils known as crystalline cellulose, with high packing densities, are formed. Complete hydrolysis of cellulose yields C_6 sugar known as glucose ($C_6H_{12}O_6$). However, the presence of hydrogen bonding makes it difficult to undergo hydrolysis.
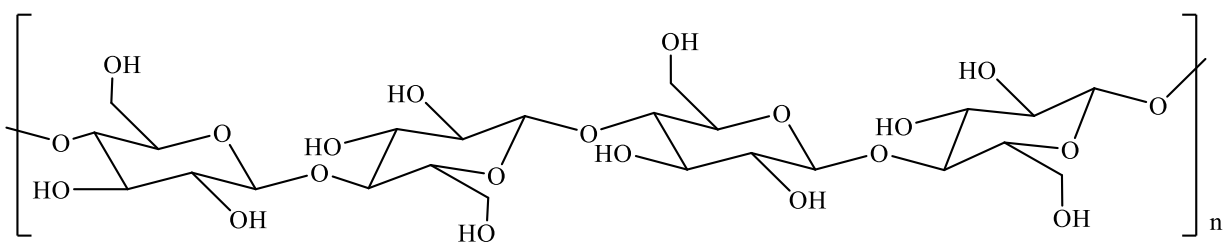
Figure 1.2. Structure of cellulose

Hemicellulose is a class of heteropolysaccharides made up of hexoses (D-glucose, D-mannose, and D-galactose), pentoses (D-xylose, L-arabinose, and D-arabinose), and deoxyhexoses (L-4 rhamnose or 6-dexoy-L-mannose and rare L-fucose or 6-deoxy-L-galactose) with small amounts of uronic acids, acetic acid, and other minor sugars present. These sugars are linked with each other by α- or β- (1,2; 1,3; 1,4; 1.6) linkages., The structure presented in Figure 1.3 [10] is for arabinoxylan. Hemicellulose typically has much lower molecular weights than cellulose. It can be readily hydrolyzed to pentose or hexose sugars it is made up of. Due to the lack of crystallinity and lower degree of polymerization than cellulose, the chemical and thermal stability of hemicellulose is lower than that of cellulose.
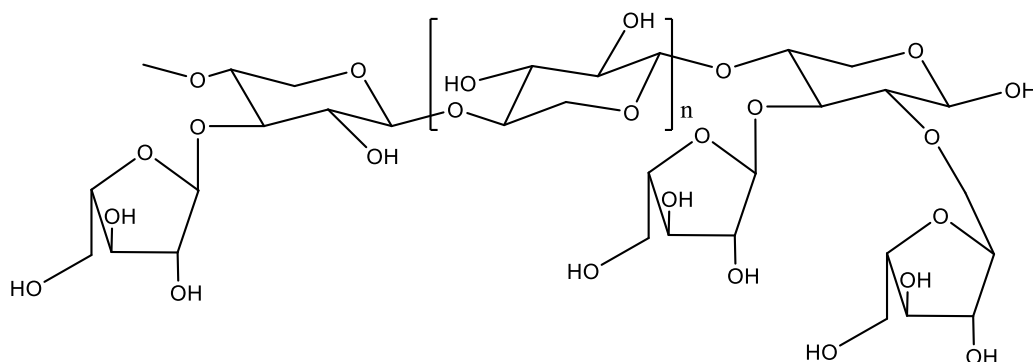
Figure 1.3. Structure of hemicellulose

Lignin is the most considerable non-carbohydrate fraction in lignocelluloses. In lignocellulosic biomass, lignin is predominantly cross-linked polymer that gives strength and rigidity to the cell wall. Lignin and hemicellulose form a sheath that is embedded with cellulose in the lignocellulosic biomass. It creates a seal around cellulose microfibrils and has limited covalent association with hemicellulose [10]. Lignin composition and its content in biomass vary between

the types of plants and also between the botanical species and even between trees and morphological parts of the tree [11]. It is known in the literature that in softwood, 30% by weight lignin is found, while in hardwood, the weight percentage falls to 20%−25% [12]. Lignin derived from grass contain only 10−15% of the total plant mass [13] (Figure 1.4 -1.5).
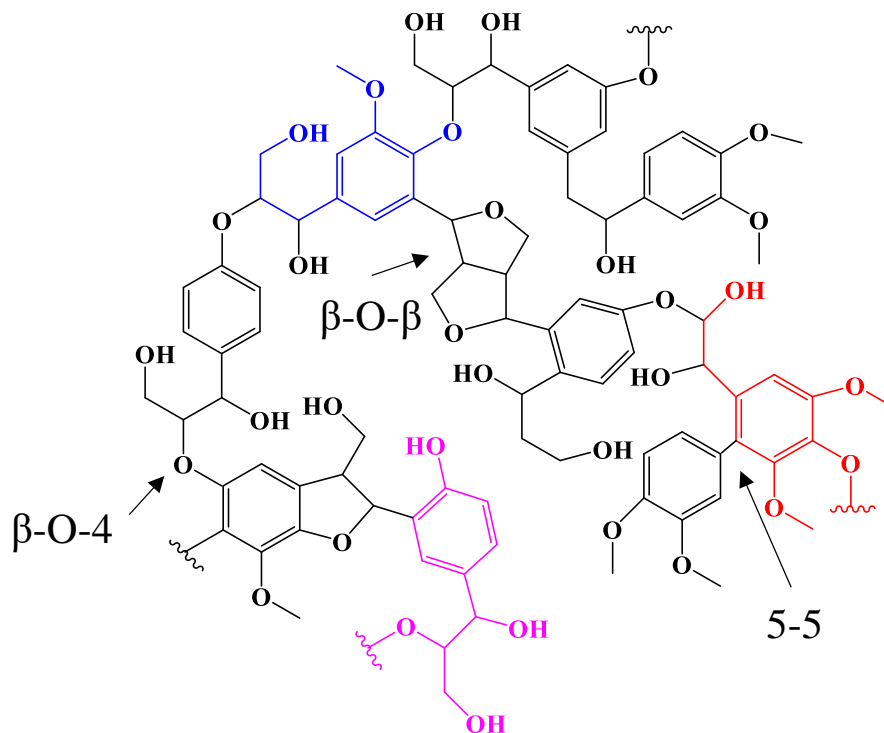
Figure 1.4. General structure of lignin
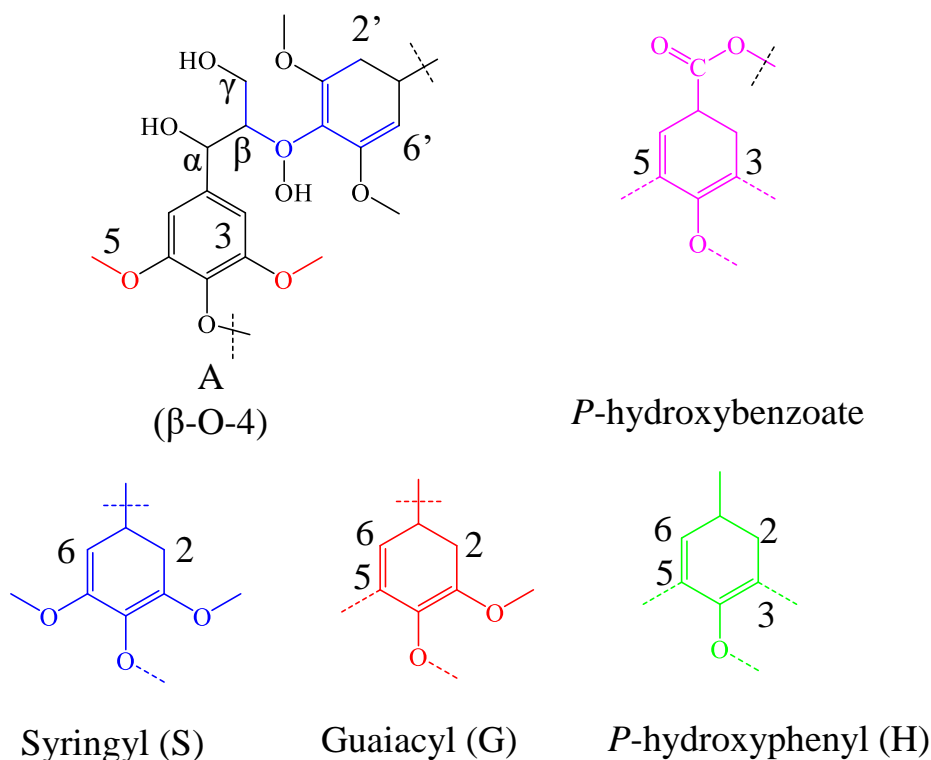
Figure 1.5. Structural units present in lignin

Lignin is a complex amorphous 3-dimensional phenyl propane based polymer made up of three primary units: sinapyl (3,5-dimethoxy 4-hydroxycinnamyl), coniferyl (3-methoxy 4-hydroxycinnamyl), and p-coumaryl (4-hydroxycinnamyl) alcohols, linked to each other via C-O-C and C−C linkages. These three monolignols are also known as syringyl (S), guaiacyl (G), and p-hydroxyphenyl (H) units, respectively (Figure 1.6). Monolignol contains a phenyl group and a propyl side chain; hence aromatic unit in lignin is usually called a phenylpropane unit (ppu). The monomers differ in the number of methoxy groups which are linked to the aromatic ring and thus are known as S, G or H. The content of each monolignol in lignin is associated with plants taxonomy. For example, while softwood (gymnosperm) lignin contains more guaiacyl units, hardwood (angiosperm) lignin has a mixture of guaiacyl and syringyl units, and grass lignin contains a mixture of all three aromatic units [12]. Depending on the composition of the three basic units in lignin, these polymers can be classified as type-G (softwood lignin),

type-G-S (hardwood lignin), type-H-G-S (grass lignin), and type-H-G (compression wood lignin) [11].
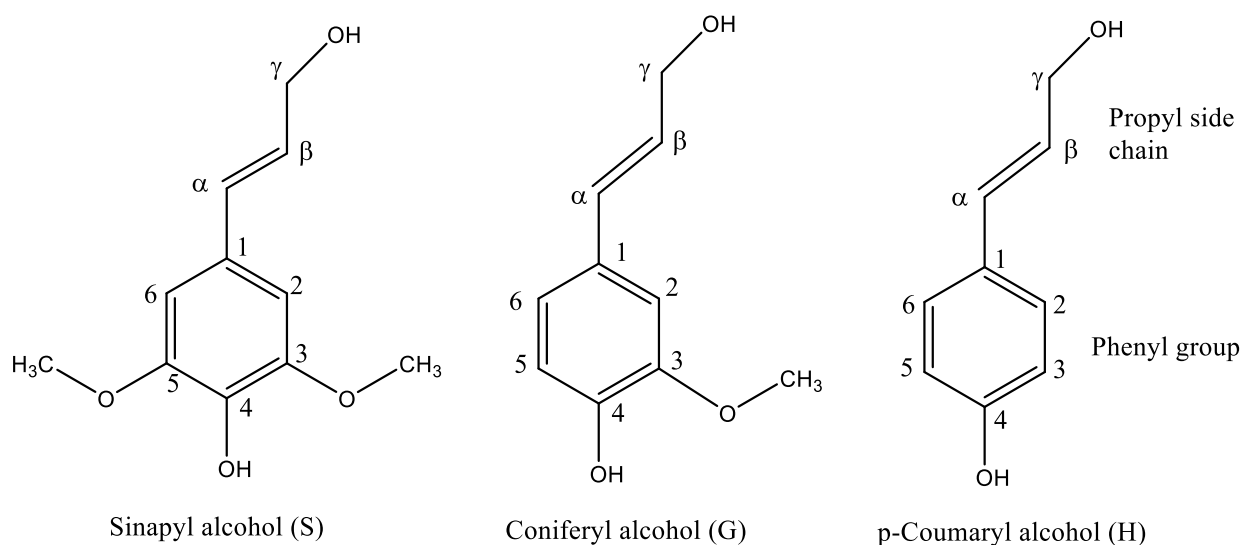
Figure 1.6. Structures of lignin monomers

1.3. Bio-refinery concept

In context to the finite availability of fossil reserves, like oil and natural gas, the use of renewable raw materials, specifically, biomass becomes a vital issue for the future chemical industries. The distribution of fossil reserves is limited to few areas, and this leads to geopolitical conflicts. However, the biomass is ample and more evenly distributed over the planet. Incorporating biomass in the industrial profile by the countries having limited fossil resources can contribute to preserve energy and chemicals independence.

In the current scenario, the generation of energy and chemicals is based mostly on the use of fossil reserves. Industries producing useful fuels, chemicals, and energy by the use of petroleum-based feedstocks gives rise to air pollution by greenhouse gases (GHGs), particle matters (PMs), toxic gases as NO_x and SO_2, as well as water and soil pollution through toxic industrial wastes. In 1965 the total world hydrocarbon consumption was about 3.7 billion toe (tons oil equivalent), which increased to 9.3 billion toe/y in 2000 and 12.7 billion toe/y in 2013 [14]. Considering the huge rise of world's population and the genuine need for a better life, it is apparent to develop bio-refinery model based on renewable resources. Figure 1.7 shows the concept of refinery and biorefinery.
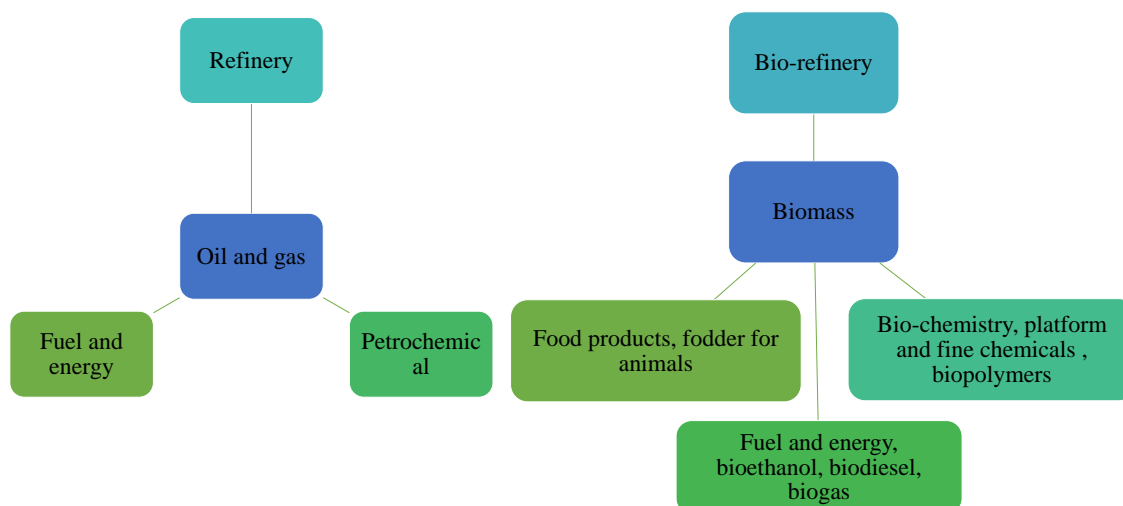
Figure 1.7. Conceptualization of refinery and Bio-refinery

Biomass is a natural energy carrier from the sun to the terrestrial life. Modern chemical technology called bio-refinery can solve the challenging task for replacing fossil hydrocarbon processing by biomass conversion into similar or new products which delivers, fuels, chemicals, and energy for substantial needs of the society. The implementation of bio-refinery could minimize the use of energetic and material resources, as well as practice recycling of waste from agriculture, industry, or domestic activities. It includes the sustainable and green approach, and compatible with sustainable development. It ensures economic development based on renewable resources, by generating opportunity in both industry and agriculture, and shielding the environment [13].
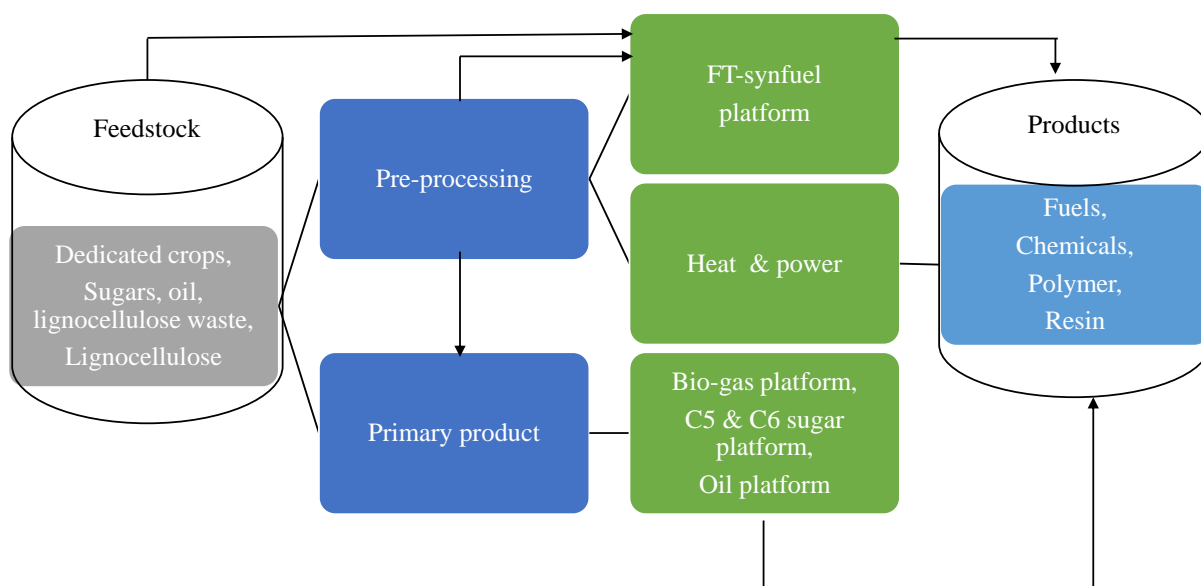
Figure 1.8. Bio-refinery concept

Figure 1.8 represents the bio-refinery concept; in the first step, the feed is subjected to pre-processing, which produces primary products directly. For example, biomass pyrolysis leads to pyrolysis oil from which some valuable chemicals such as alcohol, esters, phenols, and complex organic molecules could be formed, which otherwise requires complicated organic synthesis. After pre-processing, the treated biomass is sent to distinct technology platforms, where it is converted into targeted products.

In most of the available biorefinery literature, utilization of cellulose and hemicellulose is well reported while lignin fraction is underutilized due to its complexity and used as low-value products by burning to generate heat. In cellulosic ethanol production, a large amount of lignin is produced as a by-product. Utilization of it will boost the economy of cellulosic ethanol, which is required to enhance the use of cellulosic ethanol.

1.4. Lignin isolation techniques

Lignin isolation is achieved by giving the physical and chemical pre-treatment to solubilize it. Variation in properties of isolated lignin can be seen and dependent on the method used for its isolation. Common factors found in all the known process are the pH of the system, nature of solvent and solute participating in lignin isolation, the ability of solvent and solute to stop the recondensation and nature of the solvent to dissolve the lignin [15]. Currently, isolation of lignin

is carried out using four available processes on industrial scale, namely; Kraft, Sulfite, Organosolve, and Soda. Further, it can be categorized as sulfur free and sulfur enriched lignin. Lignin isolated using Kraft and Sulfite methods are typically enriched with sulfur while lignin isolated from Organosolv and Soda methods does not contain sulfur and shows similarity to the native structure of lignin.

1.4.1. Kraft process

Lignin isolation using Kraft process is achieved by the addition of lignocellulosic biomass into the solution of sodium hydroxide, and sodium sulfide then heated between 150 ^{o}C-180 ^{o}C around two hours, which will break the bond between cellulose, hemicellulose, and lignin followed by acidification and precipitation. Lignin produced using Kraft process contains a small amount of sulfur impurity.

1.4.2. Sulfite process

It is the largest known process used for the isolation of lignin to produce approximately 1000 tonnes per year of lignin [16]. In a typical procedure, lignocellulosic biomass is dissolved in the aqueous solution of sulfite and bisulfite salt with changing the counter ion such as calcium, magnesium, ammonium, and sodium [17]. The pH of the solution varies between 1-13.5 depending on the counter cation. Aliphatic chain of lignin is sulfonated at different positions depending on the pH of solution, which helps in the solubility of resulting lignosulfonate with hemicellulose impurity. Further purification of lignin is required to remove carbohydrate impurity using different technologies such as precipitation, ultrafiltration, and destruction of sugars.

1.4.3. Organosolv process

In this method, lignin isolation is carried out using the aqueous-organic solvent mixture, like acetone, methanol, ethanol, or acid (formic acid, acetic acid, sulphuric acid) heated up to 180 ^{o}C [18]. The high impact of this method is the use of low temperature and pressure, along with the production of sulfur free lignin. Commercial-scale production of lignin through this method is yet to explore, but in the future, it has the potential to replace the Kraft process due to the production of high purity lignin.

1.4.4. Soda process

This method is extensively used for the non-woody biomass source, e.g., sugar cane or flax. In a typical procedure, lignocellulosic biomass is first dissolved into aqueous NaOH [19] and heated

up to 160 °C. The primary step involves the depolymerization of lignin by cleaving ether linkages (α and β), resulting in the free phenolic group. Pre-treated lignin is now soluble in an aqueous medium and can be separated from pulping liquor using precipitation and filtration method. High purity sulfur free lignin is produced using this method as compared to the sulfite process, but obtained lignin has much lower molecular weight.

1.5. Lignin applications

Various functional groups (phenolic hydroxyl, aliphatic hydroxyl, carbonyl, methoxyl) present in lignin make it a versatile raw material for the various application. It has the potential to be converted into value-added products. Currently, lignin is being utilized in various ways (Figure 1.9) such as:

1.   Macromolecule synthesis

2.   Fuel-syngas production

3.   Source of aromatic compounds (phenol, hydrocarbon and oxidized product)

Among all known uses of lignin, aromatic compounds obtained from depolymerization of lignin has the highest value [20].
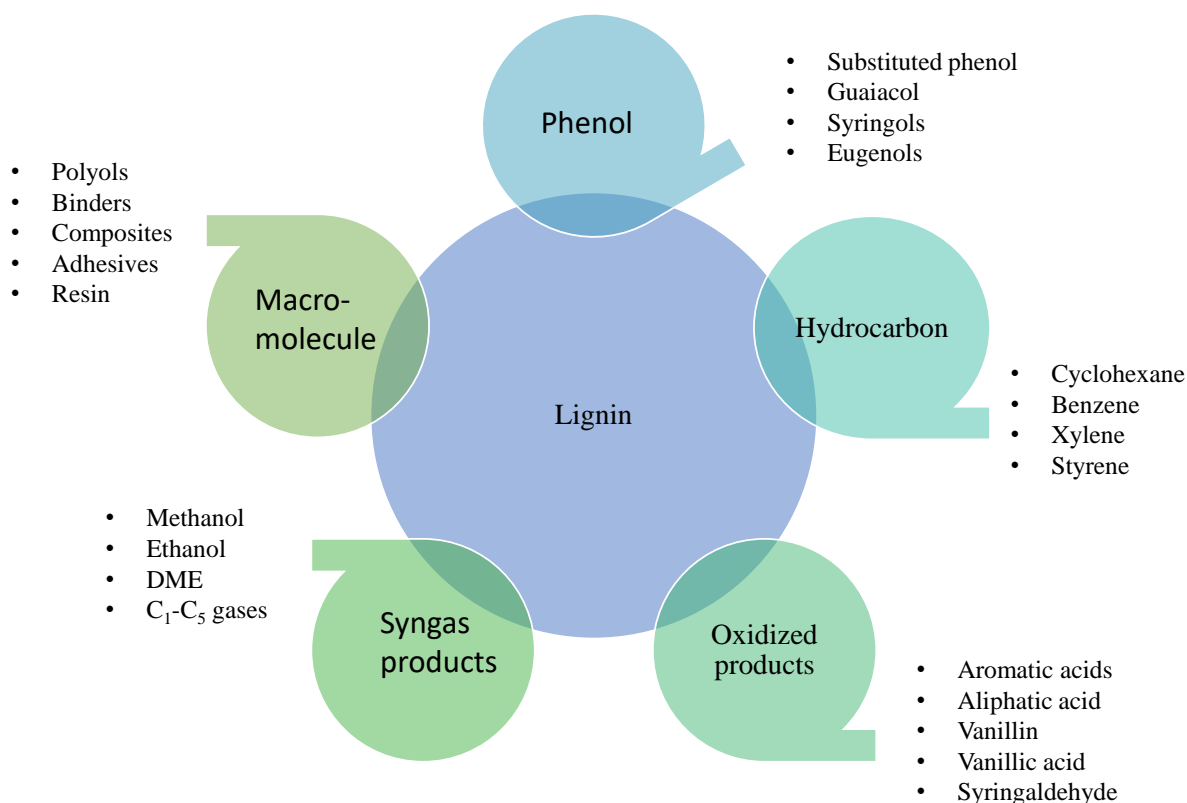
Figure 1.9. Various applications of lignin

1.6. Recent advancement in lignin depolymerization

In continuation of the above discussion, since the synthesis of chemicals adds the most value to lignin, its depolymerization into value-added chemicals is carried out using various thermal and thermo-chemical processes. In the current scenario production of the aromatic compounds from lignin instead of fossil/petroleum feedstock is gaining the attention of the researcher. Various reports have been published on the valorization of lignin. This section is dedicated to discussions on the various methodologies being used for the valorization of lignin. Figure 1.10 represents the schematic of lignin valorization under various conditions such as thermal and thermo-chemical.
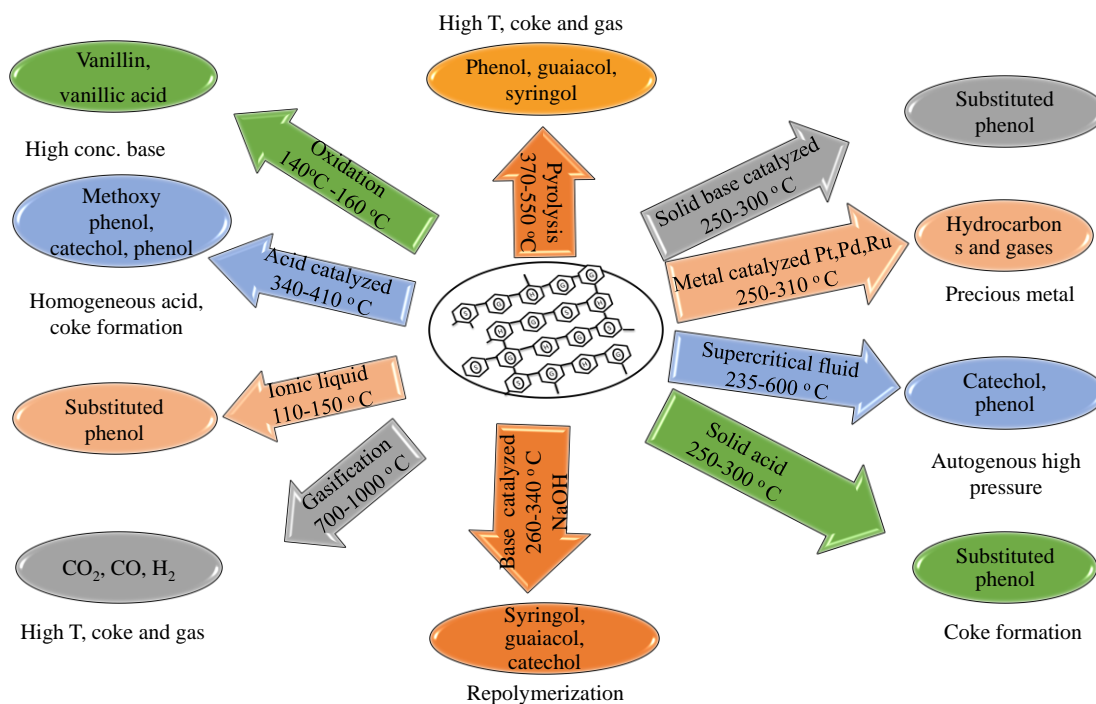
Figure 1.10. Various pathways used for the valorization of lignin

1.6.1. Thermal depolymerization

Pyrolysis and gasification of lignin come under the thermal depolymerization of lignin.

1.6.1.1. Pyrolysis

Pyrolysis process operated at high temperature (370-550 °C) under the anaerobic condition for few seconds to minutes produces mixture of low molecular weight compounds such as guaiacol, syringol derivatives. These can be used as it or can be further converted into value-added chemicals and fuels. The yield of low molecular weight compound can be increased by using catalyst Cr_2O_3/Al_2O_3 and $NiMO/SiO_2-Al_2O_3$ [21]. HZSM-5 was also reported for the pyrolysis of lignin and enhanced the yield of low molecular weight compound [22]. Pyrolysis is a known commercial-scale process for the utilization of lignin. Currently in Wisconsin, USA 50 tons of biomass/day; Vancouver, Canada 10-100 tons of biomass/day; and Finland 12 tons of biomass/day is commercially converted into value-added products [23-29].

1.6.1.2. Gasification

Gasification is a process in which biomass is gasified in the presence of an oxidant such as oxygen or air under high temperatures. Gasification of lignin is carried out using supercritical water or without it (Tc=374 °C, Pc=218 atm) for 60 minutes [30-33]. Under these conditions, a mixture of CO and H_2 (synthesis gas) along with CO, CO_2, hydrogen, methane (producer gas) are generated [30, 34]. The advantage of using this process is its thermal efficiency because it operates in aqueous media, so drying of biomass is not required. Optimization of reaction condition and catalyst help in getting many products from this route like olefin, alcohol, gasoline, and many other essential chemicals [35]. Gasification of alkyl phenol as a lignin model compound was reported for the synthesis of syngas using Ru/TiO_2 under supercritical water at 400 °C [36]. Lignin gasification activity was checked with commercial Ni catalyst and showed 20% yield of the gaseous product within 1h [37].

1.7. Thermo-chemical depolymerization

1.7.1. Acid catalyzed

Earlier lignin isolation was achieved using acid pulping from lignocellulosic biomass instead of depolymerization of lignin into value-added chemicals [38]. The same strategy was used for hydrolysis of lignin and model compounds to yield low molecular weight compounds using Lewis acids [39, 40], zeolites [41-44], acidic ionic liquids [45, 46], mineral acids [47, 48] and organic acids [38, 49]. In acid catalyzed depolymerization, hydrolytic cleavage of α and β ether linkages is more prominent as compared to C-C bond cleavage, because aryl-aryl ether and phenolic C-O bond are more stable as compared to them [50]. Lewis acid ($AlCl_3$, BF_3, $FeCl_3$, $ZnCl_2$, catalyzed lignin depolymerization uses thermodynamically favorable path and highly dependent on reaction temperature yielding low molecular weight compounds [51]. It was reported in the comparative study of crystalline and amorphous solid acids that solid acids can effectively depolymerize the various lignins to produce low molecular weight compounds at 250 °C under N_2 atmosphere in methanol and water (5:1 ratio) solvent [52, 53] to achieve ca.62% of low molecular weight compound formation.

1.7.2. Base catalyzed

Base catalyzed lignin depolymerization is usually carried out using commercially available cheaper homogeneous bases like LiOH, NaOH, KOH, and CsOH at 270-350 °C. Base catalyzed lignin depolymerization involve in the cleavage of an aryl-alkyl bond, including β-O-4, which is the weakest bond present in the lignin [54-56]. Base catalyzed lignin depolymerization is known

for high yielding low molecular weight compounds because coke and char formation can be restricted in basic media Product selectivity is dependent on the reaction parameters employed for depolymerization like time, temperature, pressure, base concentration and lignin/solvent ratio [55, 57, 58]. In base catalyzed depolymerization reaction basic strength of used bases has a high impact on lignin conversion and product selectivity [59, 60]. The extent of depolymerization is also observed to increase when the reaction is carried out in phenol or alcohol as compared to aqueous solution due to the increase of the solvolysis effect of ether linkages. Solid product formation is a significant concern in base catalyzed depolymerization due to repolymerization/condensation reactions taking place at the same time in reaction media, which in turn lowers the yield of monomers. Few efforts are made to minimize the repolymerization reactions using capping agents such as boric acid, phenol, 2-naphtol and p-cresol by capturing the reactive species responsible for repolymerization reactions [57, 61, 62]. In base catalyzed depolymerization, some acidic molecule are also formed, decreasing the active catalytic site by the time due to acid/base neutralization reaction. Efficient depolymerization of lignin is too reported using solid base in ethanol and water media at 250 $^\circ$C and shows ca. 51% yield of low molecular weight compounds [63].

1.7.3. Metal catalyzed

The effect of the metal is also well studied in the depolymerization of lignin. The depolymerization using $NiCl_2$, or $FeCl_3$ gives only 2.5% yield of catechol at 305 $^\circ$C [64]. Two-step strategy used for the depolymerization of Kraft lignin firstly treated by Si-Al catalyst in H_2O/butanol solvent followed by the use of ZrO_2-Al_2O_3-FeOx to increase the overall yield of phenol is possible with a yield of 6.5 -8.6 % of methoxy phenol [65]. The activity of 20 wt% Pt/C catalyst was checked in formic acid, and ethanol solvent for depolymerization of lignin isolated from switchgrass using Organosolv method shows improvement in the yield of guaiacol derivative. A combination of Pd with SAC-13 was checked for the depolymerization of dry spruce lignin in aqueous medium at 300 $^\circ$C gave less than 5% yield of the phenolic compound, including guaiacol, pyrocatechol, and resorcinol. Metal catalyzed depolymerization is also possible at a lower temperature (200 $^\circ$C), but lots of effort are required to understand and clarify the mechanism and function of metal and acid in depolymerization of lignin.

1.7.4. Supercritical fluid

The low viscosity of supercritical fluids helps in the dissolution of lignin, enhancing the use of it for the depolymerization of lignin. Carbon dioxide, acetone, ethanol, and methanol are known as supercritical fluids. Depolymerization of lignin and model compound using supercritical fluid such as methanol and ethanol are reported at 239 °C and 8 MPa. In addition, the use of homogeneous bases along with alcohols found to enhance the yield of low molecular weight compound (catechol, guaiacol, p-cresol, o-cresol) due to solvolysis of C-O-C linkages [66, 67] while C-C linkages remain stable. Depolymerization of Organosolv lignin is reported between 235-600 °C and up to 10 MPa in supercritical water along with phenol as a capping agent, which is helping in the suppression of repolymerization and char formation at high temperature [68]. An increase in the yield of water-soluble products such as catechol, m-cresol, p-cresol, o-cresol, and phenol was found in supercritical water at 350-400 °C, and 25-40 MPa and also evidence of both C-O-C and C-C bond cleavage is seen [69]. The advantages associated with the use of supercritical fluid is high solubility of lignin in these solvents and easy separation of depolymerized products. However, high temperatures and pressures associated with this process is a disadvantage.

1.7.5. Ionic liquid

The high solubility of lignin in ionic liquids enhances the degree of depolymerization of lignin following carbocation reaction pathway [70, 71]. An improvement in depolymerization activity was found when the ionic liquid was used in combination with Lewis acids. Lewis acids, like metal halides, help in the cleavage of β-O-4 bond [72]. In-situ generated hydrochloric acid by the hydrolysis of metal halide is an active catalytic species in this process. The ionic liquid can also act as a catalyst and solvent in the lignin depolymerization reaction. The use of 1-H-3-methylimidazolium chloride has been reported for the hydrolysis of the lignin model compound at 150 °C and resulted in 70% yield of guaiacol [73]. The reaction mechanism of the hydrolysis of the lignin model compound depends on acidity as well as the nature of cation and anion and their interaction with substrate [74]. Raw lignocellulosic biomass can be converted directly in ionic liquid due to its inherent ability to dissolve it [74]. Conversion of raw biomass is reported using (Amim)Cl ionic liquid, which is helping in the complete hydrolysis of cellulose and hemicellulose along with depolymerization of lignin into substituted phenols [75]. Efficient

depolymerization of lignin was reported using BAILs with –SO$_3$H group at 120 ^{o}C in methanol and water solvent gave 78% yield of low molecular weight aromatic compounds [76].

1.7.6. Oxidative depolymerization

Oxidative depolymerization of lignin is reported between 140-160 ^{o}C using hydrogen peroxide as an oxidant along with alkali metal and mineral acid, which increases the functionality of the depolymerized products by incorporating oxygen in the products [77]. Gaseous oxygen is also employed for the oxidative depolymerization of lignin to yield products like vanillin, syringaldehyde [78-80]. Oxidative depolymerization of lignin can be achieved using both homogeneous and heterogeneous system, but the ease of separation from reaction media make the heterogeneous system more preferable.

1.8. Applications of depolymerized products

Depolymerization of lignin produces low molecular weight compounds, and those can be used in various applications. Few of the applications are summarised below:

⚓ Guaiacol

Guaiacol can be used in the synthesis of active pharmaceutical components. It also has applications in flavoring, food, and perfumery industries. The medical application of guaiacol is also known and can be used as antiseptic and local anaesthesia.

⚓ Catechol

Catechol generally is used in the synthesis of pesticides and intermediate products of the perfumery industry. It has a potential application in the polymer industry. It can be used as a building block for the production of various polymeric materials consisting of fascinating and interesting properties such as white and black photographic developers to increase the contrast of the image.

⚓ Eugenol

Eugenol is important in dentistry due to its anaesthetic and analgesic effects. It has a potential application in the design of new drug delivery. It can also be used in the flavor and perfumery industry.

⚓ Resorcinol

Resorcinol is used as a raw material in many reactions. It is used in the rubber industry for the production of polyester, nylon, rayon fiber, etc. Moreover, it is being used in the synthesis of various fine chemicals such as fire retardants, UV absorbers, elastomers, and polycarbonates.

⊹ **Vanillin**

Vanillin is used in the food and fragrance industry. Application of vanillin in food is a flavor enhancer at many places such as chocolate, biscuit, bread, beverage, and ice-creams. It is also used to create a milk-like fragrance in cosmetics and perfumery products.

⊹ **Phenol**

Phenol is an important intermediate product used in various places, such as in the production of polycarbonates, bakelite, detergent, and herbicides.

Overall, Lignin has the potential to produce variety of chemicals, which can be used in various places. Depolymerization of lignin produces low molecular weight compounds, those have variety of potential applications. Although various reports are present for the depolymerization of lignin, those have some limitations like the use of precious metal, formation of coke, use of high temperature and pressure. It was also noted that the depolymerization of lignin produces a complex mixture of low molecular weight compounds. These low molecular weight compounds can be used in various places, but their separation or further conversion will improve the use of it.

1.9. Catalyst and Catalysis

Catalyst is a material used in many chemical reactions to help in selecting the faster path for desired product formation without affecting thermodynamics of reaction, and it remains unchanged at the end of the process. The process in which catalyst is used and participates in the reaction is called catalysis. The inherent properties and concepts related to catalysts and catalysis are summarized below:

⊹ Catalyst activity can be explained in terms of conversion (mole of reactant converted/mole of reactant charged), turnover number (mole of product/mole of active catalyst site), and reaction rate (mole of product/volume of the catalyst). However, if catalyst activity is very high and forming more selective products, then a lower quantity of catalyst is also sufficient to complete the reaction.

⊹ Higher stereoselectivity of the catalyst reduces the cost of separation of products in the chemical reaction.

⊹ Easy regeneration of the spent catalyst increases the catalytic cycle of the catalyst.

⊹ Catalyst should be economical.

Catalysis can be categorized into two categories based on phases involve in chemical reaction i.e., heterogeneous and homogeneous.

1.9.1. Heterogeneous catalysis

In heterogeneous catalytic system, phases of solvent, reactant, product, and/or catalyst are different. Generally, catalyst is present in the solid phase, and reaction and product can exist in liquid or vapor phase. Mostly, metal oxides, supported metal catalysts, zeolites, resins, inorganic solids are categorized in this category. Advantages and disadvantages of using heterogeneous catalysis are as follows:

Advantages:

- Easy separation from reaction media
- Avoid liquid waste treatment
- Avoids corrosion of the reaction vessels
- Easy and safe handling
- Easy recovery and regeneration

Disadvantages:

- Control of temperature in the exothermic reaction
- Diffusion limitation
- Restricted access to active sites
- Reproducibility of catalyst properties

1.9.2. Homogeneous catalysis

The reaction mixture, including reactants, products, solvent, and catalyst are present in the same phase. It includes organometallic complexes, soluble acids, bases, and salts. Advantages and disadvantages associated with the homogenous system are as follows:

Advantages:

- All catalytic sites are involved in the chemical reaction
- Reaction temperature of the exothermic reaction can be controlled

Disadvantages:

- Recovery of catalyst from reaction media is difficult
- Corrosion of system with homogenous acid
- Treatment cost of waste is high

⚏ Product contamination

The present work is focused on the homogeneous base catalyzed depolymerization of lignin and understanding of the products formed in the reaction. It was reported in the literature that after the depolymerization reaction and neutralization process, two-layers are formed in the reaction mixture i.e., liquid layer and solid layer. This system is interesting because in an alkaline aqueous medium, almost all lignin is soluble and thus overall process becomes homogeneous. In view of this, the present work is carried out to explore the study of base catalyzed lignin depolymerization and understanding the nature of the product.

1.10. Closest available literature for the present work

1.10.1. Lignin depolymerization

Base catalyzed lignin depolymerization was studied to explore the effect of an alkaline base such as NaOH, KOH, Na_2CO_3, and K_2CO_3. Product analysis shows that the alkaline additive promotes the depolymerization process by decarboxylation and removal of the unsaturated alkyl chain. A two-step process was developed for the base catalyzed depolymerization of lignin in which the first step is depolymerization of lignin and second step involves partial removal of oxygen, to produce mixture of compounds like phenyl, cycloalkyl methyl ethers, alkylbenzene, alkylated cycloalkane [81]. Depolymerization of softwood lignin was reported using 5% NaOH solution in aqueous media between 300-330 ºC and 9-13 MPa (N_2) pressure [82]. Organosolv lignin was depolymerized into syringol and hydroxyacetophenone at 300 ºC and 25 MPa (N_2) pressure [83]. Lignin model compound was studied using Cs_2CO_3 at 180 ºC and produced methoxy benzene as a product. Lignin model compound, 2-phenoxy-1-phenethanol was studied over Ni supported on hydrotalcite at 270 ºC in which cleavage of β-O-4 aryl ether linkages gave phenol and acetophenone as products. The same reaction condition was employed for the depolymerization of Organosolv lignin, mixture of product like guaiacol, catechol, eugenol, vanillin was observed [84]. The catalytic activity of copper supported porous metal oxide (Cu/PMO) was investigated for the Organosolv lignin depolymerization between 140-220 ºC and under 3-6 MPa H_2 to yield catechol derivative along with some oligomeric products [85]. Solid base MgO is reported for the depolymerization of pine lignin at 250 ºC, and 13% yield of substituted phenol was achieved.

1.10.2. Upgradation of lignin-derived monomers using defunctionalization/hydrodeoxygenation path

Guaiacol is one of the depolymerized product of lignin and widely studied as a model compound of lignin. It has similar types of carbon-oxygen linkages which are present in the lignin like oxygen-carbon bonds: C(sp3)–OAr (methoxy group), C(sp2)–OMe and C(sp2)–OH (hydroxyl) having bond energies about 247, 356 and 414 kJ/mol, respectively [86]. Considering this, research is devoted to use guaiacol as a representative compound of lignin-derived chemicals for hydrodeoxygenation (HDO) reactions. It is known in the literature that solid acids [87, 88] solid bases [89] and acidic ionic liquids [90, 91] can depolymerize lignin under milder conditions (<250 °C, N_2) to yield low molecular weight compounds including guaiacol.

Since cyclohexanol and cyclohexanone (KA oil) are industrially important chemicals in the synthesis of adipic acid, which is being used as an intermediate in the production of polymeric material, it is desirable to produce them from bio feedstock instead of fossil feedstock derived benzene, phenol, and cyclohexene. The expected market of adipic acid is approximately USD7000 million in 2019, which makes it one of the interesting molecule to synthesize. A large number of studies are there in literature for hydrodeoxygenation of guaiacol using the precious and nonprecious supported metal catalyst to produce cyclohexanol.

Ru supported on carbon is reported for HDO of bio-oil at 340 °C and 8 MPa H_2 in aqueous medium showing formation of mixture of upgraded monomers [92]. Ru/ZrO_2-WO_x catalyst is also reported for the formation of mixture of products (cyclohexanol, cyclohexanone, cyclopentanone) at 270 °C and 4 MPa H_2 pressure [93]. Pd-WO_x/Al_2O_3 catalyst at 300 °C and 7 MPa H_2 in n-decane solvent is reported to give 88% cyclohexane yield [94]. Comparative study of Pd, Ru (240-330 °C), and Mo_2C (330-375 °C) supported on carbon is done at 3.4 MPa H_2 in decaline solvent, and it was observed that the ring hydrogenation occurs at 240 °C and C-O bond cleavage occurs above 300 °C [95]. Previously from our group guaiacol, HDO reported in the presence of Pt, Pd, and Ru metals loaded on various supports (acidic, basic and neutral) at 250 °C under 3 MPa H_2 in hexadecane solvent and the results showed that distribution of products is a function of nature of support [96]. The comparative study of Pt/HY and Pt/HZSM5 catalyst is reported for HDO of guaiacol at 250 °C and 4 MPa H_2 in decane solvent where Pt/HY catalyst has shown better activity for the formation of complete HDO product (cyclohexane) [97]. Ru/SiO_2 catalyst has shown complete conversion of guaiacol with

55% yield of cyclohexane in n-dodecane at 300 °C and 5 MPa H_2 [98]. The activity of bimetallic RuRe/C and RuRe/MWCNT is also monitored for HDO of guaiacol at 200 °C, and 2 MPa H_2 in n-heptane medium and cyclohexanol formation was seen as a major product.[99]

Besides precious metal, significant research is also devoted to the use of non-precious transition metal based catalysts (CoMoS, NiMoS, or Mo_2N) under similar condition for the up-gradation of crude oil in flow system at 300 °C and 4 MPa H_2 [100]. However, these catalysts are associated with limitations like low activity and contamination with sulfur containing products along with desired products (cyclohexane, toluene, and catechol) [100, 101]. Few other Ni and Fe containing catalysts are also used for the HDO of lignin model compounds, but those showed respectable activities at higher temperature (>350 °C), resulting in undesired by-product formation like CH_4 and CO [102-104]. $NiCo/Al_2O_3$ catalyst is reported for the HDO of guaiacol to yield cyclohexanol as a major product (70%) at 200 °C and 5 MPa H_2 pressure in aqueous medium [105]. Recently, CuNi/Ti-MCM-41 catalyst is used for HDO of guaiacol at 260 °C and 10 MPa H_2 in heptane solvent showing 74% conversion of guaiacol with 48% selectivity of cyclohexane [106].

Typically, it is seen in the reported literature multiple factors involves in HDO reaction to get maximum yield. Among all factors nature of support and solvent has significant role in HDO activity. In a bifunctional supported metal catalyst, metal splits H_2 and support is responsible for the cleavage of C-O bond(s) [107-110].

1.10.3. Upgradation of lignin derived monomer using functionalization pathways

The depolymerization of lignin produces low molecular weight compounds. These phenolic monomers have high O/C ratio, which reduces its fuel quality, hence to improve the fuel quality of lignin derived low molecular weight compounds, the O/C ratio should be reduced, or C/H ratio should increased. HDO process is generally preferred to reduce the O/C ratio [111-114], and the alkylation process is favored to adjust the carbon number to improve the carbon number of the product [115]. The possible route for alkylation is either through C-O bond activation or through C-H bond activation [116-119].

The alkylating agent used for alkylation is either olefins or alcohols [120-122]. Alkylation of phenols is an electrophilic aromatic substitution. In the case of alcohols, the electrophile can be the protonated alcohol (an alkoxonium species) or a carbenium ion resulting from alcohol dehydration. In the alkylation reaction, O-alkylation products are formed by the electrophilic

attack on the phenolic OH while, C-alkylation products are formed when electrophile attack on the aromatic ring. It has also been proposed that C-alkylation products could be formed through intramolecular rearrangement of the kinetically favoured O-alkylation product, i.e., via an aryl alkyl ether intermediate product [116, 117, 119]. These alkylated phenolic compounds have wide applications as additives in gasoline, lubricants, and consumer products [123, 124].

Upgradation of various lignin derived phenolic monomers were carried out to produce alkylphenol over different solid acid catalysts [125-129]. The effect of acid-base property of catalyst was investigated for alkylation of phenol with methanol over modified MgO catalyst. The result showed an increase in phenol conversion and 2,6-xylenol selectivity with acidity, whereas the selectivity to o-cresol decreased since the reaction proceeds further (phenol→o-cresol→2,6-xylenol→2,4,6-trimethylphenol [125]. Immobilized ionic liquids were used as acid catalysts for the alkylation of phenol with dodecane, which showed higher selectivity for monoalkylated products [126]. α-zirconium phosphate (ZP) nanoparticles solid acid catalyst were studied in the alkylation of phenol with cyclohexanol under solvent-free conditions resulted in excellent conversion of phenol and selectivity toward 4-cyclohexylphenol [127]. The alkylation of phenol with cyclohexanol and cyclohexene in the presence of HY and dealuminated/ultrastable Y zeolite catalysts were studied over a range of temperatures 140-220 °C at atmospheric pressure for 2-12 h. A mixture of isomeric cyclohexylphenol was obtained, consisting mainly of 4-cyclohexylphenol [128]. The alkylation of m-cresol with isopropanol over HY zeolite was studied in a liquid phase system. Isopropanol favours O-alkylation while propylene favors C-alkylation.[129]. More than 85% conversion of various phenolic monomer is achieved at 250 ºC within 2 h to produce various alkylphenols without the addition of gaseous hydrogen. A series of sulphate-promoted ZrO_2 solid acid catalysts were tried for the liquid-phase alkylation of catechol to guaiacol in a fixed-bed down-flow reactor, showed 82% conversion of catechol with 84% selectivity of guaiacol at 200 °C and 0.1 MPa pressure. This study reveals the direct correlation between the catalytic activity and surface acidity of sulphated zirconia [130]. The alkylation of phenol with methanol over copper aluminum hydrotalcite catalysts has been reported. Their result showed selective C-alkylation of phenol to produce o-cresol and 2,6-xylenol due to the higher acidity of these catalysts [123]. From this literature survey, it reveals that solid acid catalyst shows better activity in the alkylation of

phenolic monomers. Hence in this thesis, we have tried to study the effect of different solid acid catalysts in the alkylation of guaiacol as a model compound with different alcohols.

1.11. Motivation of the work

Lignin is recognized as a renewable source of an aromatic compound. Depolymerization of it will produce phenolic monomers, can be utilized as a fuel additive and intermediate products in many applications such as food, chemical, and polymer industry. However, depolymerization of lignin provides complex mixture of aromatic monomers, and separation of obtained monomers is still challenging task. Various efforts were made for the value addition of lignin still there is a need to developed an effective method for the depolymerization lignin and utilization of obtained monomers. Among all known method base catalyzed depolymerization is an efficient method operated at the milder condition. Generally, the solubility of lignin is very high in an alkaline medium; however, base catalyzed depolymerization produces two separate layers after depolymerization. In this thesis, we have used homogeneous base for the lignin depolymerization and focused on understanding the product distribution based on the solubility of lignin and depolymerized product. Another perspective of this work focuses on the use of the depolymerized product by its value addition. Many reports are present for the value addition of depolymerized product using precious and nonprecious supported catalyst at high temperature and pressure, so the inspiration of this thesis is to depolymerize lignin to get aromatic monomers and their value addition using the catalytic pathway.

1.12. Objective and scope of the thesis

Based on the overall discussion about lignocellulosic biomass, depolymerization of lignin produces aromatic monomers, has a potential to replace the variety of chemical and fuel derived from the fossil feedstock, We have set following objective of my work,

- Use of actual lignin for the depolymerization process
- Use of homogeneous bases for depolymerization of lignin
- Understanding of the product distribution
- Correlation between lignin and depolymerized product
- Up-gradation of lignin model compound using supported metal and solid acid catalyst

Details background study of lignin suggests structural property of lignin is dependent on the plant species and isolation technique. Therefore before depolymerization, it is desirable to

$$Base/H_2O/250^oC/N_2$$
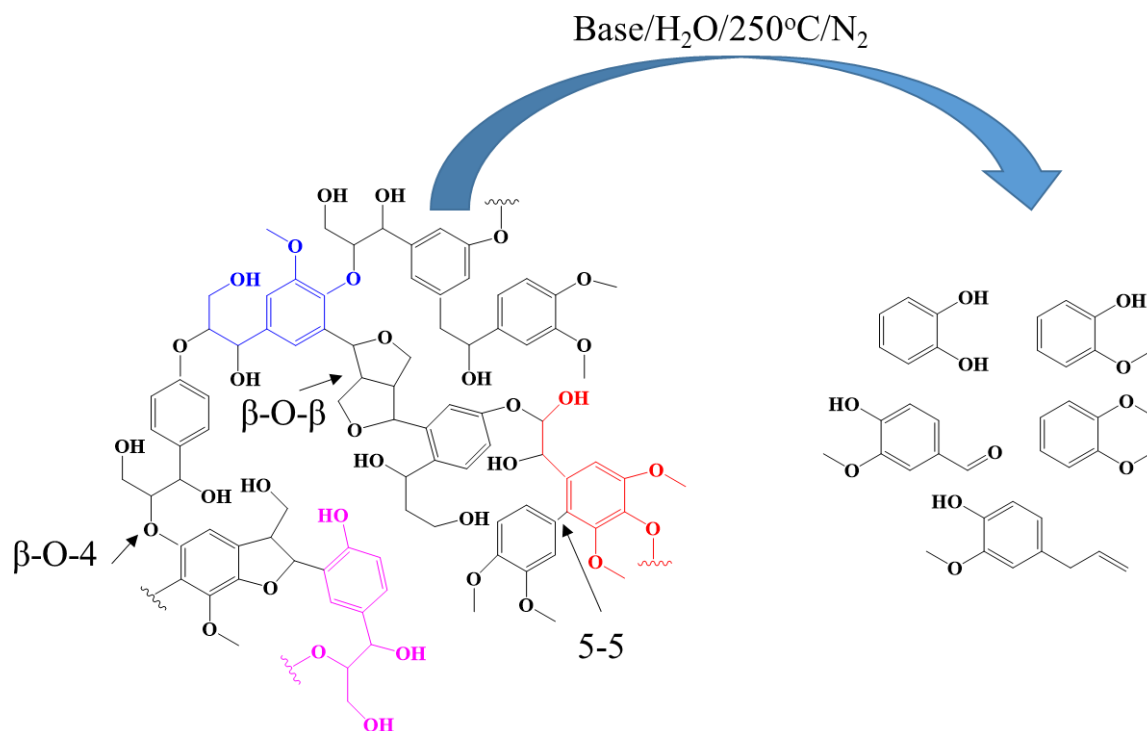
Scheme 1: Base catalyzed lignin depolymerization into monomers

understand the nature of lignin. Various physicochemical methods were used for detailed characterization of lignin such as FTIR/ATR for functional group analysis, CHNS for the correlation of molecular formula, ICP-OES for trace metal analysis, XRD for the confirmation of cellulose impurity and amorphous nature, TGA-DTA for the thermal degradation.

Synthesis of supported metal and solid acid were carried out to complete another objective of the work, i.e., upgradation of lignin model compound to provide a complete solution for the value addition of lignin.

Characterization of synthesized catalysts was done to correlate the catalytic activity of the respective catalyst.

Defunctionalization/HDO/Metal-Support

Functionalization/Alkylation/Solid acid
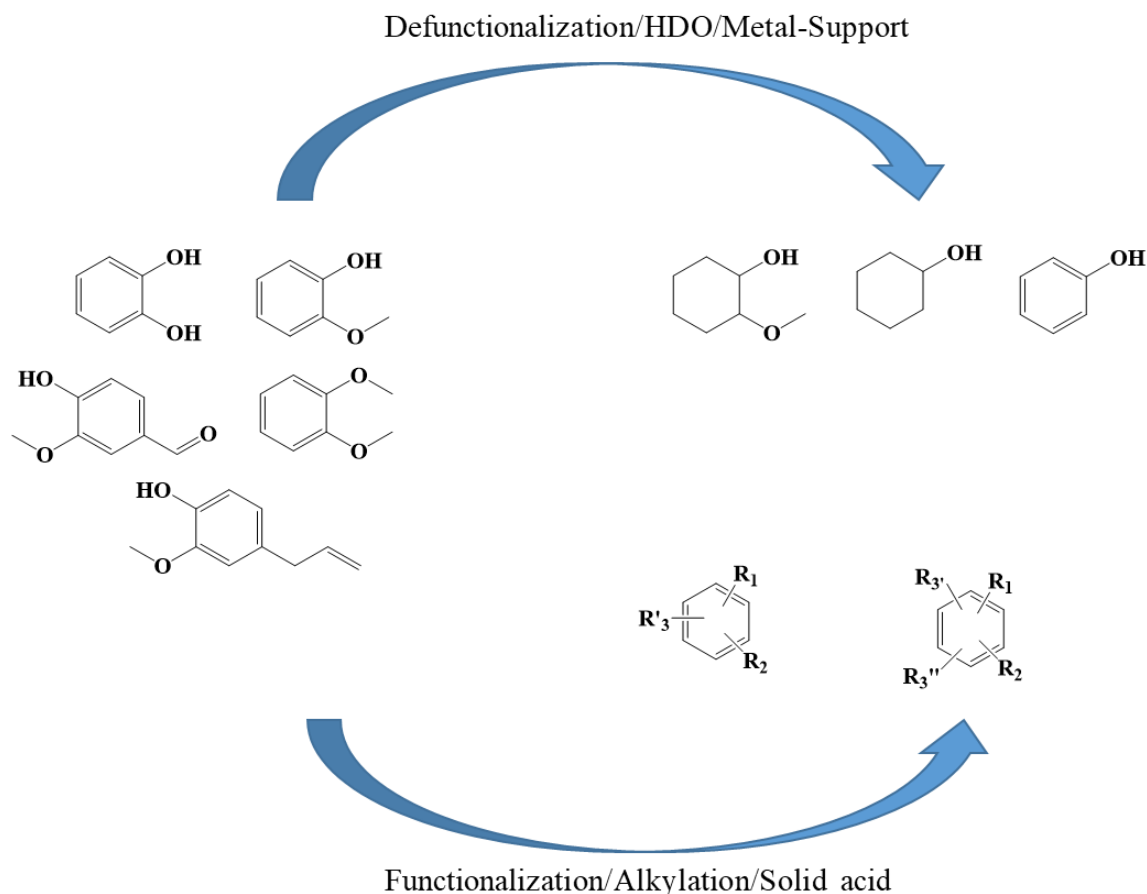
Scheme 2: Upgradation of lignin derived monomers

1.13.   Outline of the thesis

The thesis is divided into seven Chapters, the current Chapter includes discussion about the component of biomass, isolation technique used for lignin extraction from the lignocellulosic biomass, the requirement of the lignin value addition, up-gradation of lignin model compound. In the end, the motivation of the work followed by the scope and objective of the thesis incorporated in this Chapter.

The second Chapter discusses lignin characterization and catalysts characterization, which was synthesized to carry out the up-gradation of the lignin model compound. This Chapter is divided into two subparts. In 2A, various lignin used for the depolymerization were thoroughly characterized. Moreover, 2B, detailed characterization of supported metal and solid acid catalyst using XRD, NH_3/CO_2-TPD, ICP-OES, TEM, SEM, BET, CHEMISORPTION.

Chapter three, Base catalyzed lignin depolymerization into phenolic monomers and identification and quantification of products using GC, GC-MS, LC-MS, ATR. A unique model compound study is also carried out to correlate the relation between depolymerized products and lignin.

The fourth and fifth Chapters are about the up-gradation/defunctionalization of the lignin model compound using supported metal catalyst. These Chapters further divided into two subchapters. Chapter 4A, Hydrodeoxygenation/defunctionalization of lignin model compound using precious metal (Ru) and external H_2 source, Chapter 4B, is the same but using transfer hydrogenation pathways. Chapter 5A, hydrodeoxygenation/defunctionalization of lignin model compound using non-precious metal (Co,Ni) and external source of H_2, above all reactions are carried out using Parr make batch mode reaction. However, Chapter 5B discusses hydrodeoxygenation /defunctionalization of the lignin model compound using continuous flow reactor.

Chapter 6, Upgradation/functionalization of lignin derived monomers using solid acid catalyst Chapter 7, Conclusion, discuss the main results and novelty of the work.

1.14. References:

1.   Feghali, E.; Carrot, G.; Thuéry, P.; Genre, C.; Cantat, T., Convergent reductive depolymerization of wood lignin to isolated phenol derivatives by metal-free catalytic hydrosilylation. *Energy & Environmental Science* **2015,** *8* (9), 2734-2743.

2.   Tuck, C. O. P., E.; Horvath, I. T.; Sheldon, R. A.; Poliakoff.; M., Valorization of Biomass: Deriving More Value from Waste. *Science* **2012,** *337,* 695−699.

3.   Huber, G. W.; Iborra, S.; Corma, A., Synthesis of Transportation Fuels from Biomass: Chemistry, Catalysts, and Engineering. *Chemical Reviews* **2006,** *106* (9), 4044-4098.

4.   Melero, J. A.; Iglesias, J.; Garcia, A., Biomass as renewable feedstock in standard refinery units. Feasibility, opportunities and challenges. *Energy & Environmental Science* **2012,** *5* (6), 7393-7420.

5.   Gallezot, P., Conversion of biomass to selected chemical products. *Chemical Society Reviews* **2012,** *41* (4), 1538-1558.

6.   Bui, V. N.; Laurenti, D.; Afanasiev, P.; Geantet, C., Hydrodeoxygenation of guaiacol with CoMo catalysts. Part I: Promoting effect of cobalt on HDO selectivity and activity. *Applied Catalysis B: Environmental* **2011,** *101* (3-4), 239-245.

7.   Bui, V. N.; Laurenti, D.; Delichère, P.; Geantet, C., Hydrodeoxygenation of guaiacol: Part II: Support effect for CoMoS catalysts on HDO activity and selectivity. *Applied Catalysis B: Environmental* **2011,** *101* (3), 246-255.

8.   Centeno, A.; Laurent, E.; Delmon, B., Influence of the Support of CoMo Sulfide Catalysts and of the Addition of Potassium and Platinum on the Catalytic Performances for the hydrodeoxygenation of Carbonyl, Carboxyl, and Guaiacol-Type Molecules. *Journal of Catalysis* **1995,** *154* (2), 288-298.

9.   Gong, C. S., Cao, N.J., Du, J., Tsao, G.T, *Ethanol production from renewable resources. Advances in Biochemical Engineering and Biotechnology. 65, 207-241* **1999.**

10.   Tyrone Ghampson, I.; Sepúlveda, C.; Garcia, R.; García Fierro, J. L.; Escalona, N.; DeSisto, W. J., Comparison of alumina- and SBA-15-supported molybdenum nitride catalysts for hydrodeoxygenation of guaiacol. *Applied Catalysis A: General* **2012,** *435-436*, 51-60.

11.   Sepúlveda, C.; Leiva, K.; García, R.; Radovic, L. R.; Ghampson, I. T.; DeSisto, W. J.; Fierro, J. L. G.; Escalona, N., Hydrodeoxygenation of 2-methoxyphenol over Mo2N catalysts supported on activated carbons. *Catalysis Today* **2011,** *172* (1), 232-239.

12.   Calvo-Flores, F. G. D., J. A. , Lignin as Renewable Raw Material, *ChemSusChem* **2010,** *3*, 1227–1235.

13.   Kamm, B., Gruber P.R., Kamm M., *Biorefineries (editors) – Industrial processes and products, Wiley- VCH,* **2006**.

14.   *Bulletin of Romania chemical engineering society* **2015,** *2* (2).

15.   T. J. McDonough, T., **1993**, 186–193.

16.   J. Lora, M. N. B., A. Gandini *Eds. Elsevier: New York* **2008,** 225-241.

17.   J. Lora, M. N. B., A. Gandini, *Eds. Elsevier: New York* **2008**, 225-241.

18.   P. Kumar, D. M. B., M. J. Delwiche, P. Stroeve, *Ind. Eng. Chem. Res.* **2009**, 3713–3729.

19.   A. Abacherli, F. D., *U.S. Patent No. 6239198* **2001**.

20.   J.E. Holladay, J. J. B., J.F. White, D. Johnson, *Pacific Northwest National Laboratory and the National Renewable Energy Laboratory* **2007**.

21.   D. Meier, R. A., O. Faix *Bioresour. Technol.,* **1992,** *40*, 171-177.

22.   C. A. Mullen , A. A. B., *Fuel Process. Technol.* **2010,** *91*, 1446-1458.

23.   A. Gutierrez, R. K. K., M. L. Honkela, R. Siloor , A. O. I. Krause, *Catal.Today* **2009**, 239-246.

24.   D. Y. Hong, S. J. M., P. K. Agrawal, C. W. Jones, *Chem. Commun* **2010**, 1038–1040.

25.   C. Zhao, Y. K., A. A. Lemonidou, X. B. Li, J. A. Lercher *Angew.Chem.Int. Ed.* **2009**, 3987–3990.

26.   R. C. Runnebaum, T. N., D. E. Block, B. C. Gates, *Catal. Lett.* **2011**, 817–820.

27.   T. Nimmanwudipong, R. C. R., S. E. Ebeler, D. E. Block, B. C.Gates, *Catal. Lett.* **2012**.

28.   M. A. Gonzalez-Borja and D. E. Resasco, *Energy Fuels* **2011**, 4155–4162.

29.   E. Dorrestijn, L. J. J. L., I. W. C. E. Arends and P. Mulder, *J. Anal.Appl. Pyrolysis* **2000**, 153–192.

30.   A. Yamaguchi, N. H., O. Sato and M. Shirai, *Top. Catal.* **2012**, 889–896.

31.   G. P. van der Laan, A. B., *Catal. Rev. Sci. Eng.* **1999**, 255-318.

32.   P. J. A. Tijm, F. J. W. a. D. M. B., *Appl. Catal., A* **2001**, 275-282.

33.   F. L. P. Resende, S. A. F., M. J. Berger and P. E. Savage, *Energy Fuels* **2008**, 1328–1334.

34.   A. Farzaneh, T. R., E. Sklavounos,A. A. van Heiningen *BioResources* **2014**, 3052−3063.

35.   Huber, Y. C. L. a. G. W., *Energy Environ. Sci.* **2009**, 68-80.

36.   T. Sato, M. O., M. Watanabe, M. Shirai , K. Arai, *Ind. Eng. Chem. Res.* **2003,** *42*, 4277-4282.

37.   T. Minowa, F. Z., T. Ogi *J. Supercrit. Fluids,* **1998** *13*, 253-259.

38.   P. J. Deuss, M. S., F. Tran, N. J. Westwood, J. G. d. Vries and K. Barta, *J.Am. Chem. Soc. Rev.* **2015**, 7456−7467.

39.   M. M. Hepditch , R. W. T., *Can. J. Chem. Eng.* **2000**, 226–231.

40.   S. Constant, C. B., C. Dumas, F. Di Renzo, Robitzer, A. M.; Barakat,F.Quignard *Ind. Crops Prod.* **2015,,** , 180−189.

41.   R. W. Thring, S. P. R. K. a. N. N. B., *Fuel Process. Technol.*

 2000, 17−30.

42.   A. K. Deepa, P. L. D., *RSC Advances* **2014,** *4*, 12625.

43.   A. K. Deepa , P. L. D., *ACS Catalysis* **2015,** *5*, 365-379.

44.   H. X. Ben , A. J. R., *RSC Adv.* **2012**, 12892−12898.

45.   S. K. Singh , P. L. D., *Green Chemistry* **2016,** *18*, 4098-4108.

46.   B. J. Cox , J. G. E., *Bioresour.Technol.* **2012**, 584−588.

47.   J. Papadopoulos, C. L. C. a. I. S. G., *Holzforschung* **981**, 283−286.

48.   T. H. Kim, K., *J. Chem. Eng.* **2011**, 2156−2162.

49.   U. Wongsiriwan, Y. N., C. S. Song, P. Prasassarakich, Y. Yeboah, *Energy Fuels* **2012**, 3232−3238.

50. M. Meshgini , K. V. S., Holzforschung **1989**, 239−243.

51. T. R. Varga, Z. F., Y. Ikeda, H. Tomiyasu *J. Supercrit. Fluids* **2002**, 163−167.

52. Deepa, A. K., Dhepe, P. L., *RSC Adv* **2014,** *4*, 12625-12629.

53. Deepa, A. K., Dhepe, P. L. , *U.S. 0302796 A1, November 29, 2012.* **November 29, 2012**.

54. V. M. Roberts, S. F., A. Lemonidou, X. Li and J. A. Lercher, *Appl. Catal., B* **2010**, 71−77.

55. Z. Yuan, S. C., M. Leitch , C. C. Xu, *Bioresour Technol* **2010,** *101*

9308-9313.

56. J.-M. Lavoie, W. B., M. Bilodeau, *Bioresour. Technol.* **2011**, 4917−4920.

57. V. M. Roberts, V. S., T. Reiner, A. Lemonidou, X. Li, J. A. Lercher, *Chemistry* **2011,** *17*, 5939-5948.

58. N. Mahmood, Z. Y., J. Schmidt and C. C. Xu, *Bioresour. Technol.* **2013**, 13−20.

59. A. Toledano, L. S. a. J. L., *Journal of Chemical Technology &Biotechnology* **2012,** *87*, 1593-1599.

60. J. E. Miller, L. E., A. Littlewolf , D. E. Trudell, *Fuel Process. Technol.* **1999**, 1363−1366.

61. A. Toledano, L. S., J. Labidi, , *Fuel* **2014**, 617−624.

62. J. B. Li, G. H. a. G. G., *Bioresour. Technol.* **2007** 3061-3068.

63. Richa Chaudhary, P. L. D., *Green Chem.* **2017,** *19*, 778-788.

64. T. Yoshikawa, T. Y., S. Shinohara, T. Fukunaga, Y. Nakasaka, T. Tago, T.Masuda, *Fuel Processing Technology* **2013**, 69-75.

65. Q. Song, F. W., J. Cai, Y. Wang, J. Zhang, W. Yu, J. Xu, *Energy & Environmental Science* **2013,** *6*, 994-1007.

66. J. E. E. Miller, L. A. L., D. E. Trudell, *Fuel* **1999**, 1363-1366.

67. E. Minami, H. K., S. Saka *J. Wood Sci.* **2003** 158-165.

68. Z. Fang, T. S., R. L. Smith Jr, H. Inomata, K. Arai, J. A. Kozinski, *Bioresour. Technol.* **2008**, 3424-3430.

69. Wahyudiono, M. S., M. Goto, *Chem. Eng. Process. Process.Intensification* **2008**, 1609-1619.

70. X. Creary, E. D. W., M. Gagnon, *J. Am. Chem. Soc. Rev.* **2005**, 18114−18120.

71. D. Zhao, M. W., Y. Kou, E. Min *Catal. Today* **2002**, 157−189.

72. S. Y. Jia, B. J. C., X. W. Guo, Z. C. Zhang , J. G. Ekerdt *Ind. Eng. Chem.Res.* **2011**, 849−855.

73. S. Jia, B. J. C., X. Guo, Z. C. Zhang and J. G. Ekerdt, *ChemSusChem* **2010**, 1078-1084.

74. C. Z. Li, Q. W., Z. K. Zhao, *Green Chem.* **2008**, 177-182.

75.   B. F. Li, D. S. A., *Ind. Eng. Chem. Res.* **2010**, 3126-3136.

76.   Sandip K. Singha, P. L. D., Ionic liquids catalyzed lignin liquefaction: mechanistic studies using TPO-MS, FT-IR, RAMAN and 1D, 2D-HSQC/NOSEY NMR. *Green Chemistry* **2016,** *18*, 4098-4108.

77.   A. Rahimi, A. A., H. Kim, J. Ralph, S. S. Stahl *J. Am. Chem. Soc.* **2013,** *135*, 6415-6418.

78.   V. E. Tarabanko, N. V. K., A. V. Kudryashev, B. N.Kuznetsov, , *Russ. Chem. Bull.* **1995**, 367–371.

79.   J. C. Villar, A. C., F. Garcia-Ochoa *Wood Sci. Technol.* **2001**, 245–255.

80.   P. C. Rodrigues, E. A. B. d. S., A. E. Rodriguez, *Ind. Eng. Chem.Res.* **2011**, 741-748.

81.   Shabtai, J. S. Z., W.W. Chornet *E. U.S. Pat. No. 5959167* **Sep. 28, 1999.**

82.   J.-M. Lavoie, W. B. a. M. B., *Bioresour. Technol.,* **2011,** *102*, 4917-4920.

83.   V. M. Roberts, V. S., T. Reiner, A. Lemonidou , X. Li, J. A. Lercher, *Chem. Eur. J.,* **2011,** *17*, 5939-5948.

84.   M. R. Sturgeon, M. H. O. B., P. N. Ciesielski, R. Katahira, J. S. Kruger, S. C. Chmely, J. Hamlin, K. Lawrence, G. B. Hunsinger, T. D. Foust, R. M. Baldwin, M. J. Biddy, G. T. Beckham, *Green Chem.,* **2014,** *16*, 824-835.

85.   K. Barta, G. R. W., E. S. Beach, P. T. Anastas, *Green Chem.* **2014**, 191-196.

86.   Cai, Z.; Wang, F.; Zhang, X.; Ahishakiye, R.; Xie, Y.; Shen, Y., Selective hydrodeoxygenation of guaiacol to phenolics over activated carbon supported molybdenum catalysts. *Molecular Catalysis* **2017,** *441*, 28-34.

87.   Deepa, A. K.; Dhepe, P. L., Lignin Depolymerization into Aromatic Monomers over Solid Acid Catalysts. *ACS Catalysis* **2014,** *5* (1), 365-379.

88.   Deepa, A. K.; Dhepe, P. L., Solid acid catalyzed depolymerization of lignin into value added aromatic monomers. *RSC Advances* **2014,** *4* (25), 12625.

89.   Chaudhary, R.; Dhepe, P. L., Solid base catalyzed depolymerization of lignin into low molecular weight products. *Green Chemistry* **2017,** *19* (3), 778-788.

90.   Singh, S. K.; Dhepe, P. L., Ionic liquids catalyzed lignin liquefaction: mechanistic studies using TPO-MS, FT-IR, RAMAN and 1D, 2D-HSQC/NOSEY NMR. *Green Chemistry* **2016,** *18* (14), 4098-4108.

91.   Singh, S. K.; Dhepe, P. L., Isolation of lignin by organosolv process from different varieties of rice husk: Understanding their physical and chemical properties. *Bioresour Technol* **2016,** *221*, 310-317.

92.   Boscagli, C.; Raffelt, K.; Grunwaldt, J.-D., Reactivity of platform molecules in pyrolysis oil and in water during hydrotreatment over nickel and ruthenium catalysts. *Biomass and Bioenergy* **2017,** *106*, 63-73.

93.   Dwiatmoko, A. A.; Kim, I.; Zhou, L.; Choi, J.-W.; Suh, D. J.; Jae, J.; Ha, J.-M., Hydrodeoxygenation of guaiacol on tungstated zirconia supported Ru catalysts. *Applied Catalysis A: General* **2017,** *543*, 10-16.

94.   Hong, Y.-K.; Lee, D.-W.; Eom, H.-J.; Lee, K.-Y., The catalytic activity of Pd/WOx/γ-Al2O3 for hydrodeoxygenation of guaiacol. *Applied Catalysis B: Environmental* **2014,** *150-151*, 438-445.

95.   Liu, S.; Wang, H.; Smith, K. J.; Kim, C. S., Hydrodeoxygenation of 2-Methoxyphenol over Ru, Pd, and Mo2C Catalysts Supported on Carbon. *Energy & Fuels* **2017,** *31* (6), 6378-6388.

96.   Deepa, A. K.; Dhepe, P. L., Function of Metals and Supports on the Hydrodeoxygenation of Phenolic Compounds. *ChemPlusChem* **2014,** *79* (11), 1573-1583.

97.   Lee, H.; Kim, H.; Yu, M. J.; Ko, C. H.; Jeon, J.-K.; Jae, J.; Park, S. H.; Jung, S.-C.; Park, Y.-K., Catalytic Hydrodeoxygenation of Bio-oil Model Compounds over Pt/HY Catalyst. *Scientific Reports* **2016,** *6*, 28765.

98.   Leiva, K.; Garcia, R.; Sepulveda, C.; Laurenti, D.; Geantet, C.; Vrinat, M.; Garcia-Fierro, J. L.; Escalona, N., Conversion of guaiacol over supported ReOx catalysts: Support and metal loading effect. *Catalysis Today* **2017,** *296*, 228-238.

99.   Jung, K. B.; Lee, J.; Ha, J.-M.; Lee, H.; Suh, D. J.; Jun, C.-H.; Jae, J., Effective hydrodeoxygenation of lignin-derived phenols using bimetallic RuRe catalysts: Effect of carbon supports. *Catalysis Today* **2018,** *303*, 191-199.

100.   Güvenatam, B.; Kurşun, O.; Heeres, E. H. J.; Pidko, E. A.; Hensen, E. J. M., Hydrodeoxygenation of mono- and dimeric lignin model compounds on noble metal catalysts. *Catalysis Today* **2014,** *233*, 83-91.

101.   Ohta, H.; Kobayashi, H.; Hara, K.; Fukuoka, A., Hydrodeoxygenation of phenols as lignin models under acid-free conditions with carbon-supported platinum catalysts. *Chemical Communications* **2011,** *47* (44), 12209-12211.

102.   Olcese, R. N.; Bettahar, M.; Petitjean, D.; Malaman, B.; Giovanella, F.; Dufour, A., Gas-phase hydrodeoxygenation of guaiacol over Fe/SiO2 catalyst. *Applied Catalysis B: Environmental* **2012,** *115-116*, 63-73.

103.   Bykova, M. V.; Ermakov, D. Y.; Kaichev, V. V.; Bulavchenko, O. A.; Saraev, A. A.; Lebedev, M. Y.; Yakovlev, V. A., Ni-based sol–gel catalysts as promising systems for crude bio-oil upgrading: Guaiacol hydrodeoxygenation study. *Applied Catalysis B: Environmental* **2012,** *113-114*, 296-307.

104.   Wang, X.; Rinaldi, R., Solvent Effects on the Hydrogenolysis of Diphenyl Ether with Raney Nickel and their Implications for the Conversion of Lignin. *ChemSusChem* **2012,** *5* (8), 1455-1466.

105.   Zhou, M.; Ye, J.; Liu, P.; Xu, J.; Jiang, J., Water-Assisted Selective Hydrodeoxygenation of Guaiacol to Cyclohexanol over Supported Ni and Co Bimetallic Catalysts. *ACS Sustainable Chemistry & Engineering* **2017,** *5* (10), 8824-8835.

106.   Abd Hamid, S. B.; Ambursa, M. M.; Sudarsanam, P.; Voon, L. H.; Bhargava, S. K., Effect of Ti loading on structure-activity properties of Cu-Ni/Ti-MCM-41 catalysts in hydrodeoxygenation of guaiacol. *Catalysis Communications* **2017,** *94*, 18-22.

107.   Zhao, C.; He, J.; Lemonidou, A. A.; Li, X.; Lercher, J. A., Aqueous-phase hydrodeoxygenation of bio-derived phenols to cycloalkanes. *Journal of Catalysis* **2011,** *280* (1), 8-16.

108.   Zhao, C.; Kou, Y.; Lemonidou, A. A.; Li, X.; Lercher, J. A., Highly Selective Catalytic Conversion of Phenolic Bio-Oil to Alkanes. *Angewandte Chemie* **2009,** *121* (22), 4047-4050.

109.   Zhao, C.; Kou, Y.; Lemonidou, A. A.; Li, X.; Lercher, J. A., Hydrodeoxygenation of bio-derived phenols to hydrocarbons using RANEY[registered sign] Ni and Nafion/SiO2 catalysts. *Chemical Communications* **2010,** *46* (3), 412-414.

110.   Zhao, C.; Kasakov, S.; He, J.; Lercher, J. A., Comparison of kinetics, activity and stability of Ni/HZSM-5 and Ni/Al2O3-HZSM-5 for phenol hydrodeoxygenation. *Journal of Catalysis* **2012,** *296*, 12-23.

111.   Mortensen, P. M.; Grunwaldt, J. D.; Jensen, P. A.; Knudsen, K. G.; Jensen, A. D., A review of catalytic upgrading of bio-oil to engine fuels. *Applied Catalysis A: General* **2011,** *407* (1), 1-19.

112.   Yakovlev, V. A.; Khromova, S. A.; Sherstyuk, O. V.; Dundich, V. O.; Ermakov, D. Y.; Novopashina, V. M.; Lebedev, M. Y.; Bulavchenko, O.; Parmon, V. N., Development of new catalytic systems for upgraded bio-fuels production from bio-crude-oil and biodiesel. *Catalysis Today* **2009,** *144* (3), 362-366.

113.   Mortensen, P. M.; Grunwaldt, J.-D.; Jensen, P. A.; Jensen, A. D., Screening of Catalysts for Hydrodeoxygenation of Phenol as a Model Compound for Bio-oil. *ACS Catalysis* **2013,** *3* (8), 1774-1785.

114.   Mortensen, P. M.; Gardini, D.; de Carvalho, H. W. P.; Damsgaard, C. D.; Grunwaldt, J.-D.; Jensen, P. A.; Wagner, J. B.; Jensen, A. D., Stability and resistance of nickel catalysts for

hydrodeoxygenation: carbon deposition and effects of sulfur, potassium, and chlorine in the feed. *Catalysis Science & Technology* **2014,** *4* (10), 3672-3686.

115.   Zhao, C.; Song, W.; Lercher, J. A., Aqueous Phase Hydroalkylation and Hydrodeoxygenation of Phenol by Dual Functional Catalysts Comprised of Pd/C and H/La-BEA. *ACS Catalysis* **2012,** *2* (12), 2714-2723.

116.   Zhao, Z.; Shi, H.; Wan, C.; Hu, M. Y.; Liu, Y.; Mei, D.; Camaioni, D. M.; Hu, J. Z.; Lercher, J. A., Mechanism of Phenol Alkylation in Zeolite H-BEA Using In Situ Solid-State NMR Spectroscopy. *Journal of the American Chemical Society* **2017,** *139* (27), 9178-9185.

117.   Dewar, M. J. S.; Puttnam, N. A., 819. Acid-catalysed rearrangements of alkyl aryl ethers. Part II. Rearrangements in the presence of sulphuric–acetic acid mixtures. *Journal of the Chemical Society (Resumed)* **1959,** (0), 4086-4090.

118.   Ma, Q.; Chakraborty, D.; Faglioni, F.; Muller, R. P.; Goddard, W. A.; Harris, T.; Campbell, C.; Tang, Y., Alkylation of Phenol: A Mechanistic View. *The Journal of Physical Chemistry A* **2006,** *110* (6), 2246-2252.

119.   Bregolato, M.; Bolis, V.; Busco, C.; Ugliengo, P.; Bordiga, S.; Cavani, F.; Ballarini, N.; Maselli, L.; Passeri, S.; Rossetti, I.; Forni, L., Methylation of phenol over high-silica beta zeolite: Effect of zeolite acidity and crystal size on catalyst behavior; *Journal of Catalysis* **2007,** *245* (2), 285-300.

120.   Lee, S. C.; Lee, S. W.; Kim, K. S.; Lee, T. J.; Kim, D. H.; Kim, J. C., O-alkylation of phenol derivatives over basic zeolites. *Catalysis Today* **1998,** *44* (1), 253-258.

121.   Hu, C.; Zhang, Y.; Xu, L.; Peng, G., Continuous syntheses of octyl phenol or nonane phenol on supported heteropoly acid catalysts. *Applied Catalysis A: General* **1999,** *177* (2), 237-244.

122.   Sato, S.; Takahashi, R.; Sodesawa, T.; Matsumoto, K.; Kamimura, Y., Ortho-Selective Alkylation of Phenol with 1-Propanol Catalyzed by CeO2–MgO. *Journal of Catalysis* **1999,** *184* (1), 180-188.

123.   Velu, S.; Swamy, C. S., Selective C-alkylation of phenol with methanol over catalysts derived from copper-aluminium hydrotalcite-like compounds. *Applied Catalysis A: General* **1996,** *145* (1), 141-153.

124.   Schmidt, R. J., Industrial catalytic processes—phenol production. *Applied Catalysis A: General* **2005,** *280* (1), 89-103.

125. Choi, W. C.; Kim, J. S.; Lee, T. H.; Woo, S. I., Balancing acidity and basicity for highly selective and stable modified MgO catalysts in the alkylation of phenol with methanol. *Catalysis Today* **2000,** *63* (2), 229-236.

126. DeCastro, C.; Sauvage, E.; Valkenberg, M. H.; Hölderich, W. F., Immobilised Ionic Liquids as Lewis Acid Catalysts for the Alkylation of Aromatic Compounds with Dodecene. *Journal of Catalysis* **2000,** *196* (1), 86-94.

127. Hajipour, A. R.; Karimi, H., Hexagonal zirconium phosphate nanoparticles as an efficient and recyclable catalyst for selective solvent-free alkylation of phenol with cyclohexanol. *Applied Catalysis A: General* **2014,** *482*, 99-107.

128. Anand, R., Gore, K. & Rao, B., Alkylation of Phenol with Cyclohexanol and Cyclohexene Using HY and Modified HY Zeolites. *Catalysis Letters* **2002,** *81*, 33.

129. Resasco, M. Á. G. B. D. E., Reaction pathways in the liquid phase alkylation of biomass-derived phenolic compounds. *AIChE J.* **2015, ,** *61,* , 598.

130. Vishwanathan, V.; Balakrishna, G.; Rajesh, B.; Jayasri, V.; Sikhwivhilu, L.; Coville, N. J., Alkylation of catechol with methanol to guaiacol over sulphate-modified zirconia solid acid catalysts. *Reaction Kinetics and Catalysis Letters* **2007,** *92* (2), 311-317.

Chapter 2A

Lignin Characterization

2A.1. Introduction

Lignin is mainly comprised of three structural units namely, p-coumaryl, coniferyl, and sinapyl alcohols, those are joined with each other either via ether (C-O-C, β-O-4, α-O-4, 4-O-5) and C–C (β–β, β-5, β-4, 5–5) linkages [1]. Waste produced from the paper and pulp industry is rich in lignin fraction, which could be used for the production of value added chemicals. The global production of lignin in Kraft pulp mills is over 70 Mt·yr^{-1}, primarily in the form black liquor, [2] which is used for the production of electricity [3]. However, lignin is the only potential renewable source for the synthesis of high-volume aromatic compounds for the chemical industry [4, 5]. At present, more than 98% of lignin is burned as a feedstock of energy, mostly in the paper and pulp industry [6-8]. Moreover, some low value applications of lignin are known such as phenolic resins, polyurethane foams, epoxy resins, printed circuit boards, dispersing or emulsifying agents, low-grade-fuel, wood panel products, automotive brakes, etc. [9-11]. The proper utilization of this black liquor generated from paper mills will not only resolve the disposal issue but also will play significant role in the production of aromatic chemicals in biorefinery concept. The heterogeneous molecular structure of lignin creates difficulty in development of depolymerization processes for the production of commercial high-value products from lignin [12]. Different chemical processes, such as pyrolysis, hydrocracking, hydrogenolysis, hydrolysis and oxidation have been used to depolymerize lignin [13-16].

The structure and properties of lignin depend upon different factors such as age/type of plant species, weather, soil nutrients, isolations procedures, etc.[17-20]. Since, in the present work, lignin depolymerization reactions were carried out using real lignin, it is important to characterize lignin before depolymerization reactions to understand their various physico-chemical properties [21-23].

2A.2. Materials

Different types of lignin substrates purchased from commercial sources are summarized in Table 2A.1. and those were used as it is without any further pre-treatment.

Table 2A.1. Summary on the lignin substrates used in the depolymerization study

Sr.No.	Substrate	Mw (KDa)	Supplier	Product code

1	Lignin, Alkaline	60	TCI Chemicals	L0082
2	Lignin, Dealkaline	60	TCI Chemicals	L0045
3	Lignin, Alkali	28	Sigma Aldrich	370959
4	Na-lignosulfonate lignin	52	Sigma Aldrich	471038
5	Industrial -N lignin	-	-	-
6	Industrial -K lignin	-	-	-

Lignin obtained from different sources were characterized using different physico-chemical techniques because it is known from the literature that properties of lignin differ from each other.

2A.3. Lignin characterization methods

Lignins were characterized using different physico-chemical techniques like elemental analysis (C, H, N, S), TGA-DTA, XRD, ICP-OES, SEM-EDAX, ATR, NMR etc.

2A.3.1. CHNS elemental analysis

CHNS elemental analysis is used for the calculation of C, H, N and S present in given organic and inorganic matrices. It is used for the wide variety of samples in different states like solids, liquid, volatile and viscous, in the fields of pharmaceuticals, polymers, chemicals, environment, food and energy. The analysers are constructed in modular form and it is set up in number of different configurations to determine, the varying combination of elements like CHN, CHNS, CNS or N depending on the application. Various range of sample weights can be used from a fraction of a milligram to several grams (macro-systems). CHNS analysis usually carried out at high-temperature in oxygen medium and is based on the classical Pregl-Dumas method [24]. Combustion of substance can be executed in two ways i.e. static and dynamic, in static combustion fixed volume of oxygen, and in dynamic condition constant flow of oxygen is passed over the sample. Often, combustion of catalyst also can be achieved to calculation complete combustion measurement. Elemental analysis studies were done in Thermo Finnigan, Italy; model EA1112 Series Flash Elemental Analyzer. This analyser measures the amount of C, H, N and S in samples by rapid combustion of small amounts (1-2 mg) of the sample in pure O_2 (Dumas method or "flash combustion"). The analysis of all elements in the CHNS group was performed simultaneously. General monomer molecular formula of lignin sample was calculated and expressed as $C_xH_yO_z$ (x = 7-10; y = 5.4-13; z =

3-6.3). The obtained results were correlated with available literature [25, 26] and summarized in Table 2A.2 Except industrial N lignin, other lignin samples contain small amount of sulphur which is the indication of isolation procedure used for lignin i.e. Kraft process. Higher heating value (HHV) and double bond equivalence (DBE) of lignin samples were calculated and summarized in Table 2A.2. Higher heating value showed the amount of heat generated by the combustion of particular fuel. In lignin samples HHV varies between 34-46. Double bond equivalence is expressed as the degree of unsaturation in molecule. In case of benzene and phenol DBE is 4 (considering one for each double bond and one for ring). Except for Na-lignosulfonate lignin, other lignin samples have DBE between 4.5-5.1, which is an agreement of basic monomers unit of lignin (coumaryl alcohol, sinapyl alcohol, coniferyl alcohol) which have DBE number 5 similar to lignin samples.

Table 2A.2. Summary on the elemental analysis of different lignins used in depolymerization studies

Sr. No.	Lignin	Elemental composition (%)				MMF[a]	HHV[b]	DBE[c]
		C	H	O	S			
1	Lignin, Alkaline	52.0	5.0	40.9	2.0	$C_{8.7}H_{9.1}O_{5.1}S_{0.13}$	34.0	4.5
2	Lignin, Dealkaline	65.0	7.0	25.8	0.9	$C_{10}H_{13}O_3S_{0.09}$	36.8	5.1
3	Lignin, Alkali	66.1	7.0	25.9	0.7	$C_{10.}H_{13}O_3S_{0.04}$	34.5	4.5
4	Na-lignosulfo-nate lignin	42.0	5.0	49.3	3.7	$C_7H_{9.1}O_{6.2}S_{0.04}$	46.1	3.4

5	Industrial lignin	-N	32.6	4.9	61.9	-	$C_4H_{7.16}O_{5.72}$	-	1.4
6	Industrial lignin	-K	61.6	5.6	32.8	-	$C_{10}H_{10.81}O_4$	22.9	5.5

(a) MMF –monomer molecular formula

(b) HHV(MJ·kg^{-1})-higher heating value, calculated using Dulong formula,

HHV= 0.3383 x C + 1.442 x (H –O/8) + 9.248 x S

Where C = weight basis % of carbon, H = weight basis % of hydrogen, O= weight basis % of oxygen and S= weight basis % of the sulphur,

(c) DBE – double bond equivalence, calculated using formula

(d) DBE = C- (H/2) + (N/2) + 1

Where C, H and N = number of carbon, hydrogen and nitrogen atoms obtained form MMF

2A.3.2. ICP-OES

Inductively Coupled Plasma-Optical Emission Spectrometry (ICP-OES) is one of the most common techniques for quantitative elemental analysis. It is highly specific with good detection capability of multi-element, hence used in a large variety of applications. All kinds of dissolved samples can be analyzed, including solutions containing high salt concentrations to diluted acids. A plasma source is used to convert elements into its constituent atoms or ions by exciting them to a higher energy level. When it returns to the ground state it emits photons of a characteristic wavelength based on the element present. This emitted light is recorded by an optical spectrometer. Calibration against standards the technique provides a quantitative analysis of the elements present in the sample.

For ICP-OES analysis of lignin samples, SPECTRO ARCOS Germany, FHS 12 instrument was used. The preparation of the samples for ICP analysis was done by following standard protocol, in which 0.5 g of lignin sample was taken in a crucible and then kept in the muffle

furnace. Under air, sample was heated to 650 ºC for 6 h with a ramp rate of 5°C·min^{-1}. It is suggested that during this process, C, H and O will get burned off in the form of CO, CO_2, and CH_4 etc. and in the crucible only unburned residue will remain. This residue was then dissolved in millipore water and subjected to ICP-OES analysis, and obtained results are summarized in Table 2A.3.

Table 2A.3. Summary on the Na concentration present in different lignin samples

Sr. No.	Lignin	Na concentration (mg·g^{-1})
1	Lignin, Alkaline	52
2	Lignin, Dealkaline	29
3	Lignin, Alkali	70
4	Na-lignosulfonate lignin	40
5	Industrial -N lignin	23
6	Industrial -K lignin	-

ICP-OES analysis shows presence of Na metal in the lignin samples. Since these are commercial samples and details on their isolation procedures are not mentioned, it was interesting to know by which method lignins were isolated. Based on the ICP-OES data it is suggested that mostly, Kraft process is used for the isolation of lignin in which Na_2S and NaOH are used as reagent. It is also evident from the data that in case of lignin, dealkaline after isolation of lignin by Kraft method, neutralization might have performed, and hence lower Na content is observed.

2A.3.3. SEM-EDAX analysis

Another technique used to confirm the presence of elements in lignin samples was SEM-EDAX [27, 28]. In this technique, sample is exposed to a source of X-ray, which ejects an electron from inner shell and creates a hole. When an electron from a higher energy shell fills this hole, energy is released in the form of X-rays. These X-rays generated are recorded, which is characteristic

for particular element. The SEM-EDAX analysis of the lignin was performed and presented in Figure 2A.1. using Stereoscan 440 scanning electron microscope Leo Leica Cambridge UK Model, with an electron beam of 5-50 eV. SEM analysis shows irregular pattern of lignin and EDAX analysis is showing presence of sodium (Na) and sulphur element in lignin.

Lignin, Alkaline

(a)

(b)

Lignin, Dealkaline

(c)

(d)

Lignin, Alkali

(e)

(f)

Industrial lignin -N

(g)

(h)
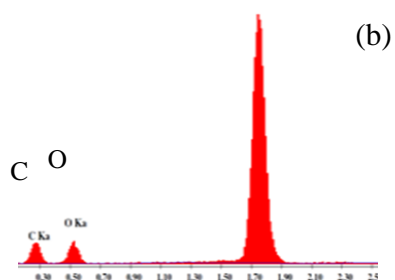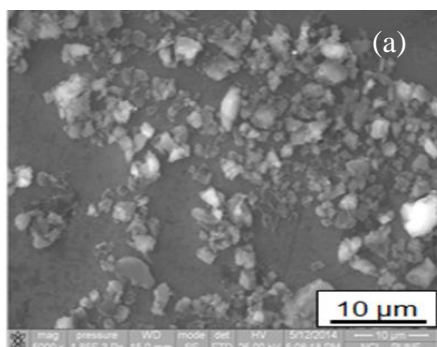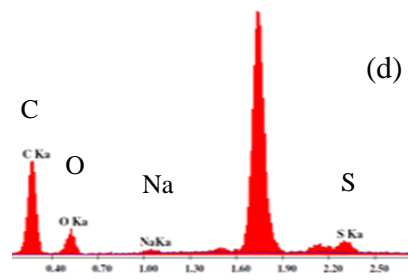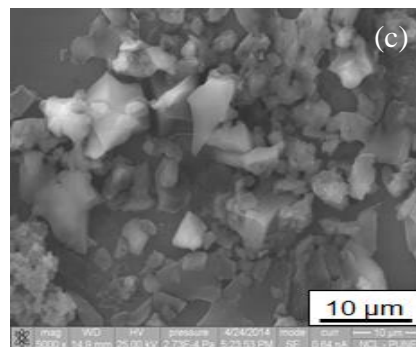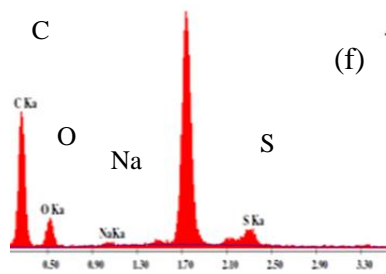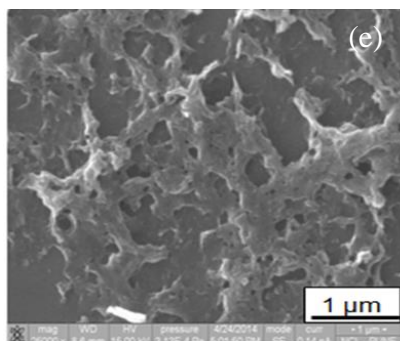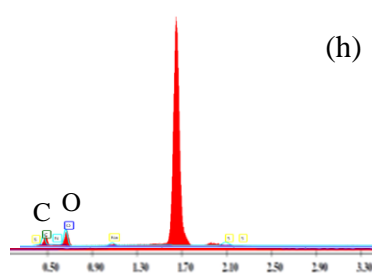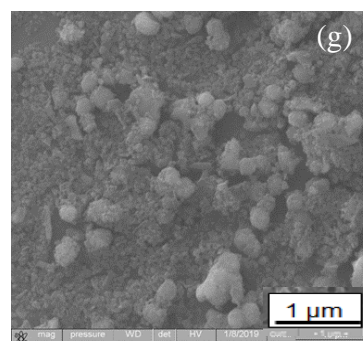
Figure 2A.1. SEM and EDAX analysis of lignin

2A.3.4. FT-IR Spectroscopy

Fourier transform infrared (FT-IR) spectroscopy involves vibration of chemical bonds in a molecule at particular frequencies depending on the elements and types of bonds. After absorption of electromagnetic radiation, the vibration frequency of a bond increases leading to transition between ground state and excited states. These excitations of vibrations of the chemical bonds are specific to the type of bond and the group of atoms involved in the vibration. The energy corresponding to these frequencies are in the range of mid-infrared region (4000–400 cm^{-1}) of the electromagnetic spectrum. The term Fourier transform (FT) refers to the collection of data and conversion of an interference pattern to an infrared absorption spectrum which is like a molecular "fingerprint". IR technique has been widely used for the identification of functional groups in lignin [29-34]. There are about 20 main asymmetric absorption bands, which are typically observed for high molecular weight compounds with irregular structures (eg. lignin). Functional group analysis of lignin was performed using Bruker Optics ALPHA-E spectrometer, USA; with a universal Zn-Se ATR (attenuated total reflection) accessory in the 600-4000 cm^{-1} region and correlated with open source literature [35, 36]. FT-IR analysis of all lignin samples are shown below in Figures 2A.2-3. And Table 2A.4.
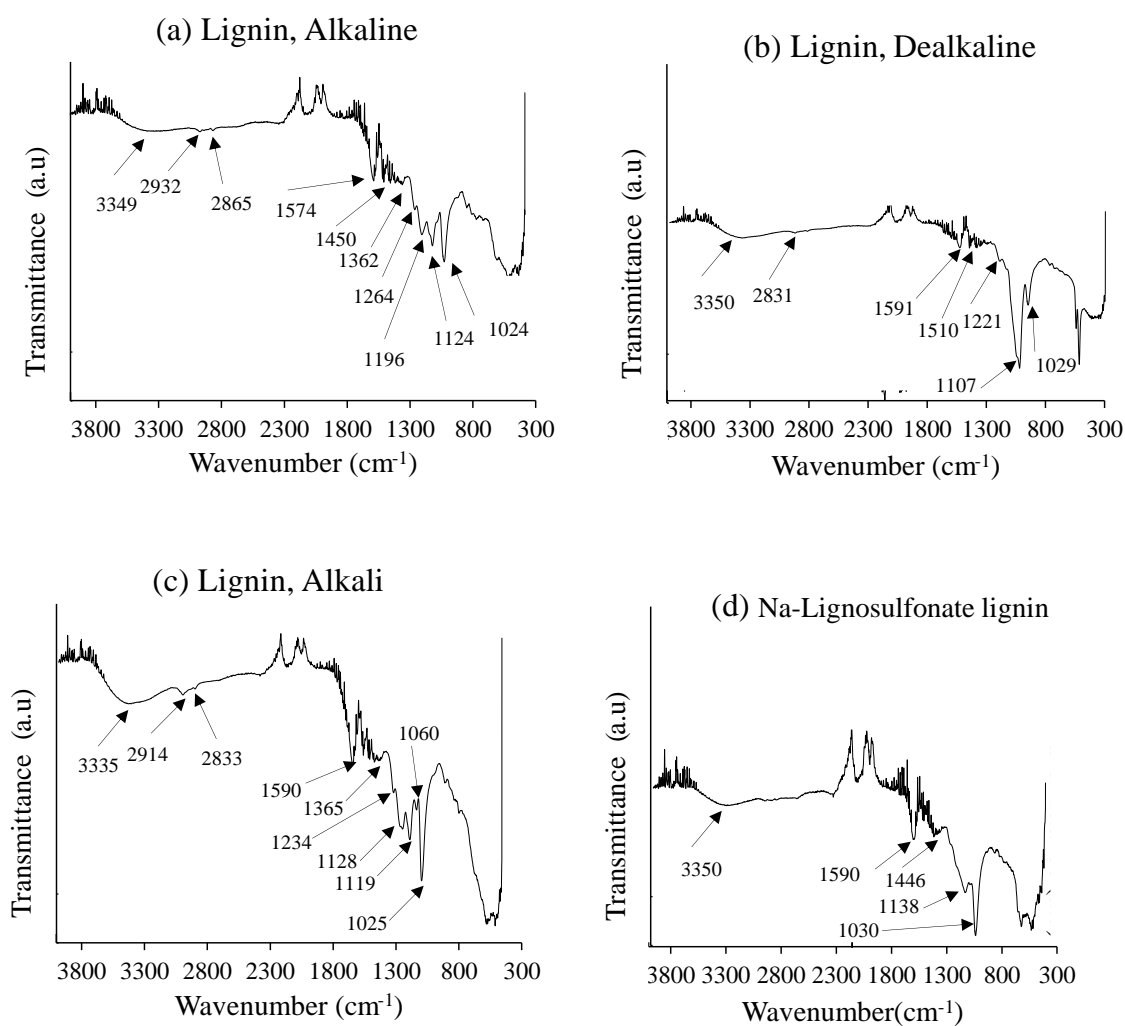
Figure 2A.2. FT-IR spectra of Lignin, (a) Lignin, Alkaline; (b) Lignin, Dealkaline; (c) Lignin, Alkali; (d) Na-Lignosulfonate lignin.
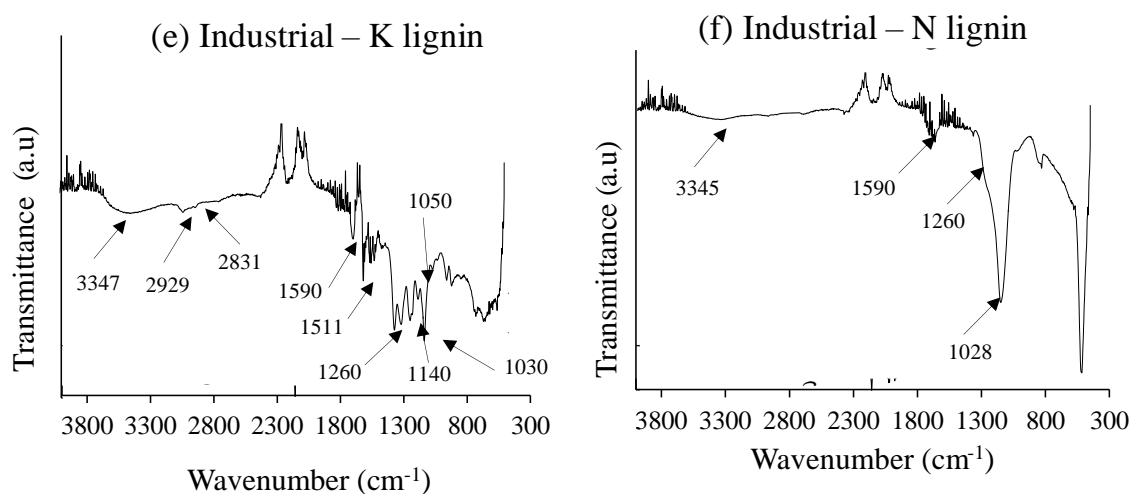
Figure 2A.3. FT-IR spectra of lignin, (e) Industrial -K lignin; (f) Industrial - N lignin

Table 2A.4. Summary on the various functional groups observed in FT-IR of different lignins

Band (cm⁻¹)	Type of vibration	Wavenumber (cm⁻¹) observed in lignin samples					
		Alkali-ne	Alka-li	Dealkali-ne	Na-lignosulfon-ate	Industrial - K	Industrial -N
3500-3100	Alcoholic and phenolic O-H stretching	3349	3335	3350	3350	3347	3345
2970-2830	C-H asymmetric stretching in methyl and	2932, 2833	2914 2833	2831	-	2929 2831	-

	methylene group						
1615-1590	C=O stretching with aromatic skeleton vibrations	-	1590	-	1590	1590	1590
1530-1500	Aromatic skeleton vibrations	1501	-	1510	-	1511	-
1470-1410	Deformation vibration of C-H bond	1450	-	-	1446	-	-
1370-1350	Aliphatic C-H stretching in methyl and phenolic OH	1362	1364	-	-	-	-
1300-1200	C-C, C-O, C=O stretching in guaiacyl units	1264	1234	1221	-	1260	1260
1195-1124	Deoformation	1164	1128	-	1138	1140	-

1030-1010	C-O stretching in alcohol, ether/ in plane deformation vibration of C-H bond in syringyl rings						
	vibration of C-H bond in syringyl rings						
1030-1010	C-O stretching in alcohol, ether/ in plane deformation vibration of C-H bond in aromatic rings	1024	1025	1029	1030	1030	1028

In Table 2A.4 peaks observed in various lignin samples are summarized. Appearance of broad peak between 3500-3100 cm^{-1} in almost all the lignins is due to presence of phenolic and alcoholic groups in lignin. Vibrational band between 2970-2830 cm^{-1} arises due to C-H stretching vibration of methoxy and aldehyde group. Group of bands appears at 1615-1590 cm^{-1}, 1530-1500 cm^{-1} and 1470-1410 cm^{-1} is dedicated to aromatic ring (C-C) vibration and stretching vibration of C=O in syringyl guaiacyl unit. An adsorption band present between 1370-1350 is arises due to stretching vibration of aliphatic –C-H and phenolic –OH. C-H stretching vibration of guaiacyl unit shows band between 1300-1200 cm^{-1} A common but major peak present in all the lignin samples between 1030-1010 cm^{-1} is designated to C-O stretching in ether and alcohol. Presence of an intense peak at 1107 cm^{-1} Lignin, Dealkaline refer to the aromatic in plane C-H deformation. Functional groups present in lignin sample are almost

similar to each other. However, difference in intensity and minimal change in position can be attributed to their slight structural change originated from different plant species and growing environment. Also, it can be due to different extraction processes employed for their isolation.

2A.3.5. Solid state ^{13}C NMR

Similar to the FT-IR analysis,^{13}C NMR analysis of lignin samples were carried out to confirm the aromaticity and functional groups present in the lignin samples. NMR spectra of lignin samples were recorded using Bruker AV300, Germany, operated at 10 kHz and pulse program Cp, av. Various reports are present in which NMR technique is used to confirm the functionality and aromatic nature of lignin.[37] ^{13}C NMR spectra of lignin samples are represented in Figure 2A.5.1- 2A.5.2 and Table 2A.5. Presence of carbonyl (R-CHO) group in lignin sample was confirmed by the peaks at chemical shift between 180-210 ppm. An intense peak appearing at 110-150 ppm resembles sp^2 carbon of alkene and aromatic compound. Presence of peak at chemical shift between 160-180 ppm confirms the presence of (R-CO-OR) ester group. A common intense peak found at 55-56 ppm can be assigned to methoxy group (R-OCH$_3$) linked to aromatic ring. Presence of chemical shift between 55-90 ppm is due to sp^3 carbon directly linked to oxygen atom of (R-CH$_2$-O, R$_1$-C-O, R$_2$-CHO, where R, R$_1$, R$_2$ refers to alkyl and aryl group). Monomer units of lignin such as guiacyl, syringyl and coumrayl alcohol can be identified using NMR chemicals shifts. Presence of basic monomers unit of lignin can be explained based on the chemical shift. Appearance of peak at 115.18 ppm is typically characteristic of guaiacyl unit, and another peak appeared at 114.6 ppm is dedicated to presence of coumaryl alcohol. Presence of syringyl unit can be seen if peak appears at 106.2 ppm. Results of lignin samples obtained using NMR and FT-IR are in good agreement with each other regarding functionality present in the lignin and can be correlated with each other. Both the technique confirms the presence of ether linkages, aromatic nature of lignin, carbonyl compound in lignin samples.

(a) Lignin, Alkaline

(b) Lignin, Dealkaline .

(c) Lignin, Alkali

(d) Na-lignosulfonate lignin.
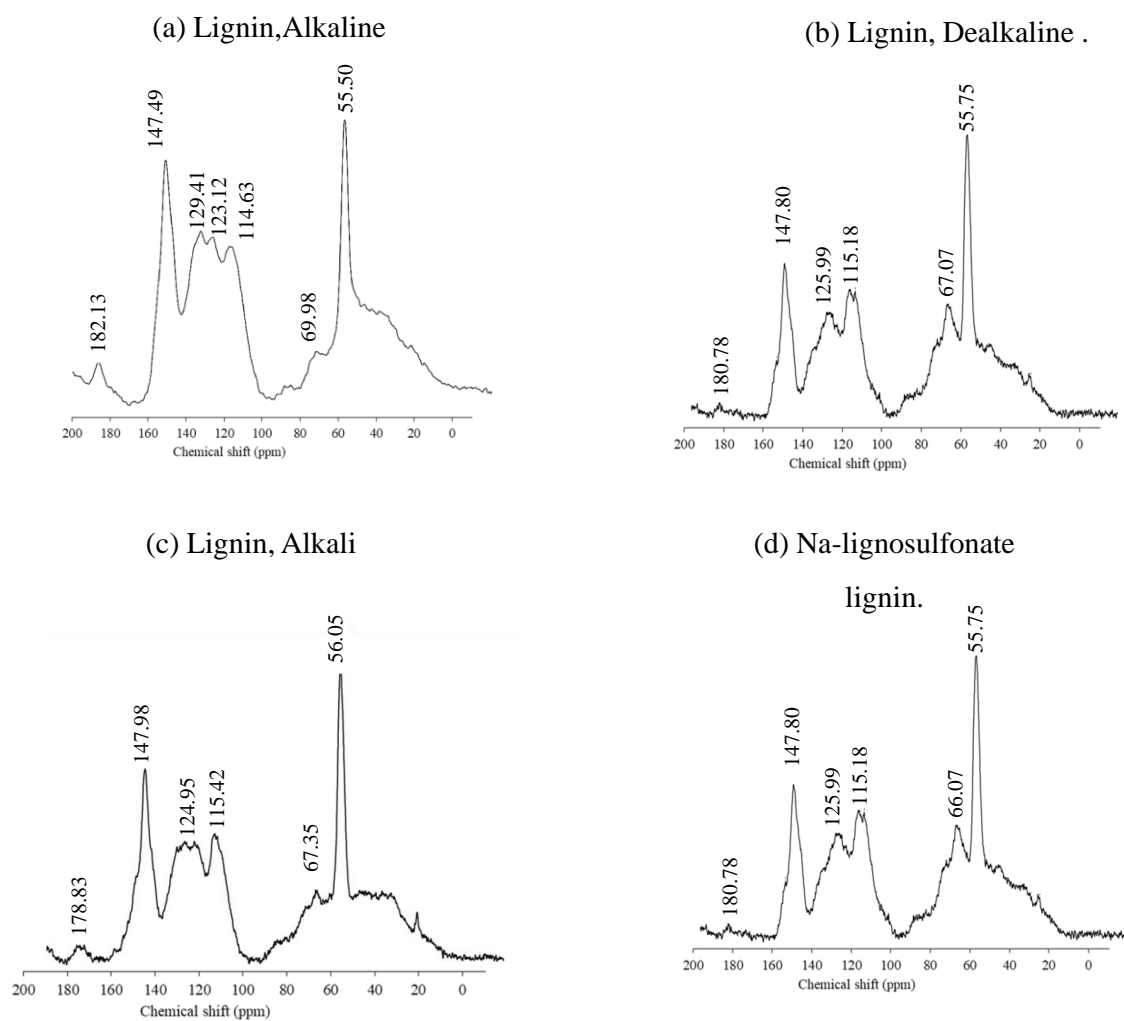
Figure 2A.5.1. Solid state ^{13}C NMR spectra of lignin (a) Lignin, Alkaline; (b) Lignin, Dealkaline (c) Lignin, Alkali (d) Na-Lignosulfonate lignin

(e) Structure units
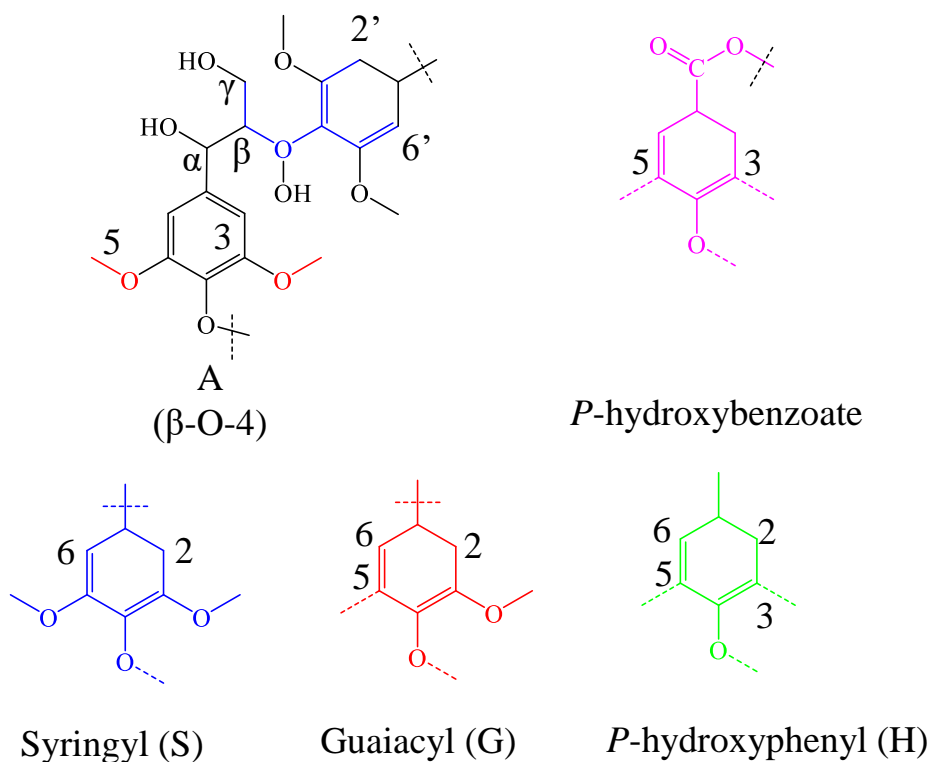
Figure 2A.5.2. Structural unit present in the lignin sample

Table 2A.5. ^{13}C NMR chemical shift summary of lignin

Functional group	Chemical Shift (ppm)			
	Alkaline	**Dealkaline**	**Alkali**	**Na-lignosulfonate**
C=O group in ketone	182.13	180.83	178.83	180.78
C$_3$ and C$_4$ in etherified guaiacyl unit	147.49	147.98	147.98	147.80
C$_{2,6}$ in *p*-hydroxyphenyl units	129.41 123.12	125.95	124.95	125.99
C$_{3,5}$ in *p*-hydroxyphenyl units	114.63	115.42	115.42	115.18
Cγ in β-O-4 substructures	69.98	-	67.35	66.07

C-H in methoxyl group	55.50	55.75	56.05	55.75

2A.3.6. XRD analysis

X Ray diffraction (XRD) technique is used on wide-angle elastic scattering of X-rays is the single most important tool to determine the structure. The XRD patterns are obtained by the measurements of the angles at which the X-ray beam is diffracted by the sample.

Bragg's equation relates the distance between two *hkl* planes *(d)* and angle of diffraction (2θ) as: nλ = 2dSinθ,

where λ = wavelength of X-rays, n = an integer known as the order of reflection (*h, k,* and *l* represent Miller indices of respective planes).

Diffraction patterns provide valuable information regarding the uniqueness of structures, purity, degree of crystallinity and unit cell parameters of the semi crystalline hybrid materials. The identification of phase is based on the comparison of a set of reflections of the sample with that of pure reference phases distributed by International centre for Diffraction Data (ICDD). Unit cell parameter of a cubic lattice can be determined by the following equation:

$$a_0 = d_{hkl}\sqrt{(h^2 + k^2 + l^2)},$$

where d = distance between two consecutive parallel planes having Miller indices *h, k,* and *l*. XRD analysis has been widely used to characterize supported metal crystallites in the nanoscale. The average size of nanoparticles can be calculated using Debye-Scherrer equation:

$$D = k\,\lambda/\,\beta\cos\theta,$$

where D = thickness of the nanocrystal, k is a constant, λ = wavelength of X-rays, β = width at half maxima of reflection at Bragg's angle 2θ.

Powder XRD analysis of lignin was performed using PANanalytical X'pert Pro, Netherlands; with duel goniometer diffractor. The source of X-ray was Cu Kα (1.5418 Å) radiation with Ni filter and sample scanning was done from a 2θ value of 5 to 90 ° at the rate of 4.3 °min⁻1 and presented in the Figure 2A.6. It is known in literature that lignin is amorphous in nature. XRD analysis of lignin samples showed the broad peak between 10-30 ° which is an agreement with the available literature for lignin and the peak is indicates amorphous nature of lignin. The

presence of some sharp peaks in Lignin, Dealkaline are due to presence of impurity (S, Na). Presence of these elements in lignin is also confirmed by ICP-OES and CHNS data. Based on these analysis, it is suggested that the isolation method used to extract lignin is Kraft process.
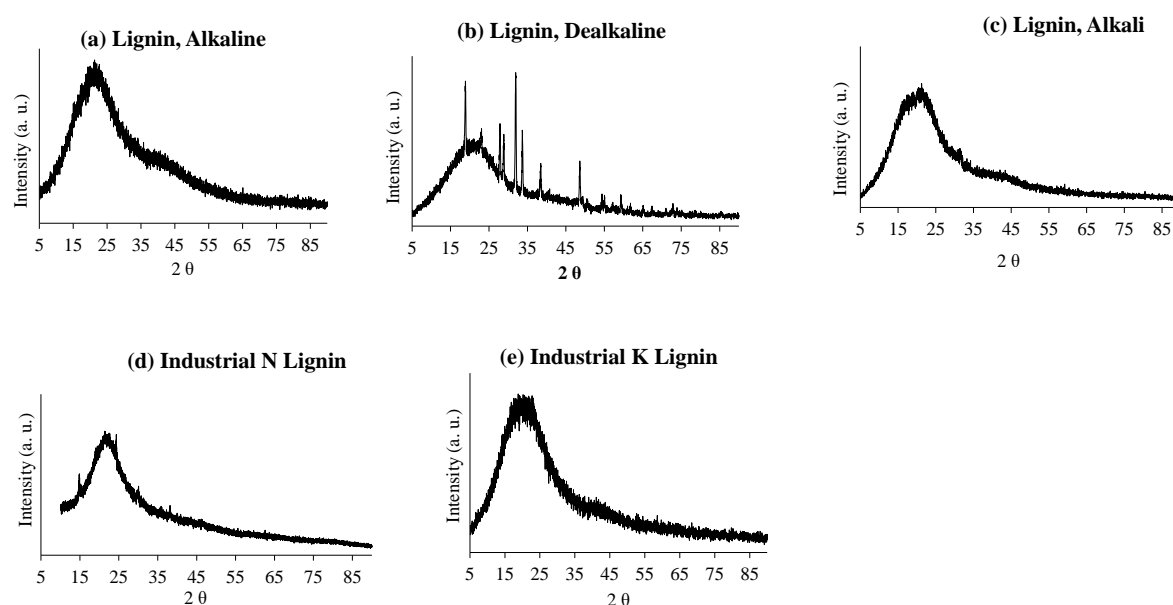
Figure 2A.6. XRD patterns of Lignin samples. (a) Lignin, Alkaline; (b) Lignin, Dealkaline; (c) Lignin, Alkali; (d) Industrial-K lignin; (e) Industrial-N lignin;

2A.3.7. TGA-DTA analysis

Thermogravimetric Analysis-Differential Thermal (TGA-DTA) analysis, used to calculate the change in weight of the sample as a function of temperature or time. TGA-DTA instruments are used to quantify loss of water, loss of solvent, decarboxylation, pyrolysis, oxidation, decomposition etc. occurring at particular temperatures and also the weight % of ash (unburnt residue or inorganics) obtained after the analysis. TGA instrument comprises a sample pan which is supported by a precision balance. Pan is placed in a furnace and is heated or cooled during the experiment. The change in the mass of the sample is checked during the experiment. A sample purge gas is used to control the sample environment. This gas may be inert or a reactive gas (air) which flows over the sample and exits through an exhaust. TGA analysis for lignin samples were studied using METTLER TOLEDO TGA/SDTA851 series, USA; instrument with a heating rate from 25°C to 900 °C at a rate of 10 °C·min^{-1}, to study the

complete decomposition. Thermal degradation studies were done in both N_2 and air atmosphere and presented in Figures 2A.7-8. All lignin samples have shown weight loss below 100 °C due to removal of moisture. Further on increasing the temperature, degradation of lignin was found between 150-400 °C, which is due to weight loss from cleavages of ether linkages followed by aliphatic side chain and then C-C bonds present in lignin. Aromatic moiety present in lignin degraded around 400-650 °C. Observed degradation pattern of lignin samples were compared with available literature and it was found that degradation pattern of lignin samples in both N_2 and air media is matching with available literature[38-41].

(a) Lignin, Alkaline N₂

(b) Lignin, Alkaline Air

(c) Lignin, Dealkaline N₂

(d) Lignin, Dealkaline Air

(e) Lignin, Alkali N₂

(f) Lignin, Alkali air

(g) Na- Lignosulfonate lignin air
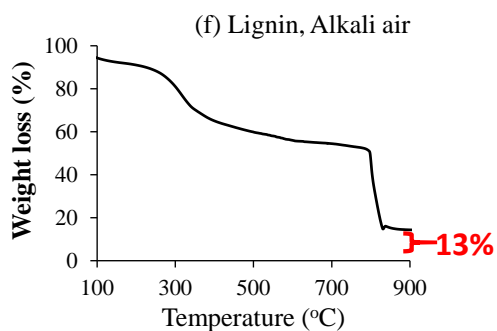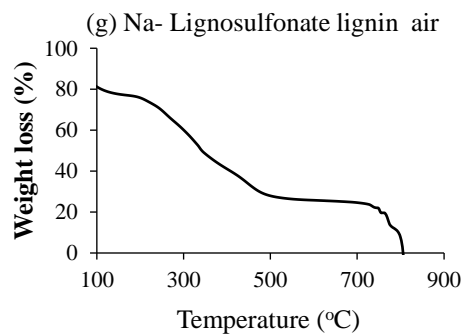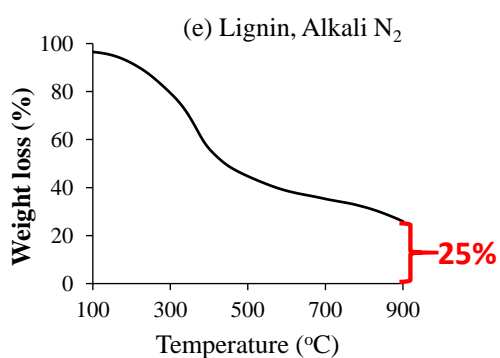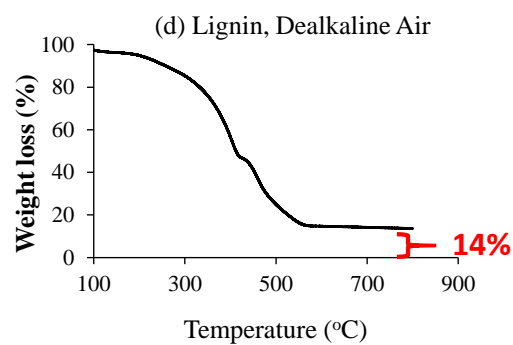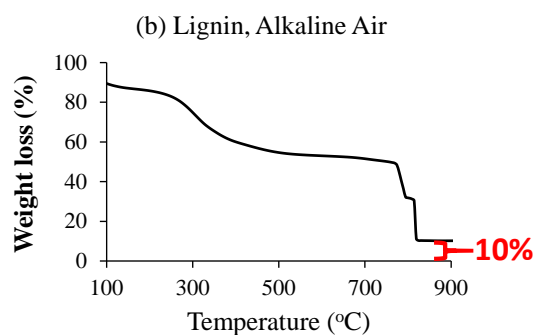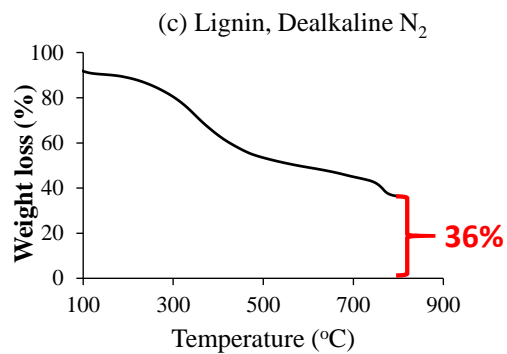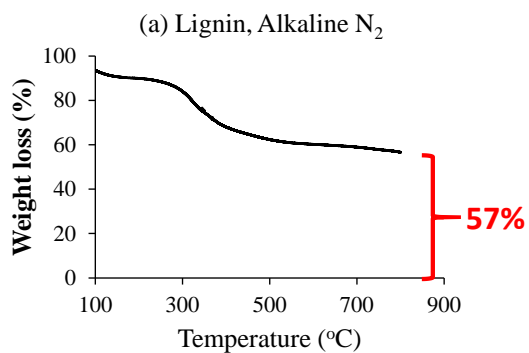
Figure 2A.7. TGA analysis of lignin samples. (a,b) Lignin, Alkaline (N_2 and Air); (c,d) Lignin Dealkaline (N_2 and Air); (e,f) Lignin, Alkali (N_2 and Air); (g) Na-lignosulfonate lignin (Air);
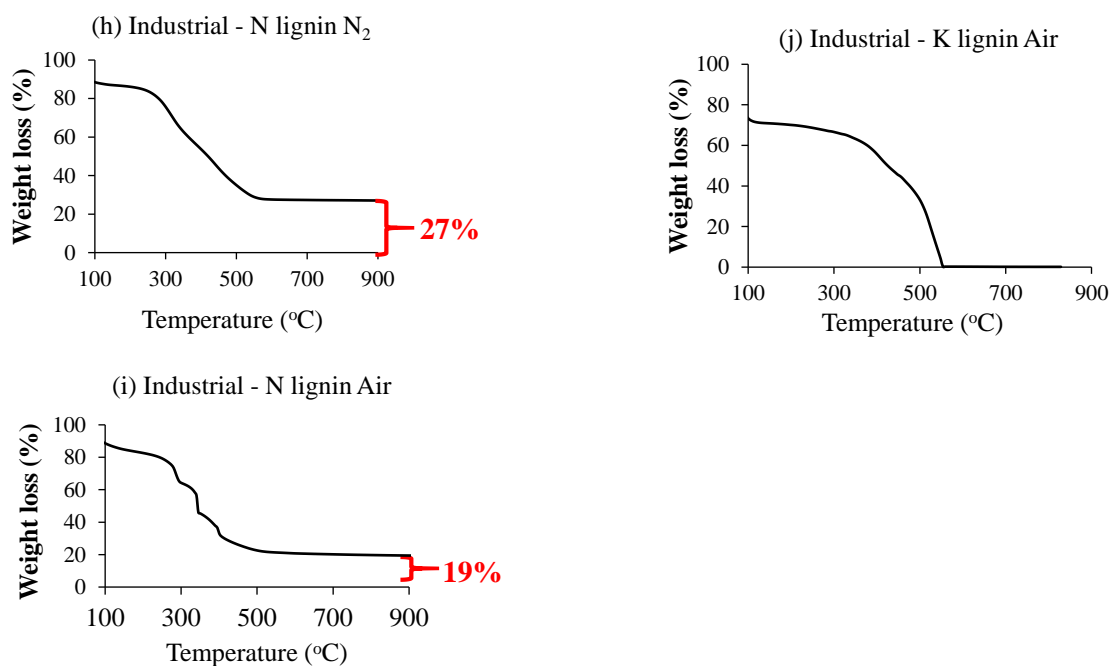
Figure 2A.8. TGA analysis of lignin samples. (h,i) Industrial - N lignin (N_2, Air); (j) Industrial-K lignin (Air);

Another aspect of TGA analysis is high unburnt residue (27-57%) if conducted in N_2 medium. Obtained results can be explained based on the elements (C,H,O) present in lignin. Under inert (N_2) medium, combustion of carbon will occur to form CO, CH_4 as per the availability of oxygen and hydrogen in lignin. It is also possible that insufficient oxygen will increase the unburnt carbon, which is contributing to high residual content. This phenomena was confirmed when TGA analysis was carried out in Air medium in which percentage of inorganic residue (0-10%) is very less compared to TGA done under N_2 medium. It was expected that complete degradation is possible when analysis was conducted in air medium, because lignin is made up of organic elements (C,H,O). Residual content present in lignin samples can be correlated with

EDX and XRD analysis of lignin samples, which shows presence of inorganic element i.e. Na, S in lignin. In air medium, these elements can form their oxide and are not degraded at high temperature.

2A.3.8. Solubility of lignin

Solubility of lignin was checked in different solvents to identify the appropriate reaction solvent to carry out depolymerization reactions and isolation of depolymerized products. Obtain Solubility data is summarized in Table 2A.6. High solubility of lignin in particular solvent will help in depolymerization reaction, however less solubility of lignin in particular solvent will be suitable for the isolation of depolymerized products.

Table 2A.6. Solubility of various lignins in different solvents

Solvent (Polarity Index)	Lignin Solubility (%)					
	Alkaline	Dealkaline	Alkali	Na-lignosulfonate	Industrial -N	Industrial -K
Water (9.0)	100	40	1.6	100	8.0	2.0
Alkaline water (pH, 12.65)	100	100	100	100	100	100
Ethyl acetate (4.4)	1.0	Insol.	0.58	Insol.	2.6	5.5
Tetrahydrofuran (4.0)	2.4	Insol.	12.5	2	5.6	92.0
Diethyl ether (2.8)	0.3	Insol.	0.52	Insol.	Insol.	4.8

Among all the solvents checked for solubility of lignin (Table 2A.6), water was found to be suitable solvent for conducting the depolymerization reactions as maximum solubility was observed in this solvent. More solubility of alkaline and Na-lignosulfonate lignin is also the evidence of its hydrophilic nature while other lignins are hydrophobic in nature. Since lignin is more soluble in water solvent, depolymerization reactions were conducted in water medium, and isolation of depolymerized product was done in diethyl ether and ethyl acetate solvents due to relatively less solubility of lignin in these solvents. It is important to note that lignin depolymerization reactions are performed in alkaline medium and at pH 12.65 lignins were completely soluble in alkaline water.

2A.4. Conclusions

Lignin characterization was completed using different physico-chemical technique like CHNS, XRD, TGA-DTA, NMR, etc., in this study four commercially available lignin along with two industrial lignin are used. Obtained result suggests that properties of lignin are differing from each other. It is due to their origin, age of plant and isolation method sued for separation of lignin. CHNS elemental analysis confirms the presence of carbon (32-66 %), hydrogen (4-7%) along with sulphur impurity. SEM-EDAX and ICP-OES analysis confirms the irregular nature of lignin along with Na and S impurity which is attribution of lignin isolation process (Kraft or Sulphite pulping). Functional group and aromatic nature of lignin samples were investigated using FT-IR and ^{13}C NMR confirm the presence of similar group in all lignin sample with different intensity. TGA-DTA analysis was conducted in both Nitrogen (N_2) and air medium shows difference in thermal degradation pattern and inorganic residue. Irregular and amorphous nature of lignin sample was also confirmed using XRD analysis. While presence of cellulose impurity in dealkaline sample was also confirmed from XRD. Further, solubility of lignin was performed in different solvent and obtained results suggest the use of water as a reaction media for depolymerization reaction and diethyl ether and ethyl acetate for the isolation of depolymerized product.

2A.5. References:

1.   Deuss, P. J. B., Katalin, From models to lignin: Transition metal catalysis for selective bond cleavage reactions. *Coordination Chemistry Reviews* **2016,** *306*, 510-532.

2.   Ferdosian F, Y. Z., Anderson M, Xu C, Synthesis of lignin-based epoxy resins: optimization of reaction parameters using response surface methodology,. *RSC Adv* **2014,** *4* (60), 31745- 31753.

3.   Laurichesse S, A. L., Chemical modification of lignins: Towards biobased polymers. *Prog Polym Sci* **2014,** *39* (7), 1266-1290.

4.   F. Cherubini, A. H. S., *Biofuels, Bioprod. Biorefin.* **2011,** *5*, 548-561.

5.   I. Delidovich, P. J. C. H., L. Deng, R. Pfützenreuter, M. Rose, R. Palkovits, *Chem. Rev* **2015,** *DOI: 10.1021/ acs.chemrev.5b00354.*

6.   J. H. Lora, W. G. G., *J. Polym. Environ* **2002,** *10*, 39-48.

7.   W. Thielemans, E. C., S. S. Morye, R. P. Wool, *J. Appl. Polym. Sci* **2002,** *83*, 323-331.

8.   W. Thielemans, E. C., S. S. Morye and R. P. Wool, *J. Appl. Polym. Sci* **2002,** *83,* , 323-331.

9.   Stewart, D., *Ind. Crops Prod* **2008,** *27*, 202-207.

10.   G. Xu, J. H. Y., H. Mao, Z. Yun, *Chem. Technol.* **2011,** *47*, 283-291.

11.   G. Vazquez, C. R.-B., S. Freire, J. Gonzalez-Alvarez,G. Antorrena, *Bioresour. Technol.* **1999,** *70*, 209-214.

12.   L. Hodásová, M. J., A. Skulcová, A. Ház, *Wood Res.* **2015,** *60*, 973-986.

13.   C. Li, X. Z., A. Wang, G. W. Huber, T. Zhang, *Chem.*

Rev. **2015,** *115*, 11559-11624.

14.   M. P. Pandey, C. S. K., *Chem. Eng. Technol* **2011,** *34*, 29-41.

15.   J. Zakzeski, P. C. B., A. L. Jongerius, B. M. Weckhuysen, *Chem. Rev* **2010,** *110*, 3552-3599.

16.   Q. Yaoa, Z. T., J.h. Guoa, Y. Zhanga, Q.Chin., *J. Chem. Phys* **2015,** *28*, 209-216.

17.   W. Boerjan, J. R., M. Baucher, , *Annu. Rev. Plant Biol* **2003,** *54*, 519-546.

18.   Frei, M., *Sci. World J* **2013,** *2013* (25).

19.   S. K. Singh, P. L. D., *Bioresour. Technol.* **2016,** *221*, 310-317.

20.   J. J. Stewart, T. A., C. Chapple, J. Ralph, S. D. Mansfield, *Plant Physiol.* **2009,** *150*, 621-635.

21.   J. S. Lupoi, S. S., R. Parthasarathi, B. A. Simmons, R. J. Henry, *Renewable Sustainable Energy Rev* **2015,** *49*, 871-906.

22.   S. H. Ghaffar, M. F., *Biomass Bioenergy* **2013,** *57*, 264-279.

23.   J.-X. Sun, X.-F. S., R.C. Sun, P. Fowler, M. S. Baird, *J. Agric. Food Chem* **2003,** *51*, 6719-6725.

24.   Zhang, Y. H. P. D., S.Y.Mielenz, J. R. Cui, J.B. Elander, R. T. Laser, M. Himmel, M. E. McMillan, J. R. Lynd, *Biotechnol. Bioeng* **2007,** *97*, 214-223.

25.   Zakzeski J, B. P., Jongerius AL,W. BM. , *Chem Rev* **2010,** *110*, 3552– 3599

26.   M. D. A. Aresta, F. D., Walter de Gruyter *GmbH &Co KG: Berlin/Boston* **2012,** *446*.

27.   Lin, S. Y. L., I. S. Ullmann's, *Encylcopedia of Industrial Chemistry. 5 ed. ed.; VCH: 1990; Vol. 15, p 305.*

28.   Shabtai, J. S. Z., W.W.Chornet, *Process for conversion of lignin to reformulated hydrocarbon gasoline. U.S. Patent 5,959,167, September 28, 1999.*

29.   Lin, S. Y. L., I. S., Ullmann's Encyclopedia of Industrial Chemistry. 5 ed. ed.; VCH: 1990; Vol. 15, p 305.

30.   Shabtai, J. S. Z., W. W. Chornet, *Process for conversion of lignin to reformulated, partially oxygenated gasoline. U.S. Patent 6,172,272, January 9, 2001.*

31.   Deepa, A. K., Dhepe, P. L. , *U.S. 0302796 A1, November 29, 2012.* **November 29, 2012**.

32.   Holladay, J. E. W., J. F. Bozell, J. J. Johnson, *Top Value Added Chemicals from Biomass: Volume II -Results of Screenings for Potential Candidates from Biorefinery Lignin* **2007**.

33.   Deepa, A. K., Dhepe, P. L., *RSC Adv* **2014,** *4*, 12625-12629.

34.   Kaplan, D. L., *Biopolymers from renewable resources. Springer: Germany*.

35.   G. Gellerstedt, J. L., I. Eide, M. Kleinert, T. Barth, *Energy Fuels* **2008,** *22*, 4240-4244.

36.   G. Zhou, G. T., A. Polle, *Plant Methods* **2011,** *7*, 1-10.

37.   E. A. Capanema, M. Y. B., J. F. Kadla, J. Agric *Food Chem.* **2004**, 1850-1860.

38.   K. Wang, F. X., R. Sun, *Int. J. Mol. Sci* **2010**, 2988-3001.

39.   D. J. Gardner, T. P. S., G. D. McGinnis, **1985**, 85-110.

40.   Balat, M., *Energ. Resour. Part A* **1981**, 620-635.

41.   M. J. Oren, M. M. N., G. D. M. Mackay, *Can., J. Spectrosc* **1984**, 10-12.

Chapter 2B

Synthesis of supported metal catalyst and characterization of supported metal catalyst and solid acid catalyst

2B.1. Introduction

As discussed in Chapter 1, current work is focused on the lignin depolymerization and up-gradation of lignin-derived low molecular weight compound. In view of this, base catalyzed lignin depolymerization was done to obtain low molecular weight compounds, and up-gradation of these low molecular weight compounds was carried out using supported metal catalysts and solid acid catalysts. It is suggested that the bifunctional nature of supported metal catalysts could alter the O/C ratio present in low molecular weight compounds. Solid acids will also alter the oxygen concentration present in the low molecular weight compounds. Two pathways were selected for the up-gradation of lignin-derived low molecular weight compounds.

+ Use of supported metal catalysts in up-gradation of lignin-derived low molecular weight compounds using defunctionalization/HDO pathway
+ Use of solid acid catalysts in the up-gradation of lignin-derived low molecular weight compounds using functionalization/alkylation pathway

The bifunctional nature of supported metal catalysts can catalyze defunctionalization/HDO process by activating molecular hydrogen if an external source of hydrogen is used [1-3]. Metal will also help in the generation of in-situ hydrogen from the hydrogen donor solvent. Solid acid-catalyzed functionalization/alkylation of lignin-derived low molecular weight compound reduces the oxygen content. In view of this, the synthesis of supported metal catalysts was done using wet impregnation process. The commercial solid acid catalyst used for the functionalization process was purchased and used as such [4-6]. Synthesized supported metal catalysts and commercial solid acid catalysts were thoroughly characterized, and catalytic activity was correlated with their morphology. Initially, defunctionalization/HDO of lignin-derived low molecular weight compounds was carried out using (Ru) metal in combination with Al_2O_3 (acidic, basic, and neutral) along with SiO_2 and SiO_2-Al_2O_3 as supports. Different supports were selected based on their nature because it is known that the nature of support alters the selectivity of the product [7]. This study was focused on the partial deoxygenating of lignin-derived low molecular weight compounds. Partial deoxygenation of lignin-derived low molecular weight compound has more industrial importance as compared to complete deoxygenated product. In the current study, guaiacol was used as a model compound because

it has similar functionality, which is present in the lignin. Partial deoxygenation of guaiacol compound produces cyclohexanol and cyclohexanone (KA oil), which is an intermediate product of adipic acid production. So, intentionally it was decided to carry out the reaction with milder acidic support, i.e. Al_2O_3, and compare the activity of this catalyst with more acidic support SiO_2-Al_2O_3, which is known for complete deoxygenation. Later in the study of defunctionalization, reactions were conducted with non-precious metal (Co, Ni) along with modified Al_2O_3 support. Also functionalization of lignin-derived low molecular weight compounds was studied by solid acid catalysts to avoid the use of expensive metal and molecular hydrogen.

2B.2. Syntheses of Ru-metal based supported metal catalysts

2B.2.1. Materials

Various supports such as SiO_2-Al_2O_3, γ-Al_2O_3 (Acidic, Basic, Neutral) and metal precursor, Ruthenium chloride ($RuCl_3 \cdot 3H_2O$) (45-50% Ru) were purchased from Sigma Aldrich, India and used as received.

2B.2.2. Synthesis of catalysts

Ru-based supported metal catalysts were synthesized using the well studied wet impregnation method. Before the synthesis of a catalyst, supports (Al_2O_3, SiO_2, SiO_2-Al_2O_3) were activated at 150 ºC under vacuum for 6 h to remove any moisture adsorbed. In a catalyst synthesis procedure, 2 g of activated support was immersed in 10 mL of water and kept under stirring for 30 min. To this, 2 mL aqueous solution of $RuCl_3$ containing 0.098 mmol of Ru (0.5 wt% Ru/Support) was added dropwise, and the resultant mixture was stirred for 16 h at room temperature. This is followed by the evaporation of water at 60 °C using a rotary evaporator. The powder obtained was dried at 60 °C in the oven for 16 h, followed by vacuum drying at 150 °C for 6 h. Further, this dry powder was reduced under flow of hydrogen (H_2, 10 mL•min^{-1}) for 2 h at 150 °C. Schematic representation of the process is represented in Figure 2B.1 The obtained catalyst was named as Ru(0.5)/Al_2O_3-Aidic. Similar procedure was used to prepare all the catalysts (Ru(0.5)/Al_2O_3-Basic, Ru(0.5)/Al_2O_3- Neutral, Ru(0.5)/SiO_2, Ru(0.5)/SiO_2-Al_2O_3).
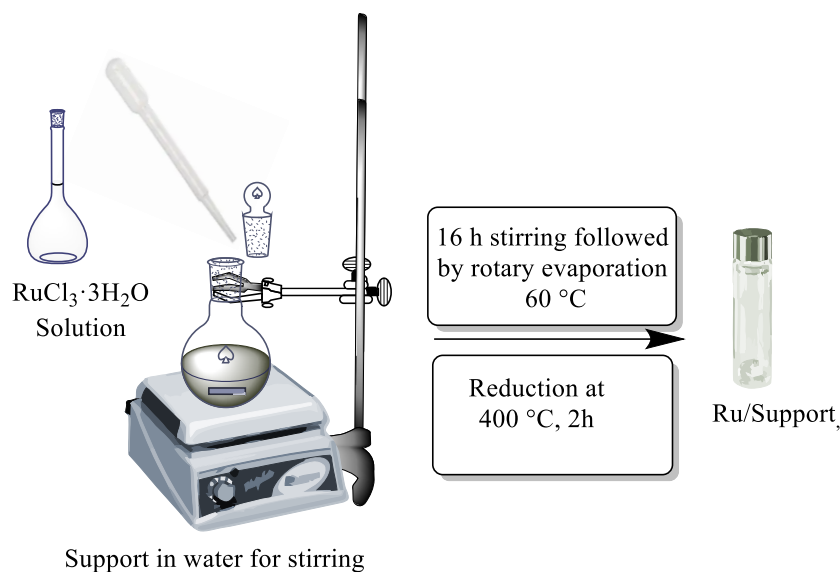
Figure 2B.1. Impregnation of metal on the supports

The synthesized catalysts are enlisted in Tables 2B.1

Table 2B.1. List of Ru based supported metal catalysts

Sr.No.	Catalyst	Metal loading (wt.%)
1	Ru/Al$_2$O$_3$-Basic	0.5
2	Ru/Al$_2$O$_3$-Neutral	0.5
3	Ru/Al$_2$O$_3$-Acidic (commercial)	0.5
4	Ru/Al$_2$O$_3$-Acidic	0.5
5	Ru/SiO$_2$	0.5
6	Ru/SiO$_2$-Al$_2$O$_3$	0.5

All the synthesized catalysts were characterized thoroughly to understand their morphology, and catalyst activity was correlated with their morphologies.

2B.3. Catalyst characterizations

Synthesized supported metal catalysts were characterized using various physico-chemical techniques such as XRD, ICP-OES, TEM, N$_2$-sorption, and NH$_3$/CO$_2$–TPD. Instrumentation and operating principles of XRD and ICP-OES are well explained in Chapter 2A Instrument

details of other techniques used in the characterization of synthesized catalysts such as N_2-sorption, NH_3/CO_2-TPD, CO chemisorption are discussed in the following sections.

2B.3.1. X-Ray diffraction (XRD) analysis

XRD analysis of synthesized catalysts was conducted to confirm the phases of metal and support. XRD patterns of all Ru catalysts are presented in Figure 2B.2. It was seen that besides characteristic peaks for support, no peak for Ru metal and RuOx were observed. This suggests that Ru is well dispersed on the supports. Another reason for the absence of Ru and RuOx peak is very low metal loading (0.5 wt%) on the supports. In the XRD patterns of the Ru/SiO_2 and Ru/SiO_2-Al_2O_3 catalysts broad peak for amorphous nature of support was observed between 12-32 °.
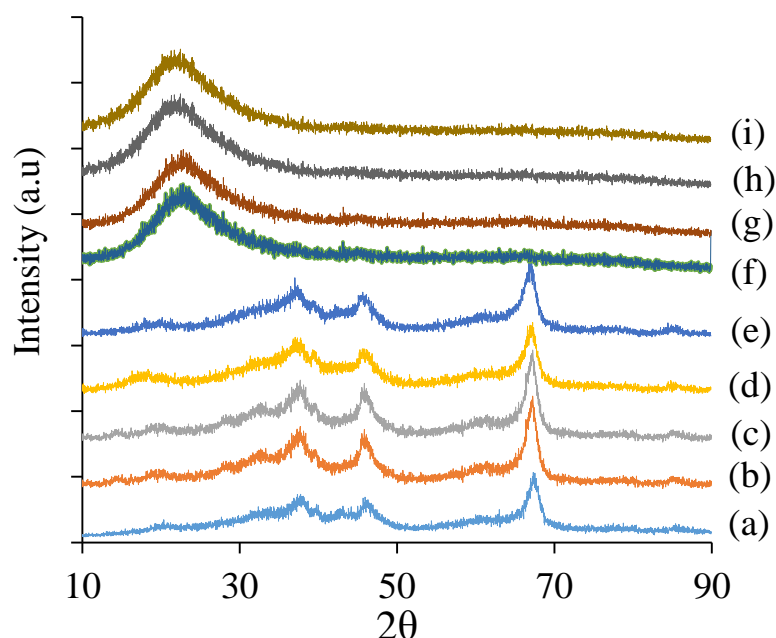
Figure 2B.2. XRD patterns of support and supported Ru catalysts. (a) Al_2O_3; (b) Ru/Al_2O_3-Acidic (commercial); (c) Ru/Al_2O_3-Acidic; (d) Ru/Al_2O_3-Neutral; (e) Ru/Al_2O_3-Basic; (f) SiO_2-Al_2O_3; (g) Ru/SiO_2-Al_2O_3; (h) SiO_2, and (i) Ru/SiO_2;

2B.3.2. N$_2$ Sorption analysis

N_2 sorption analysis is generally used for the determination of surface area and porosity of porous materials. This technique involves exposure of solid material to gases or vapors at

different conditions, and evaluation is done on the basis of uptake of weight or volume of sample. Analysis of these data provides information regarding the physical characteristics of the solid, including porosity, total pore volume (TOPV), and pore size distribution. Nitrogen gas used as the probe molecule is exposed to a solid material during analysis at liquid nitrogen temperature (i.e., 77 K). This gives adsorption isotherms of nitrogen. The surface area is calculated on the basis of measured monolayer adsorption capacity and the cross-sectional area of the molecule being used as a probe. The cross-sectional area of nitrogen is taken as 16.2 Å^2 molecule^{-1}.

The analysis was done in Autosorb iQ Quantachrome, instrument, USA. Before the starting of the analysis, the samples were activated in a vacuum at 250 °C for 3 h. The specific surface area was determined using the BET method, and pore size data was obtained using the BJH method and pore volume using the t-plot method.

The N_2 sorption analysis data for all the synthesized and commercial catalysts are summarized in Table 2B.2 The Ru/SiO$_2$ (305 m^2•g^{-1}) and Ru/SiO$_2$-Al$_2$O$_3$ (376 m^2•g^{-1}) catalysts showed higher surface area than Ru/Al$_2$O$_3$-Neutral (143 m^2•g^{-1}), Ru/Al$_2$O$_3$-Basic (147 m^2•g^{-1}), Ru/Al$_2$O$_3$-Acidic (142 m^2•g^{-1}) and Ru/Al$_2$O$_3$-Acidic (commercial) (144 m^2•g^{-1}) catalysts owing to the difference in the surface area of respective supports.

Table 2B.2. Summary of nitrogen sorption data

Catalyst	BET surface area (m^2•g^{-1})	Pore volume (V) (cm^3•g^{-1})	Pore radius (nm)
Ru/SiO$_2$	305	0.51	3.35
Al$_2$O$_3$-Acidic	155	0.22	2.51
Ru/Al$_2$O$_3$-Acidic	142	0.22	2.59
Ru/Al$_2$O$_3$-Acidic (commercial)	144	0.22	2.60
Ru/Al$_2$O$_3$-Neutral	143	0.22	2.52

Ru/Al$_2$O$_3$-Basic	147	0.23	2.52
SiO$_2$-Al$_2$O$_3$	374	0.48	3.01
Ru/SiO$_2$-Al$_2$O$_3$	376	0.43	2.29

2B.3.3. ICP-OES analysis

This technique is used for the analysis of metal in trace amounts (in ppm level). It is the type of atomic emission spectroscopy where plasma is used to excite the atoms or ions. After excitation, they emit electromagnetic radiation and goes to the ground state. The wavelength of the emitted radiation is characteristic for a particular element and shows the peak in the spectrum at that particular wavelength. The quantitative analysis of the elements can be done by calibrating the instrument with standard solutions. Metal contents in the catalysts were determined by ICP-OES analysis using SPECTRO ARCOS Germany, FHS 12 instrument. Before analysis, the sample was digested in aquaregia. All ICP-OES samples were diluted with deionized water and filtered (through 0.22 μm syringe filter). The results suggest that except in the case of SiO$_2$ support, experimental loadings are almost similar to that of theoretical loadings (Table 2B.3).

Table 2B.3. Summary on ICP-OES analysis

Catalyst	Theoretical Ru wt%	Experimental Ru wt%
Ru/SiO$_2$	0.50	0.42
Ru/Al$_2$O$_3$-Acidic	0.50	0.49
Ru/Al$_2$O$_3$-Acidic (commercial)	0.50	0.48
Ru/Al$_2$O$_3$-Neutral	0.50	0.45
Ru/Al$_2$O$_3$-Basic	0.50	0.49

Ru/SiO$_2$-Al$_2$O$_3$	0.50	0.49

2B.3.4. Transmission electron microscopy (TEM) analysis

In this technique, highly accelerated beam of electrons with high voltage (200 kV) is focused on the magnetic lens under the vacuum passes through the specimen and transmits the light. Tungsten filament is the source of the electron beam. Transmitted light carries information about the structure of the specimen in the form of an image. The vacuum is applied throughout the whole optical system in order to avoid the scattering of the electron due to the collision of an electron with an air molecule. In the column, to focus the electron beam magnetic coils are fixed. Which works as an electromagnetic condenser lens. Before analysis, the specimen stained with an electron-dense material and is placed in the vacuum. TEM images were obtained using FEI TECNAI T20 model instrument, working at an accelerating voltage of 200 kV. Samples were dispersed in isopropyl alcohol (IPA) by sonication and the drop casted on carbon-coated copper grid.

From the TEM images of Ru/Al$_2$O$_3$-Acidic (Figure 2B.3), it is seen that Ru particles with an average size of 3-5 nm are well dispersed on the support. The similar trend was found with other Al$_2$O$_3$ supported (Basic and Neutral) catalysts as seen from Figure 2B.4 With a change of support to SiO$_2$, the average particle size of metal was 10-14 nm, and with SiO$_2$-Al$_2$O$_3$ support, it was 7-11 nm (Figure 2B.5).
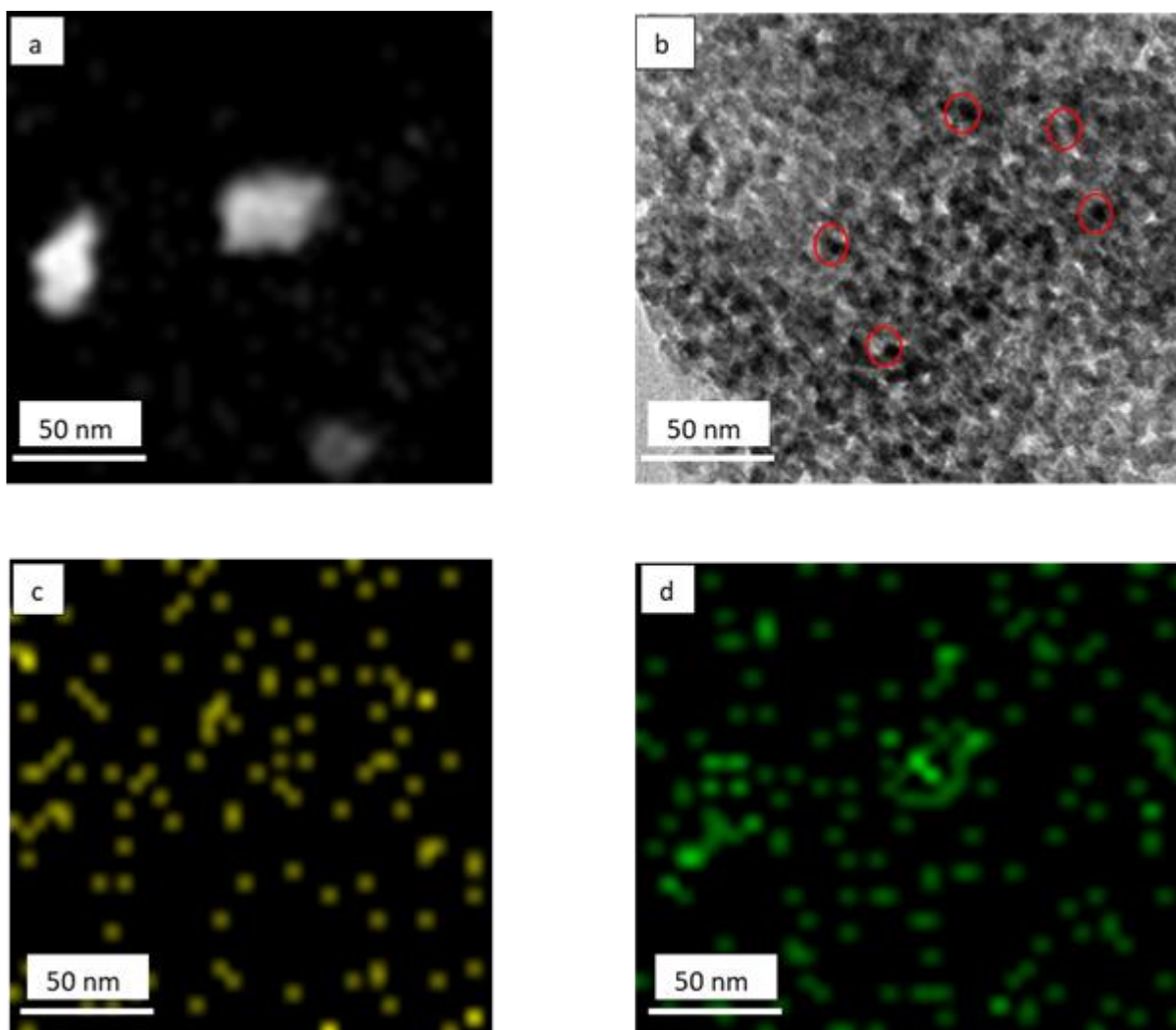
Figure 2B.3. (a) HAADF-STEM; (b) TEM; (c, d) EDX Elemental mapping of

Ru/Al$_2$O$_3$-Acidic;
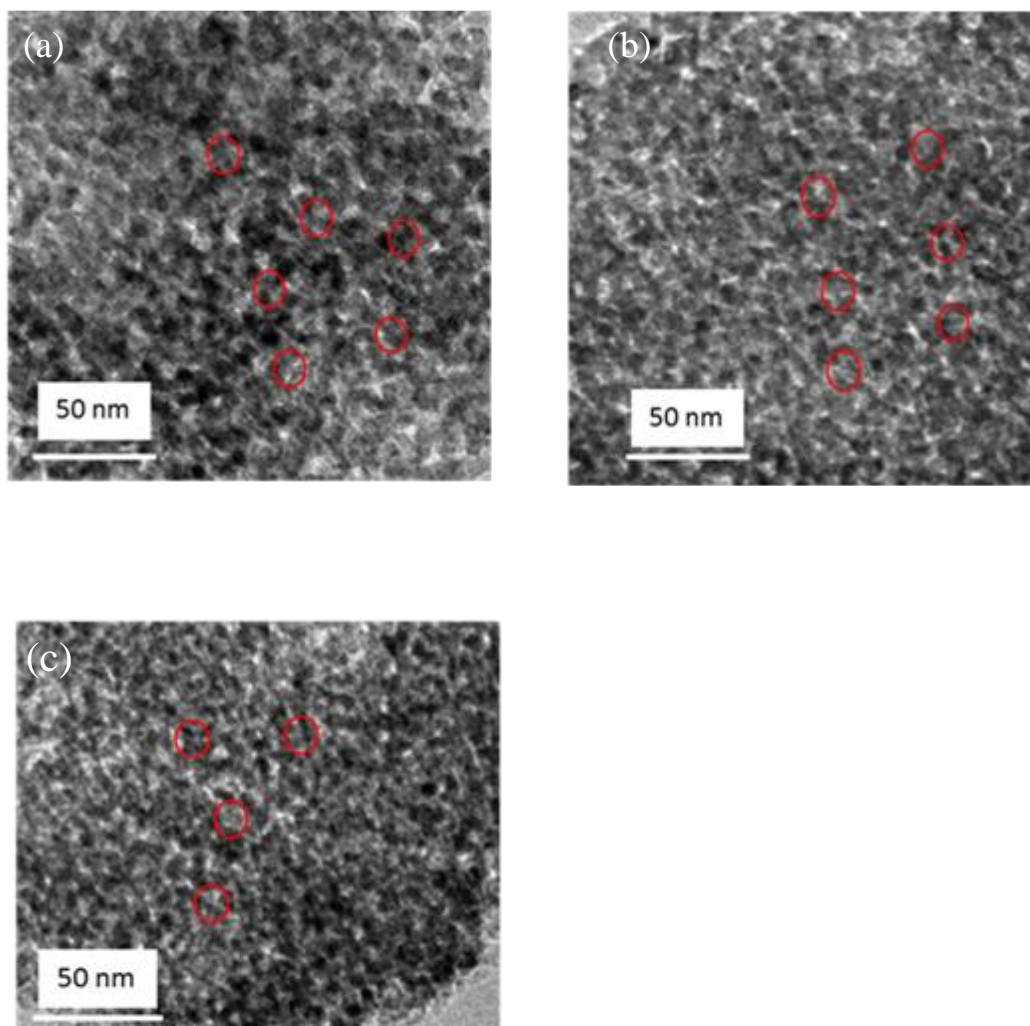
Figure 2B.4. TEM images of (a) Ru/Al_2O_3-Acidic; (b) Ru/Al_2O_3-Basic; (c) Ru/Al_2O_3-Neutral;
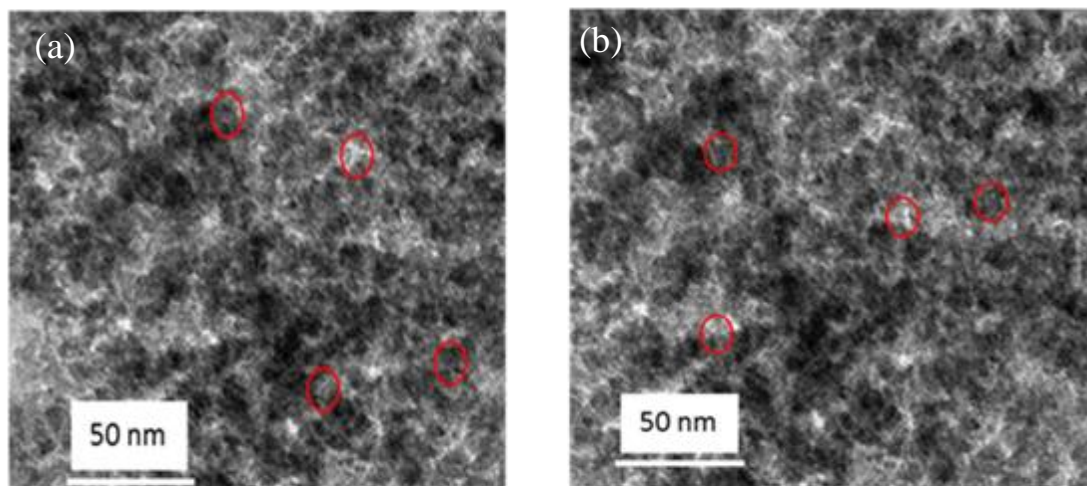
Figure 2B.5. TEM images of (a) Ru/SiO$_2$; (b) Ru/SiO$_2$-Al$_2$O$_3$;

2B.3.5. CO chemisorption

Ru metal dispersion was determined through CO chemisorption using Quantachrome Autosorb-iQ instrument. Prior to the sorption experiment, samples were in-situ reduced in H$_2$ at 150 ^{o}C for 2 h. Subsequently, samples were evacuated for 2 h at the same temperature and later were cooled to 50 ^{o}C under vacuum to record CO adsorption isotherm. The isotherm included both the physisorption and chemisorption portion. Chemisorbed CO uptake was determined by extrapolating the linear portion of isotherm to zero pressure. The dispersion of Ru metal was calculated assuming linear adsorption of CO on the metal surface.

CO chemisorption studies of synthesized catalysts are summarized in Table 2B.4 For Ru/SiO$_2$ catalyst, the volume of chemisorbed CO was 5.6 μmol•g^{-1}, which indicates 11.4% dispersion of Ru with 11.8 nm of the particle size of Ru. In the case of Al$_2$O$_3$ supported Ru catalysts, dispersion of Ru was in the range of 59 to 72% with an average particle size in the range of 1.84 to 2.27 nm, respectively which essentially reflects the fact that dispersion is almost similar, and we can compare the activity of these catalysts with each other. The Ru/SiO$_2$-Al$_2$O$_3$ catalyst showed 44% dispersion with 3.05 nm of particle size. The particle size determined from CO chemisorption data is in line with the particle size calculated from TEM images.

Table 2B.4. CO chemisorption results for supported Ru catalysts

Catalyst	Average crystallite size (nm)	Metal dispersion (%)	Monolayer uptake ($\mu mol \cdot g^{-1}$)
Ru/SiO$_2$	11.8	11.4	5.6
Ru/Al$_2$O$_3$-Acidic	1.86	70	35
Ru/Al$_2$O$_3$-Acidic (commercial)	1.84	72	35.8
Ru/Al$_2$O$_3$-Neutral	2.18	61	30.3
Ru/Al$_2$O$_3$-Basic	2.27	59	29.1
Ru/SiO$_2$-Al$_2$O$_3$	3.05	44	21.6

2B.3.6. Determination of reducibility of metal

The Temperature Programme Reduction (TPR) studies were done using Micromeritics Autochem-2920 instrument in the temperature range of 50–800 °C in the presence of 5% H$_2$ in He with a ramping rate of 5 °C $\cdot$min^{-1}. The catalyst was treated at 300 °C for 1 h in the presence of He gas before the TPR analysis. The measurement of H$_2$ consumption in the TPR analysis was done by a thermal conductivity detector (TCD) detector. TPR study reveals that Ru was reduced at very low temperature of 85 °C (Figure 2B.6), possibly due to very low loading of metal (0.5 wt%) on the support and very high dispersion (72%, Table 2B.4) observed.
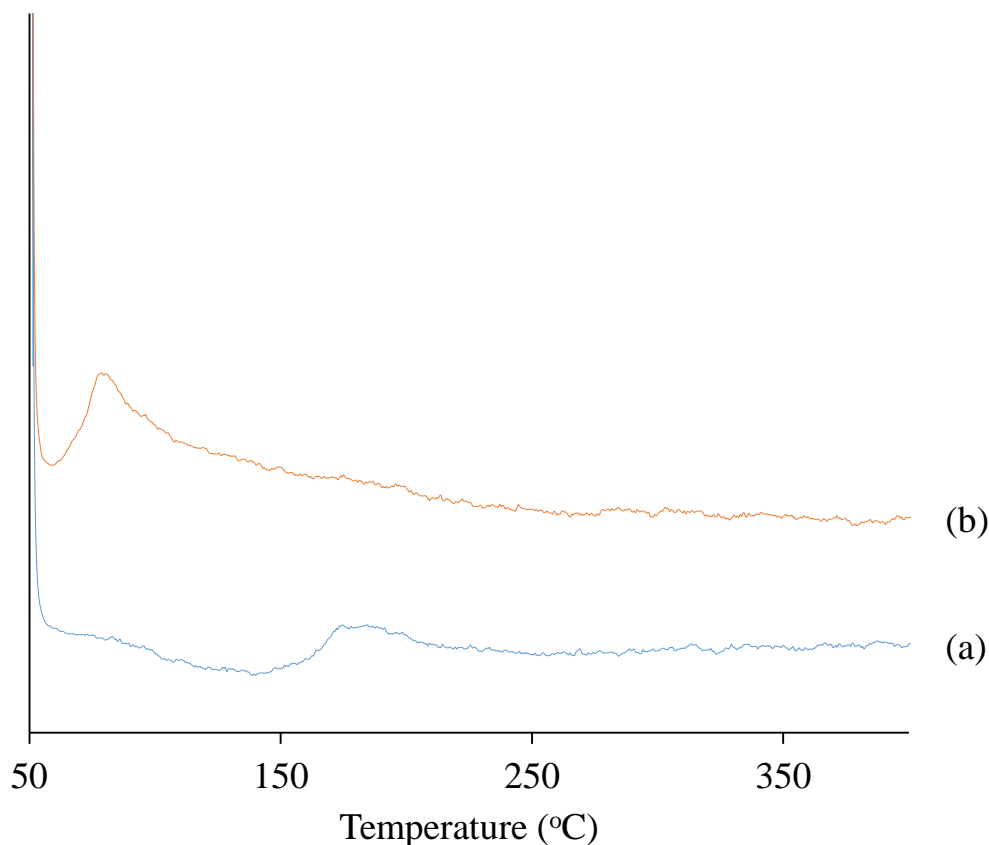
Figure 2B.6. TPR of support and supported Ru metal catalyst (a) Al_2O_3, (b) Ru/Al_2O_3-Acidic

2B.3.7. XPS analysis

It is also known as electron spectroscopy and used to provides the oxidation state of the element present on the surface of the material being studied. The average depth of XPS measurement analysis is approximately 5 nm. It can provide spectrum with a lateral spatial resolution as small as 7.5 μm. Spatial distribution information can be obtained by scanning the micro-focused X-ray beam across the sample. In this technique, the surface of a sample is excited by mono-energetic Al kα X-rays, which results in photoelectrons ejection from the sample surface. The energy of the emitted photoelectrons is measured by an electron energy analyzer. From the binding energy and intensity of a photoelectron peak, the elemental identity, chemical state, and quantity of a detected element can be determined.

The binding energy of the emitted electron is calculated by using the following formula

$$\text{Binding Energy} = E_{x\text{-ray}} - (E_{kinetic} + \Phi)$$

Where,

$E_{X\text{-ray}}$ - Energy of X-ray

$E_{kinetic}$ - Kinetic energy of ejected photoelectron

Φ - Work function depends on spectrometer and material.

XPS spectrum is plotted as binding energy *vs.* intensity, deconvolution of which gives the oxidation state of metal by comparing with reference binding energies. The electronic states of metals were analyzed by X-ray photoelectron spectroscopy (XPS, Perkin-Elmer PH 15000C) having x-ray source Al Kα radiation. The mode of the lens was LAXPS and Energy Step Size 0.1 eV. The peak in the spectrum was deconvoluted by XPSPEAK-41. All binding energy values were calibrated using the value of carbon (C1s= 284.4 eV) as a reference.Ru $3d_{3/2}$ XP spectra was observed to be overlapping with C1s (B.E. = 284.8 eV) (Figures 2B.7-2B.10) and hence no conclusion could be drawn regarding oxidation state of Ru. A small peak observed at B.E. of 279.9 eV can be attributed to the $3d_{5/2}$ level of Ru for Ru metal (0). Since, for RuO_2 species, the peak is typically observed at higher B.E. related to Ru(0), again due to overlapping of the broad peak for C1s, no conclusions could be drawn. Subsequently, XPS measurements for Ru were done at 3P level. The spectrum was deconvoluted with two peaks, peak observed at B.E. of 461.2 eV indicated the presence of Ru(0), and the peak at B.E. of 463.7 eV implied presence of RuO_2 species [8].

C1s and Ru 3d3/2

B. E. = 284.3eV, Ru/RuOx

Ru 3d5/2

B. E. = 279.9 eV, Ru(0)

B.E. (eV)

Ru 3p5/2, B. E. = 461.2

Ru 3p5/2, B. E. = 463.7 RuO2

B.E. (eV)
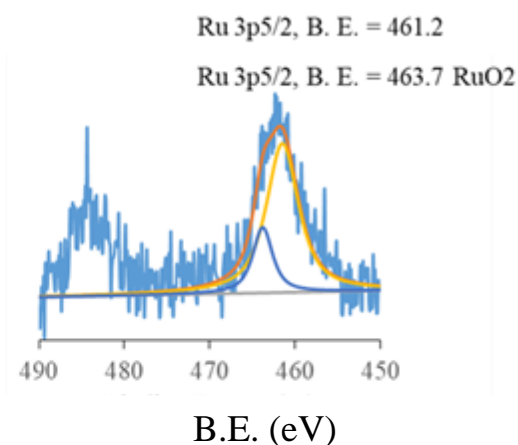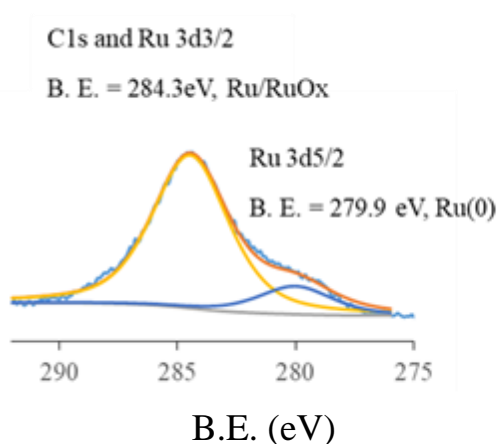
Figure 2B.7. Deconvoluted XPS spectra of Ru/Al$_2$O$_3$-Acidic catalyst

3p5/2, B. E. = 460.9 Ru(0)

3p5/2, B. E. = 462.9 RuO$_2$

C1s and Ru 3d3/2

B. E. =284.3, Ru/RuOx

3d5/2

B. E. =280.1, Ru(0)

B.E. (eV)

B.E. (eV)
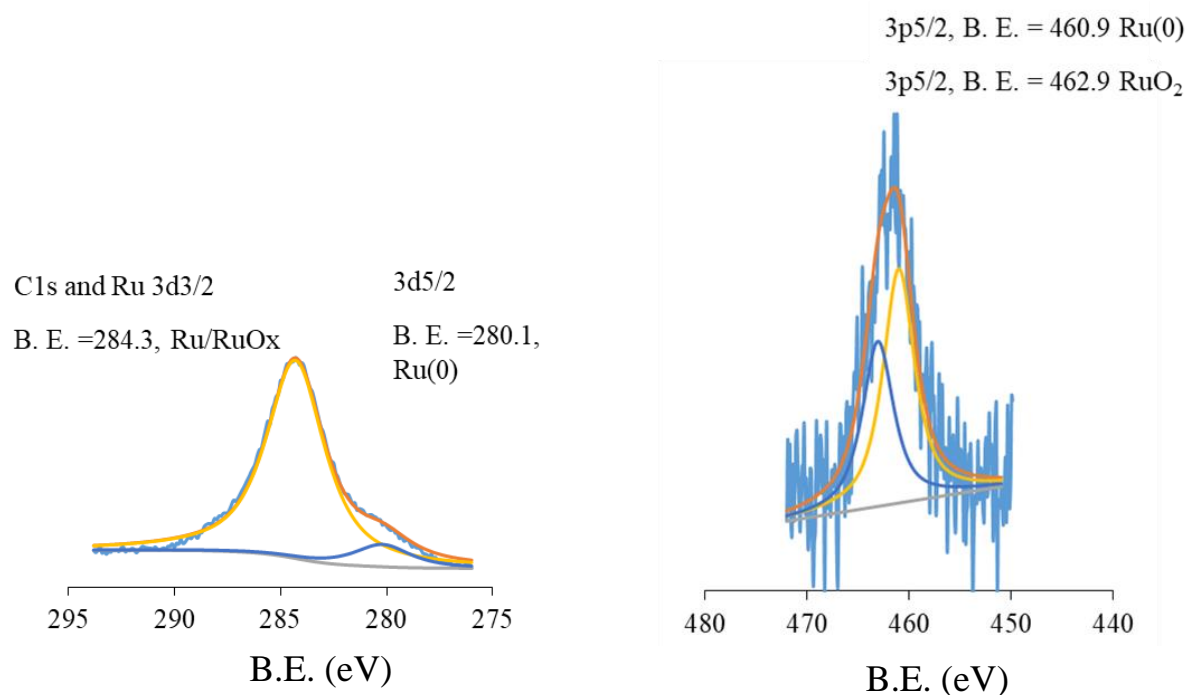
Figure 2B.8. Deconvoluted XPS spectrum of Ru/Al$_2$O$_3$-Basic catalyst
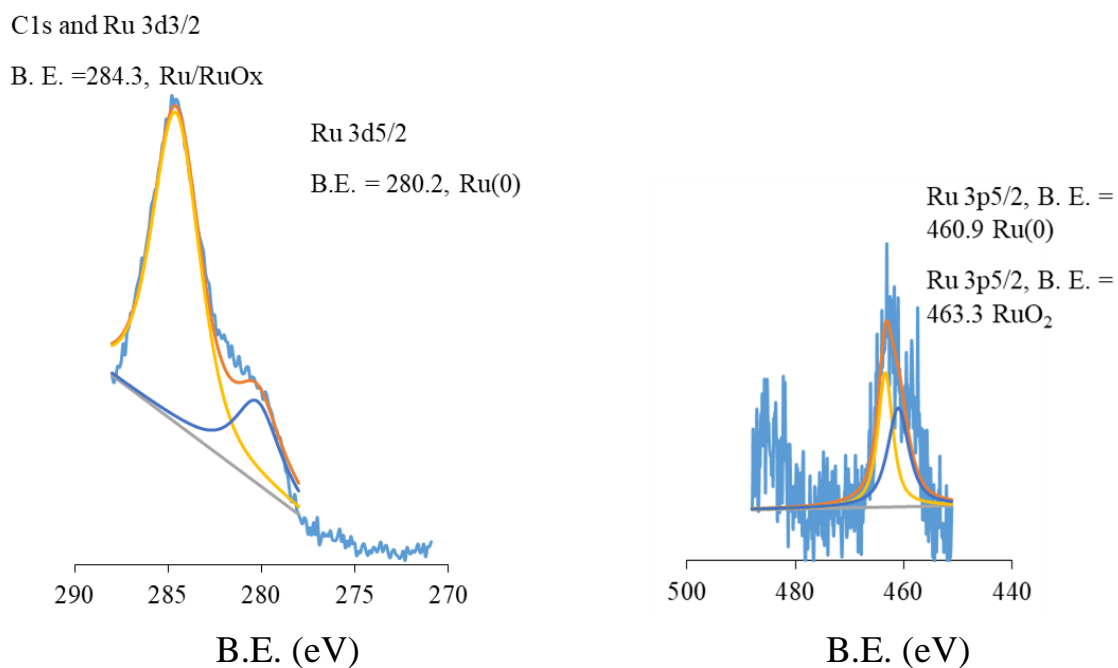
Figure 2B.9. Deconvoluted XPS spectrum of Ru/Al$_2$O$_3$-Neutral catalyst
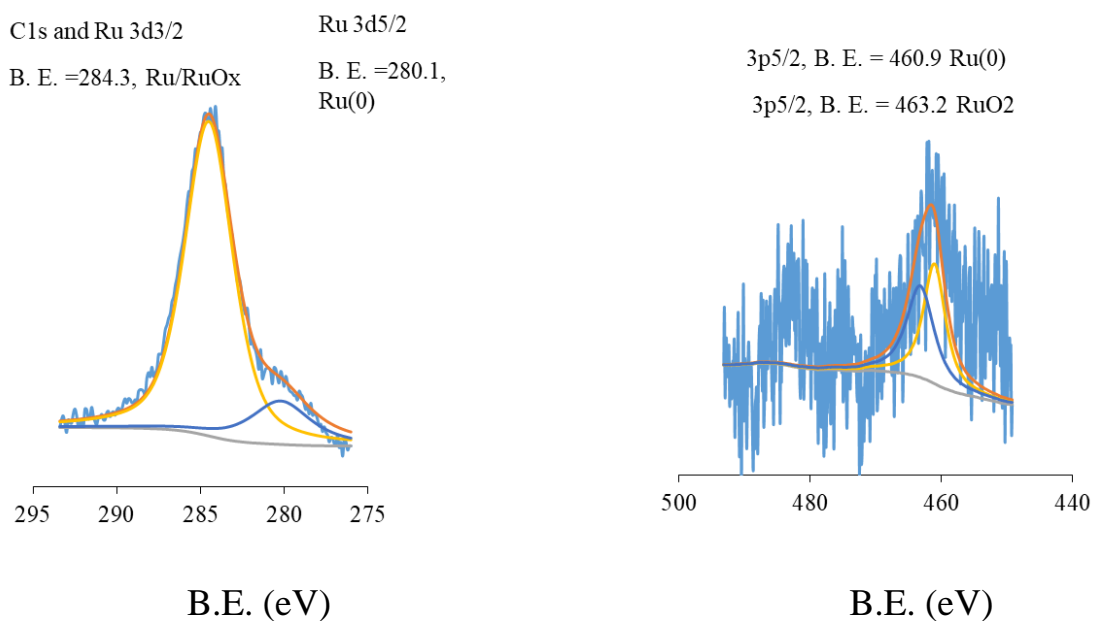
Figure 2B.10. Deconvoluted XPS spectrum of Ru/SiO$_2$-Al$_2$O$_3$ catalyst

2B.3.8. Acidity and basicity study

Temperature programmed desorption (TPD) is used to quantify the acidic or basic sites present in the material. Ammonia (NH_3) is used as a basic probe molecule which gets adsorbed on the acid sites, and carbon dioxide (CO_2) is an acidic probe molecule which adsorbs on the basic sites of the material. As the temperature increase, the probe molecule is desorbed and is recorded using a TCD detector. Analysis was conducted using Micromritics Autochem 2910 instrument. The sample was activated at 400 °C in He flow (30 mL•min^{-1}) for 1 h. Subsequently, the temperature was brought down to 50 °C, and the probe molecule was adsorbed by exposing the samples to a stream of 10% NH_3 in He (30 mL•min^{-1}) for 0.5 h. The temperature was then raised to 100 °C and flushed with He for 1 h at 100 °C to remove the physisorbed NH_3. The desorption of NH_3 was carried out in He flow (30 mL•min^{-1}) for NH_3 TPD and CO_2 for CO_2TPD, by increasing the temperature to 800 °C at 10 °C•min^{-1}, while monitoring the concentration of molecule desorbed using a thermal conductivity detector. As can be seen from the (Figure 2B.11 and Table 2B.5.) bare support Al_2O_3-Acidic showed NH_3 desorption peak at 200 °C, and when Ru was loaded on the support, an additional sharp peak for NH_3 desorption was observed at 335 °C. Similarly, an additional peak in Ru/Al_2O_3-Neutral catalyst and Ru/SiO_2-Al_2O_3 catalyst was also observed at 335 °C. The broad peak with peak maxima observed at around 200 °C in all the catalysts along with bare supports was suggested to be due to the desorption of NH_3 from the surface of the sample. However, an additional sharp peak observed after Ru loading can be assigned for the desorption of NH_3 from the different sites of the catalyst, which is indicated to be a Ru species. While electron-rich Ru in metallic state may not interact with NH_3, it is possible that Ru in electron deficient state such as Ru present in higher oxidation states (II, IV) may have interaction with NH_3. Since this interaction would be stronger than the interaction of NH_3 with Al_2O_3 support, higher desorption temperature of 335 °C was seen. Nevertheless, to prove that Ru is present in higher oxidation state, XPS analysis was performed, and data suggests that Ru is indeed present in higher oxidation state along with the metallic state. Nonetheless, with SiO_2 as a support, no peak for NH_3 desorption was seen, which was obvious because SiO_2 is considered as neutral support but, even after loading of Ru on SiO_2, no peak at around 335 °C was seen. These observations clearly suggest that metal-support interaction plays very crucial role in stabilizing Ru in different oxidation states. Later, TPD with CO_2 as a probe molecule was carried out for

Ru/Al$_2$O$_3$-Basic catalyst. However, no peak for the CO$_2$ desorption was observed. From the catalysts characterization study, it is revealed that Ru is highly dispersed on the Al$_2$O$_3$ support with small crystallite size, and mainly it is present in higher oxidation state.
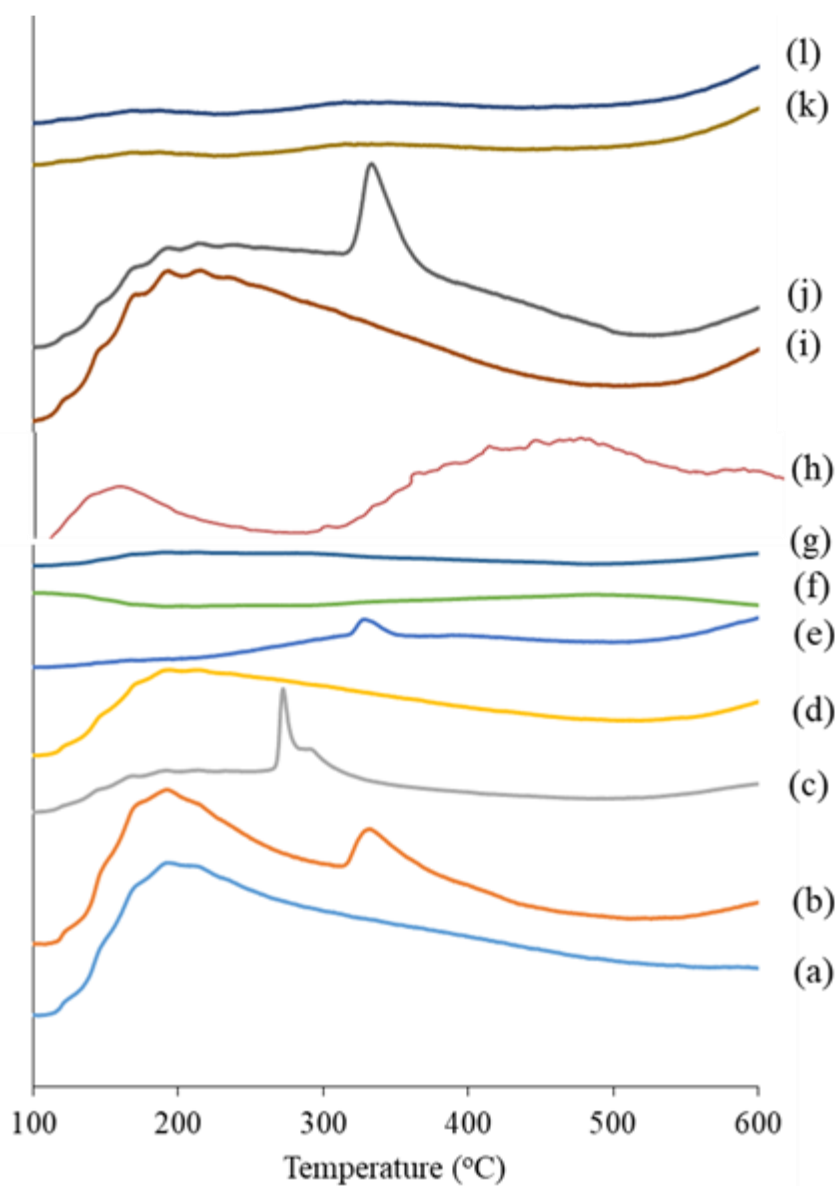
Figure 2B.11. NH$_3$-TPD of supported Ru metal catalyst (a) Al$_2$O$_3$-Acidic; (b) Ru/Al$_2$O$_3$-Acidic; (c) Ru/Al$_2$O$_3$-Acidic (commercial); (d) Al$_2$O$_3$-Neutral; (e) Ru/Al$_2$O$_3$-Neutral; (f) Al$_2$O$_3$-Basic (CO$_2$-TPD); (g) Ru/Al$_2$O$_3$-Basic (CO$_2$-TPD); (h) Ru/Al$_2$O$_3$-Basic (NH$_3$-TPD); (i) SiO$_2$-Al$_2$O$_3$; (j) Ru/SiO$_2$-Al$_2$O$_3$; (k) SiO$_2$; (l) Ru/SiO$_2$;

Table 2B.5. NH_3-TPD and CO_2-TPD study of catalysts

NH₃-TPD	
Catalyst	**Total acidity (mmol•g⁻¹)**
Ru/SiO_2	-
Al_2O_3-Acidic	0.23
Ru/Al_2O_3-Acidic	0.46
Ru/Al_2O_3-Acidic (commercial)	0.47
Ru/Al_2O_3-Neutral	0.16
SiO_2-Al_2O_3	0.54
Ru/SiO_2-Al_2O_3	0.76

CO₂-TPD	
Catalyst	**Total basicity (mmol•g⁻¹)**
Ru/Al_2O_3-Basic	0.17

2B.4. Synthesis of non-precious metal (Co, Ni) based supported catalysts

2B.4.1. Materials

Al_2O_3 powder, N-methyl-2-pyrrolidone (NMP) used as a precursor for the synthesis of Alumina hollow fiber (AHF), was purchased from Alfa Asser, India. Polysulfone (PSF) was purchased form Solvay Specialties India Pvt. Ltd. and used as received. Metal precursor, Cobalt Nitrate $(Co(NO_3)_2.3H_2O$ (97%), and $Ni(NO_3)_2.6H_2O$ (99%) were purchased from Loba chemical, India.

2B.4.2. Synthesis of Alumina fibers (AHF)

The green AHFs was extruded from the specially designed spinneret by using reported literature by well known phase inversion method [9-11]. Al_2O_3 powder (3µm) in a polymer solution of polysulfone (PSf) and N-Methyl-2-pyrrolidone (NMP) was dispersed to prepare the dope solution. This green AHF was then calcined between (800-900 ºC) for 2 to 4 h (8º•min⁻

^{1}), to remove the solvent and polymer. Further, AHF was again calcined between 1400 ^{o}C to 1600 ^{o}C for sintering to occur. The calcined AHF has been taken from the Dr. R Nandini Devis Lab as a Alumina support for the further reaction.

2B.4.3. Synthesis of Alumina fibers (AHF) supported (M/AHF) catalyst

Calcined AHF was then subjected to the metal impregnation. Capillary action was performed for the impregnation of metal to AHFs, in which the required quantity of metal precursor was dissolved in the deionized water, and AHFs was dipped into the solution about 1cm. In the impregnation procedure of metal over the AHFs, metal precursor is allowed to rise up through capillary action for 5 hours and oven-dried at 100 ^{o}C for 1 h. This action was repeated multiple times until the whole solution was deposited on the AHF support. Then, the metal deposited AHFs was subjected to reduction at 400 ^{o}C under H_2 flow ($10^o \cdot min^{-1}$) for 2h. The obtained catalyst was named as M/AHF@capillary. To compare the effect of capillary action in the catalytic activity of M/AHF@capillary, the catalyst was also synthesized using conventional wet impregnation method and reduced at 400 ^{o}C, named as M/AHF@imp. The current study is also focused on the effect of support in the catalytic activity, and since AHF is calcined between 1400-1500 ^{o}C, Al_2O_3-Acidic was also calcined at 1500 ^{o}C and metal deposited using wet impregnation method and reduced at 400 ^{o}C for the comparison of activity, and named as M/Al_2O_3-Acidic@cal@1500. The catalyst was also synthesized with γ-Al_2O_3-Acidic support and metal deposited through wet impregnation method and reduced at 400 ^{o}C and named as M/Al_2O_3-Acidic. All synthesized catalyst are summarized (Table 2B.6).

Table 2B.6. List of Cobalt (Co) and Nickel (Ni) based supported metal catalyst

Sr.No.	Catalyst	Metal loading (wt.%)
1	5 Co/Al$_2$O$_3$-Acidic	5
2	5 Co/Al$_2$O$_3$-Acidic@cal@1500	5
3	5 Co/AHF@imp	5
4	5 Co/AHF@capillary	5
5	5 Ni/AHF@capillary	5

All the synthesized catalysts were characterized thoroughly to understand their morphology, and catalyst activity was correlated with their morphologies.

2B.5. Catalyst characterizations

Synthesized supported metal catalysts were characterized using various physico-chemical techniques such as XRD, ICP-OES, TEM, N$_2$-sorption, and NH$_3$–TPD.

2B.5.1. X-ray diffraction (XRD) analysis

XRD analysis of all the synthesized catalysts was done and presented in Figure 2B.12. As can be seen from the Figure 2B.12, Al$_2$O$_3$-Acidic is present in γ-phase while Al$_2$O$_3$-Acidic@cal@1500 obtained after the calcination of γ-Al$_2$O$_3$-acidic at 1500 °C is existed in α-phase (rhombohedral, JCPDS: 80-0786). AHF support is also found in α-phase (rhombohedral, JCPDS: 80-0786). Co metal loaded in Al$_2$O$_3$-Acidic did not show any peak. While XRD pattern of Cobalt loaded Al$_2$O$_3$-acidic@cal@1500 and AHF confirmed the presence of Co in cubic (111) form (JCPDS:15-0806), Ni loaded on AHF also exists in cubic (111) form (JCPDS:04-0850).
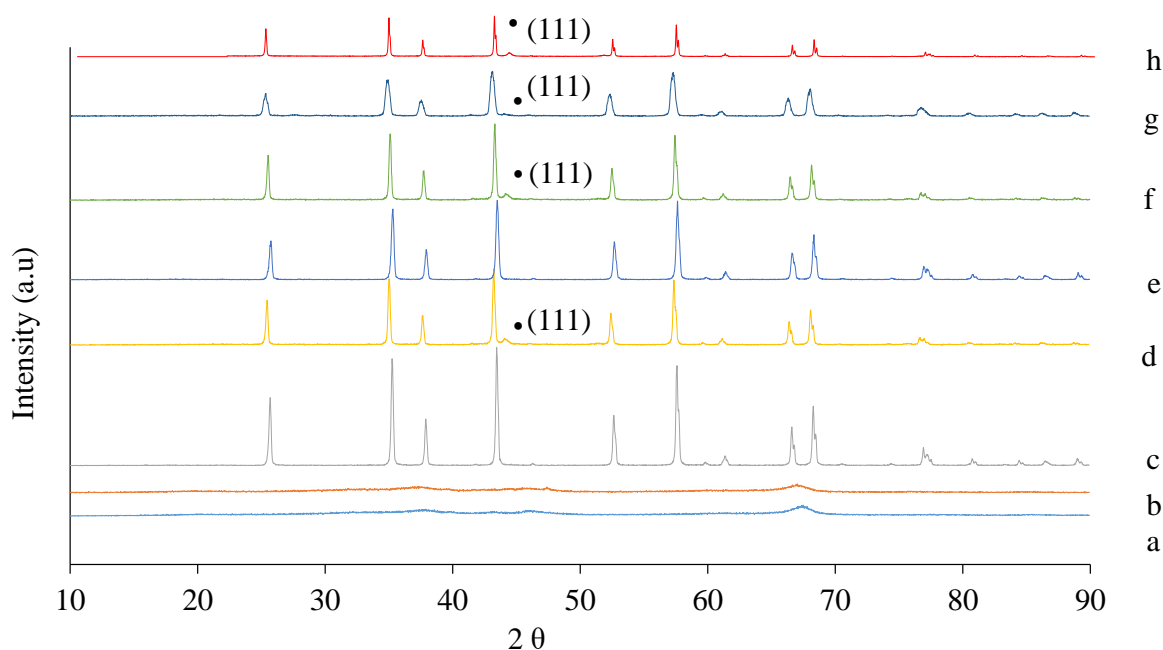
Figure 2B.12. XRD patterns of support and supported Co, Ni catalysts. (a) Al_2O_3-Acidic; (b) $5Co/Al_2O_3$-Acidic; (c) Al_2O_3-Acidic@cal@1500; (d) $5Co/Al_2O_3$-Acidic@cal@1500; (e) AHF, (f) $5Co/AHF@imp$; (g) $5Co/AHF@capillary$; (h) $5Ni/AHF@capillary$;

2B.5.2. N₂ Sorption analysis

The N_2 sorption analysis data for all the support and synthesized catalysts were summarized in Table 2B.7 Al_2O_3-Acidic (163 $m^2 \bullet g^{-1}$) and 5 Co/Al_2O_3–Acidic (148 $m^2 \bullet g^{-1}$) showed higher surface area. Al_2O_3-acidic@cal@1500 (0.7 $m^2 \bullet g^{-1}$), which is obtained after calcination of Al_2O_3-Acidic (163 $m^2 \bullet g^{-1}$), has a lower surface area due to sintering happened at higher temperature. The same trend can be seen in surface area of AHF (2.6 $m^2 \bullet g^{-1}$), which is also sintered at high temperature. Loading of metal on the support is not affecting the surface area of the catalyt. Catalysis showed similarty in the surface area as 5 Co/Al_2O_3-Acidic@cal@1500 (0.7 $m^2 \bullet g^{-1}$) and 5 $Ni/AHF@capillary$ (2.7 $m^2 \bullet g^{-1}$), 5 $Co/AHF@imp$ (2.5 $m^2 \bullet g^{-1}$) and 5 $Co/AHF@capillary$ (2.9 $m^2 \bullet g^{-1}$). Small difference in the surface area is resemble to the respective support.

Table 2B.7. Summary on nitrogen sorption data.

Catalyst	Nitrogen sorption		
	BET surface area ($m^2 \cdot g^{-1}$)	Pore volume (V) ($cm^3 \cdot g^{-1}$)	Pore radius (nm)
Al_2O_3–Acidic	163	0.260	2.1
5 Co/Al_2O_3-Acidic	148	0.270	2.4
Al_2O_3–Acidic@cal@1500	0.7	0.002	2.5
5 Co/Al_2O_3 @cal@1500 imp	0.7	0.002	2.4
AHF	2.6	0.002	2.1
5 Ni/AHF	2.7	0.001	1.8
5 Co/AHF@imp	2.5	0.002	1.6
5 Co/AHF@capillary	2.9	0.001	1.6

2B.5.3. ICP-OES analysis

Metal contents in the catalysts were determined by ICP-OES analysis as mentioned above in section 2B.3.3. The results suggest that experimental loadings are almost similar to that of theoretical loadings (Table 2B.8).

Table 2B.8. Summary on ICP-OES analysis

Catalyst	Theoretical M (wt%)	Experimental M (wt%)
5 Co/Al$_2$O$_3$-Acidic	5	4.6
5 Co/Al$_2$O$_3$ @cal 1500 imp	5	4.9
5 Ni/AHF@capillary	5	4.8
5 Co/AHF@imp	5	4.7
5 Co/AHF@capillary	5	4.8

2B.5.4. Transmission electron microscopy (TEM) analysis

TEM image of supported metal catalyst presented in Figure 2B.13., As can be seen from the Figure, metal is well dispersed on the AHF support as compared to other support. It can also be seen from the Figure, the metal deposited using capillary action is helping in more uniform distribution in case of 5 Co/AHF@capillary and 5 Ni/AHF@capillary as compared to 5 Co/AHF@imp.
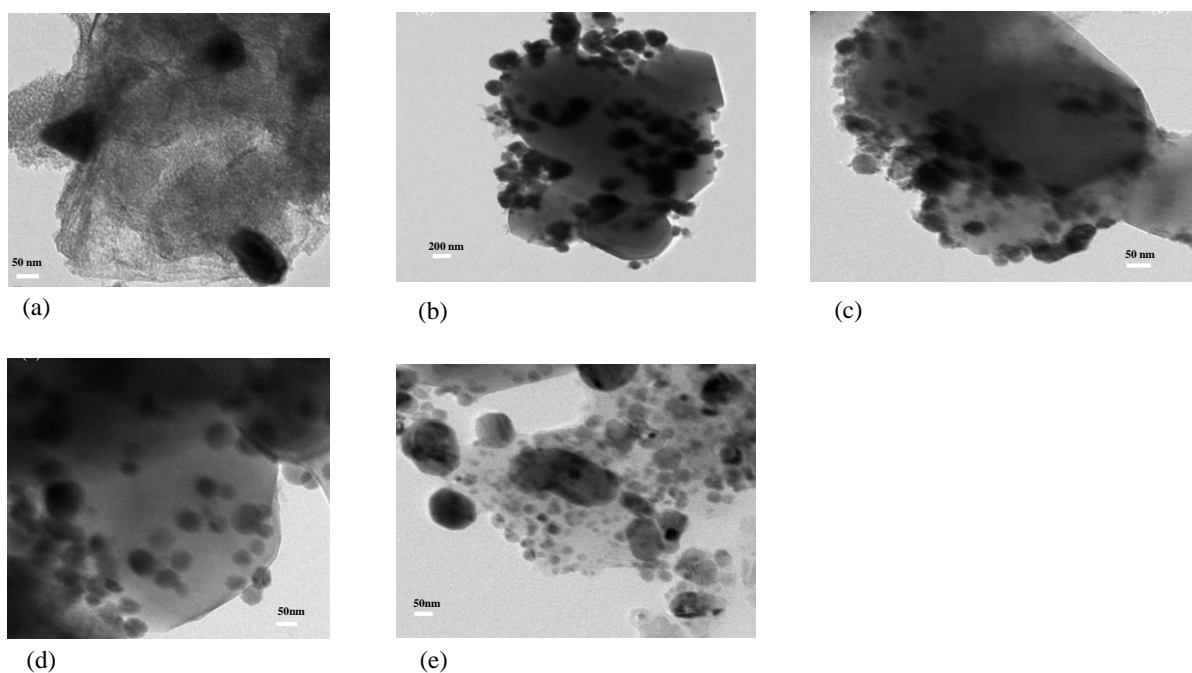
Figure 2B.13. TEM images of synthesized catalysts (a) 5 Co/Al_2O_3-Acidic; (b) 5 Co/Al_2O_3-Acidic@cal@1500; (c) 5 Co/AHF@imp; (d) 5 Co/AHF@capillary; (e) 5 Ni/AHF@capillary;

2B.5.5. CO chemisorption

CO chemisorption studies of synthesized catalyst are summarized in Table 2B.9 For 5 Co/Al_2O_3-Acidic catalyst, the volume of chemisorbed CO was 18.2 µmol•$g^{-1,}$ which indicates 2.15% dispersion of Co with 46 nm of the particle size of Co. In the case of 5 Co/Al_2O_3-Acidic@cal@1500, the dispersion of Co was 0.5 with particle size of 160 nm. While metal deposited on AHF support showed metal dispersion between 1.09-2.26 and average particle size between 40-91 nm. The particle size determined from CO chemisorption data is in line with the particle size calculated from TEM images.

Table 2B.9. CO chemisorption results for supported Ru catalysts

Catalyst	Average particle size (nm)	Metal dispersion (%)	Monolayer uptake(μmole•g^{-1})
5 Co/Al$_2$O$_3$-Acidic	46	2.15	18.2
5 Co/Al$_2$O$_3$@cal@1500	160	0.5	5.006
5 Ni/AHF	44	2.26	19.4
5 Co/AHF@imp	91	1.09	9.27
5 Co/AHF@capillary	40	2.12	20.1

2B.5.6. Determination of reducibility of metal

TPR analysis of the synthesized catalyst presented in Figure 2B.14 As can be seen from the Figure 2B.14, 5 Co/Al$_2$O$_3$-Acidic is not consuming any hydrogen, and the reduction peak is absent. However, consumption of H$_2$ can be seen in the other catalysts like 5 Co/Al$_2$O$_3$-Acidic@cal@1500, 5 Co/AHF@capillary, and 5 Ni/AHF@capillary. The above result suggested that cobalt loaded on the Al$_2$O$_3$-Acidic support might be present in oxidized form and Co loaded on the Al$_2$O$_3$-Acidic@cal@1500 and Ni, Co loaded on AHF support might be present in metallic form.
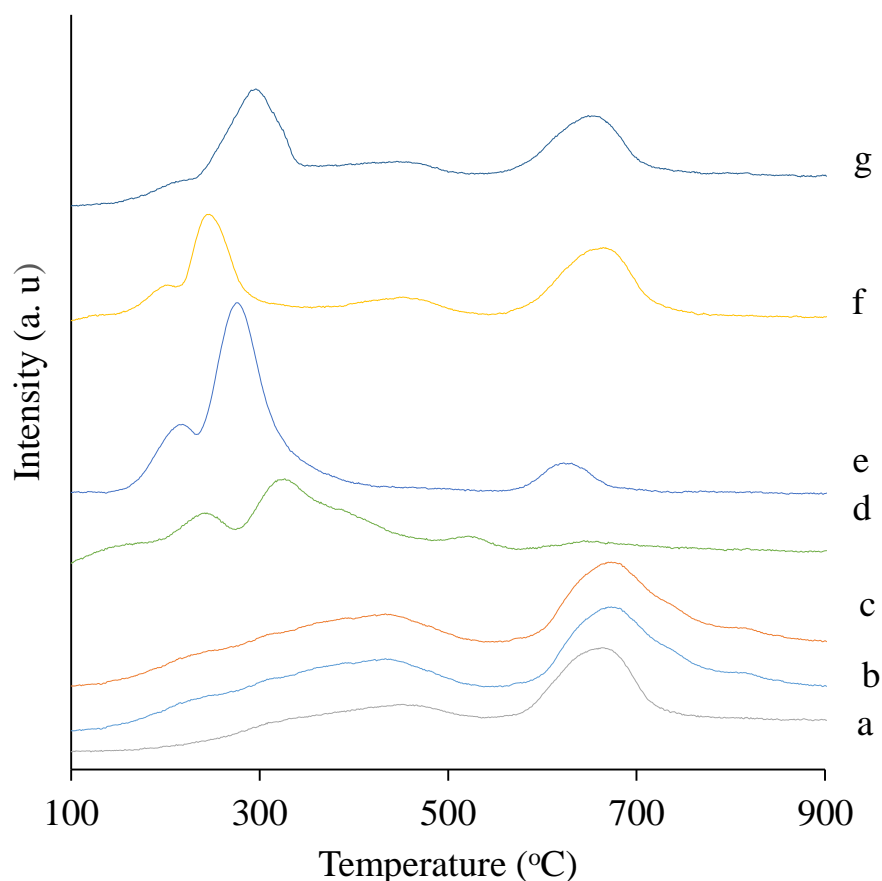
Figure 2B.14. TPR of support and supported Co, Ni catalysts. (a) Al_2O_3-Acidic; (b) 5 Co/Al_2O_3-Acidic; (c) AHF; (d) 5 Co/Al_2O_3-Acidic@cal@1500; (f) 5 Co/AHF@imp; (g) 5 Co/AHF@capillary; (h) 5 Ni/AHF@capillary;

2B.5.7. XPS analysis

XPS analysis was done to find out the oxidation state of metal and the deconvoluted spectra are represented in Figure 2B.15 All binding energy values were calibrated using the value of carbon (C1s = 284.4 eV) as a reference. Deconvoluted XPS spectra of Cobalt (Co) loaded catalyst showed, cobalt is present in the metallic state (0) as well as higher (+2/+3) oxidation state in all the catalysts. Apperence of peak at 803 eV is resemble to metallic cobalt and peak appear at 780 eV and 797 eV is dedicated to oxidized cobalt (+2/+3). XPS spectrum of 5

Ni/AHF@capillary is showed only the presence of metallic Nickel (879 eV, 873 eV, 855 eV). and oxididized Nickel.
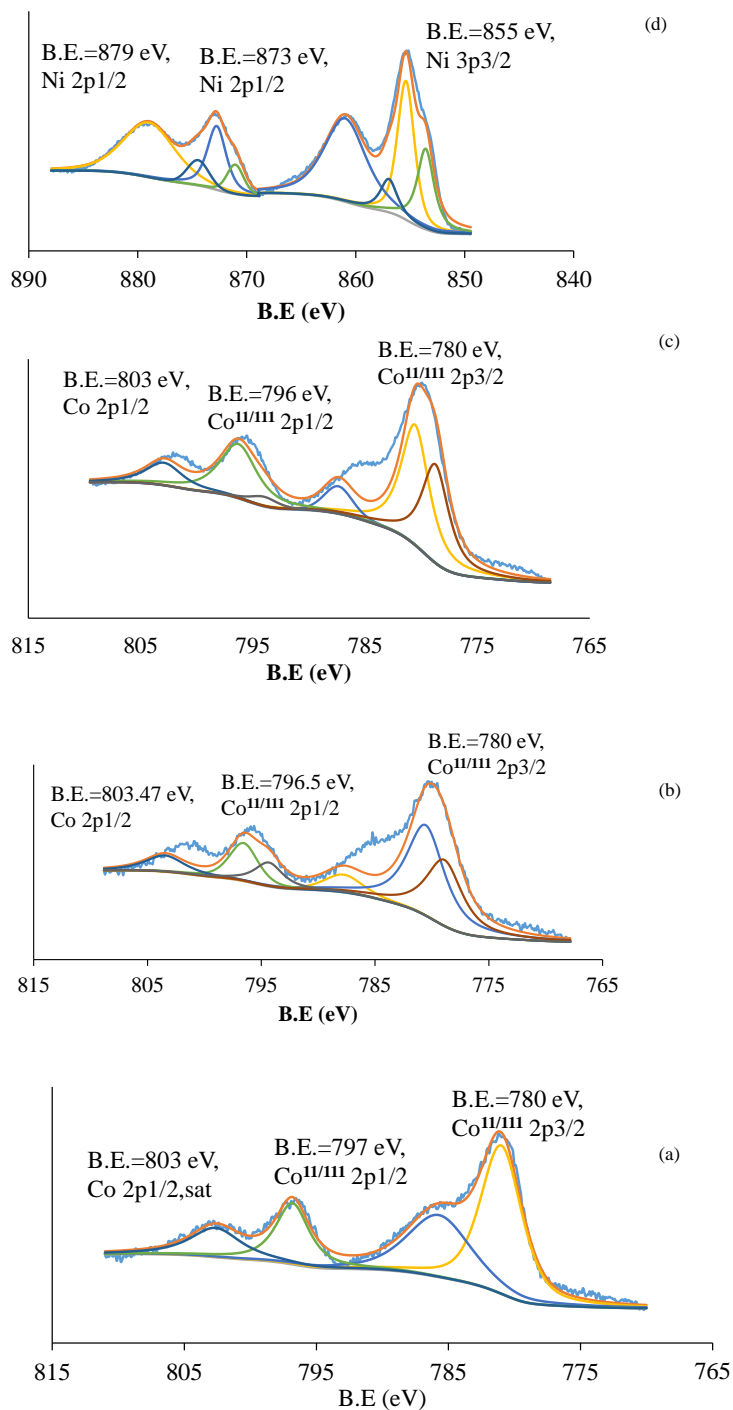
Figure 2B.15. XPS spectra of Co, Ni catalysts (a) 5 Co/Al$_2$O$_3$-Acidic@cal@1500;(b) 5 Co/AHF@imp; (c) 5 Co/AHF@capillary;(d) 5 Ni/AHF@capillary;

2B.5.8. Acidity and basicity study

NH$_3$-TPD analysis of Cobalt/Nickel supported catalyst were carried out using the same program which was used for Ru supported metal catalyst and presented in Figure 2B.16 It can be seen from the TPD analysis that only Al$_2$O$_3$-Acidic and 5 Co/Al$_2$O$_3$-Acidic catalysts are showing the desorption peak of NH$_3$ at 230 ^{o}C, and other support and metal-supported catalysts do not show any desorption peak for NH$_3$. This phenomenon could be explained based on the higher sintering temperature used for the synthesis of support which is inforcing the loss of acidity present in the support.
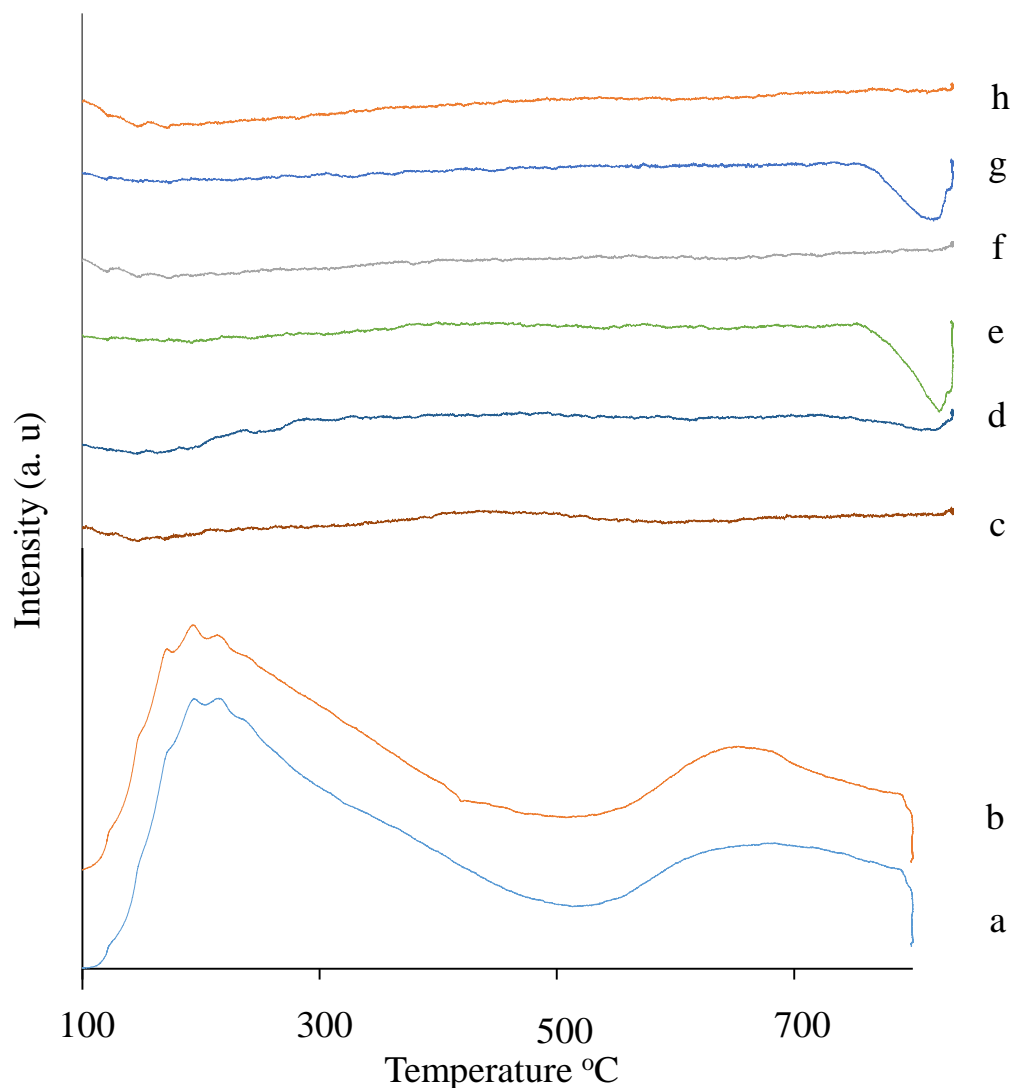
Figure 2B.16. TPD of support and supported Co, Ni catalysts. (a) Al_2O_3-Acidic; (b) 5 Co/Al_2O_3-Acidic; (c) Al_2O_3-Acidic@cal@1500; (d) 5 Co/Al_2O_3-Acidic@cal@1500; (e) AHF (f) 5 Co/AHF@imp; (g) 5 Co/AHF@capillary; (h) 5 Ni/AHF@capillary;

2B.6. Characterization of the solid acid catalysts

2B.6.1. Material

Zeolite, H-USY (Si/Al = 15), was obtained from Zeolyst International. Prior to use, zeolite was calcined at 400 °C for 16 h in air flow. $SiO_2−Al_2O_3$ (Si/Al = 5.3), K10 clay, and Al pillared clay were purchased from Sigma Aldrich, USA.

2B.6.2. X-Ray diffraction (XRD) analysis

X-Ray diffraction pattern of all the solid catalysts confirms the characteristic phase structure of solid acid catalyst (Figure 2B.17). It can be seen from Figure 2B.17 that SiO_2-Al_2O_3 is amorphous in nature, and other solid acids are crystalline in nature.
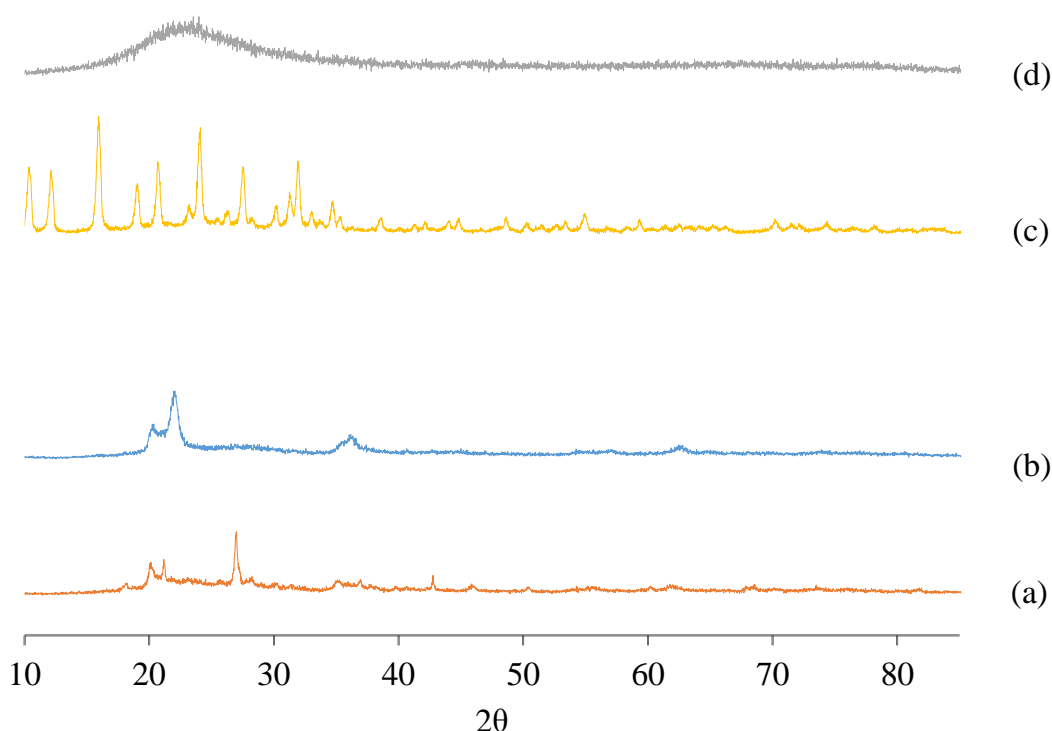
Figure 2B.17. XRD patterns of catalysts. (a) Clay K-10, (b) Al-pillared clay, (c) H-USY (Si/Al= 15), (d) SiO_2-Al_2O_3 (Si/Al= 5.3)

2B.6.3. NH₃-TPD analysis of solid acid catalysts

NH₃-TPD analysis of all solid catalysts was carried out to calculate the acidity of a solid acid catalyst (Figure 2B.18, Table 2B.11). It can be seen from the Table 2B.10 that the Al-pillared clay has maximum acidity (0.65 mmol•g^{-1}), and H-USY (Si/Al=15) showed the lowest acidity (0.28 mmol•g^{-1}).
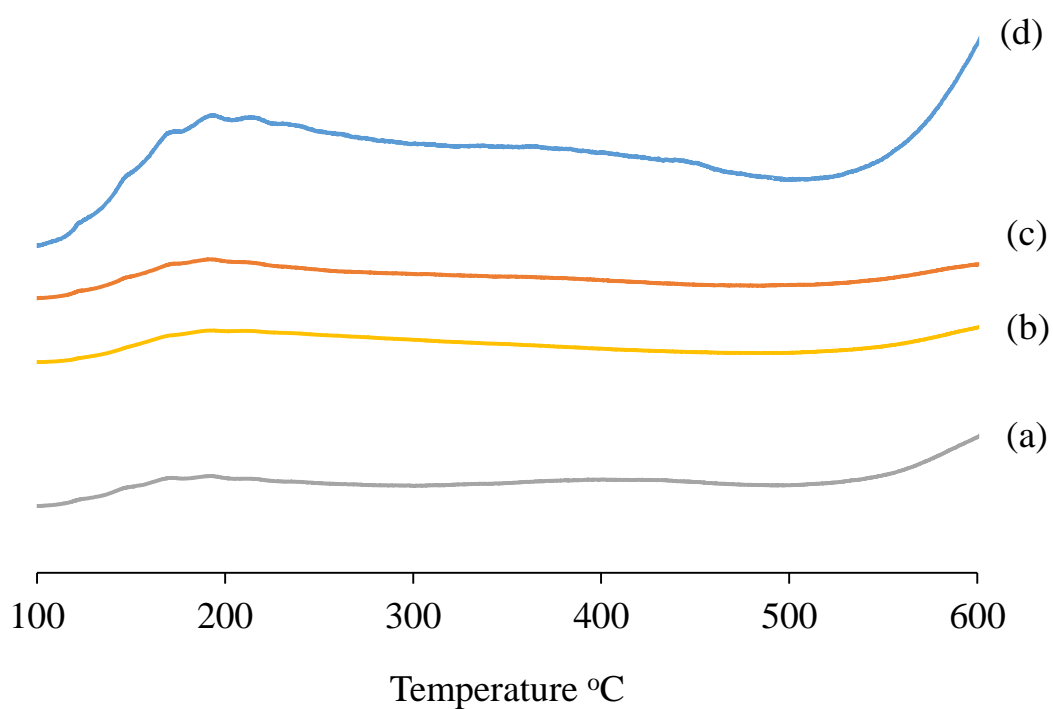
Figure 2B.18. NH$_3$-TPD of fresh catalysts. (a) Clay K-10, (b) Al-pillared clay, (c) H-USY (Si/Al=15), (d) SiO$_2$-Al$_2$O$_3$ (Si/Al=5.3)

Table 2B.10. NH$_3$-TPD study of fresh and spent catalysts.

Catalyst	Total acidity (mmol•g^{-1})
SiO$_2$-Al$_2$O$_3$ (Si/Al=5.3)	0.61
Clay K-10	0.36
Al-pillared clay	0.65
H-USY (Si/Al=15)	0.28

2B.6.4. N$_2$-sorption study of the solid acid catalysts

N$_2$-sorption study of the solid acid catalysts was done to calculate the available surface area for the catalytic reaction and summarized in Table 2B.11. As seen H-USY (Si/Al=15) (631 m^2•g^{-1}) shows the highest surface area, and Al- pillared clay (170 m^2•g^{-1}) shows the lowest surface area amongst all the catalysts used in this study.

Table 2B.11. Summary of nitrogen sorption data of fresh catalysts

Catalyst	BET surface area (m^2•g^{-1})	Pore volume (V) (cm^3•g^{-1})	Pore radius (nm)
SiO$_2$-Al$_2$O$_3$ (Si/Al=5.3)	374	0.35	3.81
Clay K-10	192	0.21	1.89
Al-pillared clay	170	0.16	1.84
H-USY (Si/Al=15)	631	0.41	nd

2B.6.5. ICP-OES analysis of solid acid catalyst

ICP-OES analysis of solid acid catalyst was done to calculate the Si/Al ratio and summarized in Table 2B.12.

Table 2B.12. Summary of ICP-OES analysis of catalysts.

Catalyst	Theoretical Si/Al ratio	Experimental Si/Al ratio of fresh catalyst
SiO_2-Al_2O_3 (Si/Al=5.3)	5.30	5.20
Clay K-10	Nd	Nd
Al-pillared clay	Nd	Nd
H-USY (Si/Al=15)	15.0	14.90

2B.7. Conclusion

Base catalyzed lignin depolymerization produces low molecular weight compounds. Upgradation of those low molecular weight compound were studied using the supported metal catalyst and solid acid catalyst. Precious metal (Ru) supported metal catalysts were synthesized using conventional wet impregnation method, and nonprecious (Co/Ni) metal-supported catalyst was synthesized using the wet impregnation and modified impregnation method i.e., capillary action.Wet impregination method was also employed for the synthesis of non-precious metal supported catalyst to compare the activity of Al_2O_3-Acidc support, which is mostly used in this study, Al_2O_3-Acidic were modified and catalyt activity checked for the upgradation of low molecular weight compound. Synthesized catalyst was characterized by several Physico-chemical methods. Solid acid catalyst used for the upgradation of low molecular weight compounds was also characterized using the various physico-chemical techniques.

2B.8. Reference:

1.   Y.K. Hong, D. W. L., H.J. Eom, K.Y. Lee, The catalytic activity of Pd/WOx/γ-Al2O3 for hydrodeoxygenation of guaiacol. *Appl. Catal. B: Environ.* **2014** *150-151* 438-445.

2.   S. Liu, H. W., K.J. Smith, C.S. Kim Hydrodeoxygenation of 2-Methoxyphenol over Ru, Pd, and Mo2C Catalysts Supported on Carbon, *Energy & Fuels* **2017,** *31* 6378-6388.

3.   A.K. Deepa, P. L. D., Function of Metals and Supports on the Hydrodeoxygenation of Phenolic Compounds, . *ChemPlusChem,* **2014,** *79* ( ), 1573-1583.

4.   W. C. K. Choi, J. S. L., Tae Hong Woo, Seong Ihl, *Catal. Today.* **2000,,** *63,* , 229-236.

5.   C. S. Decastro, E. V., M. H. Hölderich, W. F., *J.Catal.* **2000, ,** *196*, 86-94.

6.   M. A. G. Borja., E. R. D., *AIChE J.* **2015,** *61*, 598.

7.   Deepa, A. K., Dhepe, P. L., *RSC Adv* **2014,** *4*, 12625-12629.

8.   Nuermaimaiti Abudukelimu1, Hongjuan Xi2, Zhixian Gao, Yagang Zhang, Yubo Ma1 Xamxikamar Mamat and Wumanjiang Eli, Preparation and Characterization of Ru/Al2O3 Catalysts by adsorption-precipitation-activation method and Selective Hydrogenation of Dimethyl Maleate to Dimethyl Succinate. *Mater. Sci. Eng. Adv. Res.* **2015,** *1* (1), 31-37.

9.   Xiaoyao Tan, S. L., K. Li, Preparation and characterization of inorganic hollow fiber membranes. *journal of membrane science,* **2001** *188* 87-95.

10.   Shaomin Liu, K. L., R. Hughes, Preparation of porous aluminium oxide (Al$_2$O$_3$) hollow fibremembranes by a combined phase-inversion and sintering method. *ceramics international,* **2003,** *29* 875–881.

11.   J. Luyten, A. B., W. Adriansens, J. Cooymans, H. Weyten, F. Servaes, R. Leysen, Preparation of LaSrCoFeO3−x membranes. *Solid State Ionics,* **1 November 2000,** *135(1-4)*, 637-642

Chapter 3

Base catalyzed depolymerization of lignin into low molecular weight compounds

3.1. Introduction

Demand of carbon-based resources is increasing with high rate. Presently, this demand is fulfilled by fossil reserves. High consumption and limited resource of fossil reserves are limiting its availability. Lignocellulose, considered as a renewable source of carbon-based products, can be used in the production of various chemicals, which are currently being produced by fossil reserves. Lignocellulose is made up of three-components i.e., cellulose (30-50%), hemicellulose (15-40%), and lignin (10-30%). The potential use of cellulose and hemicellulose is well known, as those can be converted into cellulosic ethanol through biochemical conversion and variety of other products such as sugars, furans, acids etc. However, lignin, which is a by-product of cellulosic ethanol and pulp and paper industry is underutilized. Mostly, it is burnt to create energy and burning of it has environment concerns. Effective utilization of lignin will improve the economy of cellulosic ethanol process and also reduces the dependency of fossil reserves for the production of aromatic products because it is considered as a renewable source of aromatic products. Lignin is a 3D amorphous polymer made up of three basic units those are, *p*-coumaryl alcohol (H), guaiacyl alcohol (G), and syringyl alcohol (S). Monomer unit of lignin is connected via C-O-C and C-C linkages, namely β-O-4, α-O-4, 4-O-5 and β–β, β-5, β-4, 5–5 linkages [1]. The global production of lignin in Kraft pulp mills is over 70 Mt·yr^{-1}, primarily in the form black liquor,[2] which is used for electricity generation in pulp mills [3]. However, lignin can produce high-volume aromatic compounds for the chemical industry [4, 5]. Presently, more than 98% of lignin is burnt as a source of energy in the pulp and paper industry [6, 7]. Moreover, some low-value applications of lignin are known and being utilized in the form of low-value products such as (phenolic resins, polyurethane foams, epoxy resins, printed circuit boards, dispersing or emulsifying agents, low-grade-fuel, wood panel products, automotive brakes etc.) [8-10]. The proper utilization of lignin generated from pulp and paper industry and cellulosic ethanol plant will not only resolve the disposal issue but also will play a significant role in the production of aromatic chemicals in biorefinery concept. The heterogeneous molecular structure of lignin creates difficulty in the development of depolymerization process for the production of commercially high-value products from lignin [11]. Different chemical processes, such as pyrolysis, hydrocracking, hydrogenolysis, hydrolysis, and oxidation have been used to depolymerize lignin [12-15].

The limited solubility of relatively high molecular weight lignins in most common organic solvents at ambient temperature is another difficulty in depolymerization of lignin. Catalytic depolymerization of lignin is carried out at higher temperatures (250 °C) and leads to a variety of side reactions and favors the formation of biochar. This results in decrease of valuable carbon yield and catalyst deactivation [16]. In order to overcome this issue, various alternative reaction mediums are used, such as supercritical solvents (methanol, water) [17, 18] or ionic liquids (100-120 °C) [19, 20] for the depolymerization of lignin. Considering the complex structure of lignin, homogeneous system would have the benefit of penetrating the three-dimensional lignin structure and easy access to the target linkages. Whereas heterogeneous catalysts have limited accessibility due to the steric hindrance of the lignin backbone and the heterogeneous nature of the substrate itself [21]. This way, after deep insight into structure-activity relationships, a homogeneous catalyst is the most preferred one for depolymerization of lignin that operates under lower reaction temperatures (<300 °C) than the reported ones. An additional advantage of homogeneous catalysis is the possibility for simultaneous or cyclic processes in the presence of different catalysts by targeting different linkages. Base catalyzed depolymerization of lignin has been widely used [22, 23], in which NaOH was found to be more useful for the depolymerization of lignin [24]. Although significant advances have been made in recent research, the understanding of product distribution and effective conversion of lignins is still challenging. In the present work, homogeneous base-catalyzed lignin depolymerization is carried out and emphasis is given on the understanding of depolymerized product formation under the employed reaction conditions. Detailed model compound study is carried out to correlate the reaction results with reaction parameters.

3.2. Experimental section

3.2.1. Chemicals & materials

Lignins used in this study, were purchased from TCI chemicals, India, such as (Lignin, Alkaline, Lignin, Dealkaline, Kraft lignin). Na-lignosulfonate lignin was purchased from Sigma Aldrich, India. Two industrial lignins were also used in this study. All the lignins, including industrials lignin were used without any pre-treatments. Various aromatic monomers such as guaiacol, catechol, veretrol, eugenol, vanillin, 4-methylphenol, pyrocatechol, resorcinol, 2,6-dimethoxyphenol, homovanillic acid, 4-hydroxy benzyl alcohol, 2,4-di-tert-

butylphenol, acetovanillone,4-hydroxy-3-methoxybenzyl alcohol, 1,2,4-trimethoxybenzene were purchased from Alfa Aesar, India and used for the identification and quantification of the depolymerized products. Various bases such as NaOH, KOH, CsOH, Na_2CO_3, Cs_2CO_3, $CaCO_3$ were purchased from Loba Chemie, India, and acids HCl and H_2SO_4 were also purchased from Loba Chemie, India. Various solvents such as, diethyl ether (DEE), Ethyl acetate (EtOAc), tetrahydrofuran (THF) were purchased from Loba Chemie, India. All the catalytic runs were carried out using distilled water.

3.2.2. Homogeneous base catalyzed depolymerization of lignin

Depolymerisation of different types of lignins was performed in a 100 mL stainless steel high-pressure high-temperature Parr make reactor by charging 50 mL solvent (water); 0.5 g lignin; 3.4 mmol NaOH in the reactor. The reactor was flushed with N_2 for 3-4 times to remove any air. Then, the reactor was pressurized with N_2 up to desired pressure (1–2 MPa) and was heated slowly until desired temperature (225–250 °C) under slow stirring (100 rpm). After attaining the reaction temperature, stirring was increased to 1000 rpm, and this time was considered as the starting time of the reaction.

3.2.3. Extraction of the products

After completion of the reaction, the reactor was cooled to room temperature under air and water flow. Acidification of the reaction mixture was done with 2 N H_2SO_4 solution until the pH reached to 1–2. Acidified reaction mixture was collected in the centrifuge tube and kept for centrifugation. It was observed that the centrifuged reaction mixture has two layers, i.e., solid layer (solid cake) and liquid layer. Both layers were separated from each other. Then, the isolation of depolymerized products was done. For that, both liquid and solid obtained after centrifugation were subjected to the liquid-liquid and liquid-solid extraction. The extraction process was carried out using diethyl ether (DEE), ethyl acetate (EtOAc), and tetrahydrofuran (THF) making use of insolubility of lignin in these solvents (Chapter 2A.1., Table 2A.5). The soluble fraction was filtered and the undissolved solid (residual lignin, oligomers, trimer, or high molecular weight compounds) was oven-dried at 55 °C. The organic solutions obtained after treatment of the liquid and solid layer were vacuum evaporated to obtain the oily products. The percentage of organic solvent-soluble products were calculated based on the solid recovered after evaporating the respective solvents. The schematic flow of the procedure involved in the process is represented in Figure 3.1.

Reaction charge (lignin + NaOH + H_2O)

↓ Depolymerization

Reaction mixture (depolymerized product + NaOH + H_2O)

↓ Acidification with H_2SO_4 (pH~2)

Centrifugation

├─ Solid cake — Extraction with DEE
│   ├─ Soluble → Evaporation → Products
│   └─ Insoluble — Extraction: EtOAc
│   ├─ Soluble → Evaporation → Products
│   └─ Insoluble → Extraction THF → Products
│
└─ Liquid — Extraction with DEE
    ├─ Soluble → Evaporation → Products
    └─ Insoluble — Extraction: EtOAc
         ├─ Soluble → Evaporation → Products
         └─ Insoluble

Figure 3.1. Methodology used for the extraction of the products

3.2.4. Analysis of reaction mixture

The reaction mixture soluble in organic layer was analyzed by GC and GC-MS. GC was equipped with HP-5 capillary column (0.25 μm × 0.32 mm × 50 m), FID detector (30 mL•min^{-1} N_2 flow as carrier gas) and the oven temperature program was as follows: 100°C (hold time 4 min) to 275 °C (hold time 20 min) at 10 °C•min^{-1} ramp rate. The injector temperature was 270 °C. The detector was kept at 275 °C. The GC-MS (Agilent-7890 GC and Agilent MS-5977A MSD) equipped with the DB-5-MS column (0.25 μm × 0.25 mm × 30 m) was used for the identification of the products. The temperature program was similar to that of GC-FID. The NIST library was used for the identification of the product. The reaction mixture was also

analyzed using HPLC (Agilent make) and LC-MS (Agilent make). Both were equipped with C_{18} column (4.6 mm x 250 mm), and the RID detector kept at 40 °C. Methanol and water (1:1 *v/v*) was used as mobile phase with 0.6 ml/min flow rate. Products were identifying by injecting standards.

3.2.5. Yield calculations

Depolymerized low molecular weight compounds were extracted from the reaction mixture using diethyl ether (DEE), ethyl acetate (EtOAc), and tetra hydrofuran (THF). The percentage yield calculation of low molecular weight compounds was done on solid weight basis after evaporating the respective solvent from the reaction mixture.

Solvent contribution in the percentage weight of low molecular weight compound was avoided by keeping oily mass into an oven at 55 °C for 16 h. It was expected that pretreatment would remove solvent entrapped in the respective organic mixture. Further, vacuum drying was also done to ensure complete removal of organic solvent at 60 °C and 10^{-4} MPa under vacuum for 2 h. After this, the weight of obtained solid was collected and used for yield calculation. Moreover, to ensure the presence of the volatile components in the respective solvent, solvents collected from the collection flask of the rotary evaporator was injected in GC-FID, but the only solvent peak was observed. The quantification of identified low molecular weight compounds was done using available standards by calibrating the GC and GC-MS. Substrate weight calculation i.e., Lignin was based on the results obtained from the TGA analysis conducted in the air medium presented in Table 3.1 and results showed that Lignin, Alkaline contains around 12% moisture and 10% unburnt residue (inorganic residue/ash). Reactions were carried out using 0.5 g lignin, out of which moisture presence in the Lignin, Alklaine will be 0.06 g (12 wt%), and inorganic residue will be 0.05 g (10%). Hence,the actual weight of lignin charged in the catalytic reaction was (0.5 – (0.06 +0.05)). The actual weights of other lignins were also calculated using the same procedure.

Table 3.1. Summary on TGA analysis of various lignins

Properties	Lignin, Alkaline	Lignin Dealkaline	Lignin, Alkali	Na-lignosulfonate lignin	Industrial K lignin	Industrial N Lignin
Moisture (%)	12	10	4	21	29	13
TGA residue (%) Air	10	14	13	7	0	19

$$Yield\ of\ DEE\ soluble\ products\ (\%) = \frac{Weight\ of\ DEE\ soluble\ products\ (g)}{Weight\ of\ lignin\ (g)} \times 100$$

$$Yield\ of\ EtOAc\ soluble\ products\ (\%)$$
$$= \frac{Weight\ of\ EtOAc\ soluble\ products\ (g)}{Weight\ of\ lignin\ (g)} \times 100$$

$$Yield\ of\ THF\ soluble\ products\ (\%) = \frac{Weight\ of\ THF\ soluble\ products\ (g)}{Weight\ of\ lignin\ (g)} \times 100$$

Weight of Lignin, alkaline (g) = weight of lignin charged (g) – weight of (moisture +ash) (g)

$$= 0.5g - (0.06 + 0.05)$$
$$= 0.390\ g$$

3.2.5.1. Mass balance calculations

Mass balance of catalytic reactions were calculated using following formula,

$$Mass\ Balance\ (\%) = \frac{Initial\ mass\ (g) - final\ mass\ (g)}{Initial\ mass\ (g)} \times 100$$

The initial mass of catalytic reaction is lignin charged in the reaction, and final mass is the total weight of organic solvent soluble products.

$$Mass\ Balance\ (\%) = \frac{Weight\ of\ DEE\ soluble\ and\ EtOAc\ soluble\ prodcuts\ (g)\ +}{Weight\ of\ EtOAc\ insoluble\ prodcuts\ (g)} \times 100$$
$$\frac{}{Weight\ of\ lignin\ charged\ (g)}$$

Mass balance of catalytic reaction was calculated based on the above equation as follows:

Reaction condition: Lignin, Alkaline (0.5g), NaOH (3.4 mmol), water (50 mL), 250 $^{\circ}$C, 1 h, N$_2$, 2 MPa; 1000 rpm.

Solid charged before the reaction	Solid recovered after the reaction
Lignin, Alkaline = 0.44 g (0.5 g – 0.06 g of moisture)	Depolymerized lignin (DEE, EtOAc soluble products + EtOAc insoluble) = 0.42 g
Total solid charged = 0.44 g (including ash)	Total solid recovered = 0.42 g

Based on above observation, mass balance was calculated as

Mass balance = (0.42/0.44) x100=95%

3.2.5.2. Substrate/catalyst (S/C) calculations

The substrate to catalyst ratio was calculated by considering the average molecular weight of lignin monomer unit as 180, based on the monomeric molecular formula (MMF) of lignin (C$_{10}$H$_{12}$O$_3$), calculations are explained in detail in Chapter 2A, Section 2A.2, Table 2A.2. Mol of Lignin, alkaline was calculated based on actual lignin charged in catalytic reaction by considering the moisture and inorganic residue present in the lignin and calculated using TGA analysis as mentioned above. Hence, 0.390 g lignin was considered for the mol calculations. 0.390 g of Lignin, alkaline/180 = 2.16 x 10^{-3} mol (2.16 mmol). Mol of the catalyst was calculated based on their weight taken for the catalytic run.

3.3. Result and discussion

As discussed, homogeneous bases were used for the catalytic depolymerization of lignin in aqueous medium using batch mode reactor. After completion of the reaction, and acidification process, low molecular weight compounds were extracted in organic solvents by the liquid-liquid and liquid-solid extraction procedure.

3.3.1. Employment of various homogenous bases for the lignin depolymerization

The depolymerization of lignin was carried out to explore the catalytic activity of various bases at 250 °C for 1 h. Different types of bases were used in the catalytic run to identify the best catalytic system for the depolymerization process because different bases have different catalytic behavior and basic strengths. It was also seen from the TGA analysis that degradation of lignin substrates starts around 180 °C, and a sharp decrease was seen between 300-350 °C. Moreover, it is known in the literature that lignin has around 60-70% ether linkages. Cleavage of ether linkages (C-O-C) is possible at lower temperatures as compared to carbon linkages (C-C). It is also known in the literature that effective depolymerization of lignin is possible using solid base [25], homogeneous base [26] and mixture of solid base and homogeneous base [27] between 250 °C-300 °C. Considering this, initially, catalytic experiments were decided to be carried out at 250 °C. Moreover, all catalytic experiments were carried out with Lignin, Alkaline, unless specified. Catalytic and workup procedure was followed as mentioned in the experiment section. Here, it is also desired to mention that the presence of low molecular weight compounds is high in DEE soluble fraction compared to EtOAc and THF fraction. This observation is based on the GC and GC-MS profiles. As can be seen from Figures 3.2 and 3.3, those represents the employment of various bases in depolymerization of Lignin, Alkaline and GC-MS profile of DEE soluble product extracted from the liquid layer. Reaction results presented in Figure 3.2 showed that, on increasing the basic strength of the catalyst, the percentage of DEE soluble products increases. It is known in the literature that the basicity of homogenous base changes with change in the counter cation part, and optimum basicity of catalyst is required to maximize the depolymerized product yield. Initially, catalytic experiment was done with LiOH (pH, 11.81) and obtained 25% yield of DEE soluble products along with 27% yield of EtOAc soluble products and 42% yield of THF soluble products. Further, counter cation of the base changed to Na (NaOH; pH, 12.65) and found that yield of DEE soluble products increased from 27% to 31% whereas the yield of EtOAc soluble products decreased from 27% to 18 %. The same trend can be seen in GC-MS profile, wherein the peak intensity of depolymerized products increased on changing the counter cation. Obtained results suggest that on increasing the basic strength of catalyst, the yield of depolymerized products is increasing. So, depolymerization of lignin was done with KOH (pH, 12.88), but surprisingly yield of DEE soluble products decreased from 31% to 12%, and THF soluble products yield

increased from 46 to 63 %. The possible reason for this behavior is higher basic strength of KOH compared to NaOH, which might be encouraging the repolymerization process in the catalytic run. To confirm this behavior, the reaction was carried out with CsOH (pH, 13.11), which has higher basic strength as compared to KOH and it was found that yield of DEE soluble products is almost similar while the yield of THF soluble products decreased from 63% to 56%. The decrease in the yield of THF soluble products is contradictory to the results obtained with KOH and the expectation that with an increase in basic strength repolymerization may increase. However, DEE soluble products yield is low in CsOH catalyzed reaction and THF soluble product yield is higher compared to NaOH. These results suggest that depolymerization activity increases with increase in basic strength of a catalyst, but it also encourages the repolymerization activity in the reaction. For the minimization of repolymerization, reactions were done with the weak bases such as Na_2CO_3 (pH, 11.1), $CaCO_3$ (pH, 9.0) and Cs_2CO_3 (pH, 11.1) and found that Na_2CO_3 (24%) and $CaCO_3$ (23%) showed similar DEE soluble products compared to Cs_2CO_3 (18%). Difference in the catalytic activity of Na_2CO_3 and Cs_2CO_3 is difficult to correlate based on reaction pH (11.1), but it is well known fact that basic strength increases on increasing the size of counter cation. High basic strength encourages the repolymerization and decreases the yield of DEE soluble products. Results are consolidated and represented in Figure 3.2A and B From Figure 3.2B, it is clear that among all the bases used for the depolymerization reaction, NaOH is an efficient catalytic system producing high DEE soluble products thus further reactions are carried out with this as a catalyst. GC-MS profiles are represented in Figure 3.3,

and results are explained by selecting four peaks, guaiacol (1); catechol and creosol (2); vanillin (3); acetovanillone (4). Peak pattern is similar in all cases but intensity is changing with respect to basic strength. Although, peak intensity of DEE soluble products is similar in case of NaOH (31%) and Na_2CO_3 (24%) but the yields were different. This difference in DEE soluble yield might be due to the change in basic strength as, NaOH is considered as the strong base and Na_2CO_3 as a weak base. With strong base NaOH, the degree of depolymerization will be higher, leading to the formation of different molecular weight compounds, some of them might not be detectable (for instance due to repolymerization to dimers, trimers etc. but still those are soluble in DEE). So that, NaOH has high DEE soluble products yield but intensity is similar to Na_2CO_3.

The same trend can be seen with LiOH, CsOH, CaCO$_3$, and Cs$_2$CO$_3$, in which difference in the peak intensity and DEE soluble product yield is dependent on the basic strength of used bases.
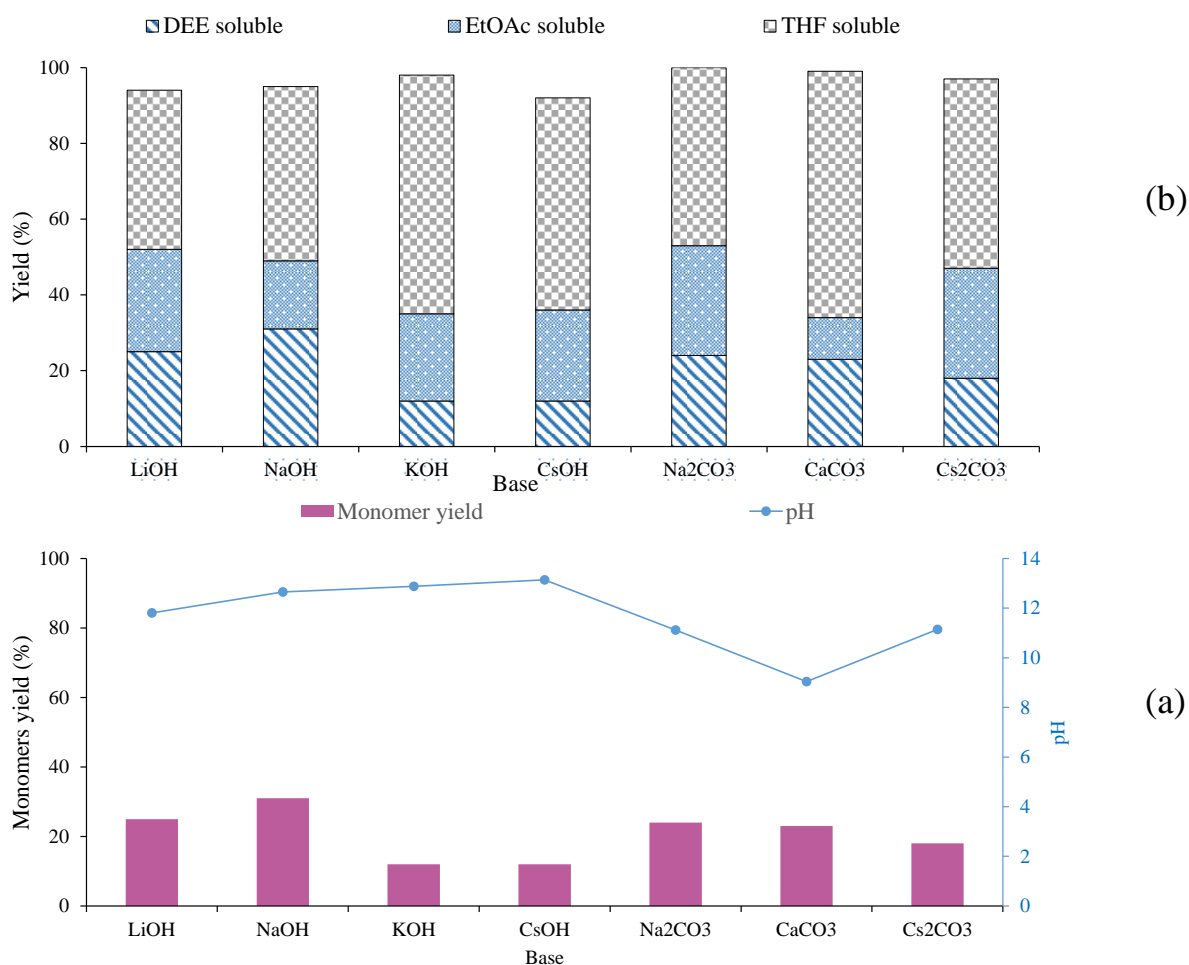
Figure 3.2. Depolymerization of lignin using various Bases

Reaction condition: Lignin, Alkaline 0.5 g; Base, 3.4 mmol; H$_2$O, 50 mL; 250 °C; 1 h; N$_2$, 2 MPa @ RT; 1000 rpm. DEE:diethyl ether, EtOAc:ethyl acetate, THF:tetrahydrofuran; (a) DEE soluble products yield; (b) DEE, EtOAc and THF soluble products yield.
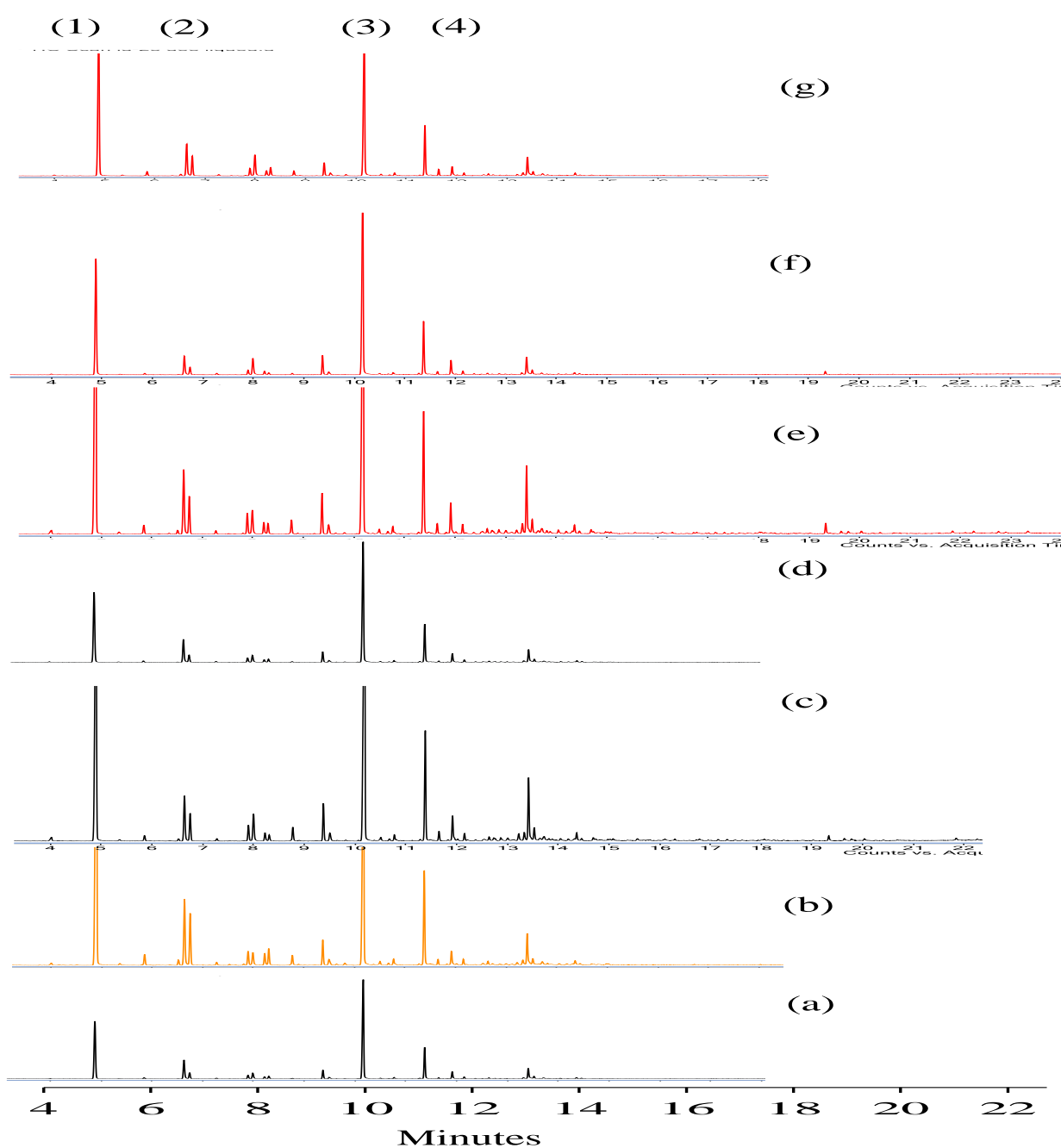
Figure 3.3. GC-MS profile of low molecular weight compounds extracted from the liquid layer using DEE solvent (a) LiOH; (b) NaOH; (c) KOH; (d) CsOH; (e) Na_2CO_3; (f) $CaCO_3$;(g) Cs_2CO_3; (1) guaiacol; (2) catechol and creosol; (3) vanillin; (4) acetovanillone;

3.3.2. Identification of depolymerized products

The identification of low molecular weight compounds formation was confirmed by GC-MS analysis. GC-MS profiles (Figure 3.4-3.6) of depolymerized products soluble in DEE and EtOAc suggests presence of low molecular weight compounds high in liquid layer compared to the solid layer, and most of them have molecular weight (Mw. < 350 Da). Obtained low molecular weight compounds were categorized as disubstituted monomer (guaiacol, 124 Da; veretrol, 138 Da; pyrocatechol, 110 Da; hydroquinone, 110 Da) and trisubstituted compound like 4-hydroxy-3-methoxybenzaldehyde, 152 Da; 1-(4-hydroxy-3methoxyphenyl)ethan-1-one, 332 Da; 1,2,3- trimethoxybenzene, 168 Da; 2,6-dimethoxyphenol, 154 Da; 3-methoxybenzne-1,2-diol, 140 Da; 3-ethyl-2-methoxyphenol, 152 Da; 2-methoxy-4methylphenol, 138Da; 1,2-dimethoxy-4propylbenzene, 180 Da; 4-(3-hydroxypropyl)-2-methoxyphenol, 182 Da).
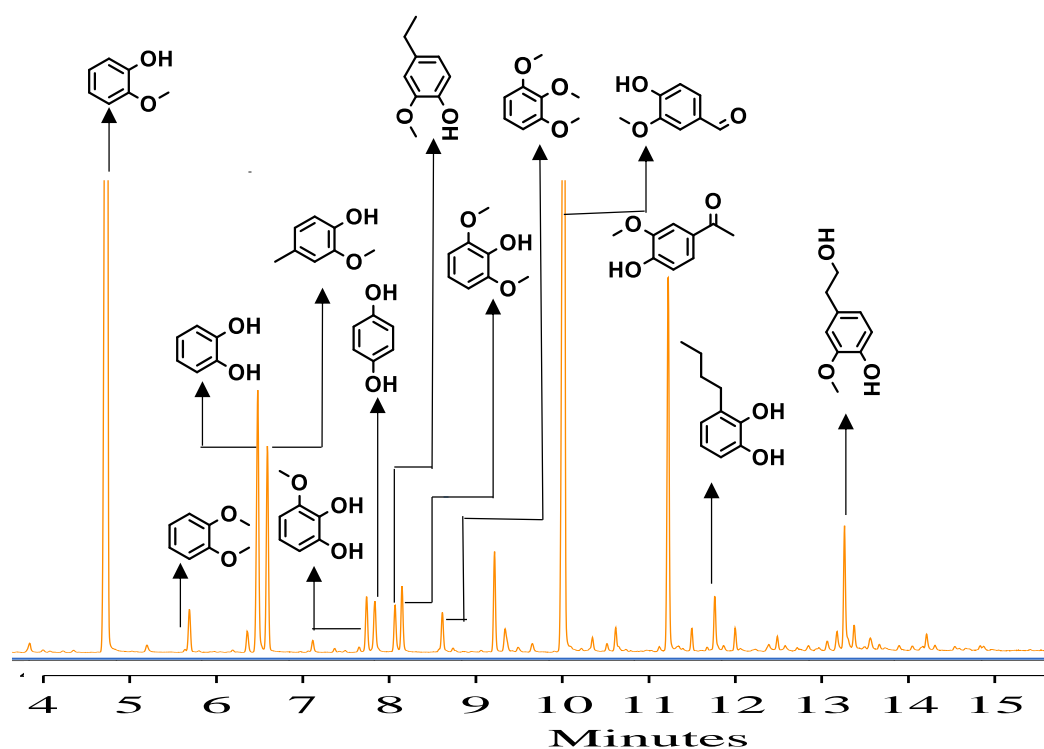
Figure 3.4. GC-MS chromatogram of products isolated in DEE ether (liquid layer)
Reaction condition: Lignin Alkaline, 0.5 g; NaOH, 3.4 mmol; H_2O, 50 mL; 250 ºC; 1 h; N_2, 2 MPa @ RT; 1000 rpm.
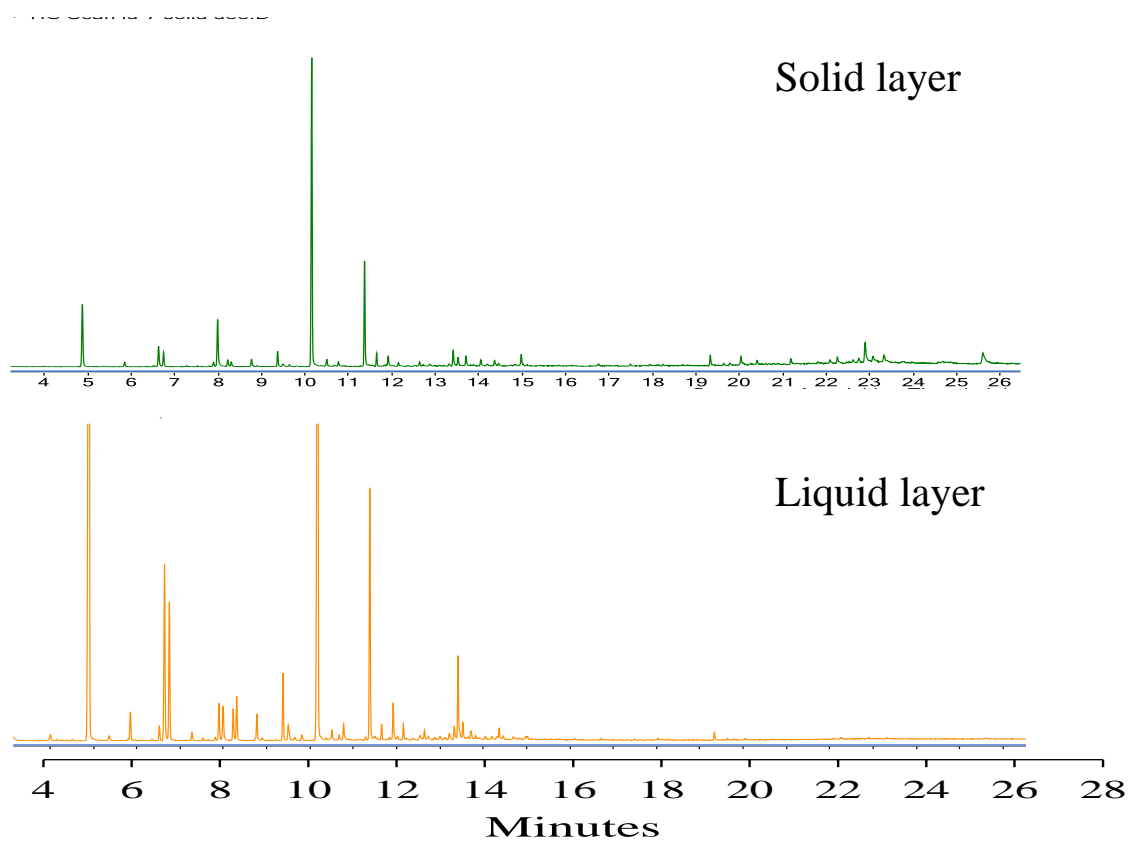
Figure 3.5. Comparative GC-MS chromatograms of products isolated in DEE (liquid layer, solid layer)

Reaction condition: Lignin Alkaline , 0.5 g; NaOH, 3.4 mmol; H_2O, 50 mL; 250 ºC; 1 h; N_2, 2 MPa @ RT; 1000 rpm

.
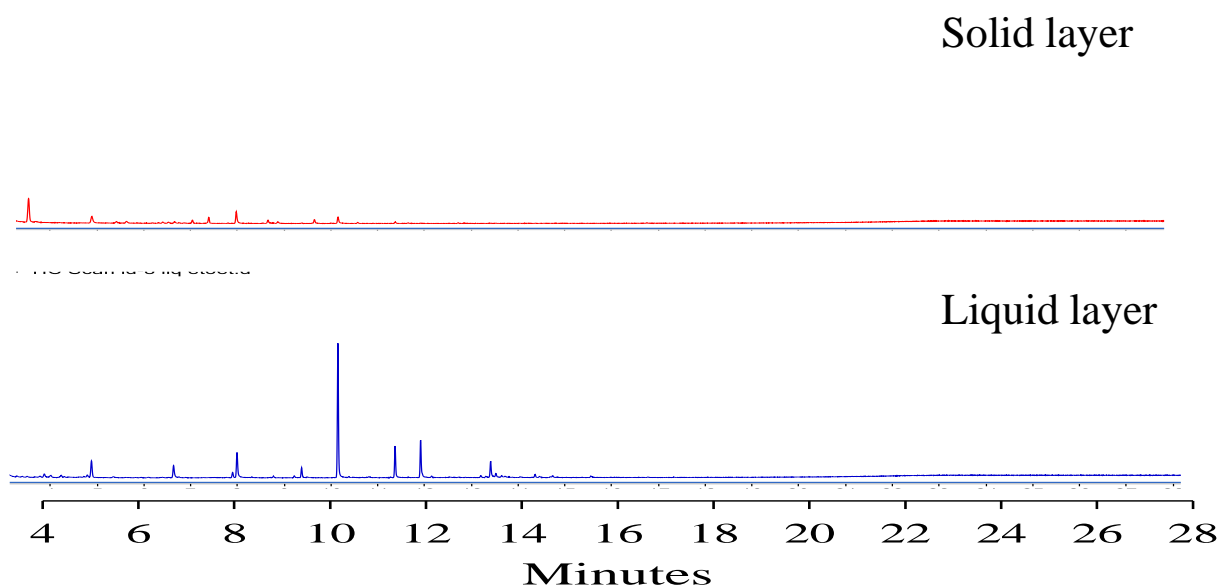
Figure 3.6. Comparative GC-MS chromatograms of products isolated in EtOAc (liquid layer, solid layer)
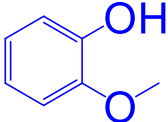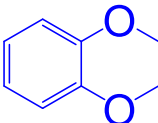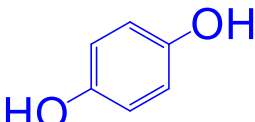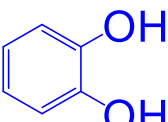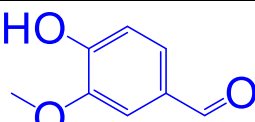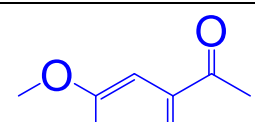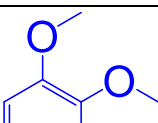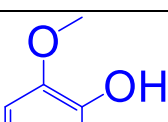
A careful analysis of GC-MS chromatograms (Figure 3.4- 3.6) of DEE and EtOAc extracted products from liquid and solid layers reveal that concentration of low molecular weight compounds is higher in liquid layer compared to solid layer. This phenomenon can be explained based on the isolation procedure, where DEE was used for the isolating products followed by EtOAc. However, the obtained weight of products isolated using EtOAc is high as compared to DEE. It is expected that low molecular weight compounds are present in the DEE layer whereas EtOAc layer contains low molecular weight compounds along with some high molecular weight compounds such as dimers and trimers.
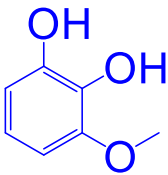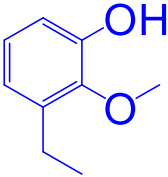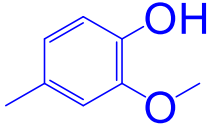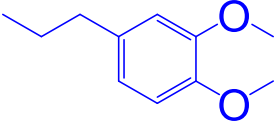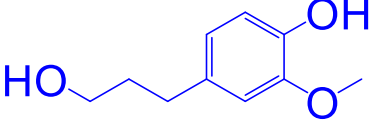
3.3.3. Quantification of depolymerized products

Lignin depolymerization produced low molecular weight compounds and identified by GC-MS analysis. Identified compounds were quantified by procuring commercially available standards. Details of quantified products and their structure are summarized in Table 3.2.

Table 3.2. Quantification of identified lignin depolymerized products

Reaction condition: Lignin, Alkaline 0.5 g; NaOH, 3.4 mmol; H_2O, 50 mL; 250 ºC; 1 h; N_2, 2 MPa@RT; 1000 rpm

Monomer	Structure	Yield (wt%)
Guaiacol		6
Veretrol		0.1
Hydroquinone		0.09
Pyrocatechol		0.8
Vanillin		2.8
Acetovanillone		1.8
1,2,3-trimethoxybenzne		0.1
2,6-dimethoxyphenol		0.08

3-methoxybenzene-1,2-diol		0.09
3-ethyl-2-methoxyphenol		0.06
2-methoxy-4-methylphenol		1.8
1,2-dimethoxy-4-propylbenzene		0.1
4-(3-hydroxypropyl)-2-methoxyphenol		0.3

Presence of alcohol functionality in almost all depolymerized products confirms the depolymerization taking place via hydrolysis path.

3.3.4. Effects of temperature and pressure

It was seen from the study with various bases that maximum yield of low molecular weight compound is possible with NaOH at 250 °C within 1 h. Further, temperature study was done to check the effect of temperature on depolymerization activity (Figure 3.7) and found that when the reaction was carried out at lower temperature 225 °C, decrease in the yield of DEE soluble products was observed from 31% to 14%. However, yield of THF soluble products is high (65%) compared to 250°C i.e., 46%. This result imply that depolymerization reaction required high energy to cleave the ether linkages, which is being supplied in the form of temperature. The same trend can be seen in GC-MS profile (Figure 3.8) wherein by lowering the temperature, peak intensity decreases and decrease in peak intensity is clear evidence of lower depolymerization activity.

Due to the decrease in depolymerized products yield upon lowering the temperature, it was decided to conduct the reaction at high temperature i.e., 275 °C but surprisingly decrease in DEE soluble products yield to 25% and an increase in the yield of THF soluble product (56%) was found. This phenomenon is the evidence of repolymerization reaction occurring at high temperatures. Moreover, it is essential to discuss that generally, depolymerization reaction was conducted at 2 MPa N_2 pressure (@RT), but system limitation restricted the use of the pressure to1.5 MPa N_2 (@RT) at 275 °C. However, it is important to note that the final pressure at both the temperatures was almost similar (7.2 MPa) and thus it is suggested that temperature plays crucial role in deciding the product distribution in the reaction. It was also decided to check the effect of pressure in depolymerization activity at constant temperature. The results are represented in Figures 3.9 and 3.10, and a reduction in the yield of DEE soluble product from 31% to 24% could be seen with reduction of pressure from 2 MPa to 1.5 MPa N_2, and further decrease in the pressure does not have significant effect on depolymerization activity.
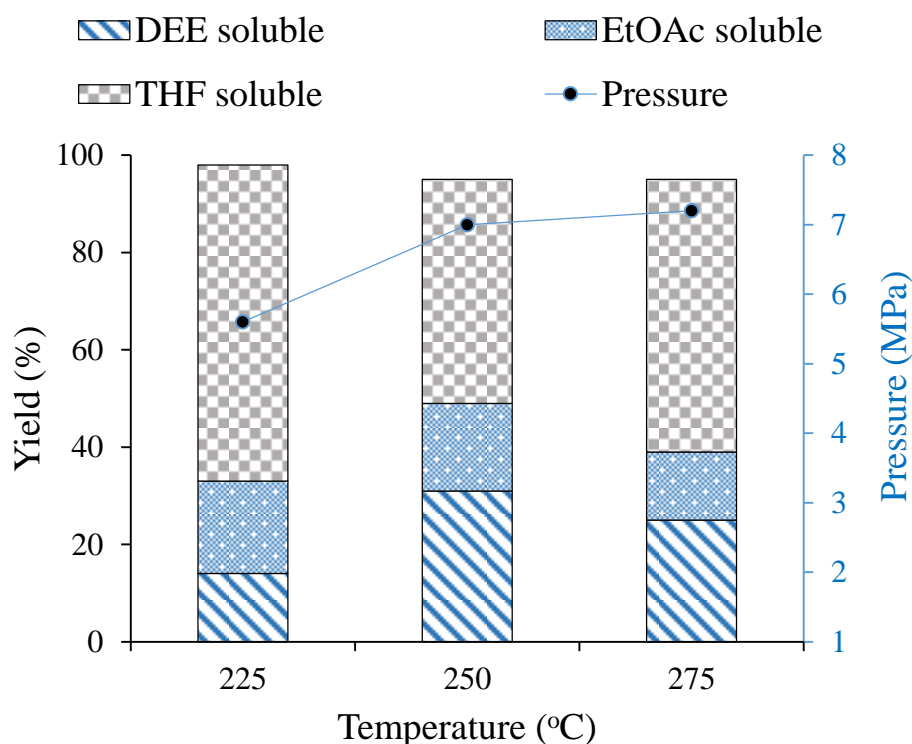
Figure 3.7. Effect of temperature on the depolymerization of Lignin, Alkaline

Reaction Condition: Lignin, Alkaline, 0.5 g; NaOH, 3.4 mmol; H_2O, 50 mL; 1 h; N_2, 2 MPa;

#At 275 ^{O}C, 1.5 MPa @RT; 1000 rpm; DEE: diethyl ether, EtOAc: ethyl acetate, THF: tetrahydrofuran
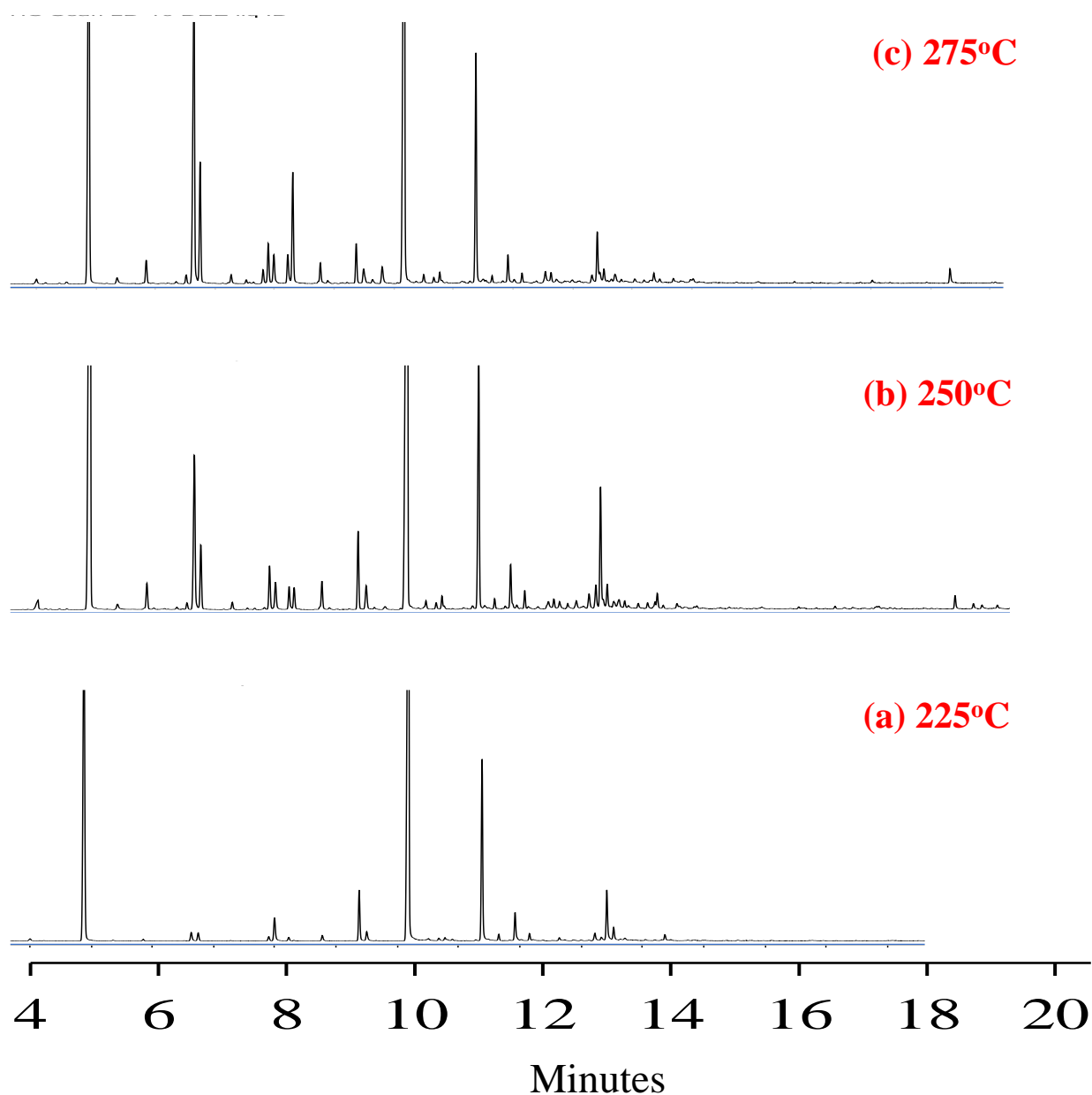
Figure 3.8. Comparative GC-MS chromatograms of DEE soluble product for the reaction conducted at different temperatures
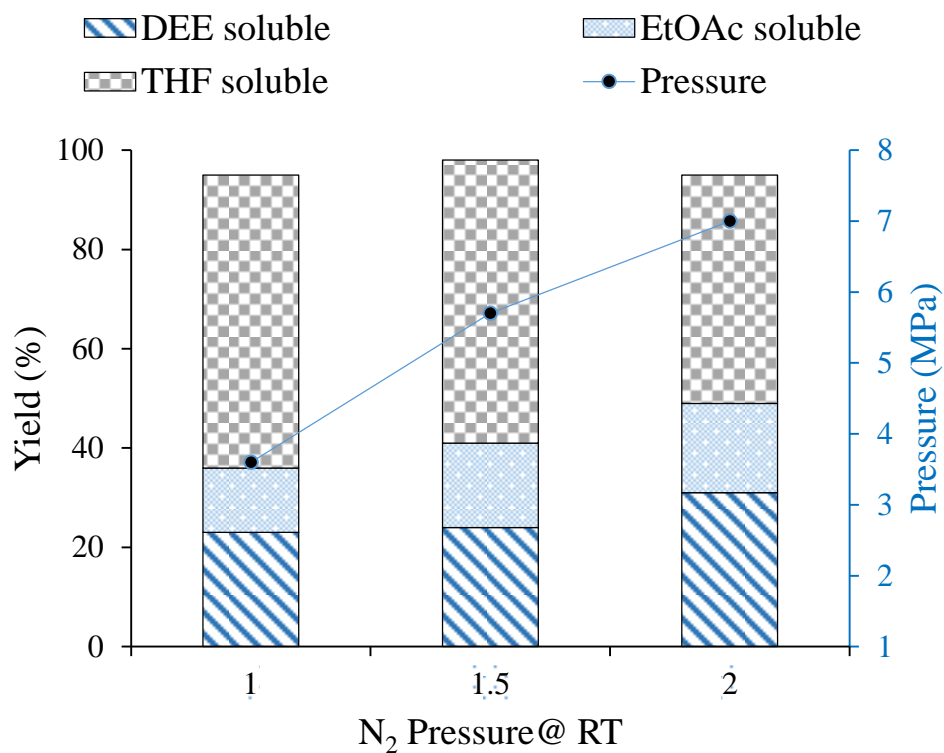
Figure 3.9. Effect of pressure on the depolymerization of Lignin, Alkaline

Reaction Condition: Lignin, Alkaline, 0.5 g; NaOH, 3.4 mmol; H_2O, 50 mL; 250 $^{\circ}$C; 1 h; 1000 rpm; DEE: diethyl ether, EtOAc: ethyl acetate, THF: tetrahydrofuran
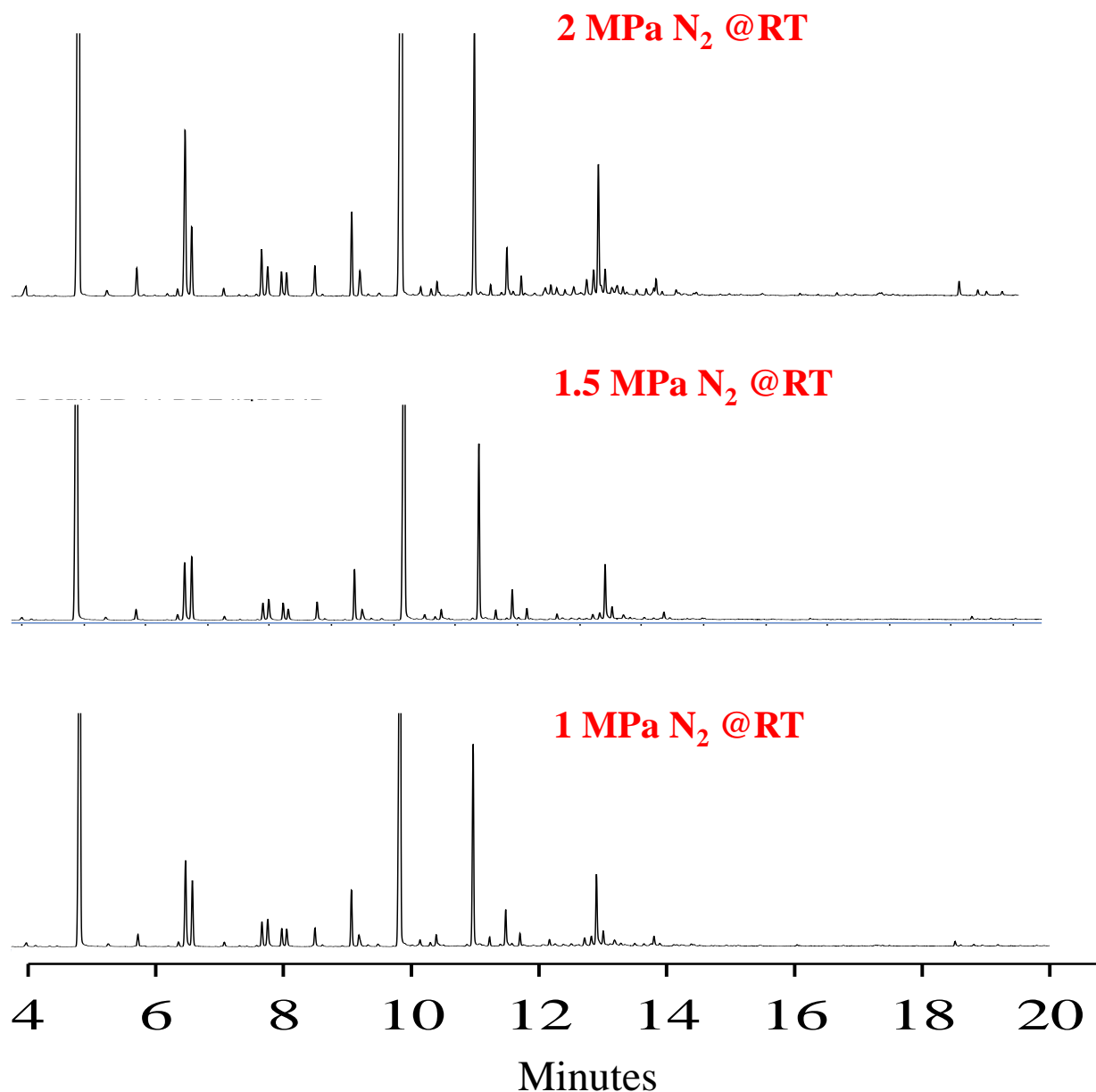
Figure 3.10. Comparative GC-MS chromatograms of reaction conducted at different pressure

3.3.5. Effects of time

Time studies were carried out to find out the effect of time on depolymerization activity. It was observed that 31% yield of DEE soluble low molecular weight compounds and 18% EtOAc, 46% THF soluble products yield was possible within 1 h at 250 ℃. It was also reported and can be seen in temperature study that repolymerization reaction is dominating under this

reaction condition. So, the reaction was carried out for 0.5 h (Figures 3.11 and 3.12), but decreased in the yield of DEE soluble products from 31% to 25% and EtOAc soluble products 14% to 12% was seen. But increase in the yield of THF soluble products from 46% to 58% was obtained. Higher yield of THF soluble products on lowering the time might be possible due to lower catalytic interaction and thus lower depolymerization activity. These results suggest that 0.5 h is not sufficient time to get maximum depolymerization products. Further, reaction time was increased to 1.5 h and found that again DEE soluble products yield decreased to 23%, which is even less than the yield obtained within 0.5 h and increased in the yield of EtOAc to 15% and THF to 54%. This indicates that on increasing the time, repolymerization of low molecular weight compounds is dominating in the reaction and responsible for the decrease in the yield of DEE soluble products.
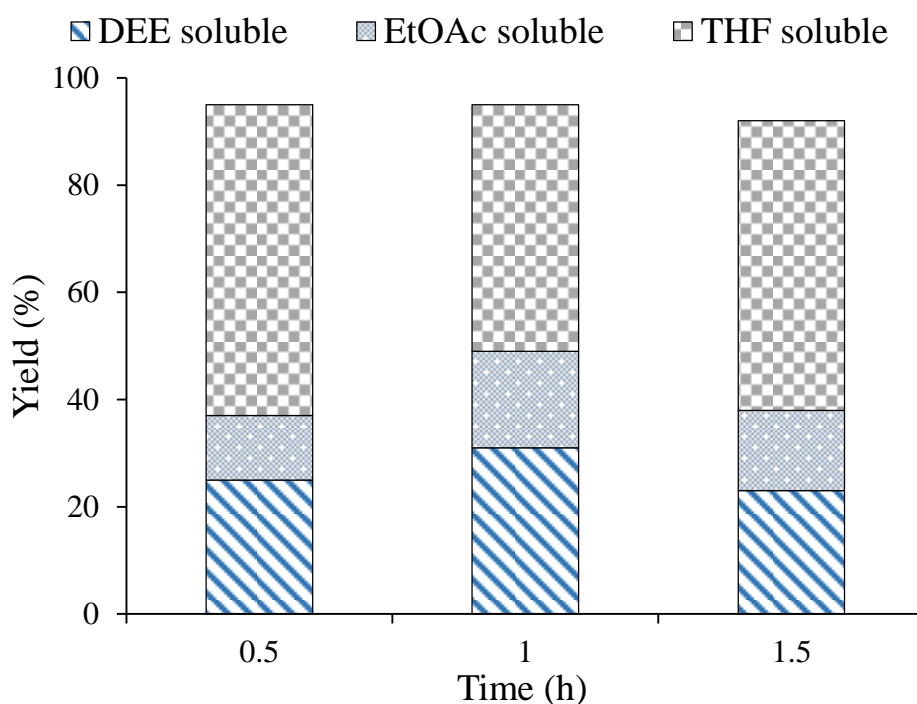
Figure 3.11. Effect of time on the depolymerization of Lignin, Alkaline
Reaction condition: Lignin, Alkaline 0.5 g; NaOH, 3.4 mmol; H_2O, 50 mL; 250 °C; N_2, 2 MPa @RT; 1000 rpm; DEE: diethyl ether, EtOAc: ethyl acetate, THF: tetrahydrofuran
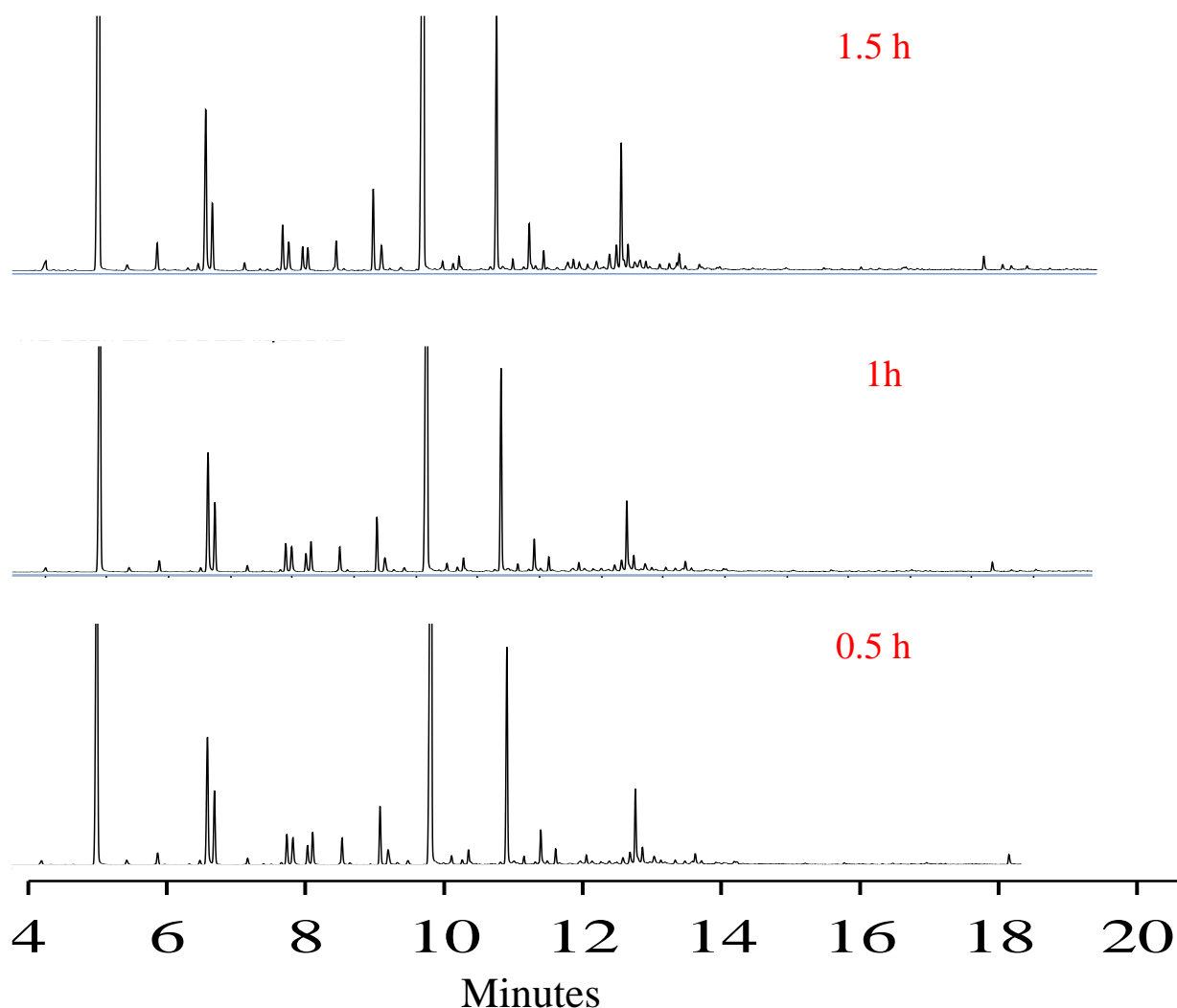
Figure 3.12. Comparative GC-MS chromatograms of DEE soluble product for the reaction conducted at different temperatures

3.3.6. Effect of lignin/NaOH ratio

All the above mentioned catalytic experiments were conducted using lignin/NaOH ratio of 3.6 (*wt/wt*) and (pH, 12.65). It was decided to increase the lignin/NaOH ratio for the depolymerization reaction. Generally, it is good to have high substrate to catalyst ratio, so catalytic activity was checked by increasing the ratio from 3.6 (pH, 12.65) to 7.3 (pH, 12.40) and 11 (pH, 12.29) Figures 3.13 and 3.14. It can be seen from the figure that the yield of DEE soluble products decreased to 19% at 7.3 and 17 % at 11 ratio. The decrease in the activity can be explained based on the availability of active catalytic sites and respective pH of the reaction mixture which is decreasing on increasing of the substrate to catalyst ratio. High substrate to

catalyst ratio implies lower catalytically active centers in the reaction. On increasing of the substrate to catalyst ratio yield of DEE soluble product is decreasing, so it was thought that lowering of the substrate to catalyst ratio may improve the yield of the DEE soluble product. So, the reaction was carried out with a ratio of 2.5 (pH,12.82) but decreased in the yield of DEE soluble products was seen, and this result is again the evidence of repolymerization, if catalytic active sites are more in the reaction mixture. Appearance of peak after 18 minute RT in the GC-MS profile of DEE soluble products presented in Figure 3.14 is a clear indication of repolymerization. It is well known fact that repolymerization is the major concern of base catalyzed depolymerization reaction. Proposed reaction mechanism in Figure 3.15 of the base-catalyzed depolymerization stated that repolymerized product formed in the reaction could not further be depolymerized due to formation of C-C bond [28].
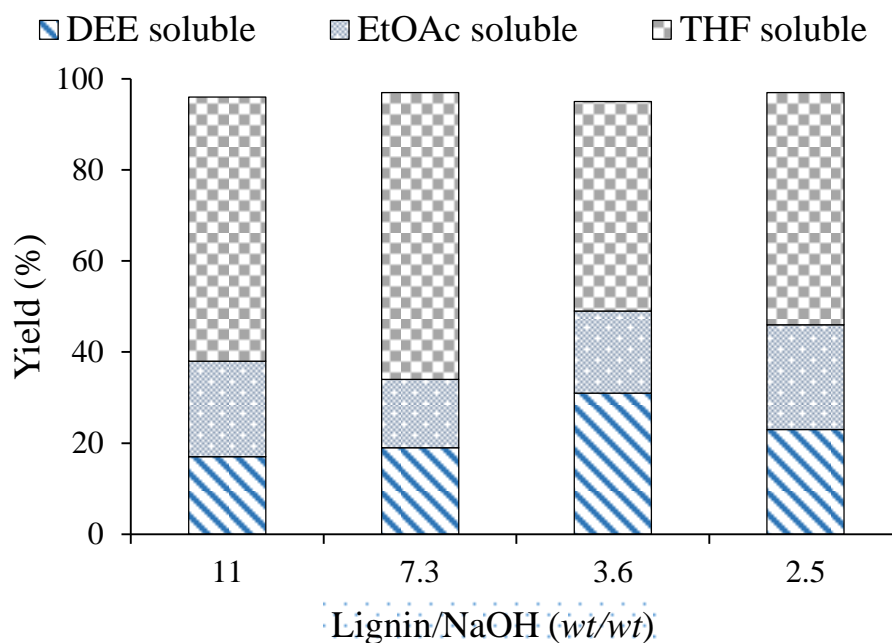
Figure 3.13. Effect of Lignin/NaOH ratio on the depolymerization of Lignin, Alkaline **Reaction condition**: Lignin Alkaline 0.5 g; NaOH; H_2O, 50 mL; 250 ℃; N_2, 2 MPa@RT; 1000 rpm; DEE: diethyl ether, EtOAc: ethyl acetate, THF: tetrahydrofuran
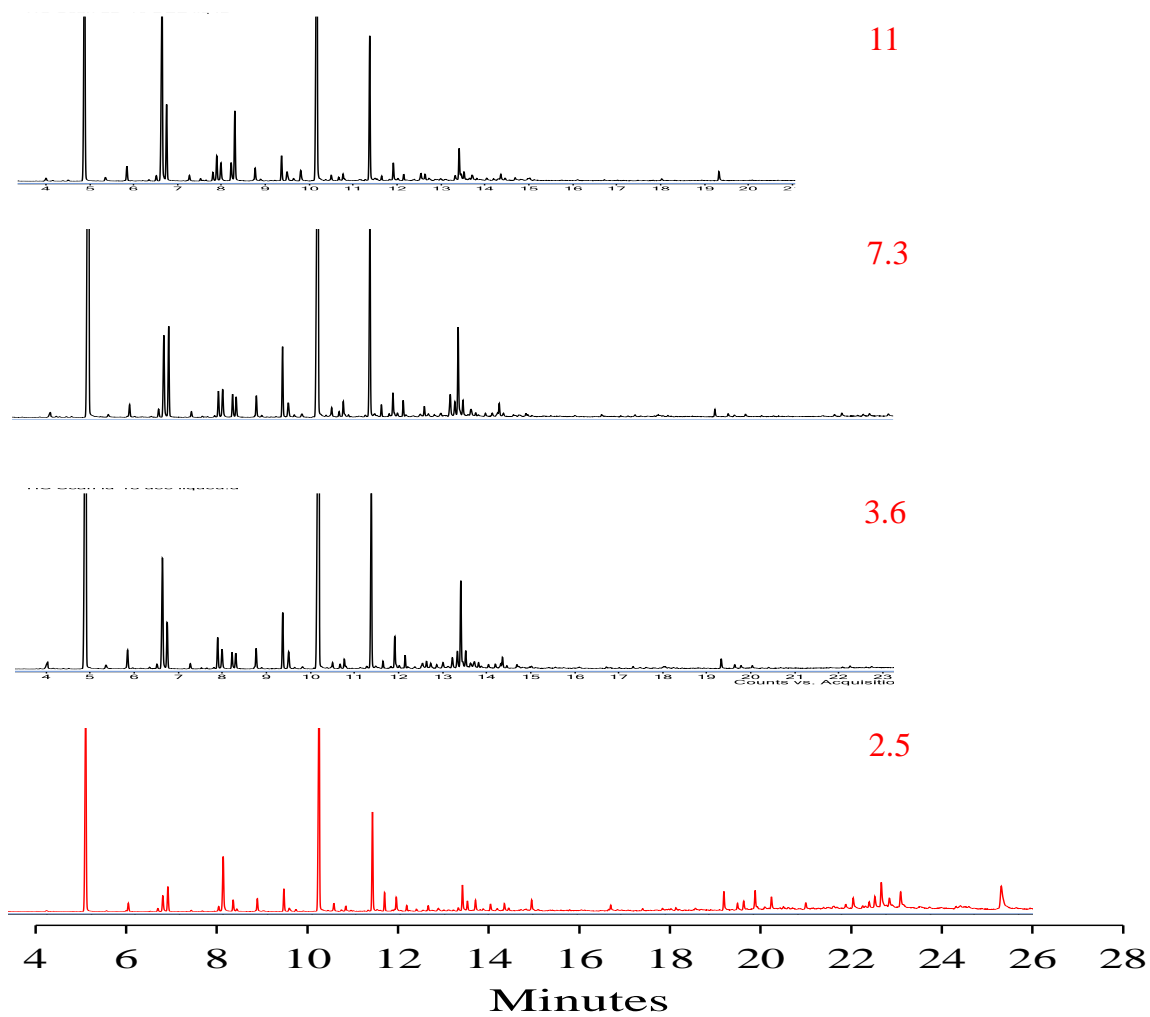
Figure 3.14. Comparative GC-MS chromatograms of DEE soluble products for the reaction conducted at different Lignin/NaOH (*wt/wt*)ratio
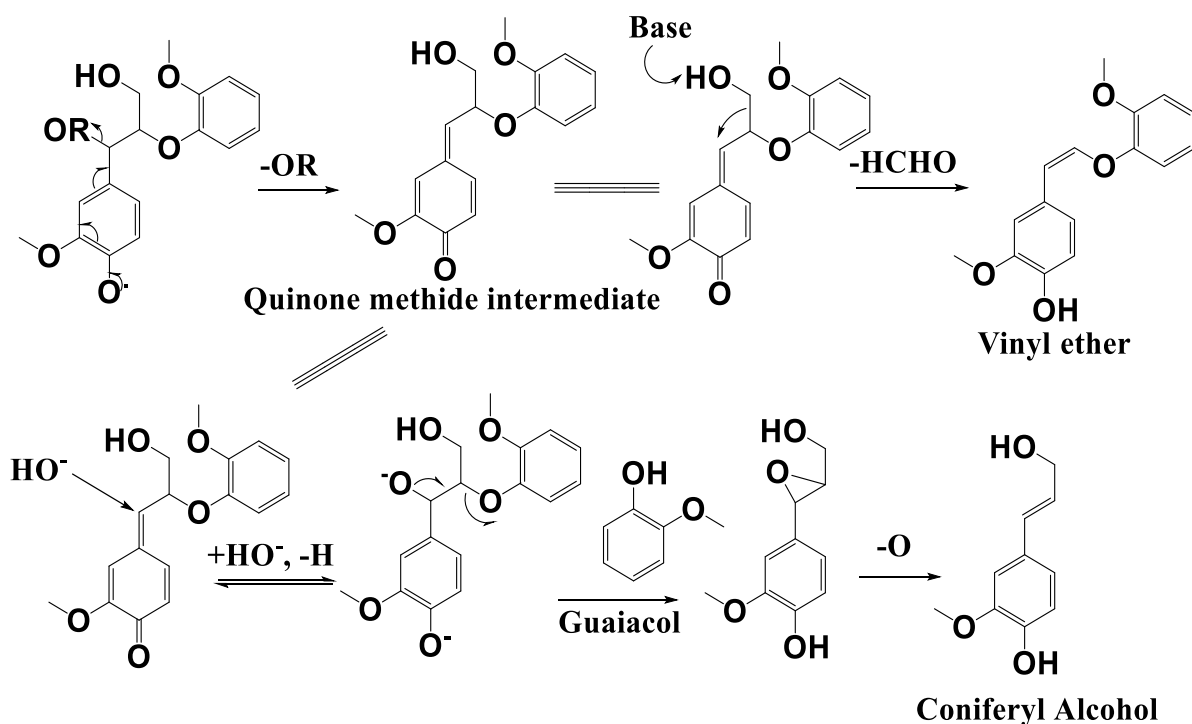
Figure 3.15. Reaction mechanism of base catalyzed depolymerization of Lignin, Alkaline [28]

3.3.7. Effect of various lignin substrates

The base catalyzed depolymerisation of different lignins (Lignin, Alkaline; Lignin, Dealkaline; Lignin, Alkali, Na-lignosulfonate lignin, Industrial K lignin, Industrial N lignin) was performed in water medium under the following reaction condition.

Lignin, 0.5 g; NaOH, 3.4 mmol; H_2O, 50 mL; 250 °C, 1 h, N_2, 2 MPa@RT

As seen in the Figures 3.16 and 3.17, with a change in lignin substrate, DEE soluble products yield was changed. Careful analysis of results suggests that catalytic activity depends on pH of the reaction mixture and molecular weight of the lignin substrate. In case of Lignin, Alkaline, DEE soluble products yield is maximum (31%) as compared to Lignin, Alkali (26%); Lignin, Dealkaline (27%) and Na-lignosulfonate lignin (29%). It was also noticed that pH of lignin sample is almost similar and vary between (12.35-12.65), but the corresponding molecular weight is different. The molecular weights of three lignins such as Lignin, Alkaline; Lignin, Dealkaline and Lignin, Alkali are in the range between 52000-60000 Da and their DEE soluble products yield varies between 27%-31%. The small difference in the activity is due to the difference in their chemical environment. However, Lignin, Dealkaline has molecular weight

of 60000 Da, and showed lower DEE soluble products yield (27%). It may be due to lower in pH of the reaction mixture and same trend can be seen in both industrial lignin, in which pH of reaction mixture is almost similar to the Lignin, Dealkaline and showed lower DEE soluble products yield i.e., industrial K lignin 25% and industrial N lignin 14%.

Mw. (Da)	60,000	28000	60,000	52,000	-	-
pH of R.M.	12.65	12.53	12.30	12.48	12.35	12.38
(%) solubility in alkaline H_2O	100	100	100	100	100	100
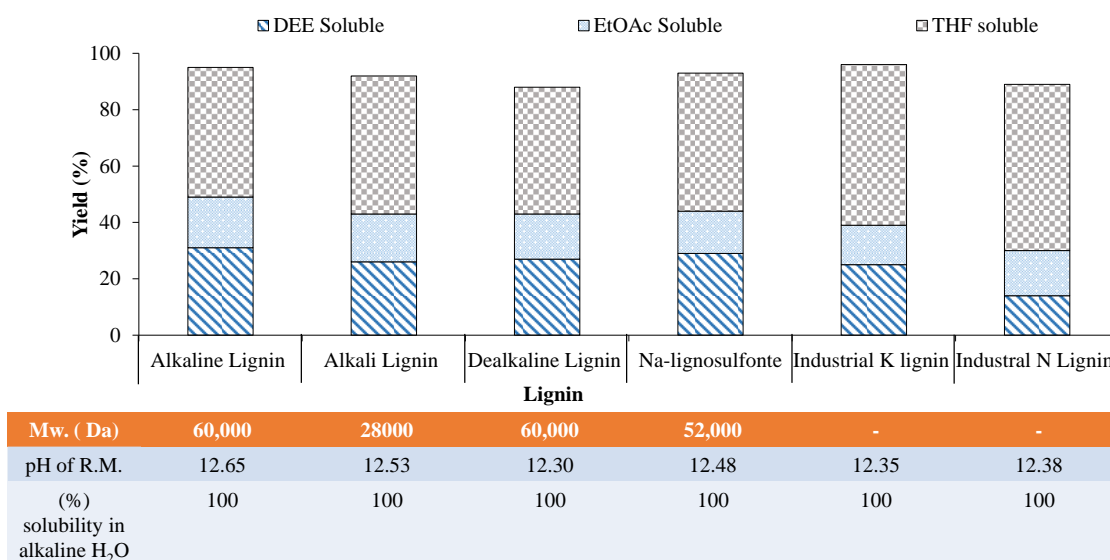
Figure 3.16. Depolymerisation of different lignin

Reaction conditions: Lignin, 0.5 g; NaOH, 3.4 mmol; H_2O, 50 mL; 250 °C; 1 h; N_2, 2 MPa; DEE: diethyl ether; EtOAc: ethyl acetate; THF: tetrahydrofuran
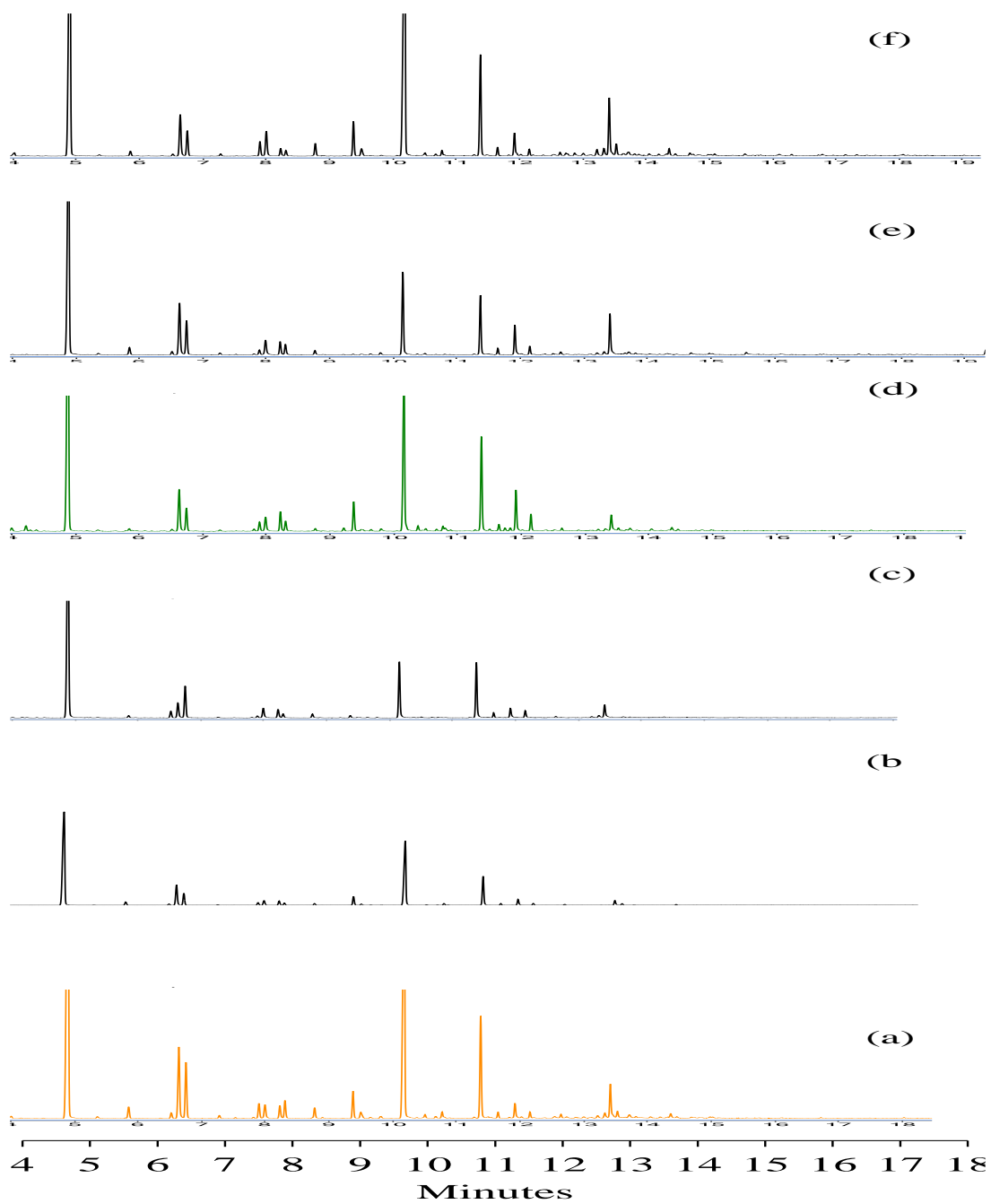
Figure 3.17. Comparative GC-MS chromatograms of DEE soluble product for the reactions conducted with different Lignin substrates

3.3.8. Confirmation of low molecular weight products formation: GC-MS, LC-MS, MALDI-MS

Initially, formation of low molecular weight compounds was confirmed by GC-MS technique. There is a chance that the products soluble in organic solvent (DEE, EtOAc), may degrade at high operating temperature of GC-MS as compared to the reaction temperature to form low molecular weight compounds. To eliminate this possibility, organic solvent-soluble products were analyzed by LC-MS and MALDI-TOF techniques. Based on these two techniques, it was found that low molecular weight compounds are present in the organic mixture. Another aspect of this study is the distribution of products isolated from the solid layer and liquid layer. It was seen that peak intensity of low molecular weight compounds is high in the liquid layer as compared to solid layer (Figures 3.5 & 3.6), and the presence of high molecular weight compounds was seen in EtOAc and THF soluble products (Figures 3.18 - 3.21). This is in agreement with previous observation, where it was stated that DEE contains low molecular weight compounds and EtOAc has low molecular weight compounds as well as oligomers and high molecular weight compounds.

LC-MS profile of depolymerized product present in liquid layer
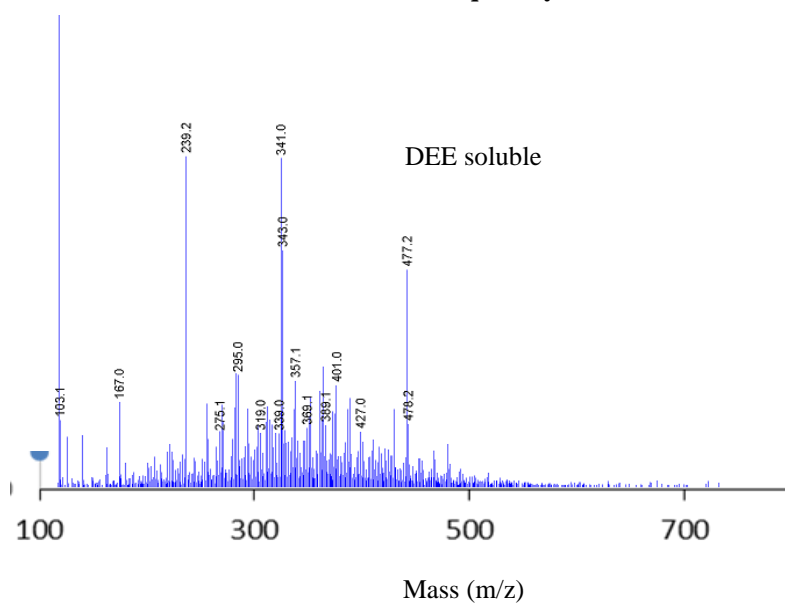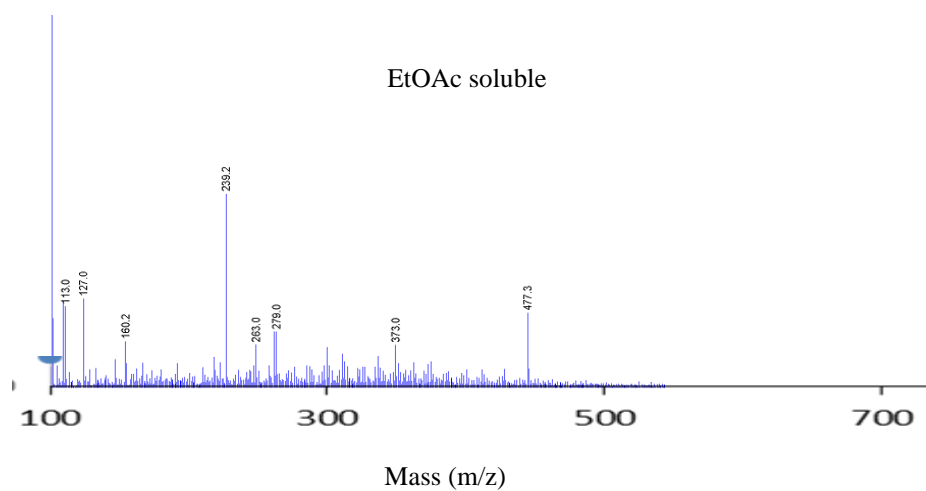
Figure 3.18. Comparative LC-MS chromatograms of depolymerized products extracted from liquid layer

LC-MS profile of depolymerized product present in solid layer
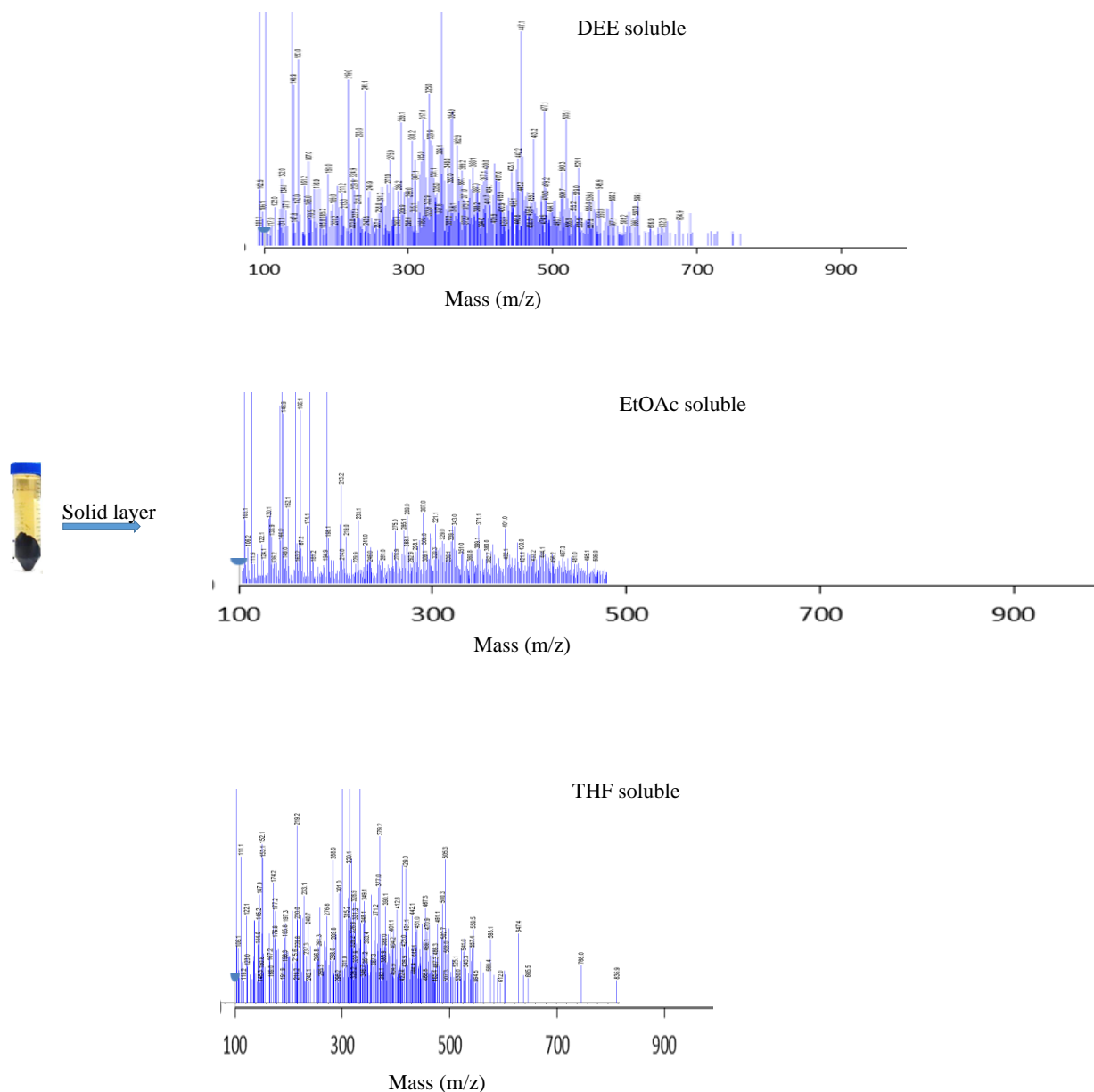
Figure 3.19. Comparative LC-MS chromatograms of depolymerized products extracted from the solid layer

DEE soluble liquid

DEE soluble solid

Figure 3.20. Comparative MALDI-MS chromatograms of depolymerized products extracted from the liquid layer
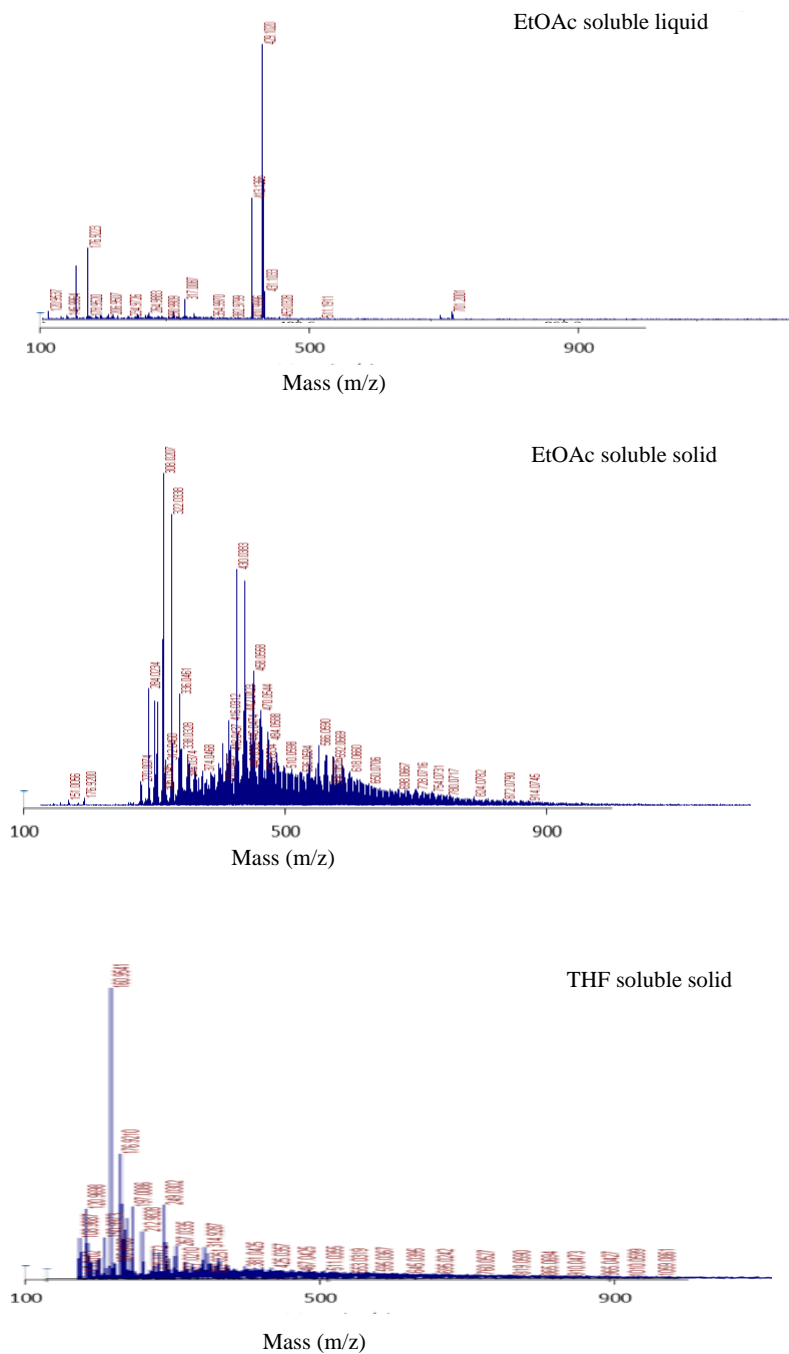
Figure 3.21. Comparative MALDI-MS chromatograms of depolymerized products extracted from the solid layer

3.3.9. Lignin and products characterization

Characterizations of the depolymerized products were done to correlate the presence of different functionalities which are present in the substrate i.e., Lignin and products. FT-IR analysis of organic solvent (DEE, EtOAc) soluble products was done and represented in Figure 3.22 A close analysis of FT-IR spectra of lignin, alkaline and depolymerized products soluble in DEE and EtOAc layer suggests that peak intensity of hydroxyl group (3500-3100 cm^{-1}), methyl and methylene group (2970-2830 cm^{-1}) has been increased in the depolymerized products. It is obvious because depolymerized products contains free hydroxyl and methoxy groups linked to aromatic backbone. The number of these groups increases after depolymerization. Other functional groups present in the lignin substrate matches well with depolymerized products. These results indicate that lignin is effectivity depolymerized into low molecular weight compounds and depolymerized products have retained the functional groups present in parent lignin sample.

Lignin, Alkaline
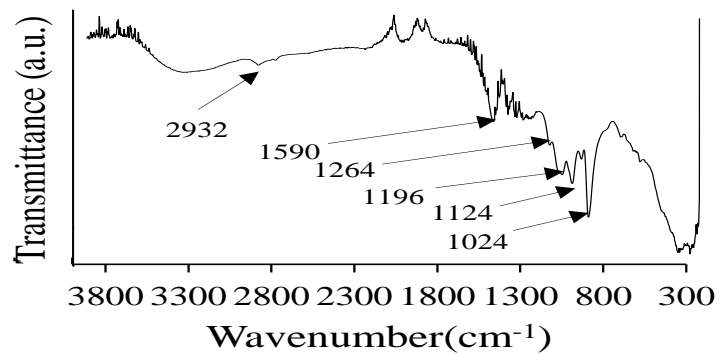
DEE Soluble liquid
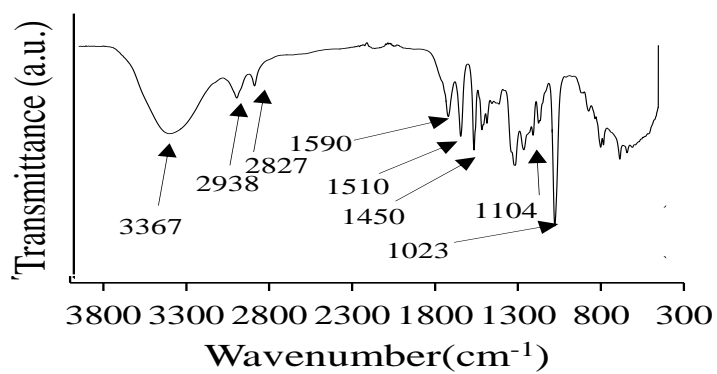
DEE soluble solid
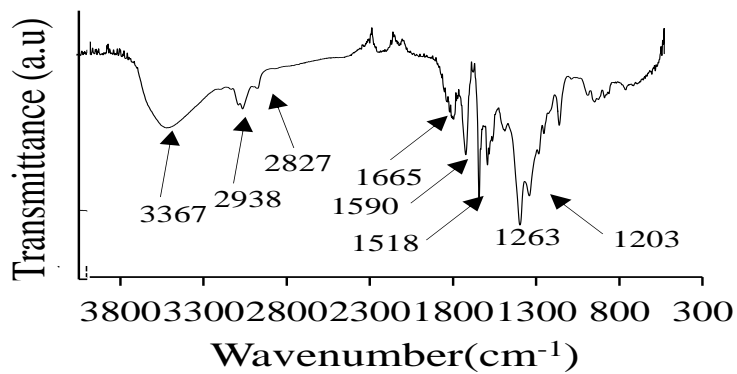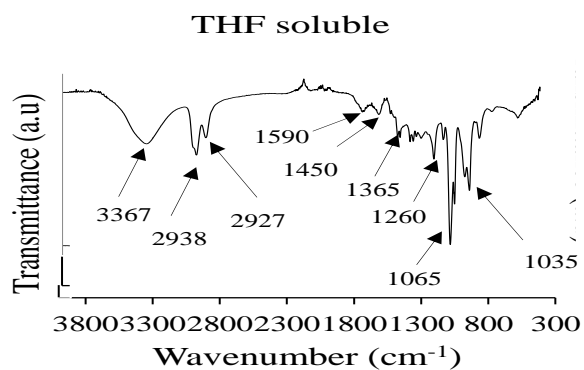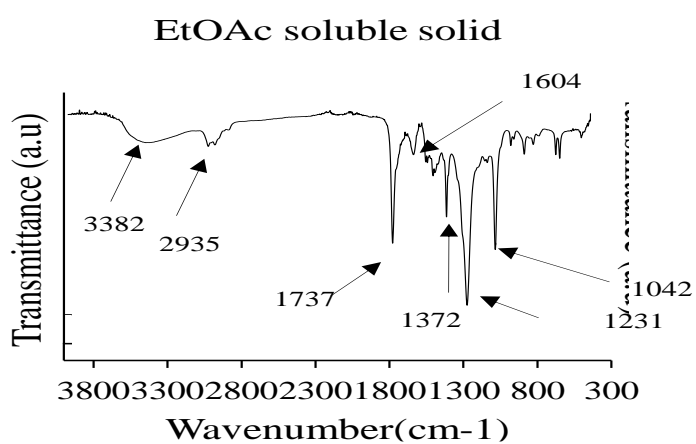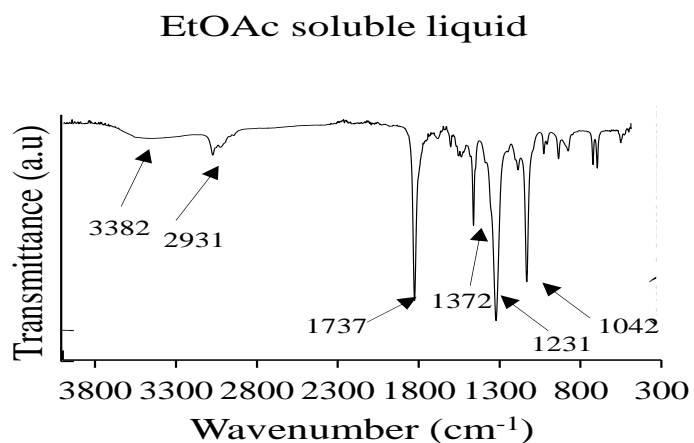
Figure 3.22. FT-IR spectra of Lignin, Alkaline and organic solvent soluble low molecular weight compounds

Table 3.3. Correlation between different functional groups of lignin and depolymerized products

Band (cm^{-1})	Type of vibration	Wavenumber (cm^{-1})		
		Lignin, Alkaline	Products extracted from liquid/solid layer using DEE	Products extracted from liquid/solid layer using EtOAc
3500-3100	Alcoholic and phenolic O-H stretching	3349	3367/3367	3382/3382
2970-2830	C-H asymmetric stretching in methyl and methylene group	2932,	2938/2938 2833/2833	2931/2935
1615-1590	C=O stretching with aromatic skeleton vibrations	1590	1590/1590	-
1530-1500	Aromatic skeleton vibrations	-	1510/1518	-
1300-1200	C-C, C-O, C=O stretching in guaiacyl units	1264	-/1263	1231
1195-1124	Deoformation vibration of C-H bond in syringyl rings	1196	1104	-
1030-1010	C-O stretching in alcohol, ether/ in plane deformation vibration of C-H bond in aromatic rings	1024	1023/1025	1023/1023

3.3.10. Proof for the solubility of lignin and depolymerized products

It was seen in catalytic experiments that initially lignin is soluble in alkaline water and after the completion of reaction when the reaction mixture was acidified by 2N H_2SO_4 and kept for

centrifugation, two layers are formed (liquid layer and solid layer). Products after the catalytic reaction were isolated from both the layers and analyzed using GC-MS, LC-MS, and MALDI-MS. It was also seen that peak intensity of products isolated from liquid layer is higher as compared to the solid layer. To confirm the probability that the solid layer may contain lignin or depolymerized products, controlled experiment was carried out without temperature and pressure treatment as represented in Figure 3.23, After the experiment, reaction mixture was acidified and centrifuged. It was seen that only one layer was present in the reaction mixture as against two layers observed in typical reaction. Thus, the results of the controlled experiment proved that solid layer may also contain the depolymerized products. It is fascinating to see that the lignin substrate is soluble in similar conditions, but the depolymerized product is not. To find out the reason of the unusual behavior, another controlled experiment was designed with lignin model compounds. In this experiment, mixture of lignin model compounds such guaiacol, vanillin, and eugenol and their mixture as represented in Figure 3.23 and 3.25 was made. Initially, substrates (guaiacol, vanillin, eugenol and mixture of three of 0.2 g each) were taken in 20 mL water. It is observed that guaiacol and vanillin are sparingly soluble in aqueous solution where as eugenol was insoluble. Possible reason of this observation is that may be due to alkyl chain present in eugenol substrate, it has become more hydrophobic than other substrates. Further, 0.05 g of NaOH was added in the corresponding solution and it was found that the solubility of all the substrates increased and dissolves completely in alkaline water. This is obvious because in alkaline water exists in ionic form. Thus their solubility was increased. Then the resultant mixture was acidified by 2N H_2SO_4 and kept for centrifugation and noticed that guaiacol and vanillin is soluble in water solution, but eugenol settled down to the bottom of the centrifuge tube. This behaviour can be explained based on hydrophobicity and hydrophilic nature of lignin and depolymerized product. Initially lignin is soluble in alkaline water because it has various functional groups (heteroatom) and attached to it, but after the depolymerization cleavage of linkages decreases the functional group present in the depolymerized product and its hydrophilic nature changed to hydrorophobic nature. A careful analysis of base catalyzed depolymerization reaction mechanism (Figure 3.13) suggested that in repolymerization process C-C bond formation is preferred, which will also decrease the functionally of depolymerized product.
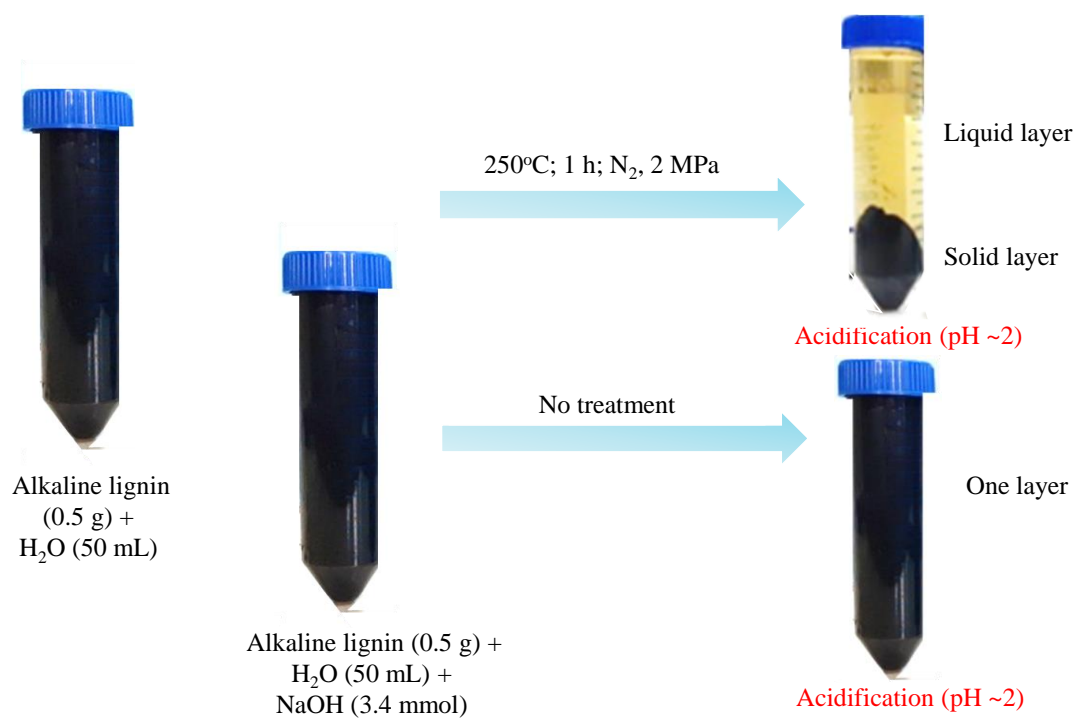
Figure 3.23. Solubility behavior of lignin and depolymerized products

Labels in figure:
- Alkaline lignin (0.5 g) + H$_2$O (50 mL)
- Alkaline lignin (0.5 g) + H$_2$O (50 mL) + NaOH (3.4 mmol)
- 250°C; 1 h; N$_2$, 2 MPa
- No treatment
- Liquid layer
- Solid layer
- One layer
- Acidification (pH ~2)
- Acidification (pH ~2)
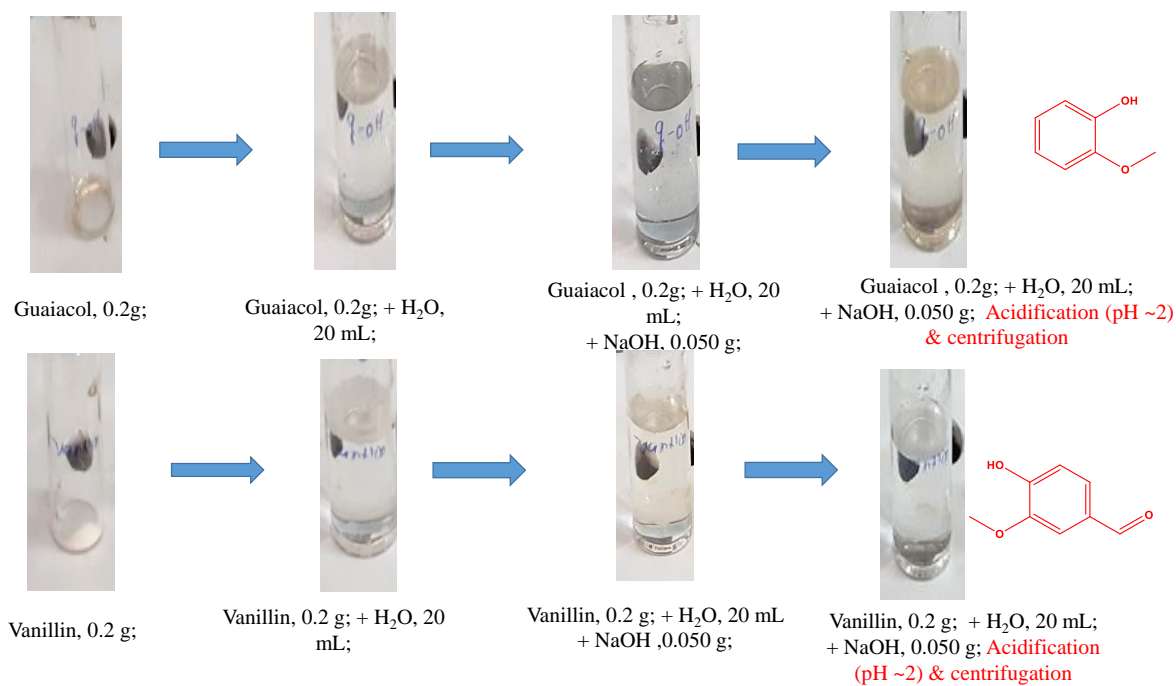
Figure 3.24. Model compound study for the solid product formation
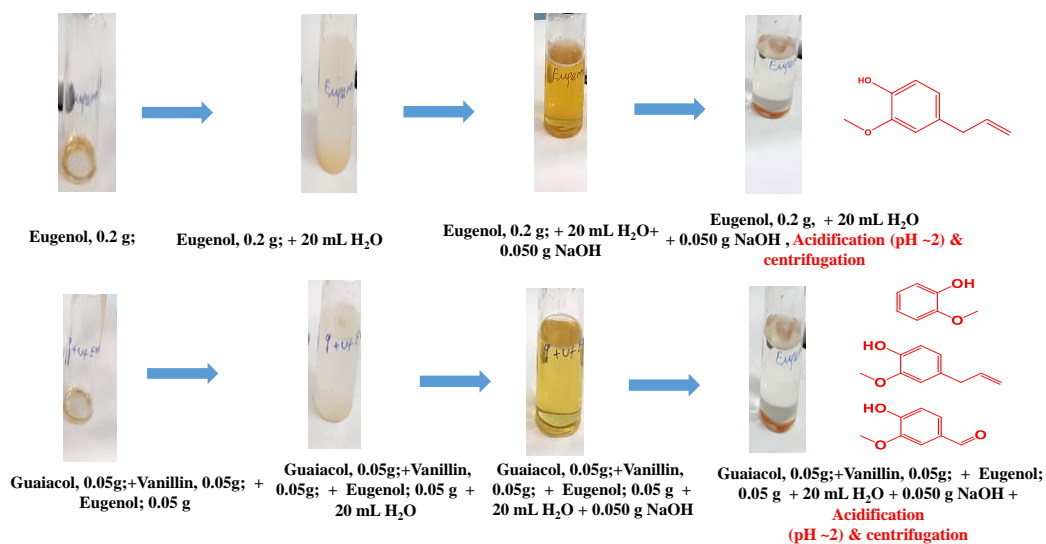
Figure 3.25. Model compound study for the solid product formation

3.4. Conclusion

In summary, various sources of lignin was effectively depolymerized into low molecular weight in alkaline water at 250 $^{\circ}$C under 2 MPa N_2 pressure using homogeneous bases. Among all used bases NaOH was found as best catalytic system for the lignin depolymerization. Model compound study was carried out to understand the product distribution of base catalyzed lignin depolymerization. It was seen that decrease in solubilty of depolymerized product is due to decrease of hydrophilicity and alkyl chain compound present in depolymerized product. FT-IR study of depolymerized product suggests that most of functional group retain, which were present in the lignin. This proves that total atom efficiency is maintained in this process.

3.5. References:

1.   Deuss, P. J.; Barta, K., From models to lignin: Transition metal catalysis for selective bond cleavage reactions. *Coordination Chemistry Reviews* **2016,** *306*, 510-532.

2.   Ferdosian F, Y. Z., Anderson M and Xu C, Synthesis of lignin-based epoxy resin: optimization of reaction parameters using response surface methodology, *RSC Adv* **2014,** *4* (60), 31745-

31753.

3.   Laurichesse S and Avérous L, Chemical modification of lignins: Towards biobased polymers. *Prog Polym Sci* **2014,** *39* (7), 1266-1290.

4.   F. Cherubini and A. H. Strømman, *Biofuels, Bioprod. Biorefin.,* **2011,** *5,* , 548-561.

5.   I. Delidovich, P. J. C. H., L. Deng, R. Pfützenreuter,; M. Rose and R. Palkovits, *Chem. Rev* **2015,** *DOI: 10.1021/ acs.chemrev.5b00354*.

6.   J. H. Lora and W. G. Glasser, *J. Polym. Environ* **2002,** *10,* 39-48.

7.   W. Thielemans, E. C., S. S. Morye and R. P. Wool; *J. Appl. Polym. Sci* **2002,** *83,* , 323-331.

8.   D. Stewart, *Ind. Crops Prod* **2008,** *27*, 202-207.

9.   G. Xu, J.-H. Y., H.-H. Mao and Z. Yun; Fuels Oils, *Chem. Technol.* **2011,** *47,* 283-291.

10.   G. Vazquez, C. R.-B., S. Freire, J. Gonzalez-; Alvarez and G. Antorrena, *Bioresour. Technol.* **1999,** *70,* 209-214.

11.   L. Hodásová, M. J., A. Skulcová and A. Ház, *Wood Res.* **2015,** *60*, 973-986.

12.   C. Li, X. Z., A. Wang, G. W. Huber and T. Zhang, *Chem. Rev.,* **2015,** *115*, 11559-11624.

13.   M. P. Pandey and C. S. Kim, *Chem. Eng. Technol* **2011,** *34,* , 29-41.

14.   J. Zakzeski, P. C. B., A. L. Jongerius and; B. M. Weckhuysen, *Chem. Rev* **2010,,** *110,* , 3552-3599.

15.   Q. Yaoa, Z. T., J.-h. Guoa, Y. Zhanga and Q.-x. Guoa, Chin., *J. Chem. Phys* **2015,** *28*, 209-216.

16.   ] K. Barta, P. C. F., *Acc. Chem. Res.* **2014,** *47* 1503-1512.

17.   A.J. Soria, A. G. M., S.R. Shook, , *Holzforschung* **2008,** *62*, 402-408.

18.   ] Ch. Schacht, C. Z., G. Brunner, *J. Supercrit. Fluids* **2008,** *46*, 299-321.

19.   H. Wang, G. G., R.D. Rogers, *Chem. Soc. Rev.* **2012,** *41*, 1519-1537.

20.   ] R. Rinaldi, R. P., F. Schüth, *Angew. Chem. Int. Ed* **2008,** *47*, 8047-8050.

21.   P.J. Deuss, K. B., J.G. de Vries, *Catal. Sci. Technol.* **2014,** *4*, 1174-1196.

22.   *J.S. Shabtai, US5959167 A (1999).*

23.   J.E. Miller, L. E., A.E. Littlewolf, D.E. Trudell, *Fuel* **1999,** *78*, 1363-1366.

24.   V.M. Robert, V. S., T. Reiner, A. Lemonidou, X. Li, J.A. Lercher, *Chem. Eur. J.* **2011,** *17*, 5939-5948.

25.   Richa Chaudhary, P. L. D., *Green Chem.* **2017,** *19*, 778-788.

26.   Shabtai, J. S. Z., W.W.Chornet, *Process for conversion of lignin to reformulated hydrocarbon gasoline. U.S. Patent 5,959,167, September 28, 1999.*

27.   Deepak Raikwar, S. M., Debaprasad Shee, *Green Chem.* **2019** *21*, 3864.

28.   *Wood.Sci.Technol* **1980,** *4*, 241-266

Chapter 4A

Understanding the influence of alumina supported Ruthenium catalyst synthesis and reaction parameters on the hydrodeoxygenation of lignin derived monomers

4A.1. Introduction

As discussed earlier (Chapter 3), base catalyzed lignin depolymerization produced low molecular aromatic compounds. It was also discussed that these low molecular weight compounds have high potential applications to replace fossil based fuel and chemicals, but complexity (mixture of various aromatic monomer) of formed low molecular weight compounds restricted their applications. Another discussion was made that up-gradation of these low molecular weight compounds will help in improving its efficiency as the potential candidates for the application as fuels and chemicals. A simple calculation for the O/C ratio of lignin, alkaline ($C_{8.7}H_{9.1}O_{5.1}S_{0.13}$, O/C, 0.58), and its derived low molecular weight compound such as guaiacol ($C_7H_8O_2$, O/C, 0.28) suggests that they have high O/C ratio. Up-gradation of these low molecular weight compounds reduces the O/C ratio and improves its potential application as a fuel and chemical. So, it was decided to carry out up-gradation of obtained low molecular weight compounds, firstly up gradation was carried out by defunctionalisation of lignin derived low molecular weight compounds using supported metal catalysts and external source of molecular H_2. This strategy is known as HDO (Hydrodeoxygenation/Defunctionalisation) of lignin derived low molecular weight compounds (Scheme 4A.1).
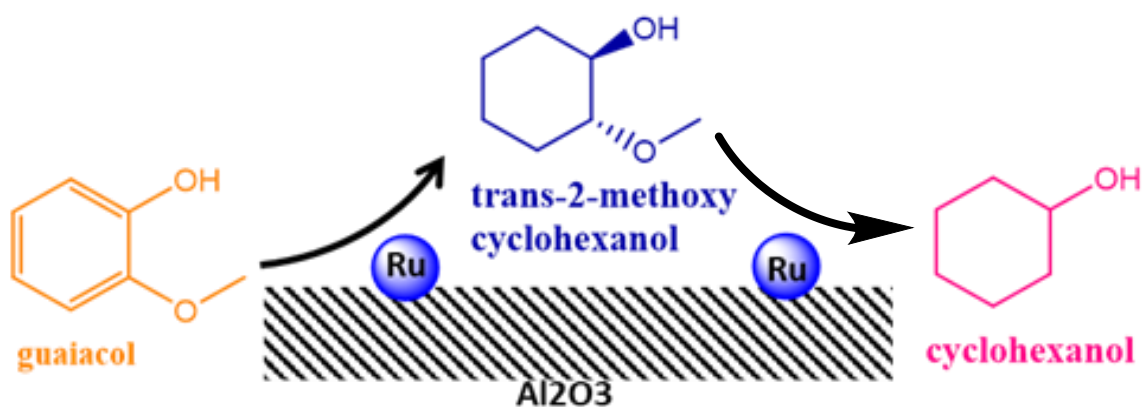
Scheme 4A.1. Hydrodeoxygenation/defunctionalisation of lignin derived low molecular weight compound, guaiacol

Various reports describe the HDO of lignin derived low molecular weight compound, and it was seen that HDO is improving the fuel efficiency of lignin derived low molecular weight compounds. So, it was decided to carry out catalytic hydrodeoxygenation (HDO) reaction to lower the oxygen content and improve its energy value [1, 2]. Thus, in order to produce fuels from lignocellulosic biomass two prong strategy needs to be developed in which first step is the conversion of lignocellulosic biomass to crude bio-oil and in a second step, up-gradation of bio-oil through HDO process to decrease the oxygen content is required [3]. Further, cyclohexanol and cyclohexanone (KA oil) are the intermediates in the synthesis of adipic acid however, currently KA oil is obtained either by hydrogenation of phenol or oxidation of cyclohexane/cyclohexene which are obtained from fossil feedstock [4]. It can be suggested that if the KA oil is obtained from lignin instead of fossil feedstock, it would be beneficial for the bio-refinery concept. The expected market for adipic acid is approximately USD7000 million in 2019, which makes it one of the most interesting molecule to synthesize. In view of this, research is devoted on the KA oil synthesis from lignin via depolymerisation and HDO-ring hydrogenation of depolymerized aromatic monomers. In a typical HDO process, oxygenates are reacted with hydrogen in the presence of a catalyst to remove oxygen via C-O bond cleavage [5-7]. Precious metals like Ru, Pt, Pd with high loading decorated over various supports are required for the HDO of bio-oil at elevated temperatures (>300 °C) and pressures (~7 MPa H_2) to cleave C-O bonds due to i) higher bond dissociation energy (414 kJ/mol) and ii) partial double bond character to C-O bond in phenolic compounds due to resonance [8, 9]. Guaiacol is one of the depolymerized product of lignin, and it has different types of oxygen-carbon bonds similar to those found in lignin: Ar(C)-O-CH_3 [C(sp3)–OAr (methoxy group), C(sp2)–OMe] and C(sp2)–OH (hydroxyl) having bond energies of 247, 356 and 414 kJ/mol, respectively [10]. Considering this, much of the research is devoted on the use of guaiacol as a representative compound of lignin derived chemicals for HDO reactions. In the earlier works, from our group it is shown that the solid acids,[11, 12] solid bases [13] and acidic ionic liquids [14, 15] can depolymerize lignin under milder conditions (<250 °C, N_2) to yield low molecular weight compounds including guaiacol.

It is reported that Ru/C could catalyze HDO reaction of bio-oil at 340 °C under 8 MPa H_2 pressure in aqueous medium to yield mixture of upgraded monomers [9]. Ru/ZrO_2-WO_x catalyst is too reported for the formation of mixture of products (cyclohexanol, cyclohexanone, cyclopentanone) at 270 °C and 4 MPa H_2 pressure [16]. Pd-WO_x/Al_2O_3 catalyst at 300 °C and 7

MPa H_2 in n-decane solvent is shown to give 88% cyclohexane yield [17]. Comparative study of Pd, Ru (240-330 °C) and Mo_2C (330-375 °C) supported on carbon is done at 3.4 MPa of H_2 in decaline solvent and it was observed that at lower temperatures (240 °C) predominantly ring hydrogenation occurs and at elevated temperature of 300 °C, C-O bond cleavage is possible [18]. Earlier from our group it has been exemplified that with a change of support from basic (HT) to neutral (AC) to acidic (Al_2O_3), product selectivity (ring hydrogenation to partial HDO) alters and with highly acidic support (SiO_2-Al_2O_3), complete HDO activity is possible to achieve. Incidentally, change in selectivity of the products was devoid of metal used (Pt, Ru, Pd with 3.5 wt% loading) [19]. Recently, in a comparative study of Pt/HY and Pt/HZSM5 catalysts on the basis of strength and amount of acidic sites, HDO of guaiacol at 250 °C and under 4 MPa H_2 in decane solvent is reported. It has been shown that due to optimal acidic properties in Pt/HY catalyst compared with Pt/HZSM5 catalyst, it showed better HDO activity [20]. Ru/SiO_2 catalyst has shown complete conversion of guaiacol with 55% yield of cyclohexane in n-dodecane at 300 °C and 5 MPa H_2 [21]. The HDO activities of bimetallic catalysts like, 4wt%-1wt%RuRe/C and RuRe/MWCNT are also evaluated at 200 °C and 2 MPa H_2 in n-heptane medium and with guaiacol as a substrate, approximately 60% cyclohexanol formation was seen [22]. A careful look at the literature suggests that with precious metals, high activity is obtained at high temperatures (typically >250 °C) and high hydrogen pressures (2 MPa – 8 MPa). It is also suggested that since precious metals are highly active, those may catalyse further reactions and coke formation and gaseous products formation becomes predominant at the expense of desired compounds, cyclohexanol and cyclohexanone.

Though precious metals demonstrate good HDO activity, but due to high loadings (>3wt%) required to achieve respectable activity, researchers have extensively focused their works on the use of non-precious transition metal based catalysts. In view of this, CoMoS, NiMoS or Mo_2N catalysts are evaluated for HDO at 300 °C and 4 MPa H_2 [23-29]. However, these catalysts have exhibited lower activity and contamination of products with sulfur was also seen [23-30]. Besides sulfur containing catalysts, Ni and Fe based catalysts are also used for the HDO of lignin model compounds but those showed respectable activities at very high temperatures (>350 °C) resulting in undesired by-product formation like CH_4 and CO [31-33]. NiCo/Al_2O_3 catalyst is also reported for the HDO of guaiacol to yield cyclohexanol as a major product (70%) at 200 °C and 5 MPa H_2 pressure in aqueous medium [34]. Recently, CuNi/Ti-MCM-41

catalyst is demonstrated for HDO of guaiacol at 260 °C and 10 MPa H_2 in heptane solvent to achieve 74% conversion of guaiacol with 48% selectivity to cyclohexane [35].

Typically, it is seen that the catalysts with higher acid sites show better activity for HDO. Additionally, different studies have shown that the activation of hydroxyl group is possible in presence of the transition metal along with acid sites. In a bifunctional supported metal catalyst, metal splits H_2 and acidic sites are responsible for the cleavage of C-O bond(s) [36-39].

A careful study of the published research reveals that with aqueous and high boiling solvents like decane (174.1 °C), dodecane (216.3 °C) and hexadecane (286.9 °C), HDO reactions typically occur ≥250 °C and >3 MPa H_2 pressure. However in low boiling solvents such as heptane (98.4 °C), HDO activity can be achieved at lower temperatures and lower H_2 pressures (<250 °C and <2 MPa H_2). This indicates that for a HDO reaction to occur, minimum threshold pressure is required which can be achieved with high boiling solvents at higher temperatures but with low boiling solvents is achieved at lower temperatures. Nevertheless, possibility of solubility of hydrogen in these solvents at given temperatures is required to be examined. Thus, it becomes essential to understand this underlying chemistry and develop a catalytic system which would use lower precious metal loading and operate under lower temperature and pressures. It is anticipated that in the presence of low boiler solvent, and bifunctional catalyst having noble metal in combination with acidic support, could be the better alternative to achieve HDO activity under moderate temperature (175-225 °C) and lower H_2 pressure (<2 MPa). Moreover, in most of the earlier studies, higher loading (> 3wt%) of precious metals is reported which might not be economically viable. Hence the objective of this work was to use very low loading of noble metal and study the effect of support in presence of low boiler as well as thermally stable solvents like hexane (B.P = 68 °C) and cyclohexane (80.7 °C). Earlier it is shown by experimental and theoretical evidence that cyclohexane is stable at higher temperature [40, 41]. Additionally, effect of catalytic system on various other lignin derived aromatic monomers was also checked.

4A.2 Experimental section

4A.2.1. Materials

n-hexane (99%), cyclohexane (99.9%), phenol (99.5%), eugenol (99%), $RuCl_3$ (45–55%), Ru/Al_2O_3-Acidic (commercial) catalyst and various supports (SiO_2-Al_2O_3, γ-Al_2O_3 acidic, basic, and neutral) used in the catalyst synthesis were procured from Sigma Aldrich Chemicals, USA. It is typically known that Al_2O_3 when precipitated during synthesis is done under alkaline

condition (pH ~10) and later it can be washed with acid to make either neutral or acidic. Acidic Al_2O_3 has typically pH of 4-6. Guaiacol (99%), anisole (99%), veratrol (98%), and 4-propyl cylohexanol (>98%) were purchased from Loba Chemie, India. 2-methoxy cyclohexanol (99%) was procured from Alfa Aesar, India. 4-propyl phenol (99%) was purchased from TCI Chemicals, India. Besides supports, all the other chemicals were used as received.

4A.2.2. Catalyst synthesis

Supported Ru metal catalysts (Ru/Al_2O_3, Ru/SiO_2, Ru/SiO_2-Al_2O_3) with 0.5 wt% Ru loading were prepared by wet impregnation method. More details on the materials and synthesis procedure used for the synthesis of supported metal catalyst are described earlier (Refer chapter 2B, Section 2B.2.2).

4A.2.3. Catalytic runs

Hydrodeoxygenation of guaiacol was performed in a 100 mL hastelloy high pressure high temperature Parr make reactor. In a typical reaction, 2.15 wt% guaiacol solution (23 g) in cyclohexane with guaiacol/Ru molar ratio of 165 was charged in the reactor. The reactor was flushed with H_2 for 3-4 times to remove any air. Then, the reactor was pressurised with H_2 up to desired pressure (0.3–1 MPa at R.T) and was heated under slow stirring (100 rpm) until desired reaction temperature (175–250 °C) was reached. After attaining the reaction temperature, stirring was increased to 1000 rpm and this time was considered as a starting time of the reaction. Reactions with other substrates (eugenol, veretrol, anisole, phenol) were carried out using similar charge. With 1 MPa pressure charged at R.T, under reaction temperature of 225 °C, 3.1 MPa pressure was observed.

4A.2.4. Recycle experiments

After completion of a reaction, the catalyst (solid) was recovered by centrifugation of the reaction mixture. The recovered wet catalyst was used in the next reaction without any pre-treatment. In addition, to check the catalyst activity by maintaining S/C ratio (substrate to catalyst molar ratio) constant, the residual solvent of recovered wet spent catalyst from third run was removed by heat treatment of catalyst at 60 °C for 12 h. The dried catalyst was used to carry out the fourth run without further treatment.

4A.2.5 Analysis of reaction mixture

After completion of reaction, reactor was allowed to cool to room temperature under air flow. The reaction mixture was collected and centrifuged to separate solid and liquid. The liquid was then filtered through a 0.22 μm syringe filter and used for gas chromatography (Agilent GC)

analysis. GC was equipped with HP-5 capillary column (0.25 μm × 0.32 mm × 50 m), flame ionization detector (FID) (30 mL•min^{-1} N$_2$ flow as carrier gas) and the oven temperature programme was as follows: 100 °C (hold time, 1 min) to 270 °C (hold time, 10 min) at 10 °C•min^{-1} ramp rate. The injector temperature used was 270 °C. Detector was kept at 275 °C. The GC-MS (Agilent-7890 GC and Agilent MS-5977A MSD) equipped with DB-5 MS column (0.25 μm × 0.25 mm × 30 m) was used for the analysis. Temperature program used was similar to that for GC-FID. The NIST library was used for product identification. Following formulae are used for the calculation of conversion and yields.

$$Conversion\ (\%) = \frac{\text{moles of substrate converted (based on GC)}}{\text{moles of substrate charged}} x\ 100$$

$$Yield\ (\%) = \frac{\text{moles of product formed (based on GC)}}{\text{moles of theoretical product formed based on substrate converted}} x\ 100$$

4A.3. Result and discussion

4A.3.1. Catalyst characterization

All the synthesized catalysts were characterized thoroughly to understand their morphology and to correlate the activity of the catalysts with their morphologies. For details of characterization technique used Refer (Chapter 2B, Figure 2B.2. XRD analysis). XRD analysis of supported metal catalysts was done to confirm the phase of support and metals. ICP analysis was done to confirm the % of metal loading in respective catalyst (Chapter 2B, Section 2B.3.3. Table 2B.3. ICP analysis). NH$_3$/CO$_2$ TPD analysis of synthesized catalysts was done to calculate respective acidity and basicity present in catalyst (Chapter 2B, Figure 2B.11. and Table 2B.5). XPS analysis was done to check the oxidation state of metal (Chapter 2B, Figure 2B.7.-2B.10.). N$_2$ physisorption analysis of synthesized catalysts were done to check available surface area for the catalytic activity (Chapter 2B, Table 2B.2.). CO chemisorption analysis was done to calculate % metal dispersion and crystallite site of the synthesized catalyst and tabulated in (Chapter 2B, Table 2B.4.). TEM analysis was done to check the particle size of supported metal catalyst (Chapter 2B, Figure 2B.3-2B.5).

4A.3.2. Catalyst activity

Hydrodeoxygenation (HDO) reactions were carried out in high pressure high temperature batch mode reactors and the analysis of the reaction mixture was done on GC (for details please refer experimental section, 4A.2).

4A.3.2.1. Effect of support on the HDO of guaiacol
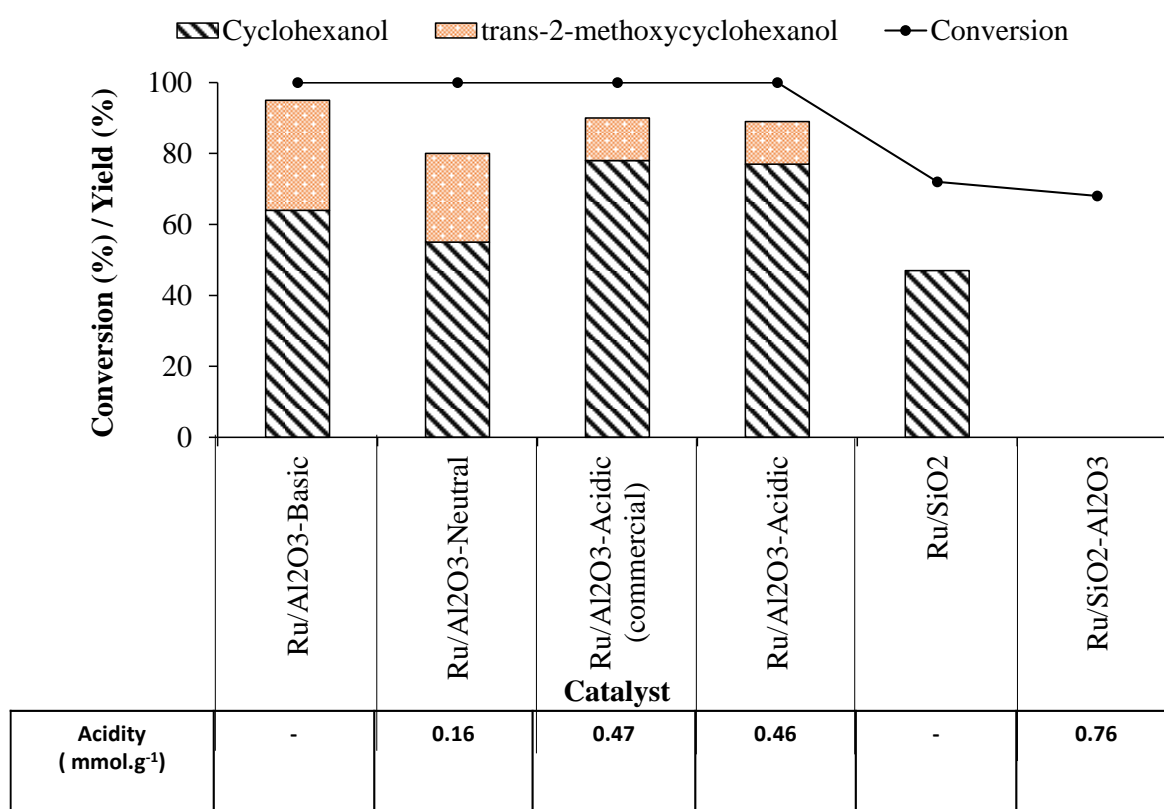
Figure 4A.1. Effect of support on the hydrodeoxygenation of guaiacol.

Reaction condition: Guaiacol/Ru molar ratio, 165; 2.15 wt% Guaiacol in cyclohexane; H_2, 1 MPa at room temperature; 225 °C; 4 h; 1000 rpm.

As can be seen from the Figure 4A.1, with constant Ru (0.5wt%) loading but with the change in the support; activity of the catalyst with selectivity for the product formation has changed

when reactions were carried out at 225 $^{\circ}$C under 1 MPa H$_2$ pressure for 4 h in cyclohexane as a solvent. With neutral SiO$_2$ as a support, formation of 47% cyclohexanol was observed with 72% conversion of guaiacol. However, when instead of SiO$_2$, Al$_2$O$_3$-Neutral was used to support Ru, increase in the conversion (100%) was seen along with increase in cyclohexanol formation (55%). Additionally, formation of an intermediate product, trans-2-methoxycyclohexanol with 25% yield was also seen. This result was surprising considering that both SiO$_2$ and Al$_2$O$_3$-Neutral were considered as neutral supports. However, as shown above, in case of Al$_2$O$_3$-Neutral support very weak acidity (0.16 mmol•g^{-1}) was seen. Moreover, CO chemisorption data indicated that crystallite size of Ru on Al$_2$O$_3$-Neutral was too small (2.18 nm) compared to on SiO$_2$ support (11.8 nm). These two factors might have played important role in increasing the overall activity of the catalyst. Considering this, acidic Al$_2$O$_3$ was used to support Ru and the activity was evaluated under similar conditions. As observed, with Ru/Al$_2$O$_3$-Acidic catalyst, improvement in the yield for cyclohexanol (77%) was achieved compared to neutral Al$_2$O$_3$ (55%). Besides cyclohexanol as a product, formation of trans-2-methoxycyclohexanol (12%) was seen, which was lower than Al$_2$O$_3$-Neutral supported catalyst (25%). In view of this result, crystallite size of Ru was checked for both the catalysts (Al$_2$O$_3$-Neutral, Al$_2$O$_3$-Acidic) and it was seen that over both the supports, Ru crystallite size is almost similar (1.86 nm, 2.18 nm; Chapter 2B, Table 2B.4). Hence, it can be effectively said that the acidity of the support is playing an important role in the cleavage of C-O bond and thus acidic Al$_2$O$_3$ supported Ru catalyst showed higher cyclohexanol yield than neutral Al$_2$O$_3$ supported Ru catalyst. These results suggest that the adsorption of oxygenated compound(s) on the acidic supports might be higher which results in the formation of cyclohexanol as a product. In regard to this, activity of basic Al$_2$O$_3$ supported Ru catalyst was evaluated and it was seen that the catalyst gave 64% cyclohexanol yield with 31% yield for trans-2-methoxycyclohexanol. As expected on the basic support, C-O cleavage activity was lower however, higher GC based carbon balance (considering GC based conversions and yields of products) was observed (95%) compared to acidic Al$_2$O$_3$ (89%) and neutral Al$_2$O$_3$ (80%) supported Ru catalysts. This can be explained on the basis of coke formation on the catalyst during the reaction. In order to substantiate this suggestion, CHNS elemental analysis of spent Ru/SiO$_2$-Al$_2$O$_3$ and spent Ru/Al$_2$O$_3$-Basic catalysts was carried out and it proved the adsorption of coke on the catalyst surfaces was more on acidic support [Ru/SiO$_2$-Al$_2$O$_3$ (9.50% C and 1.12 % H) than Ru/Al$_2$O$_3$-Basic (4.15% C and 0.54% H)]. This is due to a well-known fact that on

basic supports formation of coke is always lower compared to acidic supports over which cracking reactions are predominant. To discuss this further, on acidic sites if noble metals are present they show higher hydrogenation activity due to higher dispersion and stability of metals and thus can reduce the coke formation but with relatively higher acidity, problems of strong adsorption of substrate/intermediate/products is possible, which will lead to coke formation by undergoing further degradation reactions. In this work, since very low loading of Ru (0.5wt%) is used, it was believed that it may not be possible to use highly acidic supports as it may lead to coke formation and the same is proven by above data. Moreover, phenolic compounds are mildly acidic and thus can interact with basic supports weakly by losing H+ and forming phenoxide ion and thus these supports can be of use to carry out these reactions. Since, best cyclohexanol formation activity was seen on Ru/Al$_2$O$_3$-Acidic catalyst, commercially procured Ru/Al$_2$O$_3$-Acidic (commercial) catalyst, which is known to have mild acidity was also checked for its activity and almost similar activity was observed with the catalyst synthesized in the laboratory. Later, Ru/SiO$_2$-Al$_2$O$_3$ catalyst was also evaluated for its activity for HDO of guaiacol nevertheless even if 68% conversion of guaiacol was observed, no cyclohexanol formation was seen. This can be explained on the fact that SiO$_2$-Al$_2$O$_3$ has higher acidity (0.54 mmol•g^{-1}) with Ru crystallite size of 3.05 nm and thus catalyst might be highly active to yield cyclohexane as a product, which incidentally we could not quantify as reaction media is same.

To compare the activity of different catalysts and the role of support on the reaction, TOF calculations were done while reactions were performed for shorter time of 1 h at 225 °C under 1 MPa H$_2$ pressure. Following order of TOF was observed:

Ru/SiO$_2$ 36% (4 h^{-1}) < Ru/SiO$_2$-Al$_2$O$_3$ 34% (13 h^{-1}) < Ru/Al$_2$O$_3$-Basic 40% (22 h^{-1}) < Ru/Al$_2$O$_3$-Neutral 42% (24 h^{-1}) ~ Ru/Al$_2$O$_3$-Acidic 37% (24 h^{-1}) < Ru/Al$_2$O$_3$-Acidic (commercial) 39% (26 h^{-1})

TOF calculation was done for the all the catalyst, and it can be seen from the obtained result, Ru/SiO$_2$ catalyst has lowest TOF, it is obvious due to bigger particle size of Ru compared to other catalysts, and all Al$_2$O$_3$ supported catalyst showed higher TOF due to better metal dispersion and lower particle size. Nonetheless, TOF values need to be explained based on the structure sensitive/insensitive aspect of HDO reaction.

To check whether during the reactions methane is obtained as methanol would form after the cleavage of C-O bond (Ar-OCH$_3$), vent gas was analysed by GC equipped with TCD. However, formation of methane or any other gases was not detected. Moreover, based on the GC equipped with FID analysis of reaction mixture, formation of methanol with almost 92% equivalent to HDO of guaiacol was seen, which confirmed that methanol does not undergo any further conversions.

4A.3.2.2. Effect of temperature

Since, Ru/Al$_2$O$_3$-Acidic catalyst showed the best cyclohexanol yield (77%) in the reaction amongst all the catalysts when reaction was carried out at 225 ^{o}C, to improve the yield of cyclohexanol further, effect of reaction temperature (175, 200, 225 and 250 °C) on the HDO activity of this catalyst was studied and the results are shown in Figure 4A.2. Catalyst could even at 175 ^{o}C exhibit 100% conversion of guaiacol however, at this temperature, C-O bond cleavage activity was lower as is evident from the higher yield of ring hydrogenation product, trans-2-methoxycyclohexanol (40%). With an increase in temperature to 200 ^{o}C, enhancement in the yield of cyclohexanol (82%) along with 17% yield of trans-2-methoxycyclohexanol was observed (99% carbon balance). However, with further increase in temperature to 225 ^{o}C, catalyst showed slight decrease in cyclohexanol yield (77%) and also trans-2-methoxycyclohexanol yield (12%) (89% carbon balance). In order to check whether at higher temperature, cyclohexanol yield remains constant, reaction was done at 250 ^{o}C but lower yields were seen.
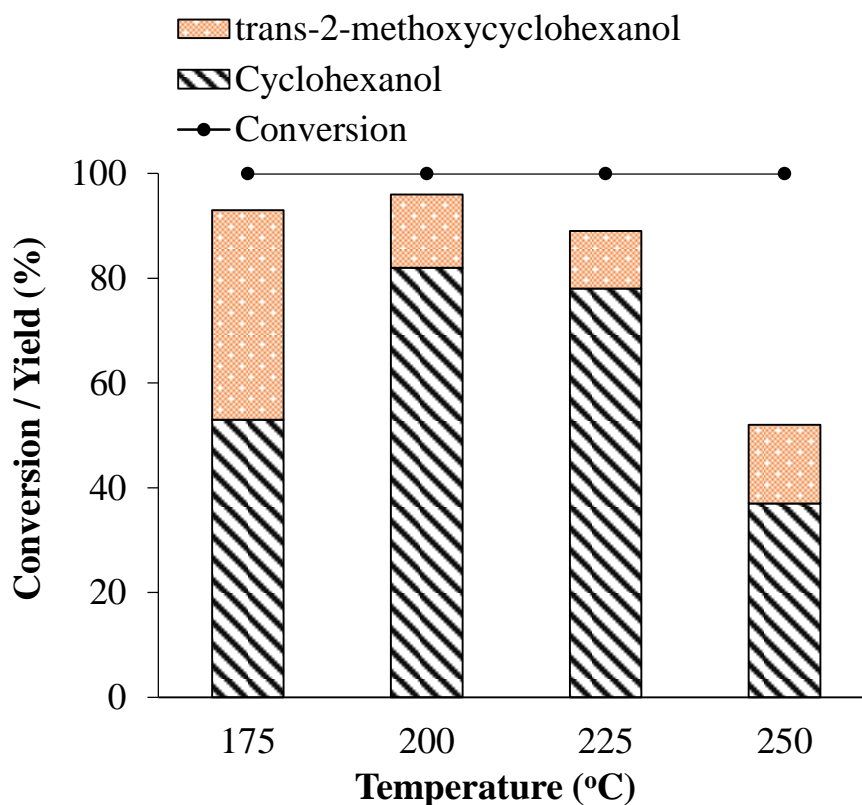
Figure 4A.2. Effect of temperature on the hydrodeoxygenation of guaiacol

Reaction condition: Guaiacol/Ru molar ratio, 165; 2.15 wt% Guaiacol in cyclohexane; H_2, 1 MPa at room temperature; 4 h; 1000 rpm.

Based on these results, it can be suggested that at lower temperature (175 °C) the activity of catalyst for the formation of HDO product is low and at 250 °C since the significant decrease in the yield of cyclohexanol (37%) was observed with only 15% trans-2-methoxycyclohexanol formation, side reactions such as coke formation or gaseous products formation are predominant. Moreover, this is implied due to observance of lower carbon balance (52%) with an increase in temperature to 250 °C. To check whether gaseous products are formed at higher reaction temperatures, after the reaction, gas analysis was done on GC equipped with TCD but no gaseous product formation was seen. As one of the possibility, the decrease in the yield of cyclohexanol at 250 °C could be due to its complete HDO to form cyclohexane, which incidentally we could not analyze as same is used as a reaction media. In order to check this possibility, the stability study of cyclohexanol was carried out at 225 °C under N_2 and H_2 atmospheres under similar reaction conditions. The result showed that under N_2 atmosphere

cyclohexanol was more stable with 20% conversion compared to under H_2 atmosphere wherein 50% conversion of cyclohexanol was seen (Figures 4A.3.1-4A.3.2). Incidentally, as mentioned above, quantification of cyclohexane as product was not possible since reactions were carried out in the same solvent. However, stability study results imply that under the reaction conditions employed in this study, cyclohexanol is unstable and converted into deoxygenated product cyclohexane or coke. Further, to investigate the loss in carbon balance at higher reaction temperature, spent Ru/Al_2O_3-Acidic catalyst was subjected to the elemental analysis and TGA analysis (Table 4.1, and Figure 4A.4). The calculated weight loss at 225 ^oC was 9.4% (TGA, difference in weight loss between spent and fresh catalyst at 800 ^oC) which reflects into loss of 0.046 g of substrate or product. Further, based on the mass balance (89% GC based), loss of substrate was calculated to be 0.055 g. Thus it is suggested that lower mass balance is due to strongly adsorbed substrate or product on the catalyst surface or coke formation. However, the first possibility is negligible because it can happen at lower temperature too like at 200 ^oC but where higher mass balance was achieved (99%). Surprisingly, at higher reaction temperature of 250 ^oC, calculated weight loss was 6.3% based on TGA study. The similar trend was also observed from CHNS elemental analysis. As summarized in Table 4A.1, in fresh Ru/Al_2O_3-Acidic catalyst, no carbon was present. But, over Ru/Al_2O_3-Acidic@200 spent catalyst, 1.20% carbon and on Ru/Al_2O_3-Acidic @225 spent catalyst, the content of carbon was 5.35%. This shows that with an increase in reaction temperature, either coke formation or adsorption of reactant/products on the catalyst surface is possible. Moreover, with an increase in reaction temperature to 250 °C, decrease in carbon content (3.67%) was observed. From this it is concluded that in the temperature range of 200-225 °C, the formation of partial oxygenated products was predominant and those were adsorbed on the acidic support and can further be converted into carbonaceous deposits. There is a possibility that once carbon (either in coke or intermediate oxygenated products form) is deposited on the catalyst, active sites are buried under it and thus adsorption of reactant and/or intermediate products is prohibited on these active sites. This may result in the lower yield of desired products. The TGA and elemental analysis data are complimentary with each other and this proves that with an increase in temperature from 175 to 225 °C, adsorption of oxygenated products or coke on the catalyst surface increases. Now to investigate further on whether coke is deposited on the catalyst surface or oxygenated intermediate products, it is essential to delve deeper into the elemental and TGA results. A simple calculation of elemental analysis suggests that if cyclohexanol

($C_6H_{12}O$) is considered as a product adsorbed on the catalyst surface then with the consideration of carbon content (5.35%, spent catalyst @225 °C from elemental analysis), 1.18% of oxygen (5.35x16/72) is present on the catalyst. Additionally, 0.89% of H will be present (5.35x12/72). However, from elemental analysis we understand that only 0.62% H is calculated. The total for cyclohexanol adsorption should give 7.44% weight loss (5.35+1.18+0.89=7.42%). Yet, TGA analysis of spent catalyst @225 °C, showed 9.4% weight loss. Along with this, there is a mismatch between hydrogen present on catalyst, experimentally (0.62%, elemental analysis) and theoretically should be present from cyclohexanol adsorption (0.89%). Considering this, it is expected that partially, oxygenates and coke are deposited on the catalyst.
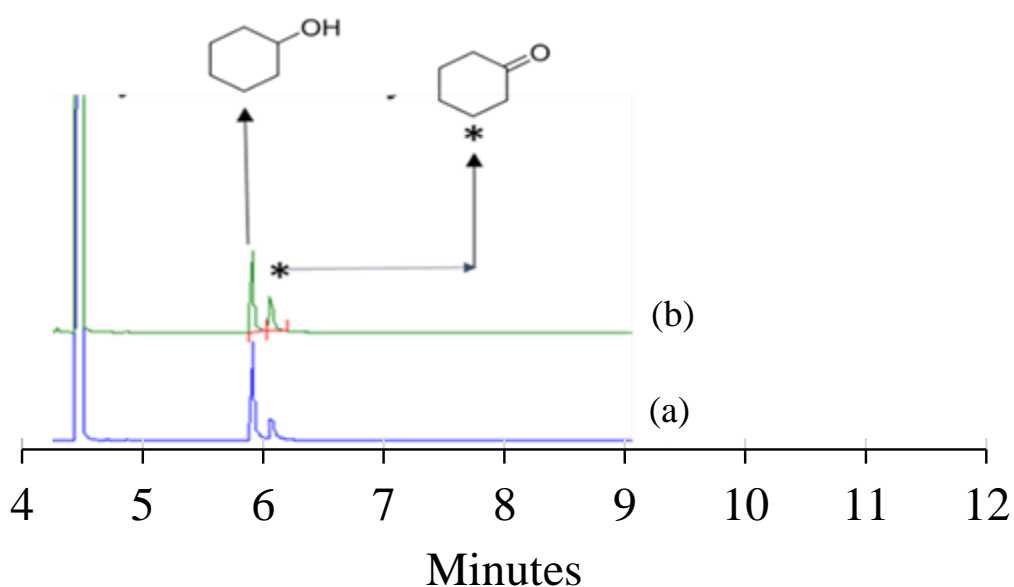
Figure 4A.3.1. cyclohexanol stability in N_2; (a) before reaction; (b) after reaction
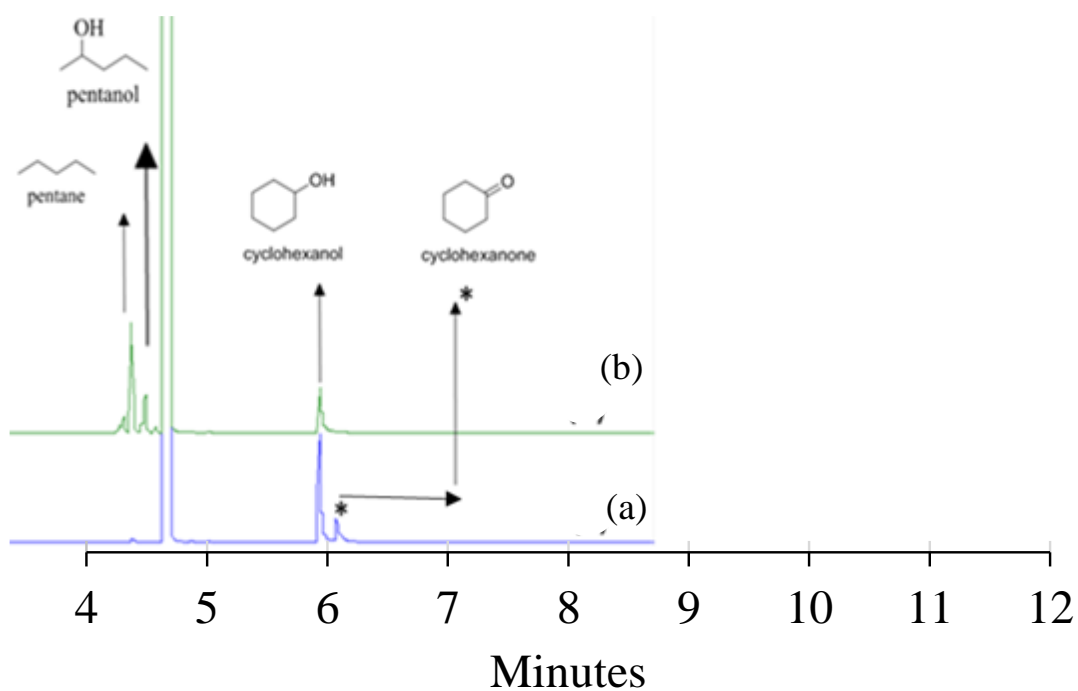
Figure 4A.3.2. Cyclohexanol stability in H_2

Table 4A.1. CHNS analysis of spent and fresh catalyst reaction done at different temperature

Catalysts		Ru/Al₂O₃-Acidic Fresh	Ru/Al₂O₃-Acidic @ 200 °C - Spent	Ru/Al₂O₃-Acidic @ 225 °C - Spent	Ru/Al₂O₃-Acidic @ 250 °C - Spent
Elemental analysis of catalyst (%)	C	0	1.20	5.35	3.67
	H	0.44	0.35	0.62	0.42
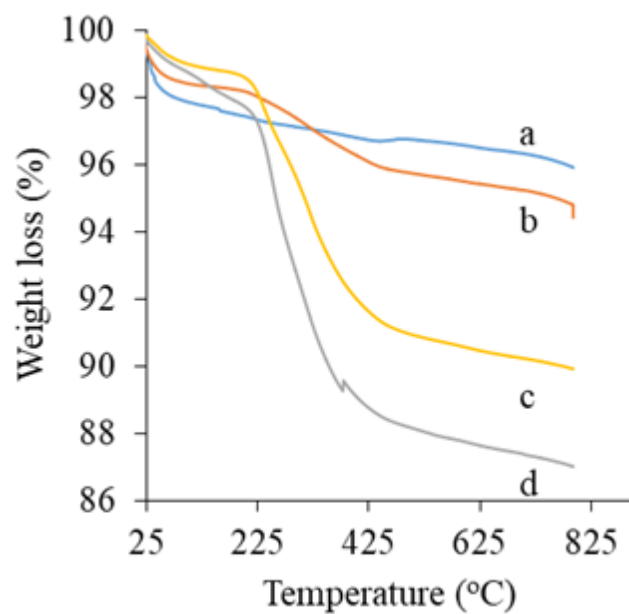
Figure 4A.4. TGA pattern of fresh and spent Ru metal catalyst (a) Fresh Ru/Al$_2$O$_3$-Acidic;(b) Spent Ru/Al$_2$O$_3$-Acidic @200; (c) Spent Ru/Al$_2$O$_3$-Acidic @250; (d) Spent Ru/Al$_2$O$_3$-Acidic @225;

4A.3.2.3. Effect of S/C (substrate to Ru catalyst) molar ratio
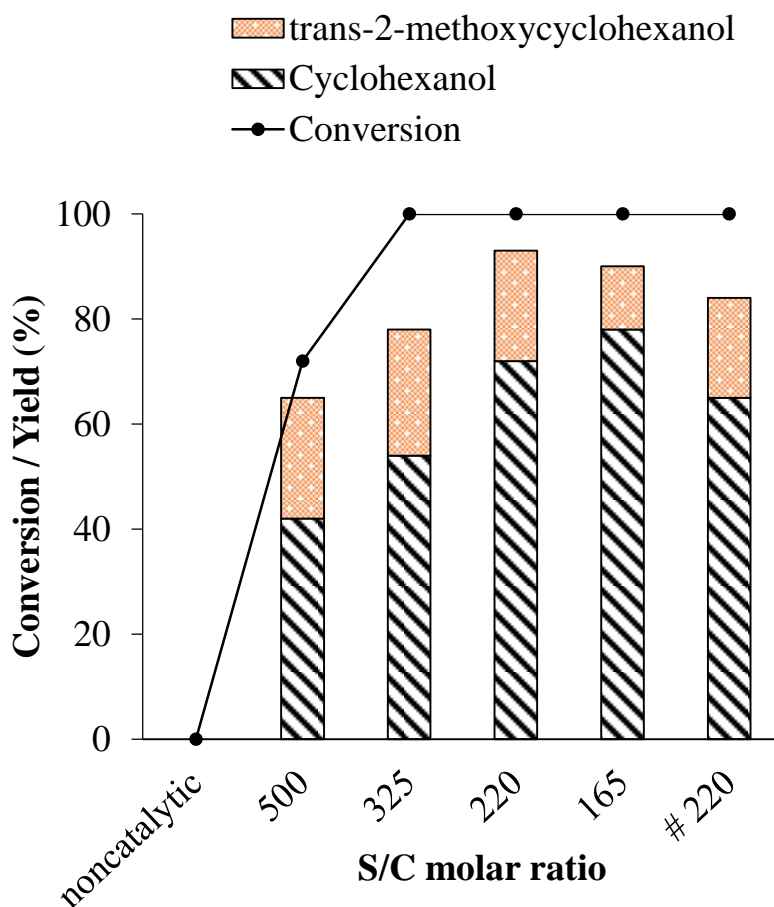
Figure 4A.5. Effect of substrate to catalyst (S/C) molar ratio

Reaction condition: 2.15 wt% Guaiacol in cyclohexane; H_2, 1 MPa at room temperature; 225 °C; 4 h; 1000 rpm. # 8 h reaction.

To achieve the best results with lower Ru content, molar ratio of substrate to Ru was varied from 165 to 500 and the results are summarized in Figure 4A.5. With highest S/C molar ratio of 500, 72% conversion with 42% yield of cyclohexanol and 23% yield of trans-2-methoxycyclohexanol was achieved. Reaction with S/C molar ratio of 325 showed 100% conversion of guaiacol with 54% yield of cyclohexanol and 24% yield of trans-2-methoxycyclohexanol. Subsequently, ratio of 220 was used and 100% conversion with 72% yield of cyclohexanol and 21% yield of trans-2-methoxycyclohexanol was observed. Further,

decrease in the S/C molar ratio to 165, 78% yield of cyclohexanol with 12% yield of trans-2-methoxycyclohexanol was achieved. This shows that with a deficiency of the catalyst or active sites (Ru), side reactions are predominant. Interesting observation is that reaction carried out without catalyst showed no conversion, which means that guaiacol is thermally stable compound at 225 °C. But it eventually suggests that in the absence of Ru, Al_2O_3 itself can catalyse guaiacol conversion however, to undesired products (which could not be detected on GC/GCMS). With decrease in ratio, improvement in overall mass balance was seen which means that with presence of Ru active sites, mass balance improves and also conversion of guaiacol and intermediate, trans-2-methoxycyclohexanol to cyclohexanol enhances. Later with lower ratio of 220 reaction was carried out for 8 h and slightly lower yield of cyclohexanol (65%) and trans-2-methoxycyclohexanol (19%) was observed as compare to 4 h reaction with similar ratio. This might be because of two reasons, 1) due to conversion of cyclohexanol to cyclohexane over Ru or 2) contribution of Al_2O_3 to yield side products from intermediate or cyclohexanol due to lack of Ru active sites. To ascertain this fact, reaction with only Al_2O_3 was carried (225 °C, 4 h, 1 MPa H_2) out and found that cyclohexanol is stable under reaction condition. TGA (Figure 4A.6.) and elemental analysis (C, 3.99%; H, 0.57%) of Al_2O_3 suggested very low adsorption of cyclohexanol on the surface.
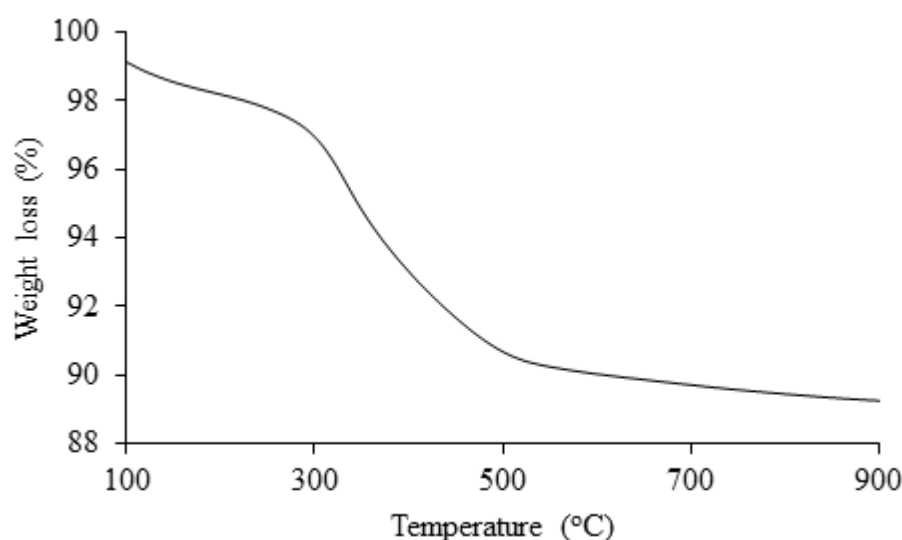
Figure 4A.6. TGA profile of cyclohexanol reaction carried out with Al_2O_3-Acidic

4A.3.2.4. Effect of time on hydrodeoxygenation of guaiacol

As shown above with S/C molar ratio of 165, within 4 h, it was possible to achieve 77% yield for cyclohexanol with complete conversion of guaiacol at 225 °C. As complete conversion of guaiacol was possible within 4 h and as per my earlier observation that cyclohexanol is unstable at 225 °C, reactions with shorter time were carried out (Figure 4A.7.). It was observed that within 2 h of reaction, mass balance was improved but cyclohexanol formation was decreased to 65% compared to 77% observed within 4 h.
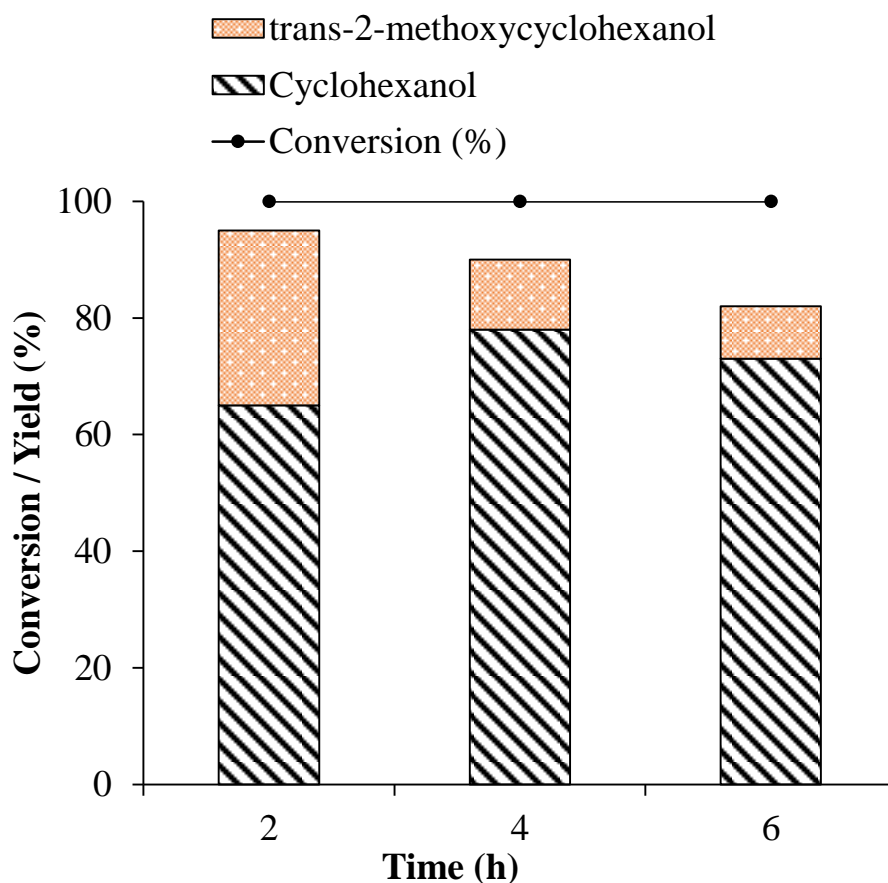
Figure 4A.7. Effect of time on the HDO of guaiacol.

Reaction condition: Guaiacol/Ru molar ratio, 165; 2.15 wt% Guaiacol in cyclohexane; H_2, 1 MPa at room temperature; 225 °C; 1000 rpm.

Additionally, as expected, intermediate formation was increased to 30% from 12%. The improvement in the mass balance reflects the fact that shorter reaction times are better to

suppress side reactions of cyclohexanol. Later, to check whether cyclohexanol yield can improve with further conversion of intermediate, reaction was carried out for 6 h. It was expected that with longer reaction time, trans-2-methoxycyclohexanol will convert into cyclohexanol and on the same line decrease in the yield of intermediate was seen (9%) compared to 4 h (12%). However, this decrease in the intermediate concentration did not reflect in the formation of cyclohexanol as lower yield of it was observed (73%) compared to 4 h reaction (77%). From the time study, it was observed that the first step in this reaction is formation of trans-2-methoxycyclohexanol which further gets converted in to cyclohexanol and cyclohexanone by the cleavage of C-O bond. Hence it is believed that reaction proceeds via cyclohexanone species which further undergoes hydrogenation to yield cyclohexanol. From this, it is proposed that on the catalyst surface ring hydrogenation of guaiacol occurs to form cis and trans-2-methoxycyclohexanol, however the trans form is more stable than cis form hence the trans-2-methoxycyclohexanol was observed in reaction and cis-methoxycyclohexanol immediately gets converted to cyclohexanol due to its low stability. To prove this, reaction was carried out with trans-2-methoxycyclohexanol as a substrate under similar reaction condition (225 °C, 4 h) and it was observed that trans-2-methoxycyclohexanol isomerise into cis-2-methoxycyclohexanol which further converts into cyclohexanol (Figure 4A.8).
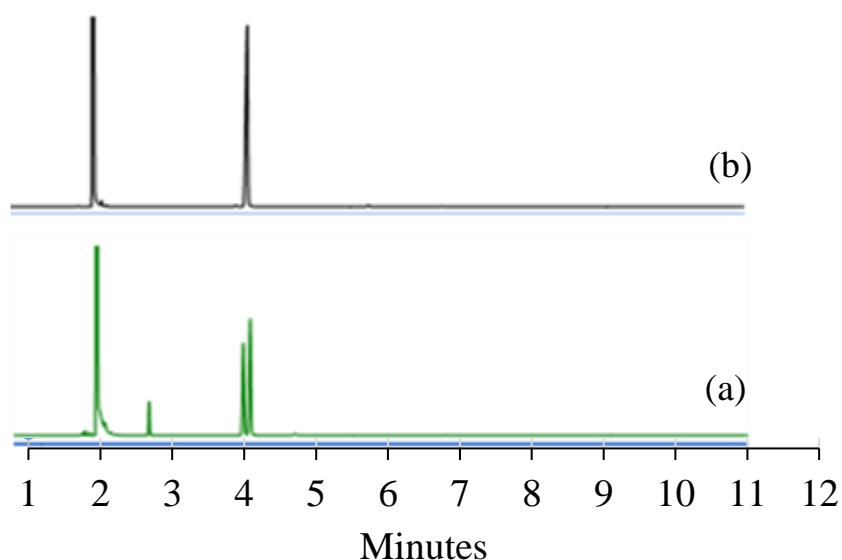
4A.3.2.5. Effect of H$_2$ pressure

Typically, literature reports HDO reactions under high H$_2$ pressure (>3 MPa)[9, 16, 19] however, in this work it is shown that HDO can be achieved even at 1 MPa pressure with high yield of cyclohexanol (82%). In order to check whether Ru/Al$_2$O$_3$-Acidic catalyst could show consistent HDO activity further under lower H$_2$ pressures, reactions were carried out using 0.5 MPa H$_2$ pressure and the results are summarized in Figure 4A.9.
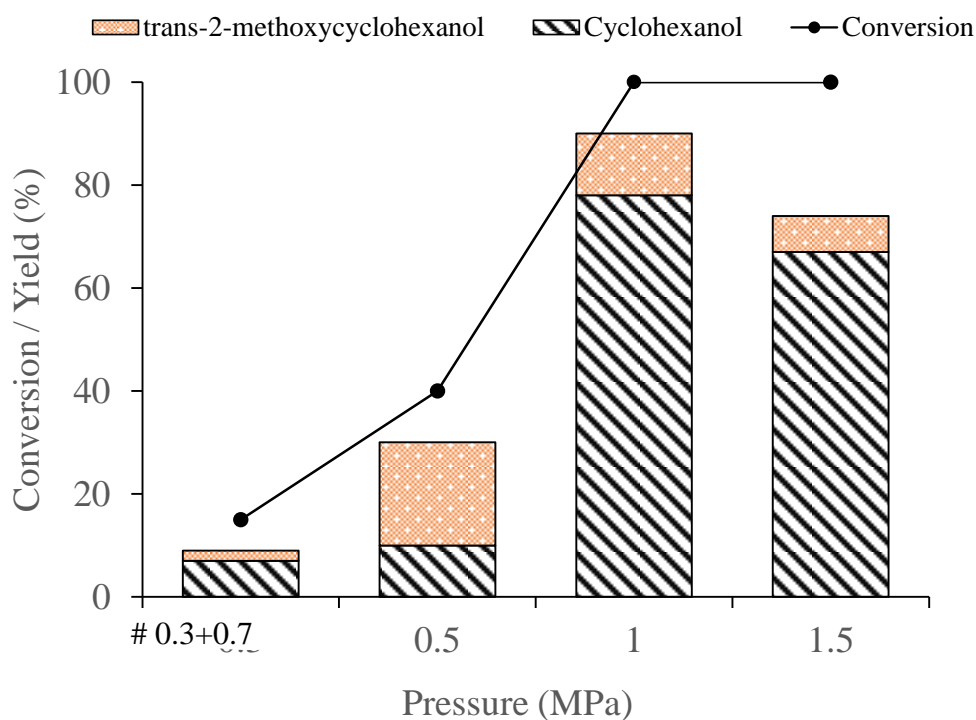
Figure 4A.9. Effect of H$_2$ pressure

Reaction condition: Guaiacol/Ru molar ratio, 165; 2.15 wt% Guaiacol in cyclohexane; 1000 rpm. # 0.3 MPa H$_2$ + 0.7 MPa N$_2$; 225 °C; 1000 rpm.

However, at lower pressure, conversion of guaiacol was decreased to 40% with only 10% cyclohexanol and 20% trans-2-methoxycyclohexanol formation. This result is very poor

compared with 1 MPa pressure reaction (guaiacol conversion, 100%; cyclohexanol yield, 77% and trans-2-methoxycyclohexanol yield, 12%). The better activity observed at 1 MPa may be attributed to two factors, 1) increased solubility of H_2 in cyclohexane, which in turn gives more concentration of H_2 on the catalyst and 2) better interaction between substrate (solubalized) and catalyst (solid). To check these possibilities, reaction was carried out with 0.3 MPa partial pressure of H_2 + 0.7 MPa partial pressure of N_2 (total 1 MPa pressure). Under this reaction condition, the conversion of guaiacol was only 15% with 7% cyclohexanol and 2% trans-2-methoxycyclohexanol formation. This suggests that even if total pressure of 1 MPa is applied with lower partial pressure of hydrogen, reaction does not proceed and in turn it leads to the conclusion that availability of hydrogen on the catalyst is more important than increase in interaction between catalyst and substrate due to higher pressures. Further, in order to study the effect of higher H_2 pressure, reaction was carried out at 1.5 MPa H_2 and 100% conversion of guaiacol was obtained but the yields of both, cyclohexanol (67%) and trans-2-methoxycyclohexanol (7%) were decreased. The possible reason behind this could be the excess availability of H_2 resulted in the formation of the complete deoxygenated product i.e cyclohexane, which as mentioned earlier I could not detect due to same is used as a reaction media. The hydrogen solubility study [42] reveals that in all the organic solvents like methylstyrene, cumene, cyclohexene, and cyclohexane; solubility of hydrogen increases with increase in temperature (30 ℃-100 ℃) and pressure (0.68 MPa to 6.89 MPa). Interestingly, maximum hydrogen solubility was observed in cyclohexane as a solvent. In yet another study, solubility of hydrogen in organic solvents such benzene, cyclohexane, decaline, phenol, and cyclohexanol was checked and it was found that cyclohexanol had the second highest hydrogen solubility after decaline under atmospheric pressure between 25-150 ℃ [43].

4A.3.2.6. Effect of solvent

Since, lignin depolymerization reactions are typically carried out in alcohol-water mixture,[11-14] it was decided to carry out HDO reactions in the presence of MeOH:H_2O (5:1 *v/v*). Although, this solvent system is good for depolymerization reaction but it unfortunately did not yield good HDO activity (Figure 4A.10). This might be because of competition between guaiacol, methanol and water to interact with catalyst surface. Water (29.27 $Å^2$) and guaiacol (29.46 $Å^2$), have almost similar Molecular Polar Surface Area (PSA), i.e., surface belonging to polar atoms, which is higher compared to methanol (20.23 $Å^2$) and this might play role in the interaction with catalyst surface.
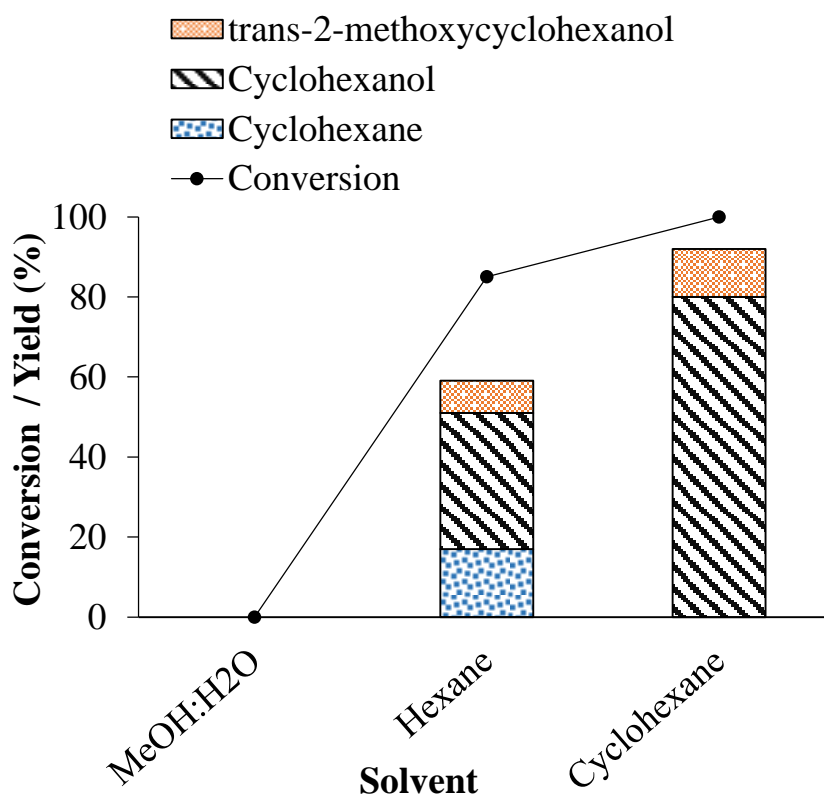
Figure 4A.10. Effect of solvent on the HDO of guaiacol.

Reaction condition: Guaiacol/Ru molar ratio, 165; 2.15 wt% Guaiacol; H_2 pressure, 1 MPa at room temperature; 225 °C; 4 h; 1000 rpm.

Al_2O_3 is predominantly considered as polar material with some ionic character to Al-O bond due to Al being electropositive and O being electronegative. Even though, water and guaiacol can interact with Al_2O_3 almost with a similar extent however, difference in concentration of those in the reaction system reduces the extent of interaction of guaiacol (4 mmol) with Al_2O_3 surface in comparison to water (227 mmol). This less interaction with catalyst surface of guaiacol in turn can lower its interaction with active sites and thus, reaction did not progress. Moreover, oxygenated solvents (polar solvents) may interact with catalyst surface and thus devoid any interaction of guaiacol with catalyst surface. When reaction was carried out in presence of hexane (PSA, 0.00 Å^2 due to absence of surface 'O' atoms), conversion of guaiacol reached to 85% with the formation of 17% cyclohexane along with 34% cyclohexanol and 8% trans-2-methoxycyclohexanol (69% carbon balance). However, when the reaction was carried out in the presence of cyclohexane (PSA, 0.00 Å^2 due to absence of surface 'O' atoms), complete conversion of guaiacol was achieved along with 77% yield of cyclohexanol and 12%

yield of trans-2-methoxycyclohexanol. As seen, non-oxygenated (non-polar) solvents may not interfere with the interaction of guaiacol with catalyst surface and thus can enhance the activity of a catalyst. The decrease in the activity of a catalyst in presence of hexane could be due to deactivation of catalyst by the adsorption of coke on the catalyst surface as in this solvent, either cyclohexanol was further converted into cyclohexane and then into coke or hexane itself is converted to coke. To check this, reaction was carried out under similar reaction condition (225 °C, 4 h) in absence of substrate (guaiacol) in both, cyclohexane and hexane solvents and the spent catalysts were subjected to elemental analysis (Table 4A.2). As seen, almost double the quantity of carbon was deposited on the catalyst used in hexane solvent compared to cyclohexane. Moreover, lower carbon balance observed using hexane as a solvent, implies that it might not be a good solvent to carry out reactions. Another interesting fact was seen about the extent of adsorption of guaiacol on the catalyst surface in different solvents. With polar solvent such as water+methanol mixture, guaiacol adsorption on catalytic surface was negligible but with nonpolar solvent such as cyclohexane and hexane, it was 52% and 46%, respectively (Figure 4A.11). This is obvious because as discussed above, due to difference in PSA of water and non-polar solvents, interaction of guaiacol with catalyst surface is lower.

Table 4A.2. CHNS analysis of spent and fresh catalyst to evaluate the stability of solvent

Catalysts		Fresh Ru/Al$_2$O$_3$-Acidic	Spent Ru/Al$_2$O$_3$-Acidic	
			Cyclohexane	Hexane
Elemental analysis (%)	C	0	0.95	1.95
	H	0.44	0.36	0.42
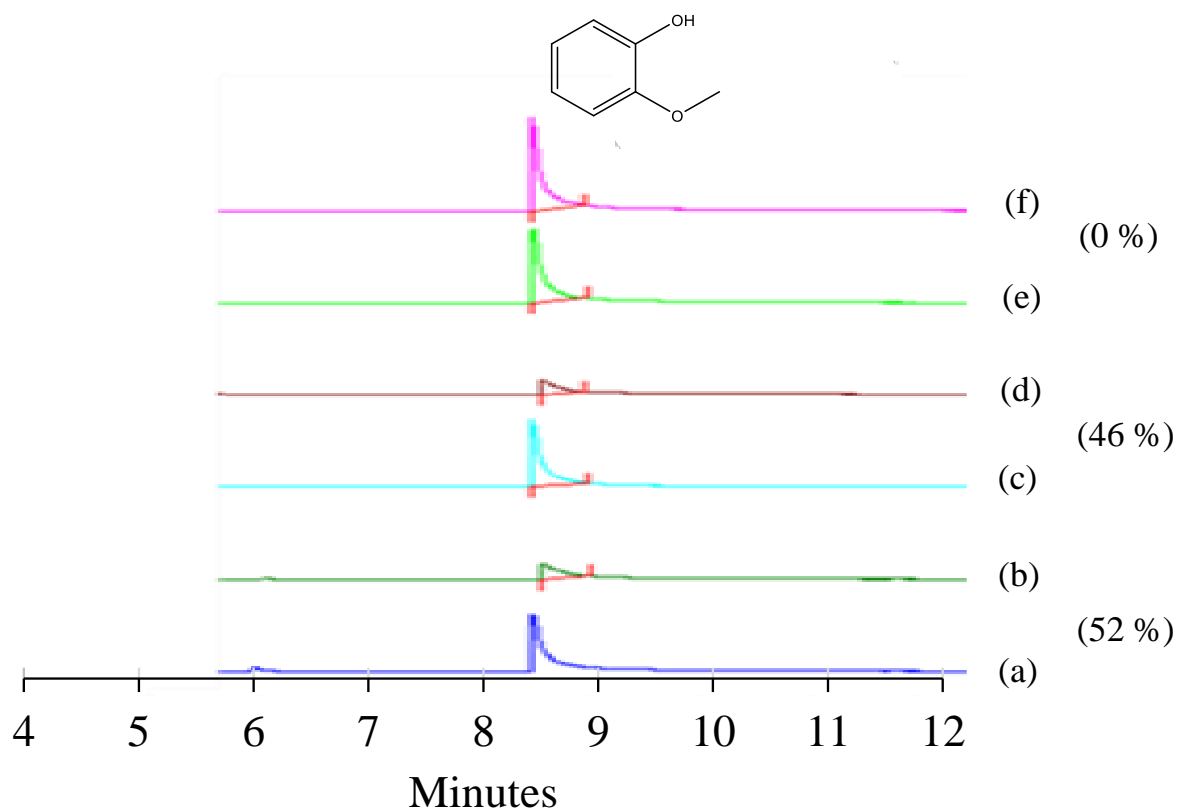
Figure 4A.11. Representative GC spectra of guaiacol adsorption in different solvent Guaiacol, 0.1 g; Al_2O_3, 1 g; solvent, 10 mL; room temperature; 4 h; (a) Cyclohexane (Before); (b) Cyclohexane (After); (c), Hexane (Before); (d), Hexane (After); (e), MeOH : H_2O (Before); (f) MeOH : H_2O (After);

4A.3.2.7. Effect of reduction temperature of catalyst on the catalytic activity

Typically, metal catalysts are reduced at higher temperatures (>300 ^oC) in order to achieve complete reduction of metal. In view of this, initially Ru/Al_2O_3-Acidic catalyst was reduced at 400 ^oC and the activity of the catalyst was evaluated at 225 ^oC for 4 h under 1 MPa H_2 in hexane solvent (Figure 4A.12). Although, 50% conversion of guaiacol was observed but no formation of cyclohexanol or trans-2-methoxycyclohexanol was seen. But in this reaction, 11% yield of cyclohexane was obtained (hexane was used as a solvent). To understand whether at lower reduction temperatures, activity increases, catalyst was reduced at 250 ^oC and 150 ^oC and with decrease in reduction temperature, higher activity of the catalyst was seen (Figure 4A.12). The same trend of dependence of catalytic activity as a function of reduction temperature was observed with cyclohexane as a reaction solvent (Figure 4A.13). With cyclohexane as solvent

complete conversion of guaiacol was achieved with all the catalysts. In presence of Ru/Al$_2$O$_3$-Acidic catalyst, the yield of cyclohexanol reached up to 77% with 12% yield of trans-2-methoxycyclohexanol. The catalyst reduced at 150 °C showed almost similar activity (76% cyclohexanol and 9% trans-2-methoxycyclohexanol yield) as that with non-reduced catalyst. However, the activity of catalyst drastically reduced with increase in the reduction temperature to 250 °C (48% cyclohexanol yield and 8% trans-2-methoxycyclohexanol yield) and 400 °C (cyclohexanol yield, 25%). This proves that with an increase in reduction temperature, interaction of substrate with active catalyst site is either reduced [44, 45]. The other plausible explanation is want of higher oxidation state metal in this reaction. However, this aspect needs further probe to be done.

To understand whether with an increase in reduction temperature crystallite size of Ru has increased which in turn has reduced the concentration of active sites for the reaction, CO chemisorption analysis was performed and the results are summarized in Table 4A.3. However, almost similar crystallite size was seen for all the catalysts, which then emphasize the fact that besides particle size, some other factor is playing a role in deciding the catalyst activity. To study this further, elemental analysis of catalysts was done and the results are summarized in Table 4A.4. As seen, with an increase in the catalyst reduction temperature, higher amount of carbon was deposited on the catalyst surface which suggests that in the initial time, activity of the catalyst may actually increase for the catalysts reduced at higher temperatures however, later coke formation may happen, that would bury the active sites and thus lower the conversion and yields for desired products.
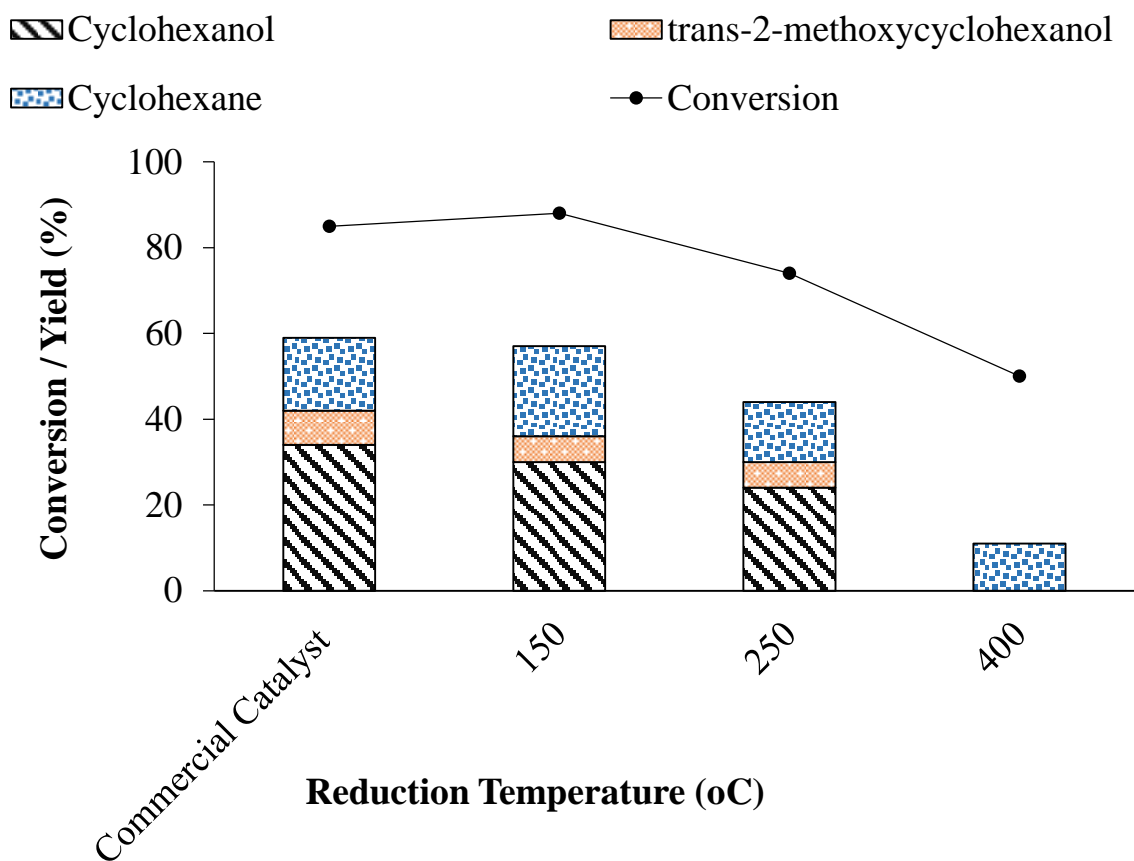
Figure 4A.12. Effect of catalyst reduction temperature with hexane as a reaction solvent. **Reaction condition:** Guaiacol/Ru molar ratio, 165; 2.15 wt% Guaiacol; hexane; H_2 pressure, 1 MPa at room temperature; 225 °C; 4 h; 1000 rpm.

Similarly, all the catalyst with different reduction temperature were used in the presence of cyclohexane solvent and the results are shown in Figure 4A.13.
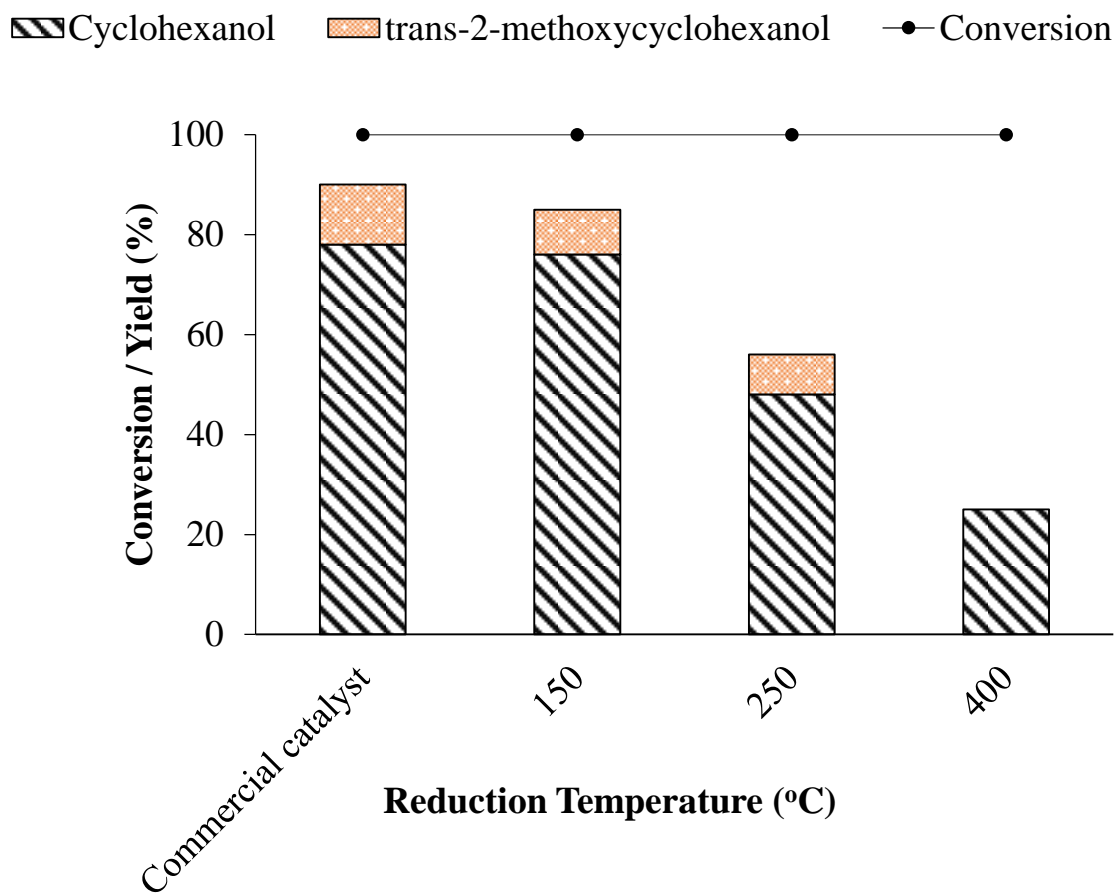
Figure 4A.13. Effect of catalyst reduction temperature with cyclohexane as a reaction solvent.

Reaction condition: Guaiacol/Ru molar ratio, 165; 2.15 wt% Guaiacol; cyclohexane, H_2 pressure, 1 MPa at room temperature; 225 °C; 4 h; 1000 rpm.

Table 4A.3. CO chemisorption study of the catalyst reduced at different temperatures

Catalyst	Average crystallite size (nm)	Metal dispersion (%)	Monolayer uptake ($\mu mol \cdot g^{-1}$)
Ru/Al$_2$O$_3$-Acidic	1.8	72.7	35.7

Ru/Al$_2$O$_3$-Acidic @250	1.6	80.7	39.6
Ru/Al$_2$O$_3$-Acidic @400	1.5	88.4	43.4

Table 4A.4. CHNS analysis of fresh and spent catalysts for reaction carried out in hexane solvent

Catalysts		Ru/Al$_2$O$_3$-Acidic fresh	Ru/Al$_2$O$_3$-Acidic@spent	Ru/Al$_2$O$_3$-Acidic @150@spent	Ru/Al$_2$O$_3$-Acidic @250@spent	Ru-Al$_2$O$_3$-Acidic @400@spent
Elemental analysis (%)	C	0	3.21	4.58	6.09	6.12
	H	0.44	0.37	0.44	0.44	0.38

4A.3.2.8. HDO of different substrates

Since Ru/Al$_2$O$_3$-Acidic catalyst was active in guaiacol conversion into cyclohexanol, it was worth evaluating catalysts HDO performance with other lignin derived substrates like phenol, veratrole, anisole, and eugenol. Reactions with these substrates were carried out under similar reaction conditions those were used for guaiacol. In all the reactions, complete conversion of substrate was achieved. With phenol as a substrate, (Figures 4A.14.1- 4A.14.2) yield of cyclohexanol was 20% with the formation of pentane, cyclopentane as other products. There is a possibility of formation of cyclohexane in reaction mixture which could not be quantified due to similar reaction medium. Reaction with veratrole (Figures 4A.15.1- 4A.15.2.) showed 20% cyclohexanol and 9% trans-2-methoxycyclohexanol formation along with observance of dimethoxy cyclohexanol. HDO of anisole (Figures 4A.16.1- 4A.16.2) gave 22% cyclohexanol and 15% methoxycyclohexane formation and in HDO of eugenol (Figures 4A.17.1- 4A.17.2) 27% propyl cyclohexanol (2-propylcyclohexan-1-ol) yield was obtained. As can be seen from

the GC and GCMS profiles of all these reactions various ring hydrogenated and partial hydrogenated products could be identified however, few of those could not be quantified due to lack of commercial samples.
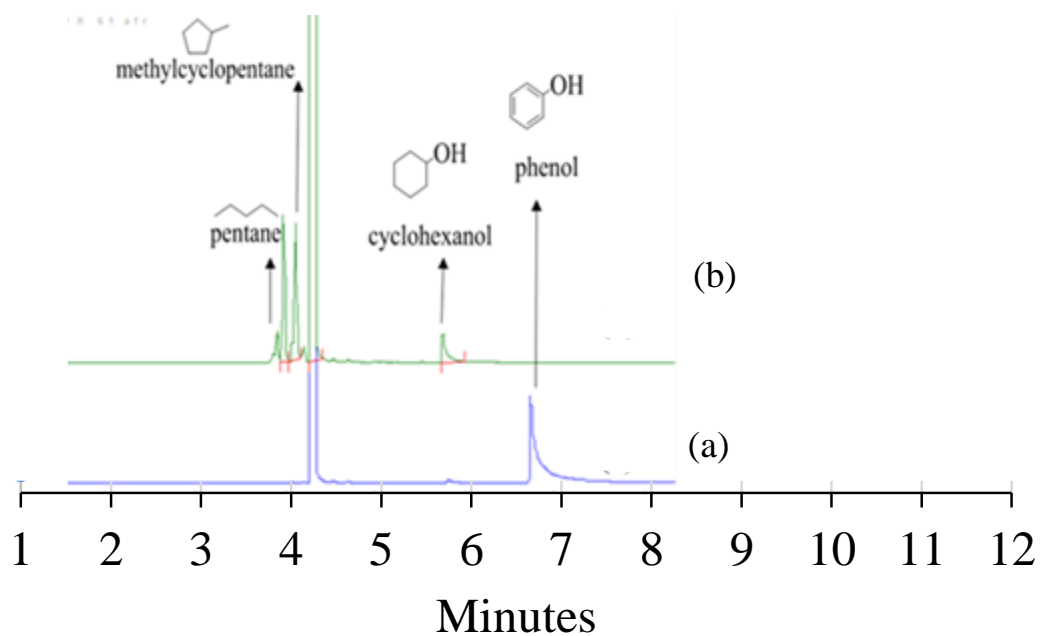
Figure 4A.14.1. Representative GC profile. Phenol, 4.0 mmol; Ru/Al$_2$O$_3$-Acidic, 0.0245 mmol of Ru; cyclohexane, 30 mL; H$_2$ pressure, 1 MPa at room temperature; 4 h; 1000 rpm.

(a) Before reaction (b) After reaction
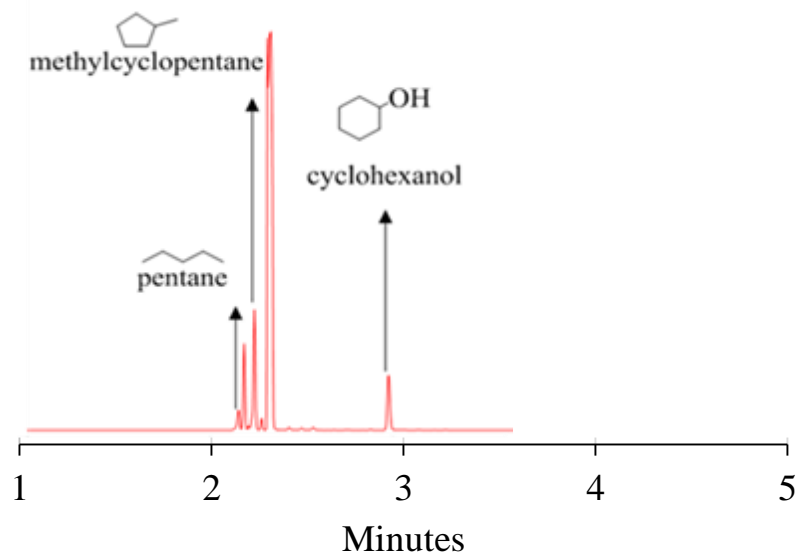
Figure 4A.14.2. Representative GC-MS profile. Phenol, 4.0 mmol; Ru/Al$_2$O$_3$-Acidic (commercial), 0.0245 mmol of Ru; cyclohexane, 30 mL; H$_2$ pressure, 1 MPa at room temperature; 4 h; 1000 rpm.
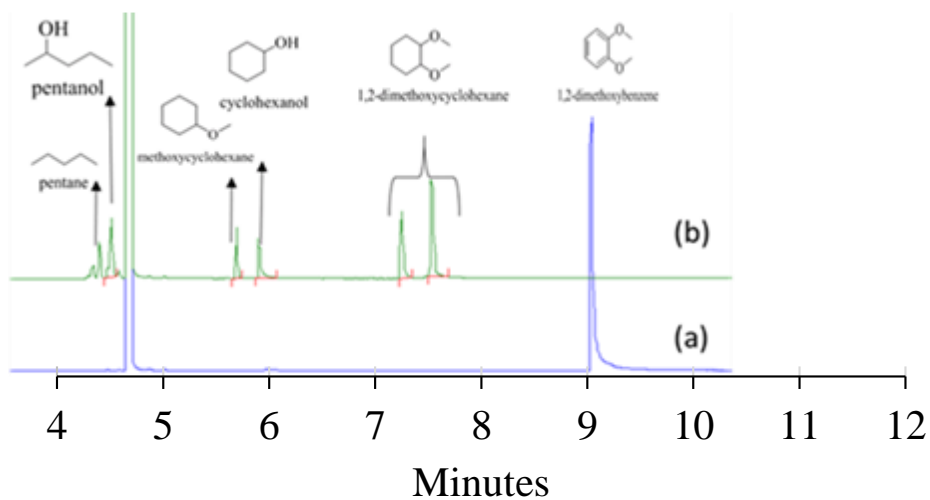
Figure 4A.15.1. Representative GC profile. Veratrol, 4.0 mmol; Ru/Al$_2$O$_3$–Acidic, 0.0245 mmol of Ru; cyclohexane, 30 mL; H$_2$ pressure, 1 MPa at room temperature; 4 h; 1000 rpm.
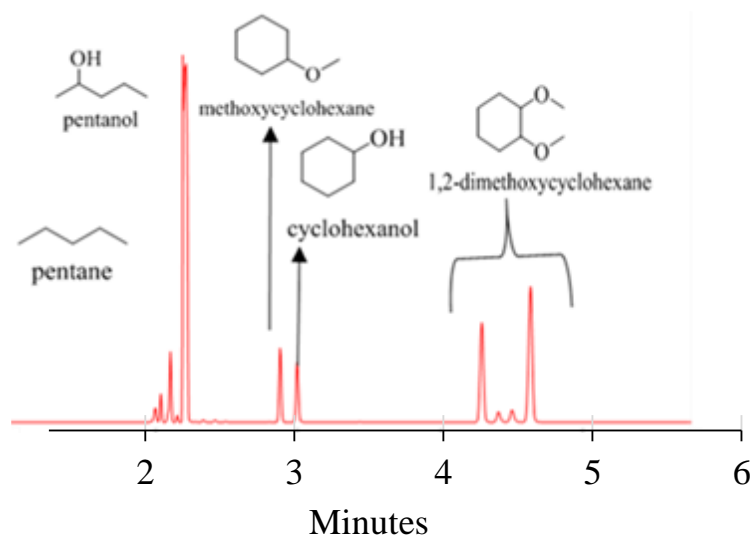
Figure 4A.15.2. Representative GC-MS profile. Veratrol, 4.0 mmol; Ru/Al$_2$O$_3$–Acidic, 0.0245 mmol of Ru; cyclohexane, 30 mL; H$_2$ pressure, 1 MPa at room temperature; 4 h; 1000 rpm.
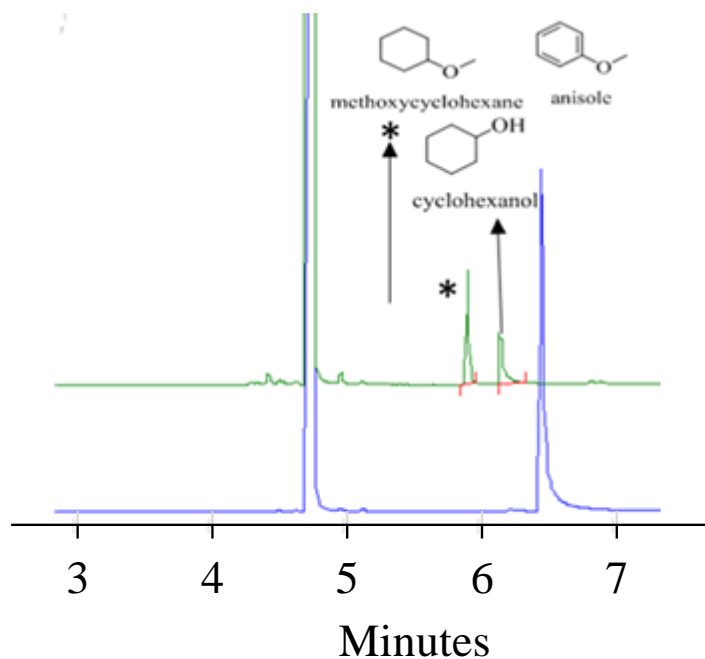
Figure 4A.16.1. Representative GC profile. Anisole, 4.0 mmol; Ru/Al$_2$O$_3$–Acidic, 0.0245 mmol of Ru; cyclohexane, 30 mL; H$_2$ pressure, 1 MPa at room temperature; 4 h; 1000 rpm.
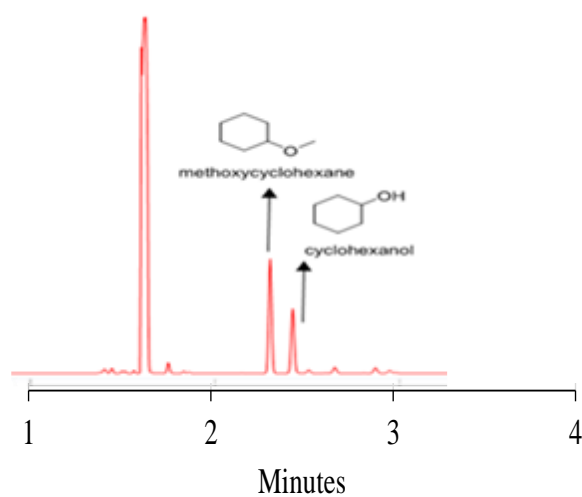
Figure 4A.16.2. Representative GC-MS profile. Anisole, 4.0 mmol; Ru/Al$_2$O$_3$–Acidic, 0.0245 mmol of Ru; cyclohexane, 30 mL; H$_2$ pressure, 1 MPa at room temperature; 4 h; 1000 rpm.
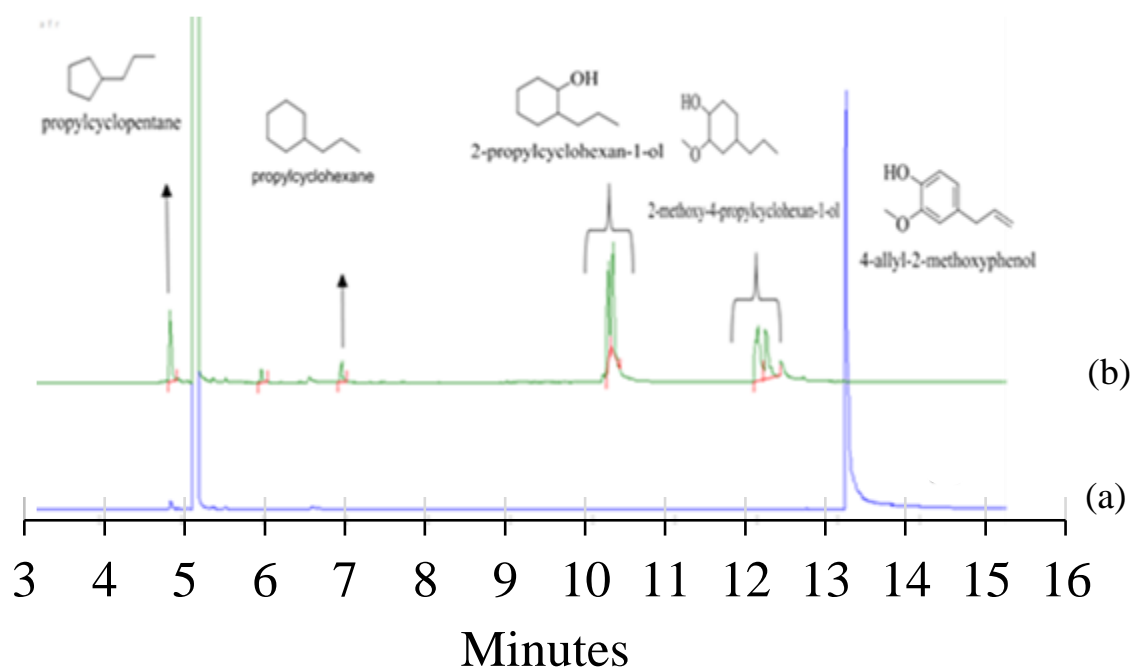
Figure 4A.17.1. Representative GC profile. Eugenol, 4.0 mmol; Ru/Al$_2$O$_3$-Acidic, 0.0245 mmol of Ru; cyclohexane, 30 mL; H$_2$ pressure, 1 MPa at room temperature; 4 h; 1000 rpm.
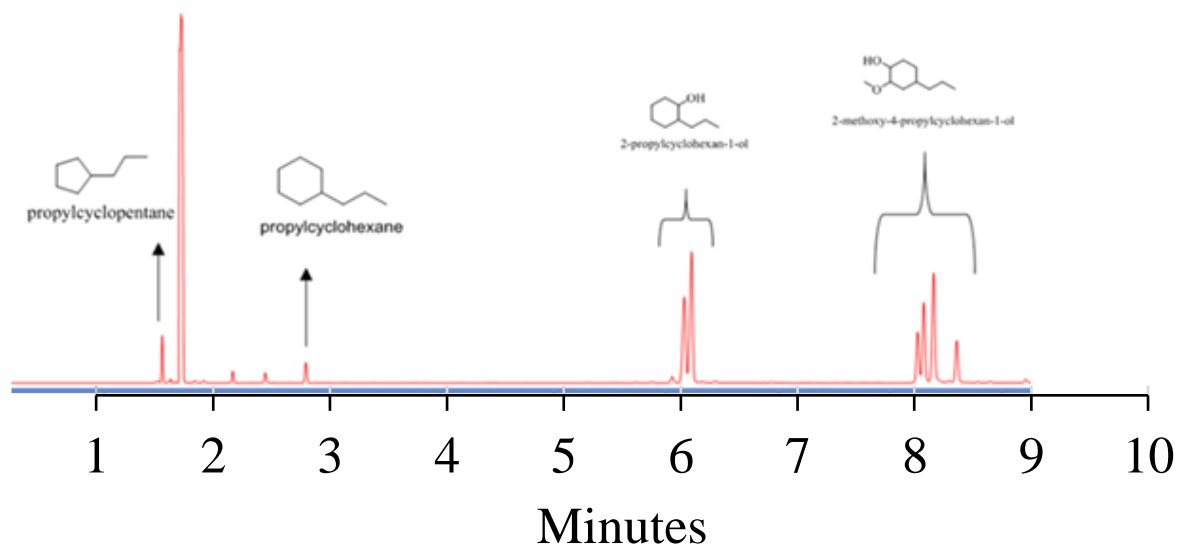
Figure 4A.17.2. Representative GC-MS profile. Eugenol, 4.0 mmol; Ru/Al$_2$O$_3$-Acidic, 0.0245 mmol of Ru; cyclohexane, 30 mL; H$_2$ pressure, 1 MPa at room temperature; 4 h; 1000 rpm.

4A.3.2.9. Recycle study of catalyst

The reusability of Ru/Al$_2$O$_3$-Acidic catalyst was done by carrying out multiple catalytic runs with spent catalyst. During the recycle study the recovery of spent catalyst was done by centrifugation. The recovered wet catalyst was used in the next catalytic run without any pre-treatment. In addition, to check the catalyst activity by maintaining S/C ratio constant, the recovered wet catalyst obtained after 3rd catalytic run was dried at 60 °C for 12 h and used for 4th run.
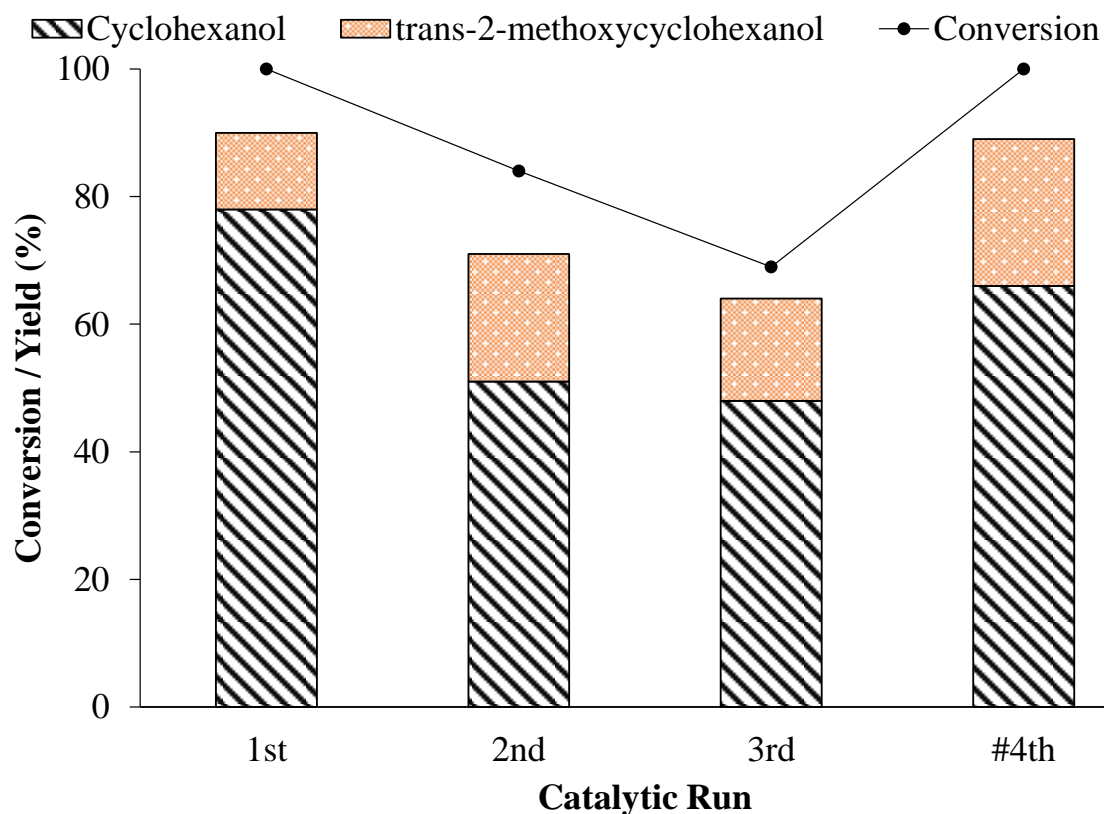
Figure 4A.18. Recycle study of catalyst.

Reaction condition: Guaiacol/Ru molar ratio, 165; 2.15 wt% Guaiacol; cyclohexane, H_2 pressure, 1 MPa at room temperature; 225 °C; 4 h; 1000 rpm. In the 2nd and 3rd run, Guaiacol/Ru molar ratio was not maintained as catalyst was not dried. # In 4th run, wet recovered catalyst from 3rd run was dried at 60 °C for 12 h and Guaiacol/Ru molar ratio of 165 was maintained.

Recycle study shown in Figure 4A.18. represents drop in the catalyst activity till 3rd run this was due to increase in substrate to catalyst ratio due to loss of catalyst during recovery of spent catalyst. Hence in fourth run S/C ratio was maintained which showed improvement in the activity of catalyst correlating with the result of 1st catalytic run. This shows that catalyst is stable under reaction condition and reusable till 4th run.

4A.4. Characterization of spent catalyst

The N_2 sorption data of spent Ru/Al_2O_3-Acidic catalyst shows slight decrease in the surface area of spent catalyst (114 $m^2 \bullet g^{-1}$). This is due to adsorption of coke on the catalyst surface as is proven above. ICP-OES analysis shows no leaching of Ru metal as the Ru content in fresh and spent was same. CO chemisorption data also showed similar crystallite size of fresh and spent catalyst (1.8 nm) with 72% dispersion. The TPR profile of fresh and spent catalyst were exactly matching with each other as shown in (Figure 4A.19.). TEM profile shows similar morphology of spent catalyst (Figure 4A.20.). Due to the stability of the catalyst, it showed similar activity in recycle runs.
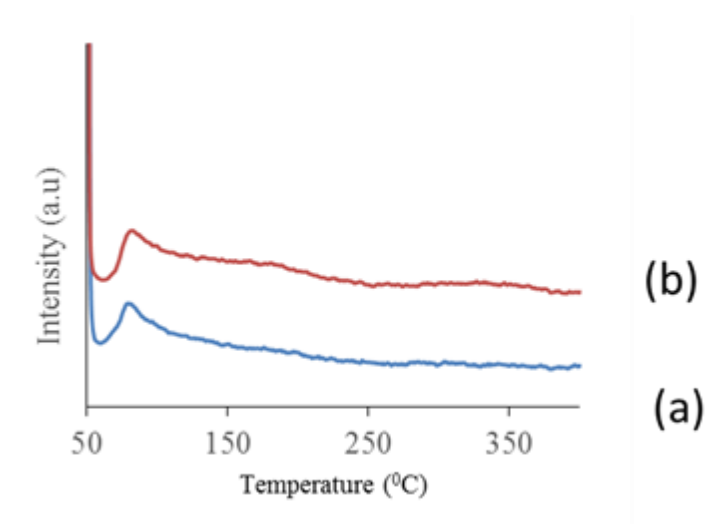
Figure 4A.19. TPR of spent catalyst (a) fresh catalyst (b) spent catalyst
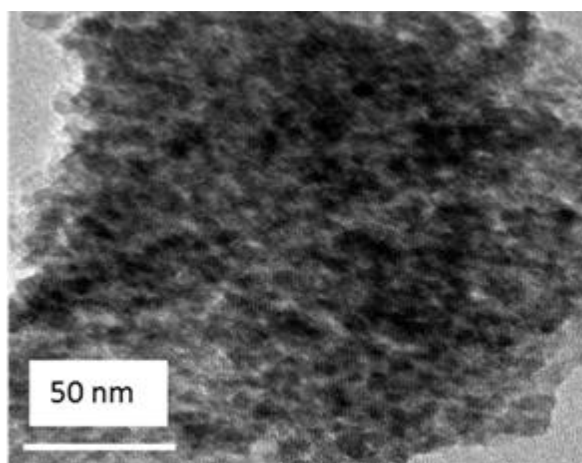
Figure 4A.20. TEM of spent Ru/Al$_2$O$_3$-Acidic (commercial) catalyst

4A.5. Conclusion

Hydrodeoxygenation reactions of guaiacol and various other lignin derived monomers were carried out in presence of different Ru based supported metal catalyst. Effect of support study shows that acidic support plays an important role in the improvement of catalyst activity towards HDO reaction. A unique study on the effect of reduction temperature of catalyst shows that with decrease in reduction temperature activity of catalyst increases due to metal is partially present in higher oxidation state that helps in suppressing coke formation. In cyclohexane medium in presence of Ru/Al$_2$O$_3$-Acidic catalyst, 82% yield of cyclohexanol was achieved with 100% conversion of guaiacol, which is one of the highest reported until now. The recycle study of catalyst shows that catalyst is stable under reaction condition.

4A.6. References:

1.   Kim, T.-S.; Oh, S.; Kim, J.-Y.; Choi, I.-G.; Choi, J. W., Study on the hydrodeoxygenative upgrading of crude bio-oil produced from woody biomass by fast pyrolysis. *Energy* 2014, *68* (C), 437-443.

2.   Elkasabi, Y.; Mullen, C. A.; Pighinelli, A. L. M. T.; Boateng, A. A., Hydrodeoxygenation of fast-pyrolysis bio-oils from various feedstocks using carbon-supported catalysts. *Fuel Processing Technology* 2014, *123*, 11-18.

3.   Xu, X.; Zhang, C.; Liu, Y.; Zhai, Y.; Zhang, R., Two-step catalytic hydrodeoxygenation of fast pyrolysis oil to hydrocarbon liquid fuels. *Chemosphere* 2013, *93* (4), 652-660.

4.   Michael Tuttle Musser, E. I. D. P. D. N., Cyclohexanol and Cyclohexanone. 2005, *10.1002/14356007.a08_217*.

5.   Lai, Q.; Zhang, C.; Holles, J. H., Hydrodeoxygenation of guaiacol over Ni@Pd and Ni@Pt bimetallic overlayer catalysts. *Applied Catalysis A: General* 2016, *528*, 1-13.

6.   Dickerson, T.; Soria, J., Catalytic Fast Pyrolysis: A Review. *Energies* 2013, *6* (1), 514.

7.   Kim, T.-S.; Oh, S.; Kim, J.-Y.; Choi, I.-G.; Choi, J. W., Study on the hydrodeoxygenative upgrading of crude bio-oil produced from woody biomass by fast pyrolysis. *Energy* 2014, *68*, 437-443.

8.   Elkasabi, Y.; Liu, Q.; Choi, Y. S.; Strahan, G.; Boateng, A. A.; Regalbuto, J. R., Bio-oil hydrodeoxygenation catalysts produced using strong electrostatic adsorption. *Fuel* 2017, *207*, 510-521.

9.   Boscagli, C.; Raffelt, K.; Grunwaldt, J.-D., Reactivity of platform molecules in pyrolysis oil and in water during hydrotreatment over nickel and ruthenium catalysts. *Biomass and Bioenergy* 2017, *106*, 63-73.

10.   Cai, Z.; Wang, F.; Zhang, X.; Ahishakiye, R.; Xie, Y.; Shen, Y., Selective hydrodeoxygenation of guaiacol to phenolics over activated carbon supported molybdenum catalysts. *Molecular Catalysis* 2017, *441*, 28-34.

11.   Deepa, A. K.; Dhepe, P. L., Lignin Depolymerization into Aromatic Monomers over Solid Acid Catalysts. *ACS Catalysis* 2014, *5* (1), 365-379.

12.   Deepa, A. K.; Dhepe, P. L., Solid acid catalyzed depolymerization of lignin into value added aromatic monomers. *RSC Advances* 2014, *4* (25), 12625.

13.   Chaudhary, R.; Dhepe, P. L., Solid base catalyzed depolymerization of lignin into low molecular weight products. *Green Chemistry* 2017, *19* (3), 778-788.

14.   Singh, S. K.; Dhepe, P. L., Ionic liquids catalyzed lignin liquefaction: mechanistic studies using TPO-MS, FT-IR, RAMAN and 1D, 2D-HSQC/NOSEY NMR. *Green Chemistry* 2016, *18* (14), 4098-4108.

15.   Singh, S. K.; Dhepe, P. L., Isolation of lignin by organosolv process from different varieties of rice husk: Understanding their physical and chemical properties. *Bioresour Technol* 2016, *221*, 310-317.

16.   Dwiatmoko, A. A.; Kim, I.; Zhou, L.; Choi, J.-W.; Suh, D. J.; Jae, J.; Ha, J.-M., Hydrodeoxygenation of guaiacol on tungstated zirconia supported Ru catalysts. *Applied Catalysis A: General* 2017, *543*, 10-16.

17.   Hong, Y.-K.; Lee, D.-W.; Eom, H.-J.; Lee, K.-Y., The catalytic activity of Pd/WOx/γ-Al2O3 for hydrodeoxygenation of guaiacol. *Applied Catalysis B: Environmental* 2014, *150-151*, 438-445.

18.   Liu, S.; Wang, H.; Smith, K. J.; Kim, C. S., Hydrodeoxygenation of 2-Methoxyphenol over Ru, Pd, and Mo2C Catalysts Supported on Carbon. *Energy & Fuels* 2017, *31* (6), 6378-6388.

19.   Deepa, A. K.; Dhepe, P. L., Function of Metals and Supports on the Hydrodeoxygenation of Phenolic Compounds. *ChemPlusChem* 2014, *79* (11), 1573-1583.

20.   Lee, H.; Kim, H.; Yu, M. J.; Ko, C. H.; Jeon, J.-K.; Jae, J.; Park, S. H.; Jung, S.-C.; Park, Y.-K., Catalytic Hydrodeoxygenation of Bio-oil Model Compounds over Pt/HY Catalyst. *Scientific Reports* 2016, *6*, 28765.

21.   Leiva, K.; Garcia, R.; Sepulveda, C.; Laurenti, D.; Geantet, C.; Vrinat, M.; Garcia-Fierro, J. L.; Escalona, N., Conversion of guaiacol over supported ReOx catalysts: Support and metal loading effect. *Catalysis Today* 2017, *296*, 228-238.

22.   Jung, K. B.; Lee, J.; Ha, J.-M.; Lee, H.; Suh, D. J.; Jun, C.-H.; Jae, J., Effective hydrodeoxygenation of lignin-derived phenols using bimetallic RuRe catalysts: Effect of carbon supports. *Catalysis Today* 2018, *303*, 191-199.

23.   Bui, V. N.; Laurenti, D.; Afanasiev, P.; Geantet, C., Hydrodeoxygenation of guaiacol with CoMo catalysts. Part I: Promoting effect of cobalt on HDO selectivity and activity. *Applied Catalysis B: Environmental* 2011, *101* (3-4), 239-245.

24.   Bui, V. N.; Laurenti, D.; Delichère, P.; Geantet, C., Hydrodeoxygenation of guaiacol: Part II: Support effect for CoMoS catalysts on HDO activity and selectivity. *Applied Catalysis B: Environmental* 2011, *101* (3), 246-255.

25.   Centeno, A.; Laurent, E.; Delmon, B., Influence of the Support of CoMo Sulfide Catalysts and of the Addition of Potassium and Platinum on the Catalytic Performances for the Hydrodeoxygenation of Carbonyl, Carboxyl, and Guaiacol-Type Molecules. *Journal of Catalysis* 1995, *154* (2), 288-298.

26.   Ruiz, P. E.; Frederick, B. G.; De Sisto, W. J.; Austin, R. N.; Radovic, L. R.; Leiva, K.; García, R.; Escalona, N.; Wheeler, M. C., Guaiacol hydrodeoxygenation on MoS2 catalysts: Influence of activated carbon supports. *Catalysis Communications* 2012, *27*, 44-48.

27.   Tyrone Ghampson, I.; Sepúlveda, C.; Garcia, R.; García Fierro, J. L.; Escalona, N.; DeSisto, W. J., Comparison of alumina- and SBA-15-supported molybdenum nitride catalysts for hydrodeoxygenation of guaiacol. *Applied Catalysis A: General* 2012, *435-436*, 51-60.

28.   Sepúlveda, C.; Leiva, K.; García, R.; Radovic, L. R.; Ghampson, I. T.; DeSisto, W. J.; Fierro, J. L. G.; Escalona, N., Hydrodeoxygenation of 2-methoxyphenol over Mo2N catalysts supported on activated carbons. *Catalysis Today* 2011, *172* (1), 232-239.

29.   Güvenatam, B.; Kurşun, O.; Heeres, E. H. J.; Pidko, E. A.; Hensen, E. J. M., Hydrodeoxygenation of mono- and dimeric lignin model compounds on noble metal catalysts. *Catalysis Today* 2014, *233*, 83-91.

30.   Ohta, H.; Kobayashi, H.; Hara, K.; Fukuoka, A., Hydrodeoxygenation of phenols as lignin models under acid-free conditions with carbon-supported platinum catalysts. *Chemical Communications* 2011, *47* (44), 12209-12211.

31.   Olcese, R. N.; Bettahar, M.; Petitjean, D.; Malaman, B.; Giovanella, F.; Dufour, A., Gas-phase hydrodeoxygenation of guaiacol over Fe/SiO2 catalyst. *Applied Catalysis B: Environmental* 2012, *115-116*, 63-73.

32.   Bykova, M. V.; Ermakov, D. Y.; Kaichev, V. V.; Bulavchenko, O. A.; Saraev, A. A.; Lebedev, M. Y.; Yakovlev, V. A., Ni-based sol–gel catalysts as promising systems for crude bio-oil upgrading: Guaiacol hydrodeoxygenation study. *Applied Catalysis B: Environmental* 2012, *113-114*, 296-307.

33.   Wang, X.; Rinaldi, R., Solvent Effects on the Hydrogenolysis of Diphenyl Ether with Raney Nickel and their Implications for the Conversion of Lignin. *ChemSusChem* 2012, *5* (8), 1455-1466.

34.   Zhou, M.; Ye, J.; Liu, P.; Xu, J.; Jiang, J., Water-Assisted Selective Hydrodeoxygenation of Guaiacol to Cyclohexanol over Supported Ni and Co Bimetallic Catalysts. *ACS Sustainable Chemistry & Engineering* 2017, *5* (10), 8824-8835.

35.   Abd Hamid, S. B.; Ambursa, M. M.; Sudarsanam, P.; Voon, L. H.; Bhargava, S. K., Effect of Ti loading on structure-activity properties of Cu-Ni/Ti-MCM-41 catalysts in hydrodeoxygenation of guaiacol. *Catalysis Communications* 2017, *94*, 18-22.

36.   Zhao, C.; He, J.; Lemonidou, A. A.; Li, X.; Lercher, J. A., Aqueous-phase hydrodeoxygenation of bio-derived phenols to cycloalkanes. *Journal of Catalysis* 2011, *280* (1), 8-16.

37.   Zhao, C.; Kou, Y.; Lemonidou, A. A.; Li, X.; Lercher, J. A., Highly Selective Catalytic Conversion of Phenolic Bio-Oil to Alkanes. *Angewandte Chemie* 2009, *121* (22), 4047-4050.

38.   Zhao, C.; Kou, Y.; Lemonidou, A. A.; Li, X.; Lercher, J. A., Hydrodeoxygenation of bio-derived phenols to hydrocarbons using RANEY[registered sign] Ni and Nafion/SiO2 catalysts. *Chemical Communications* 2010, *46* (3), 412-414.

39.   Zhao, C.; Kasakov, S.; He, J.; Lercher, J. A., Comparison of kinetics, activity and stability of Ni/HZSM-5 and Ni/Al2O3-HZSM-5 for phenol hydrodeoxygenation. *Journal of Catalysis* 2012, *296*, 12-23.

40.   Thermal Stability of Cyclohexane and.pdf

41.   Gong, C.-M.;   Li, Z.-R.; Li, X.-Y., Theoretical Kinetic Study of Thermal Decomposition of Cyclohexane. *Energy & Fuels* 2012, *26* (5), 2811-2820.

42.   Mordechay Herskowttz, J. W., and Lussy Skladman, Hydrogen Solubility in Organic Solvent. *J. Chem. Eng. Data* 1983, *28*, 164-166

43.   Noble, S. K. A. P. P., Solubility of hydrogen in benzene, cyclohexane, decalin, phenol, cyclohexanol*, Chem. Revs.* 1941.

44.   Tauster, S. J., Strong Metal-Support Interactions. *Account of chemical research* 1987.

45.   S. J. Tauster, S. C. F., and R. L. Garten, Strong Metal-Support Interactions.Group 8 Noble Metals Supported on TiO$_2$; *journal of the American Chemical Society* 1978.

Chapter 4B

Pathway for the transfer hydrogenation of lignin derived monomers: Mechanistic and kinetic study over the alumina supported Ruthenium catalysts

4B.1. Introduction

Reducing O/C content of lignin derived monomers via hydrodeoxygenation (HDO) is mainly used in up gradation to produce value-added chemicals and fuel grade products. Organic molecule such as alcohol, can transfer hydrogen to minimise the O/C ratio in monomer called catalytic transfer hydrogenation (CTH). However, it is less studied compare to molecular hydrogen based HDO process. Herein we are reporting up gradation of lignin derived monomers via catalytic transfer hydrogenation (CTH) to make overall bio-refinery process economical. Although, few studies are devoted based on (CTH). Strategic development in the study of commercially viable (low loading of metal, mild conditions, high selectivity, etc.) is necessary under mild conditions. Herein, we report, the systematic (CTH) study over the numerous supports (SiO$_2$, Al$_2$O$_3$ (acidic, basic and neutral), SiO$_2$-Al$_2$O$_3$) on the (CTH) of lignin monomers like phenol, veretrol, eugenol and guaiacol by using minor concentration of Ru i.e 0.5wt% Ru metal in the catalyst. Drift IR technique was used to understand the mechenistic pathways for the of (CTH) process. We could achieve 74% cyclohexanol yield from guaiacol by using isopropyl alcohol (IPA) solvent and Ru/Al$_2$O$_3$ as an acidic catalyst at 225 °C in the presence of 0.7 MPa N$_2$ gas. Based on guaiacol conversion detailed kinetic study has been done based on nature of various (CTH) agent, stability of both reactants & products. Our observation justify the formation of less stable targeted products which undergoes further reactions. Detailed characterization of fresh and spent catalysts was studied to understand catalytic behavior of (CTH) process. Lignocellulosic biomass, a renewable resource is an alternate resource to fossil feedstock and is profusely available for the synthesis of chemicals and fuels. Lignin, the third largest component of lignocellulosic biomass is available in plenty as a by-product in the pulp and paper industry and as a by-product in the synthesis of bio-ethanol. Lignin is an amorphous aromatic biopolymer made up of substituted oxygenated aromatic monomers such as, coniferyl, sinapyl, *p*-coumaryl alcohols linked together via various ≡C-C≡ and ≡C-O-C≡ linkages [1, 2]. Lignin upon depolymerization produces phenolic monomers, those may find utilization in the manufacture of variety of precursors for polymers, fuels, and other high value added industrially important products. Thus, valorization of lignin, is considered as a key to make the overall bio-refinery process economically viable. Lignin has typically oxygen to carbon ratio (O/C) of 0.3-0.5 and importantly this ratio is also retained after depolymerization of lignin when carried out in presence of either solid acids, solid bases, or

ionic liquid catalysts [3-5]. The bio-oil obtained after depolymerization consists of mixture of various oxygen containing compounds like substituted phenols, furans, etc. with varying concentrations [6, 7]. Though, these chemicals are very important, but their further conversions into various other useful chemicals are also targeted via various functionalization and defunctionalisation reactions. One of the way to upgrade these chemicals is subject them to catalytic dehydration and hydrodeoxygenation (HDO) reactions, both of which are known as defunctionalization reactions. Through these reactions, oxygen from these monomers can be either partially or fully removed via loss of water, cleavage of C-O bonds, hydrogenation of double bonds etc. Hydrodeoxygenation over heterogeneous catalysts has received substantial consideration in the last couple of years for the valorization of oxygenates obtained from biomass to yield fuels and chemicals [8-12]. HDO reactions usually occur on metal, acid, and bifunctional sites present in optimal amount on a catalyst. The typical reactions involved in HDO are hydrogenation, deoxygenation by decarbonylation, cleavage of C-O bond etc. and thus make HDO process a complicated one. Consequently, the choice of active sites for achieving these reactions in controlled manner is critical when designing effective heterogeneous catalysts for HDO processes [7, 13, 14]. One of the chemical which can be targeted to be obtained from lignin is cyclohexanol as it is derived from phenol, which is currently obtained from fossil feedstock and similar type of monomers are also typically obtained after depolymerization of lignin. Thus by combining lignin depolymerization and up-gradation of bio-oil obtained through dehydration/HDO reactions can yield cyclohexanol as a product. As is known, commercial production of adipic acid proceeds via two key intermediates formation namely cyclohexanol and cyclohexanone (KA oil), which in turn are obtained either from hydrogenation of phenol or oxidation of cyclohexane/cyclohexene, both of which are derived from fossil feedstock [15]. It is anticipated that successful establishment of the bio-refinery model is possible if the KA oil is obtained from lignin. In reference to this, lignin derived KA oil via depolymerisation, HDO and ring hydrogenation of aromatic monomers has been widely studied over various catalysts. Most of the HDO reactions are performed using molecular hydrogen as a hydrogen source in presence of organic solvents since the chemistry is very well known and activation of substrates and molecular hydrogen is easily possible over various precious metals. Generally, precious metals like Ru, Pt, Pd loaded over various supports as catalysts are known to catalyse HDO reactions with molecular hydrogen as hydrogen source

under high temperatures (>275 °C) and pressures (>5 MPa H_2). The employment of severe reaction conditions is necessary to cleave strong C-O bonds (bond dissociation energy, 414 kJ/mol) present in phenolic compounds [16, 17]. Guaiacol having almost similar chemical environment (C-O bonds) as present in lignin: Ar(C)-O-CH$_3$ [C(sp3)–OAr (methoxy group), C(sp2)–OMe] and C(sp2)–OH (hydroxyl) having bond energies of 247, 356 and 414 kJ/mol, respectively is typically used as a model compound for these reactions [18]. The effects of various metals [19-35], supports [36, 37], solvents etc. are well studied in these reactions. Besides, precious metal, these reactions are also catalyzed by sulfided Co and Mo catalysts [38-50]. Although effective way for HDO, the low solubility of molecular hydrogen in most solvents used in these reactions, demands use of higher hydrogen pressures. Moreover, employment of higher hydrogen pressure, may also lead to side reactions. Additionally, infrastructure required to handle high hydrogn pressures in a safe way also adds up the cost of the process. To ally these issues, few reports demonstrate that catalytic transfer hydrogenation (CTH involving addition of hydrogen across C=C or C=O bonds) and/or catalytic transfer hydrogenolysis (CTH involving cleavage of C-C and C-O bonds) can be an alternative methodology. Through this methodology, in-situ hydrogen generation from organic solvents (hydrogen donors) is achieved. In view of this, Ru/C and RuRe/C catalysts are reported for CTH of guaiacol in isopropanol system at 200 °C and 2 MPa N_2 pressure and within 5 h, cyclohexanol formation was observed as a major product (60%) [51]. Recently, comparative study based on CTH of lignin is reported in presence of PtRe/TiO$_2$, Re/TiO$_2$, Pt/TiO$_2$ at 240 °C in inert He media [52]. However, it is emphasized that more research in this area is required to evaluate detailed catalytic parameters to achieve better results in terms of selectivity, TON etc [53]. It is shown that over Ni/C catalyst, in-situ generation of hydrogen from various alcohols (methanol, ethanol, and ethylene glycol) thus in effect CTH pathway is more effective than high-pressure hydrogen (5 MPa) for the depolymerization of birch sawdust [54]. CTH with supercritical methanol over Cu decorated porous metal oxides (Cu-PMO) is also disclosed for depolymerization of lignin [55]. Supported Pd/Ag bimetallic catalyst, is also shown to be active for the CTH of vanillin, a lignin derived monomer [56]. CTH using Raney Ni catalyst in presence of isopropanol as a hydrogen source is known from the literature[57, 58]. Besides this, use of Pd metal supported on Fe$_3$O$_4$ is also known in presence of isopropanol as a hydrogen source to carry out CTH of benzyl phenyl ether[59]. Although, huge body of work is done on CTH for other substrates, work on HDO with

CTH pathway for reduction of oxygen content from lignin derived monomers is in initial stages[60-62]. CTH of lignin derived monomers opens up a scope for the designing and optimization of HDO processes. It is known that organic hydrogen donors transfer hydrogen via different mechanistic pathways such as intermolecular hydride transfer etc. and competition amongst adsorption of organic hydrogen donors with reactants, intermediates and products is also challenging to study and thus achieve alternate results.

4B.2. Experimental section

4B.2.1. Materials

For the details on all the materials used in this study, please refer Chapter 4, section 4A.2.1.

4B.2.2. Catalyst synthesis

Supported Ru metal catalysts (Ru/Al$_2$O$_3$, Ru/SiO$_2$, Ru/SiO$_2$-Al$_2$O$_3$) with 0.5 wt% Ru loading were prepared by wet impregnation method. More details on the materials and synthesis procedure used for the synthesis of supported metal catalyst are described earlier (Refer Chapter 2B, Section 2B.2.2)

4B.2.3. Catalytic runs

CTH of guaiacol was carried out in high pressure, high temperature 100 mL hastelloy make Parr reactor. 2.13 wt% guaiacol solution in (24 g) IPA with Guaiacol/surface exposed Ru metal molar ratio, 35520 is charged in the reactor. At the starting of the reaction, reactor was flushed with N$_2$ for 3-4 times to make autoclave environment free of air. Then, N$_2$ gas was filled in the reactor (0–1.5 MPa at R.T) and heating was started with slow stirring rate (100 rpm) until desired reaction temperature was attained (175–250 °C). After attaining the reaction temperature, stirring rate was increased up to 1000 rpm and this time was recorded as initial time of the reaction. CTH reactions of other aromatic monomers (phenol, anisole, veretrol, eugenol) were carried out by following similar protocol mentioned above. It was also noticed that with an initial 0.7 MPa N$_2$ pressure charged at R.T, at desired reaction temperature of 225 °C, final pressure of the reaction reached upto 5.4 MPa.

4B.2.4. Recycle experiments

After completing the reaction, wet catalyst was recovered from the reaction mixture via centrifugation and subsequently next reaction with the same wet catalyst was carried out without any treatment. In addition, experiments are also carried out by maintaining S/C ratio (substrate to catalyst molar ratio) constant after drying the catalyst. Spent catalyst recovered after the third run was given heat treatment at 60 °C for 12 h after centrifugation. Then this dried catalyst was used for subsequent fourth run.

4B.2.5. Analysis of reaction mixture

Reaction mixture was analysed using GC and GC-MS techniques and for the details about the methodologies used and instruments used for the analysis of reaction mixture, please refer Chapter 4, section 4A.2.5.

$$Conversion\ (\%) = \frac{\text{moles of substrate converted (based on GC)}}{\text{moles of substrate charged}} x\ 100$$

$$Yield\ (\%) = \frac{\text{moles of product formed (based on GC)}}{\text{moles of theoretical product formed based on substrate converted}} x\ 100$$

4B.3. Result and discussion

4B.3.1. Catalyst characterization

Before employing the catalysts for the CTH reactions, those were characterized to understand their morphologies and properties.

4B.3.1.1. Determination of catalysts morphology

All the synthesized catalysts were characterized thoroughly to understand their morphology and to correlate the activity of the catalysts with their morphologies. For details of characterization technique used Refer (Chapter 2B, Figure 2B.2. XRD analysis). XRD analysis of supported metal catalysts was done to confirm the phase of support and metals. ICP analysis was done to confirm the % of metal loading in respective catalyst (Chapter 2B, Section 2B.3.3.

Table 2B.3. ICP analysis). NH_3/CO_2 TPD analysis of synthesized catalysts was done to calculate respective acidity and basicity present in catalyst (Chapter 2B, Figure 2B.11. and Table 2B.5). XPS analysis was done to check the oxidation state of metal (Chapter 2B, Figure 2B.7.-2B.10.). N_2 physisorption analysis of synthesized catalysts were done to check available surface area for the catalytic activity (Chapter 2B, Table 2B.2.). CO chemisorption analysis was done to calculate % metal dispersion and crystallite site of the synthesized catalyst and tabulated in (Chapter 2B, Table 2B.4.). TEM analysis was done to check the particle size of supported metal catalyst (Chapter 2B, Figure 2B.3-2B.5).

4B.3.2 Catalyst activity

Catalytic transfer hydrogenation (CTH) reactions were conducted in high temperature, high pressure, batch mode reactors and reaction mixture was analysed by using gas chromatography (please refer experimental section for details).

4B.3.2.1. Effect of support on the HDO of guaiacol

Figure 4B.1. Effect of support on the CTH of guaiacol.

Reaction condition: Guaiacol/surface exposed Ru metal molar ratio, 35520; 2.13 wt% Guaiacol in IPA; N_2, 0.7 MPa at room temperature; 225 °C; 2 h; 1000 rpm.

It has been seen from the Figure 4B.1 that catalytic activity and selectivity for the formation of product has changed from different supports with constant Ru (0.5 wt%) loading. Reactions were carried out at 225 ^oC, under 0.7 MPa N_2 pressure for 2 h by using IPA as a solvent. 28% cyclohexanol and 10% trans-2-methoxycyclohexanol formation was observed with 48% guaiacol conversion by using SiO_2 (Neutral) as a support. When Al_2O_3-Neutral was used as a support instead of SiO_2 (Neutral), increase in the guaiacol conversion (55%) was seen along with the increase in the formation of cyclohexanol (39%) and 12 % trans trans-2-methoxycyclohexanol. This observation was not surprising since both SiO_2 and Al_2O_3 are known as neutral supports. Regardless, as shown above, very weak acidity (0.16 mmol•g^{-1}) was seen in case of Al_2O_3-Neutral support. Also, CO chemisorption data indicated that crystalline size of Ru on Al_2O_3-Neutral was too small (2.18 nm) compared to SiO_2 support (11.8 nm). These two factors are playing significant role in increasing the overall activity of the catalyst. Additionally, presence of Ru in different oxidation states on Al_2O_3 (+2/+3) SiO_2 (+2/+3 is also responsible for the change in activity. Considering this fact, acidic Al_2O_3 was used to support Ru metal or particles and the catalytic activity was estimated under similar conditions. As an evidence of acidity playing a role, enhancement in the yield for cyclohexanol (74%) with Ru/Al_2O_3-Acidic catalyst, was attained as compared to neutral Al_2O_3 (39%). Besides this, formation of trans-2-methoxycyclohexanol (9%) and 5 % cyclohexane with cyclohexanol as a product was seen, which was lower than Al_2O_3-Neutral supported catalyst (12%). Taking everything into account, crystallite size of Ru was examined for both the catalysts (Al_2O_3-Neutral, Al_2O_3-Acidic) and it was perceived that over both the supports, Ru crystallite size is nearly equivalent 1.8 nm, 2.1 nm; Chapter 2B, Table 2B.4). Moreover, it has been observed that on both Al_2O_3 supported Ru, it is present in higher oxidation state as is evident from TPD studies. Hence, it can be effectively proven that the acidity of the support has a significant role in the cleavage of C-O bond and hence, acidic Al_2O_3 supported Ru catalyst is showing higher cyclohexanol yield than neutral Al_2O_3 supported Ru catalyst. These results recommended that the adsorption of oxygenated compound(s) on the acidic supports has

greater influence and it has resulted into the formation of higher cyclohexanol as a product. With reference to this, activity of basic Al_2O_3 supported Ru catalyst was estimated and it was found that the catalyst showed 33% cyclohexanol yield along with 21% yield for trans-2-methoxycyclohexanol. It was likely to give lower C-O cleavage activity on the basic support. As noticed, best cyclohexanol formation activity was found with Ru/Al_2O_3-Acidic catalyst, which is identified to have milder acidity. Later, Ru/SiO_2-Al_2O_3 catalyst was also examined for CTH activity of guaiacol however, no conversion of guaiacol was observed. Yet, acid catalyzed dehydration of solvent (IPA) was predominant resulting in the formation of ether. This might be because of the fact that SiO_2-Al_2O_3 has higher acidity (0.54 mmol•g^{-1}) than Al_2O_3-Acidic with Ru crystallite size of 3.05 nm and thus catalyst might be highly active to dehydrate alcohols yielding ether as a product. Another aspect in this study was lower mass balance reported in the reaction. This phenomena is due to formation of isomeric intermediate product (cis-2/trans-2 methoxy cyclohexanol). Nonetheless, unavailability of standard compound (cis-2-methoxycyclohexanol) restricted its quantification. Moreover, considerable similarity in GC area of both the isomers suggested similar quantity of cis-2.methoxy cyclohexanol which is forming in almost similar amount.

To compare the activity of different catalysts and the role of support on the reaction, TOF calculations were done while reactions were performed for shorter time of 0.5 h at 225 °C under 0.7 MPa N_2 pressure. Following order of TOF was observed:

Ru/SiO_2 12% (2.4 (0.5 h^{-1})) < Ru/Al_2O_3-Neutral 15% (7.2 (0.5 h^{-1})) < - Ru/Al_2O_3-Basic 13% (14.2 (0.5 h^{-1})) < Ru/Al_2O_3- Acidic 37% (48 (0.5 h^{-1}))

Higher TOF was seen for Ru/Al_2O_3 catalyst in shorter reaction time, which is obvious due to smaller particle size of Ru compared to other catalysts, showed conversions (100%, 2 h) and high yield of cyclohexanol (74%, 2 h). Nonetheless, TOF values need to be explained based on the structure sensitive/insensitive aspect of CTH reaction.

To check whether during the reactions methane is obtained as methanol would form after the cleavage of C-O bond (Ar-OCH$_3$), vent gas was analysed by GC equipped with TCD. However, absence of any peak for methane or any other gas was seen and thus it is suggested

that methanol does not undergo any reaction. Based on the GC equipped with FID analysis of reaction mixture, formation of methanol with almost 75% equivalent to CTH of guaiacol was seen, which confirmed that methanol does not undergo any further conversions.

4B.3.2.2. Effect of Temperature

Amongst all the catalytic systems, with Ru/Al$_2$O$_3$-Acidic catalyst higher CTH activity with formation of 74% cyclohexanol was achieved when reaction was carried out at 225 ^{o}C. For the improvement of cyclohexanol yield, further effect of reaction temperature (175, 200, 225 and 250 $^\circ$C) on the CTH activity of Ru/Al$_2$O$_3$-Acidic catalyst was studied and the results are presented in Figure 4B.2, At 175 ^{o}C no conversion of guaiacol has been seen, which can be explained based on the fact that normally CTH does not happen <170 ^{o}C. When temperature was increased to 200°C, 50% yield of cyclohexanol along with 22% yield of trans-2-methoxycyclohexanol and 2 % cyclohexane was found. With further increase in temperature to 225 ^{o}C, CTH activity of catalyst increased with formation of cyclohexanol (74%) and trans-2-methoxycyclohexanol yield (9%) and 5% cyclohexane seen. In order to investigate whether at higher temperature, more cyclohexanol yield is possible, reaction was carried out at 250 ^{o}C but lower yields of cyclohexanol (68%) with 6% trans-2-methoxycyclohexanol and 14 % cyclohexane formation were seen. This is obvious since, at higher temperature, further HDO of cyclohexanol is possible to yield cyclohexane as product. Interesting fact in all these results is that intermediate is not completely converted into cyclohexanol. This suggests that cleavage C-O bond is RDS.

Figure 4B.2. Effect of temperature on the hydrodeoxygenation of guaiacol

Reaction condition: Guaiacol/ surface exposed Ru metal molar ratio, 35520; 2.13 wt% Guaiacol in IPA; N_2, 0.7 MPa at room temperature; 2 h; 1000 rpm.

Based on the obtained results, it can be suggested that at lower temperature (175 °C) the CTH activity of catalyst is low due to lower partial pressure generated (2.1 MPa). It was seen that very high pressure was observed (7.3 MPa) at 250 °C, that encourages the higher CTH activity.

4B.3.2.3. Effect of S/C (Substrate to Ru catalyst) molar ratio
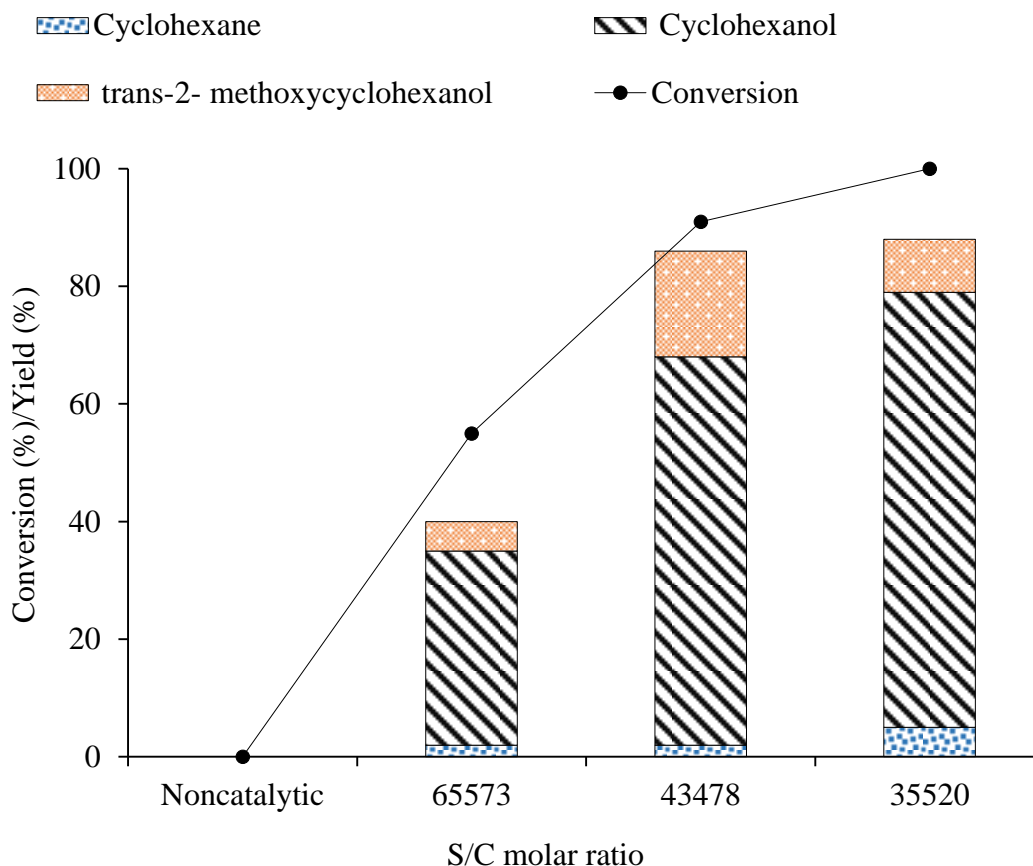
Figure 4B.3. Effect of Substrate to catalyst surface exposed Ru metal (S/C) molar ratio. **Reaction condition:** 2.13 wt% Guaiacol in IPA; N_2, 0.7 MPa at room temperature; 225 °C; 2 h; 1000 rpm.

To achieve the best results with lower Ru content, molar ratio of substrate to surface exposed Ru metal was varied from 35520 to 65573 and the results are summarized in Figure 4B.3. With highest S/C molar ratio of 65573, 55% conversion with 33% yield of cyclohexanol and 5% yield of trans-2-methoxycyclohexanol with 2% cyclohexane was achieved. Reaction with S/C molar ratio of 43478 showed 91% conversion of guaiacol with 66% yield of cyclohexanol and 18% yield of trans-2-methoxycyclohexanol with 2% yield of cyclohexane. Subsequently, ratio of 35520 was used and 100% conversion with 74% yield of cyclohexanol and 9% yield of

trans-2-methoxycyclohexanol and 5% cyclohexane was observed. One of the interesting observation is that in non-catalytic reaction, guaiacol did not show any conversion which indicates that guaiacol is thermally stable compound until 225 ℃.
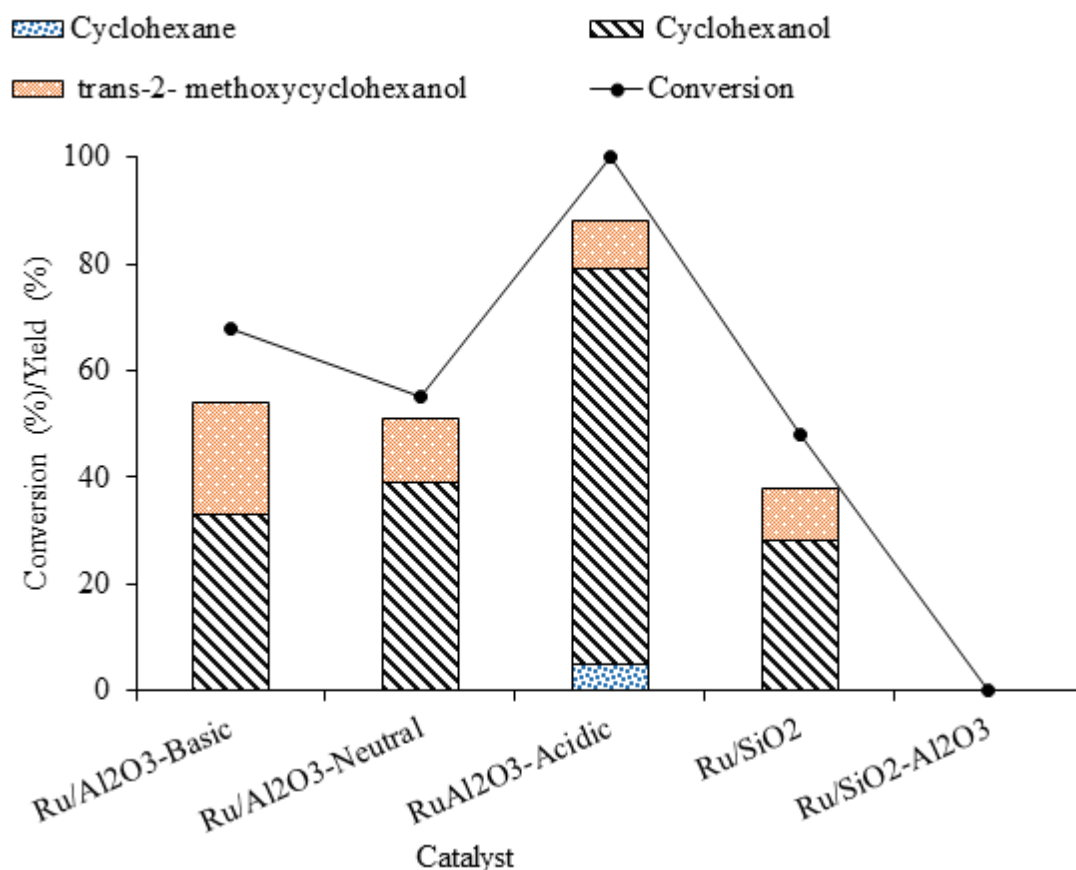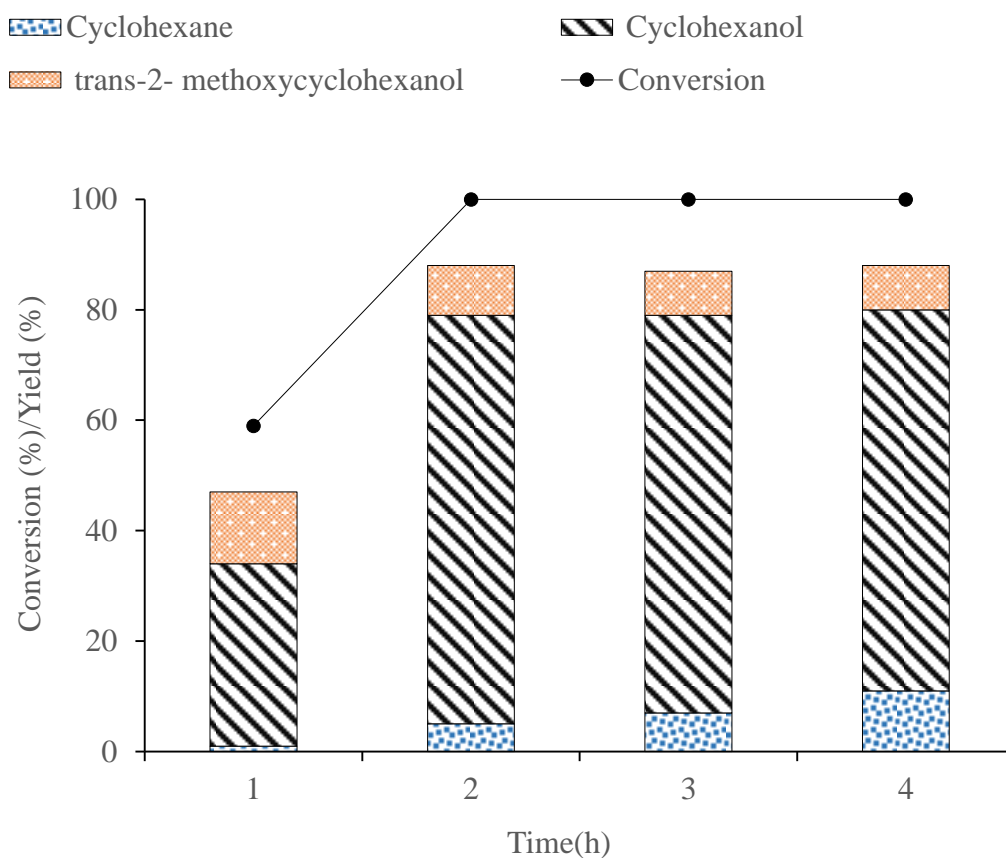

Figure 4B.4. Effect of time on the HDO of guaiacol.

Reaction condition: Guaiacol/surface exposed Ru metal molar ratio, 35520; 2.13 wt% Guaiacol in IPA; N_2, 0.7 MPa at room temperature; 225 °C; 1000 rpm.

4B.3.2.4. Effect of time on hydrodeoxygenation of guaiacol

As mentioned above with S/C molar ratio of 35520, within 2 h, it was possible to attain 74% yield for cyclohexanol with complete conversion of guaiacol at 225 ℃. As 100% conversion of guaiacol was achieved within 2 h, reaction was carried out by shortneing the reaction time from 2 h to 1 h. It was found that guaiacol conversion decreases to 59% with decrease in yield of cyclohexanol (33%) (Figure 4B.4). Conversely, reaction time increased from 2 h to 3 h

and100 % conversion of guaiacol was achieved but there was marginal decrease in the yield of cyclohexanol (72%) at the expense of formation of cyclohexane. To check the stability of cyclohexanol in a reaction further, reaction time was increased to 4 h and it was found that again cyclohexanol yield was decreased to 69% with increase in the yield of cyclohexane upto 11%. From these observations, it can be suggested that cyclohexanol is slightly unstable under reaction conditions and gets converted to fully deoxygenated product i.e.cyclohexane.

Time study reveals that the first step in this reaction is formation of cis-2-/trans-2-methoxycyclohexanol. Further, cleavage of C-O bond gives cyclohexanol and cyclohexanone as products. Hence, it is believed that reaction proceeds via cyclohexanone species which further undergoes hydrogenation to yield cyclohexanol. From this fact, it is anticipated that hydrogenation of guaiacol occurs on the catalyst surface to form cis-2-/trans-2-methoxycyclohexanol. However, since formation of cis-2-methoxycyclohexanol was not observed in the GC, it was believed that the trans-2-methoxycyclohexanol form is more stable than cis-2-methoxycyclohexanol form and hence, the trans-2-methoxycyclohexanol was observed in the reaction and cis-2-methoxycyclohexanol instantly get consumed to form cyclohexanol due to its lower stability. To prove this fact, reactions were carried out with both guaiacol and trans-2-methoxycyclohexanol as a substrate under similar conditions (0.5 h). It was seen that guaiacol conversion was 37% with 19% of cyclohexanol formation. On the other hand, when reaction was carried out with trans-2-methoxycyclohexanol, 21% conversion was seen with the 9% formation of cyclohexanol. This means guaiacol conversion to cyclohexanol is faster and it is happening through cis-2-methoxycyclohexanol isomer formation, which is less stable than trans-2-methoxycyclohexanol. When trans-2-methoxycyclohexanol was used as a substrate, from the GC-MS profiles it is suggested that with the decrease in intensity of peak for trans-2-methoxycyclohexanol (RT=3.87) another peak was appeared (RT=3.74). Since, this peak is very close to trans-2-methoxycyclohexanol it is considered as peak for cis-2-methoxycyclohexanol. Moreover, mass fragmentation patterns of both the peaks is observed to be analogous. Hence, it is proposed that these peaks are for cis-2-/trans-2-methoxycyclohexanol isomers. This is a natural phenomena that trans-2-methoxycyclohexanol will be more stable than cis-2-methoxycyclohexanol due to highly unfavorable steric interaction of functionality present in cis-2-methoxycyclohexanol isomer compared to trans-2-methoxycyclohexanol isomer of same. This in turn is because of difference in the exothermic

heat of combustion factor of isomers. Conventionally, it is known that thermodynamically trans-2-methoxycyclohexanol form of disubstituted cyclic hydrocarbon is more stable than cis form. Hence, we believe that cis-2-methoxycyclohexanol is an intermediate for final product cyclohexanol (Figure 4B.5).
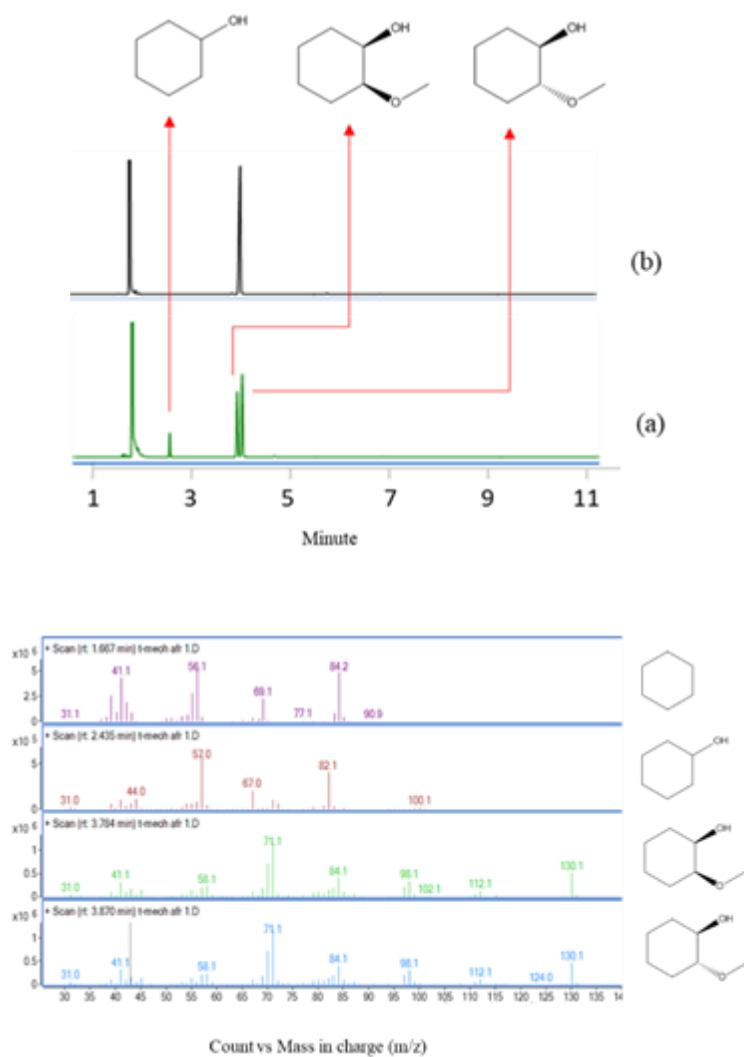
Figure 4B.5. Reaction with trans-2-methoxycyclohexanol. (A) GC-MS profile for (a) after reaction, (b) before reaction. (B) GC-MS fragmentation profile.

Reaction condition: 225 °C; H$_2$, 1 MPa; 1 h;

4B.3.2.5. Effect of N₂ pressure

Typically, HDO reactions are reported under high H_2 pressure (>3 MPa) [17, 29, 30, 51] however, in this work high yield of cyclohexanol (74%) could be achieved even at 0.7 MPa N_2 pressure with CTH process generated in-situ H_2. Furthermore, under lower N_2 pressures, reactions were carried out using 0.1 MPa N_2 pressure in order to check consistent HDO activity of Ru/Al₂O₃-Acidic catalyst and the results are summarized in Figure 4B.6.
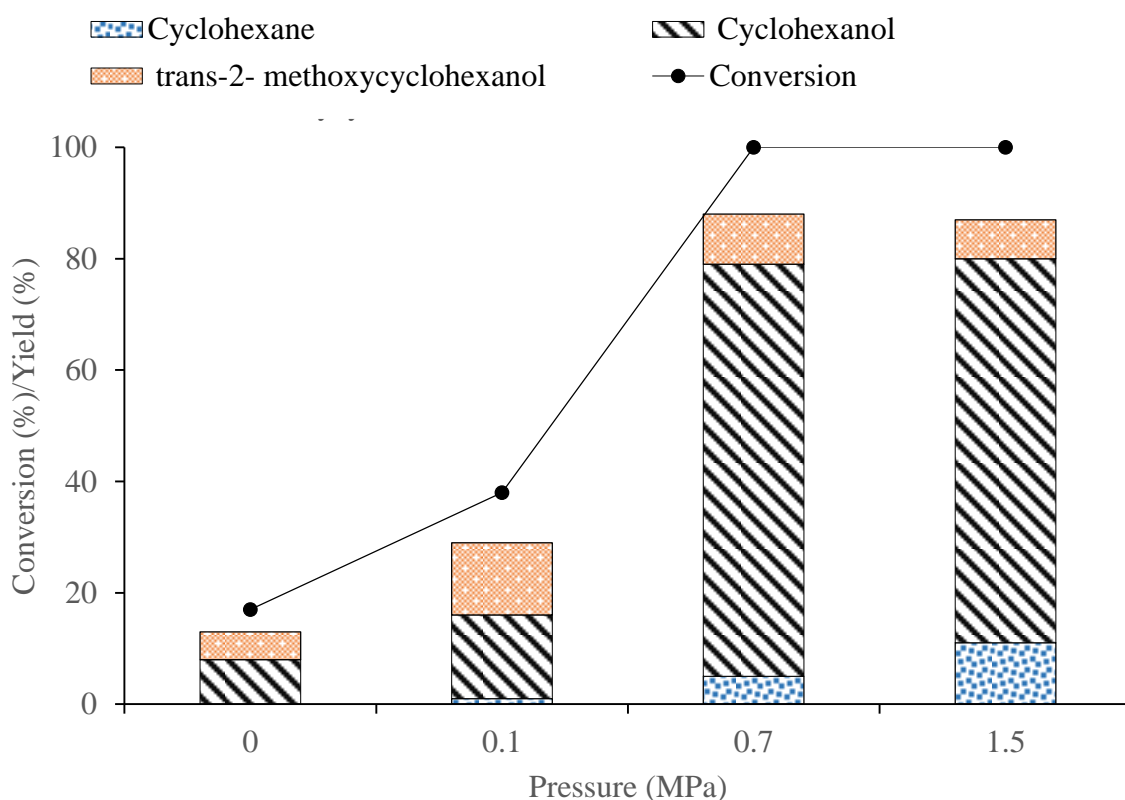
Figure 4B.6. Effect of N_2 pressure

Reaction condition: Guaiacol/surface exposed Ru metal molar ratio, 35520; 2.13 wt% Guaiacol in IPA; 1000 rpm. 225 °C; 1000 rpm.

It is seen from the Figure 4B.6 that at lower pressure of 0.1 MPa, conversion of guaiacol was decreased to 38% with only 15% cyclohexanol, 13% trans-2-methoxycyclohexanol and 1 % cyclohexane formation. Obtained result was not satisfactory as compared with 0.7 MPa N_2 pressure reaction (guaiacol conversion, 100%; cyclohexanol yield, 74% and trans-2-

methoxycyclohexanol yield, 9% cyclohexane 5%). The better activity observed at 0.7 MPa pressure can be attributed to two factors, 1) Increased solubility of in-situ generated H_2, which in turn gives more concentration of H_2 on the catalyst and 2) Better interaction between substrate (solubalized) and catalyst (solid) at high autogenous pressure (5.4 MPa). To check these possibilities, reaction was carried out without pressurizing N_2 (total final pressure 2.1 MPa). Under this reaction condition, the conversion of guaiacol was only 17% with 8% cyclohexanol and 5% trans-2-methoxycyclohexanol formation. If nitrogen developed pressure was not playing any role and only in-situ generated hydrogen was driving the reaction, then under similar temperature condition with same catalyst, even without nitrogen, reactions should have shown similar results like obtained under 0.7 MPa N_2 pressure reaction. Since, this is not the fact, it is believable that nitrogen developed pressure plays crucial role in the reaction, which is better interaction between substrate and catalyst. Further, in order to study the effect of higher N_2 pressure, reaction was conducted at 1.5 MPa N_2 pressure and 100% conversion of guaiacol was obtained but the yields of both, cyclohexanol (69%) and trans-2-methoxycyclohexanol (7%) decreased with increase in the yield of cyclohexane (11%). This might be because of the fact that there can be stronger and better interaction between catalyst and substrate/product to drive the reaction further.

4B.3.2.6. Effect of solvent

Since, IPA is well known CTH reagent, it was obvious choice to carry out the reaction in same. It is well reported in the literature that most of the lignin depolymerization processes are carried out in alcohol-water mixture,[3-5] and hence it would be interesting to check whether CTH reaction can be done in this solvent system (Figure 4B.7). As known, when reaction was carried out in IPA solvent, conversion of guaiacol reaches upto 100% with formation 74% yield of cyclohexanol and 9% yield of trans-2-methoxycyclohexanol.
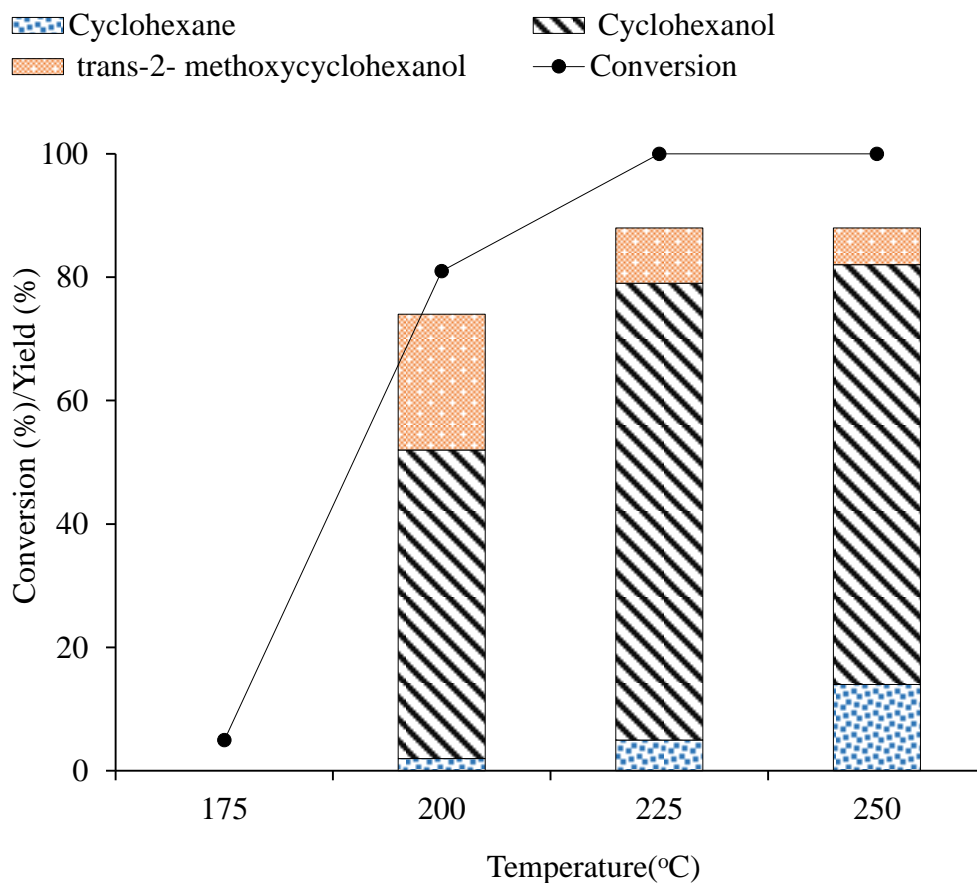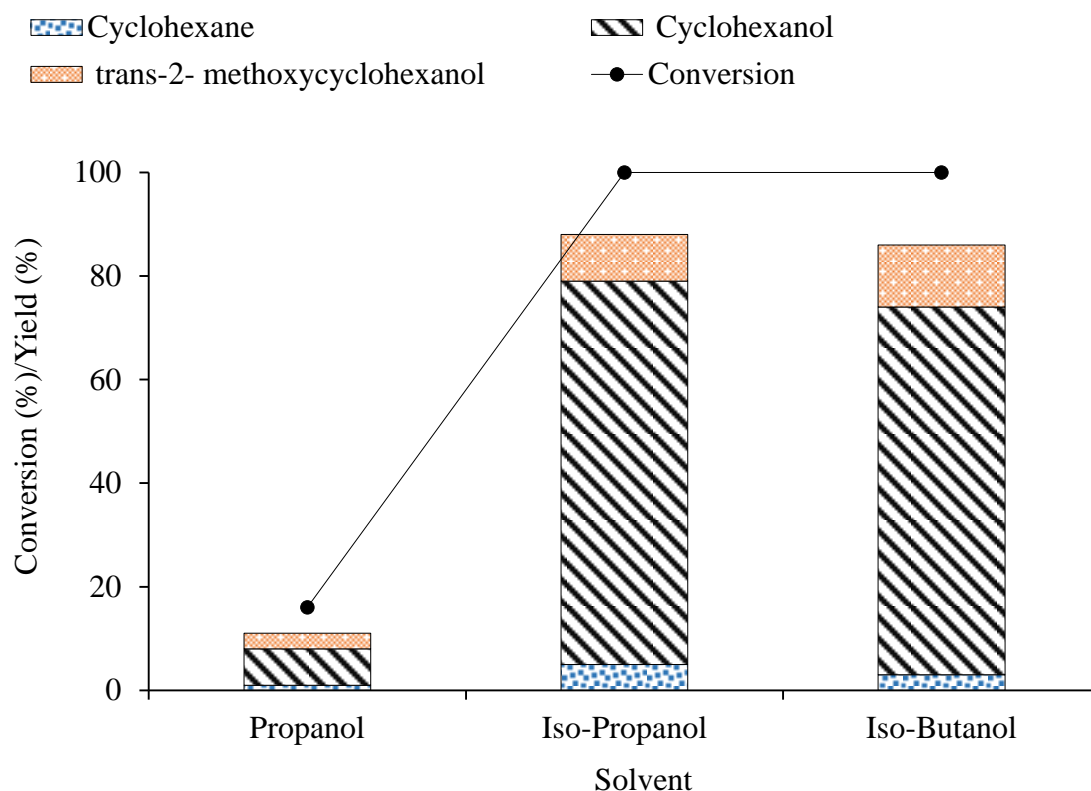
Figure 4B.7. Effect of solvent on the HDO of guaiacol

Reaction condition: Guaiacol/surface exposed Ru metal molar ratio, 35520; 2.13 wt% Guaiacol in solvent; 0.7MPa N_2, 1000 rpm. 225 °C; 1000 rpm.

Although the reaction was carried out in the presence of n-propanol solvent, only 16 % conversion of guaiacol was achieved along with 7% yield of cyclohexanol and 3% yield of trans-2-methoxycyclohexanol. As seen, n-propanol, which is a primary alcohol is less active for CTH process in comparison with IPA (secondary alcohol). This is because, IPA is more active due to formation of corresponding ketone, a stable form. To prove this fact, another secondary alcohol Iso-Butanol was tested for CTH process, and 100 % guaiacol conversion, 71% yield of cyclohexanol with 12 % yield of trans-2-methoxycyclohexanol were achieved. From the obtained results, it is suggested that secondary alcohol is more active for CTH process than primary alcohol.

4B.3.2.7. Effect of reduction temperature of catalyst on the catalytic activity

Typically, reduction of supported metal catalyst was carried out at high temperature (>300 °C) in order to attain complete reducton of metal. In view of this, initially Ru/Al$_2$O$_3$-Acidic catalyst was reduced at 400 °C and the catalyst activity was estimated at 225 °C for 2 h under 0.7 MPa N$_2$ in IPA solvent (Figure 4B.8.) At 400 °C, only 39 % conversion of guaiacol was achieved with 22% cyclohexanol, 6% trans-2-methoxycyclohexanol, and 2 % cyclohexane formation. To understand whether lower reducing temperatures will help in better CTH activity, catalyst was reduced at 250 °C and 150 °C and with the decrease in reduction temperature, higher activity of the catalyst was seen (Figure 7) in IPA as a solvent. When reaction were carried out at 225°C, with a catalyst reduced at 250 °C, guaiacol conversion reaches upto 65% with corresponding yield of cyclohexanol of 41 %, trans-2-methoxycyclohexanol of 14%, and cyclohexane of 3%. With catalyst reduced at 150 °C, guaiacol conversion reached upto 100% with corresponding yield of cyclohexanol of 74%, trans-2-methoxycyclohexanol of 9%, and cyclohexane of 5%. This proves that with increase in reduction temperature, interaction of substrate with active catalyst site decreases either due to change in oxidation state or change in particle size[63, 64]. Another acceptable reason is that higher oxidation state metal is required to carry this reaction. Moreover, this characteristic phenomena requires further investigation. Another aspect is increase in crystallite size of active metal at higher reduction temperature, for that CO chemisorption analysis was done and tabulated in Table 4B.1. However, almost similar crystallite size were found for all the catalysts. Apart from particle size some other unknown factor is playing a role. There is room for futuristic investigation in this area of research.

Table 4A.3. CO chemisorption study of the catalyst reduced at different temperatures

Catalyst	Average crystallite size (nm)	Metal dispersion (%)	Monolayer uptake (µmol•g^{-1})
Ru/Al$_2$O$_3$-Acidic	1.8	72.7	35.7
Ru/Al$_2$O$_3$-Acidic @250	1.6	80.7	39.6

Ru/Al$_2$O$_3$-Acidic @400	1.5	88.4	43.4

Figure 4B.8. Effect of catalyst reduction temperature

Reaction condition: Guaiacol/surface exposed Ru metal molar ratio, 35520; 2.13 wt% Guaiacol in IPA; 0.7 MPa N$_2$, 1000 rpm. 225 °C; 1000 rpm.

4B.3.2.8. Kinetics of guaiacol hydrogenolysis

As presented in Scheme 4B.1, hydrogenation of guaiacol and hydrogenolysis of intermediate 2-methoxycyclohexanol are main steps involved in guaiacol CTH, so detailed kinetic evaluation were carried out over Ru/Al$_2$O$_3$-Acidic catalyst. Conversion versus time and Arrhenius plot for CTH of guaiacol to cyclohexanol are plotted in Figure 4B.9.A-4B.9.B. The R (reaction rate in mmol•g•cat^{-1}•h^{-1}) and corresponding activation energy (Ea) are tabulated in Table 4B.2. It was found that the reaction rate of guaiacol conversion increases with increase in temperature.
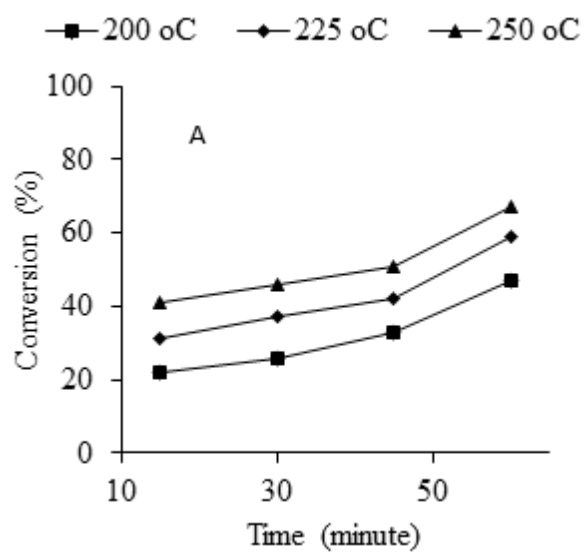
Figure 4B.9A. Conversion of guaiacol over Ru/Al$_2$O$_3$ –Acidic catalyst with different temperature and time

E_a= 15.35 KJ•mole^{-1} , R^2 = 0.99
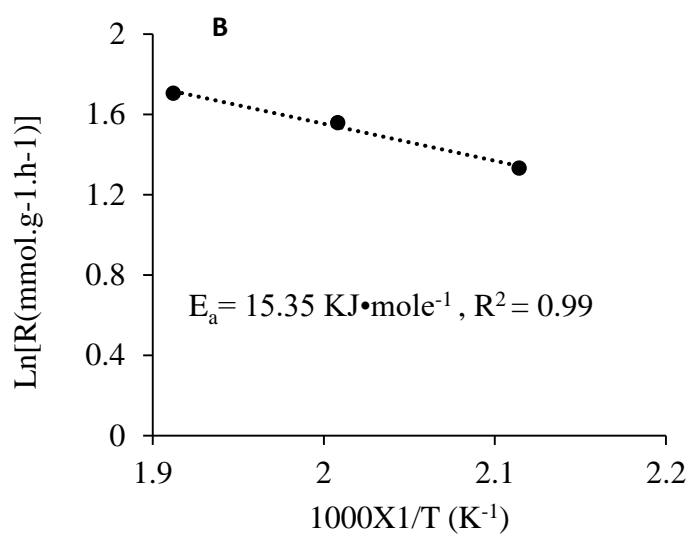
Figure. 4B.9 (B) Arrhenius Plot

Reaction Condition: Guaiacol/surface exposed Ru metal molar ratio, 35520; 2.13 wt% Guaiacol in IPA; 0.7MPa N$_2$, 1000 rpm. Temperature; 1000 rpm.
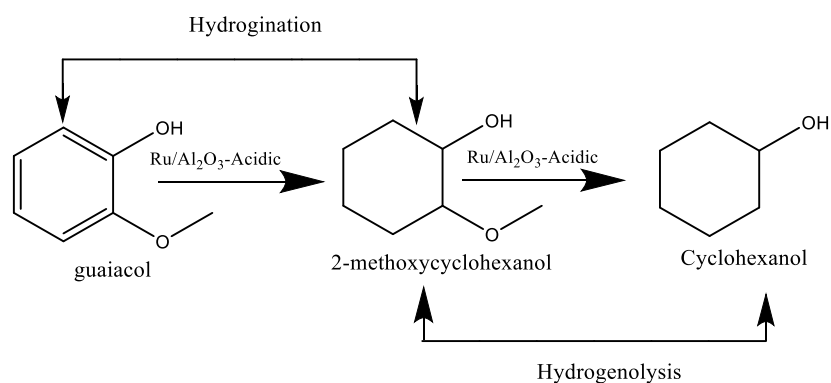
Scheme 4B.1. Reaction paths for guaiacol HDO over Ru/Al$_2$O$_3$-Acidic

Table 4B.2. Rate and activation energy of Guaiacol HDO

Hydrogenation of guaiacol	Rate (mmol•g$_{cat}^{-1}$•h^{-1})			Ea (KJ•mole^{-1})
	200	220	250	
	3.79	4.75	5.49	15.35

4B.3.2.9. Comparative Drift study towards mechanistic path of phenolic CTH over Ru/Al₂O₃-Acidic Catalyst
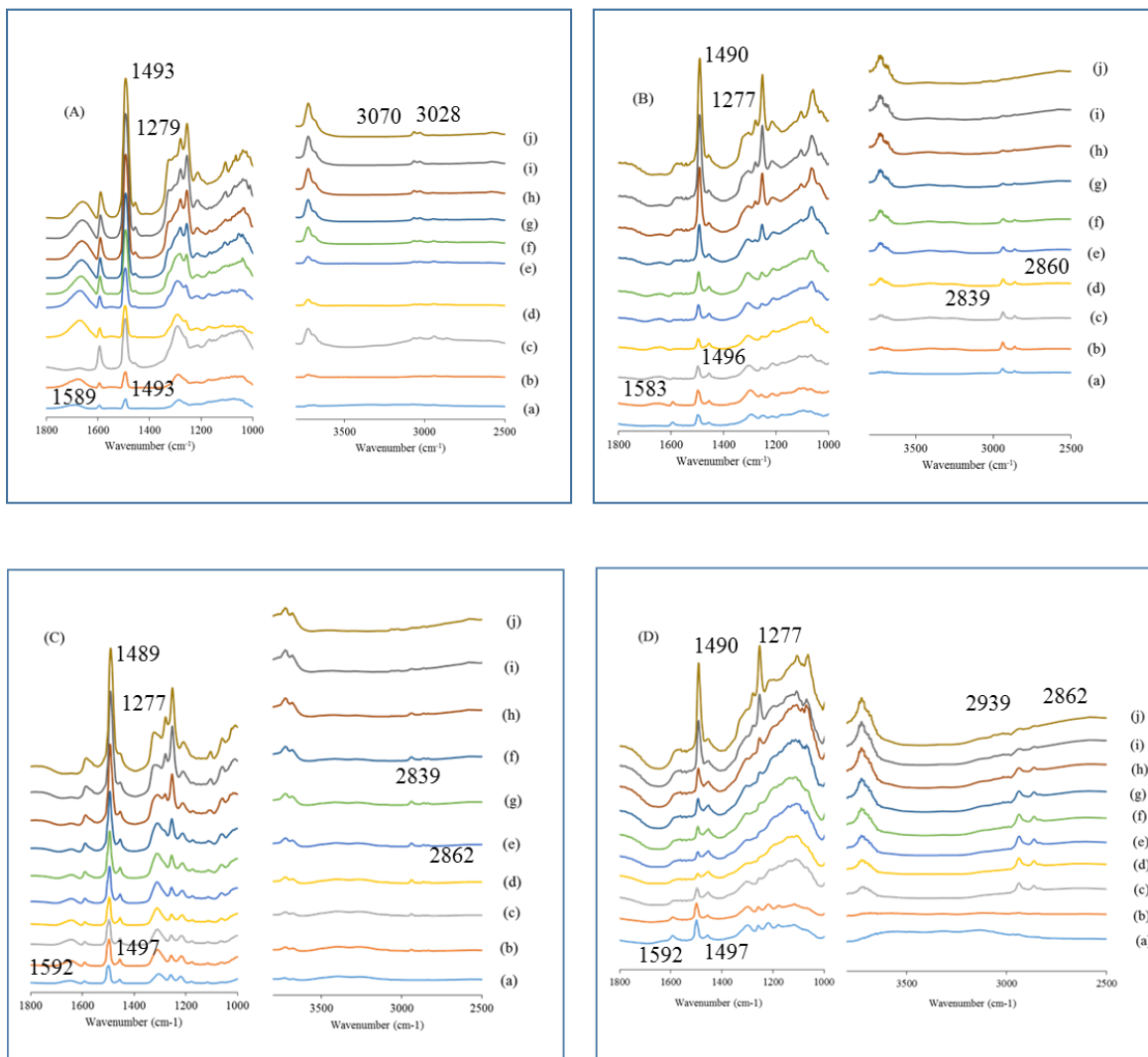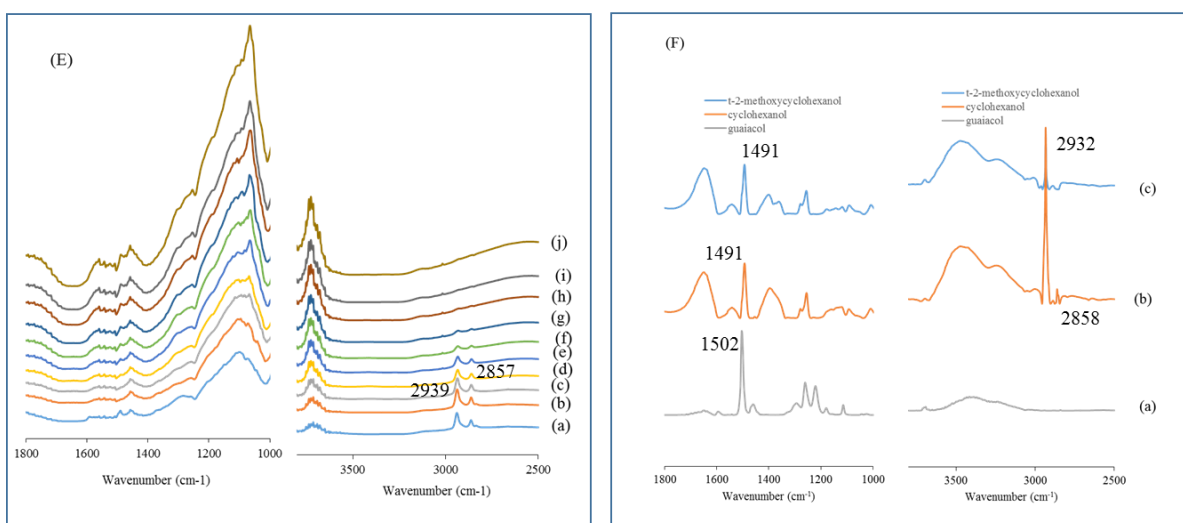
Figure 4B.10. DRIFT spectra of (A) Guaiacol adsorption over Al₂O₃, (B) Anisole adsorption over Ru/Al₂O₃-Acidic, (C) Guaiacol adsorption over Ru/Al₂O₃-Acidic, (D) Phenol adsorption over Ru/Al₂O₃-Acidic, (E) Successive adsorption of Phenol and Anisole over Ru/Al₂O₃-Acidic, Summary of FT-IR bands present in lignin and products. (F) Adsorption of guaiacol, cyclohexanol and t-2-methoxycylohexanol at R.T

Reaction condition: Substrate 0.5 g, cyclohexane 30 mL, P (H₂), (a) 100 °C, (b) 125 °C, (c) 150 °C, (d) 175 °C, (e) 200 °C, (f) 225 °C, (g) 250 °C, (h) 275 °C,(i) 300 °C, (j) 325 °C

The Drift spectra of phenolic compounds (guaiacol, anisole, phenol) was carried out using Bruker Tensor 27 spectrometer in diffuse reflectance mode (DRIFT) equipped with MCT detector and Harrick praying mantis reaction chamber with Zn-Se window, scan and resolution was 232 and 4 cm⁻¹. For the experiment, Al₂O₃-Acidic support and Ru/Al₂O₃-Acidic catalyst were kept inside the reflectance cell under H₂ (10 ml•min⁻¹) medium and background spectra was collected before analysis. At the start of experiment 5 microlitre sample was injected at room temperature, then the sample was heated inside the diffuse reflectance cell, and spectrum was recorded by increasing the temperature interval of 25 °C starting from 100 to 325 °C. Spectrum was recorded in Kubelka-Munk mode, respective data over the in Table 4B.3

Table 4B.3. Vibrational band of the Guaiacol adsorption

Bands (cm^{-1})	Type of vibration	Substrate	Catalyst	Wavenumber (cm-1)	Results
1493, 1589 1279 3028, 3070	C=C stretching of aromatic ring CO of phenoxy species C=H Stretching	Guaiacol	Al$_2$O$_3$-Acidic	1493,1589 1279 3028,3070	Aromatic character retain
1497, 1592 1277 2839, 2862	C=C stretching of aromatic CO of phenoxy C-H Stretching	Guaiacol	Ru/Al$_2$O$_3$-Acidic	1497 ↓ 1489 3028 ↓ 2868 3070 ↓ 2862	Aromatic character shifting to Single bonding character C=H shifting to C-H Stretching
1496, 1583 1277 2839,	C=C stretching of aromatic ring CO of phenoxy species	Anisole	Ru/Al$_2$O$_3$-Acidic	1496 ↓ 1490	Aromatic character shifting to Single bonding character

				2839,2860	C=H shifting to C-H Stretching
2860	C-H Stretching				
1497, 1592 1277 2862, 2939	C=C stretching of aromatic ring CO of phenoxy species C-H Stretching	Phenol	Ru/Al$_2$O$_3$-Acidic	1497 ↓ 1490 2862,2939	Aromatic character shifting to Single bonding character C=H shifting to C-H Stretching
1491 2858, 2932	C-C Stretching C-H Stretching	Cyclohexanol	Ru/Al$_2$O$_3$-Acidic	1491 2852,2932	C-C Stretching C-H Stretching
1491	C-C Stretching	trans-2-methoxycyclohexanol	Ru/Al$_2$O$_3$-Acidic	1491	C-C Stretching

Initially, adsorption of guaiacol was carried out over Al$_2$O$_3$-Acidic support which was used in catalytic experiment, various adsorption mode of guaiacol was confirmed with open literature.

At 100 ºC, guaiacol adsorbed over oxide, when temperature increases after 200 ºC, guaiacol adsorption increases and broad peak converting into sharp peak is confirmation of methoxy phenate species at 1277 cm^{-1}. These frequencies are developed due to the unidentate and bidentate adsorption of –OH present in Guaiacol. Aromaticity of guaiacol was confirmed by

the observance of peak around 1592 cm^{-1}, 1497 cm^{-1} attributed to mode of $V(C=C_{ring})$ vibration. Appearance of bands at 3070 cm^{-1} and 3028 cm^{-1} shows the characteristics of V (C=C-H-).

When the experiments were carried out with Ru/Al$_2$O$_3$-Acidic, initially all characteristic peaks belongs to guaiacol were observed but on increasing temperature,bands obtained at 1497 cm^{-1} (C=C) is shifting to lower wavenumbers 1489 which is characteristic significance of C-C. Presence of bands at 2862 cm^{-1} and 2839 cm^{-1} are confirmatory bands for guaiacol conversion into cyclohexnol.

For comparative adsorption mode of guaiacolic (-OH and -OCH$_3$), three controlled experiments were carried out like (1) adsorption of Anisole (2) adsorption of Phenol (3) Successive adsorption of Phenol and guaiacol. Obtained results were tabulated in Table 2. Phenol adsorbed at slightly higher wavenumber due to occurrence of adsorption peak at 1592 cm^{-1} and 1497 cm^{-1} as compare to anisole 1583 cm^{-1} and 1496 cm^{-1} charecterisitic peak for Aromatic (C=C). On increasing temperature, peak obtained at 1497 cm^{-1} in phenol is shifting to lower site 1490 cm^{-1} and same trend was seen with anisole, where peak obtained at 1496 cm^{-1} is shifted to lower wavenumber 1490 cm^{-1}. This observation is due to phenomenal change in doubly bonded character of aromatic (Phenol and Anisole) to singly bonded character. When successive adsorption of phenol and anisole were conducted, significant difference can not be attained due to the broadening of peaks in aromatic region, when phenolic compound

are adsorbed on catalytic surface peaks obtained at 2857 cm^{-1} and 2939 cm^{-1} . It can be suggested that phenolic –OH adsorb first compared to –OCH$_3$.

To confirm this the experiment IR spectra of cyclohexanol and trans-2-methoxycyclohexanol were recorded. Peaks obtained at 1491 cm^{-1}, 2858 cm^{-1}, 2932 cm^{-1} are significant proof of our earlier experiment performed.

4B.3.2.10. HDO of different substrates

Since, achieved good CTH activity with Ru/Al$_2$O$_3$-Acidic catalyst in guaiacol conversion into cyclohexanol, reactions were carried out with other lignin derived monomers like phenol, veratrole, anisole, and eugenol. Reactions were carried out under similar reaction conditions with all the substrates which were used for guaiacol. Complete conversion of substrate was

achieved in all the reactions. When phenol was used as a substrate, (Figures 4B.11) the yield of cyclohexanol was 90 % with formation of 5 % cyclohexane. CTH of anisole (Figures 4B.12) shown 28% cyclohexanol yield with 61% conversion. CTH of eugenol (Figures 4B.13) showed 100% propyl eugenol yield. It can be seen from the GC and GC-MS profiles of substrate study that various ring hydrogenated and partial hydrogenated products were formed.
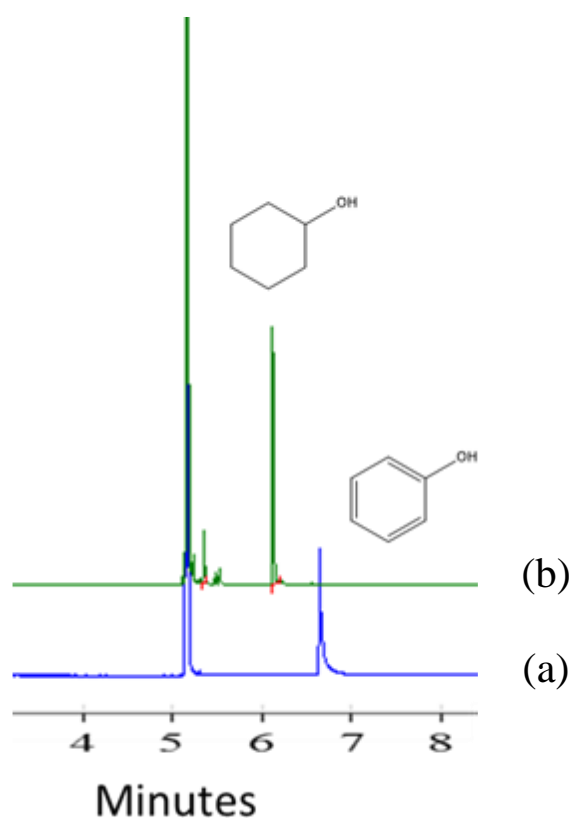
Figure 4B.11. Representative GC profile. Phenol, 4.0 mmol; Ru/Al$_2$O$_3$-Acidic, 0.0245 mmol of Ru; cyclohexane, 30 mL; H$_2$ pressure, 1 MPa at room temperature; 4 h; 1000 rpm.

(a) Before reaction; (b) After reaction
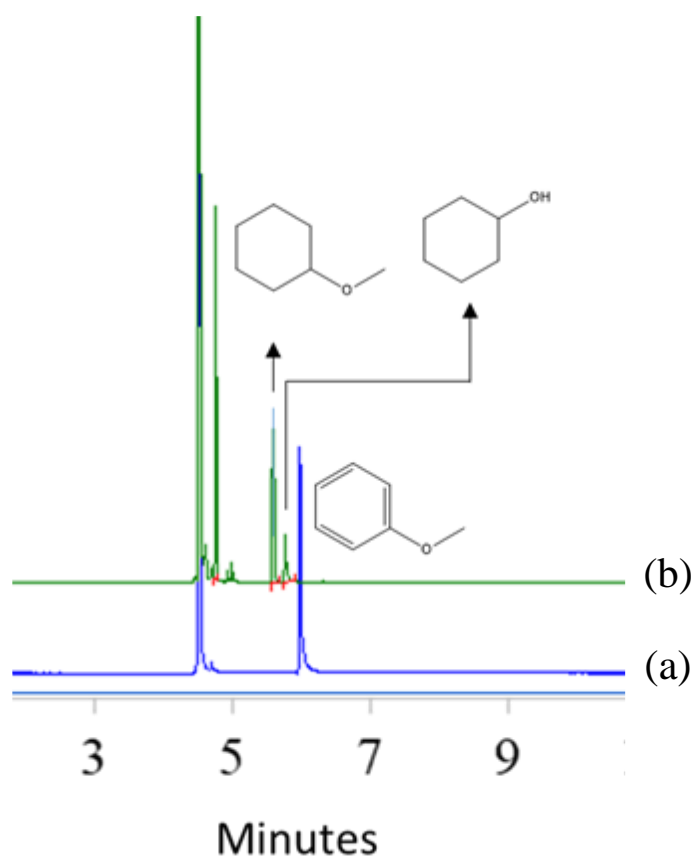
Figure 4B.12. Representative GC profile. Anisole, 4.0 mmol; Ru/Al$_2$O$_3$–Acidic, 0.0245 mmol of Ru; cyclohexane, 30 mL; H$_2$ pressure, 1 MPa at room temperature; 4 h; 1000 rpm.

(a) Before reaction; (b) After reaction;
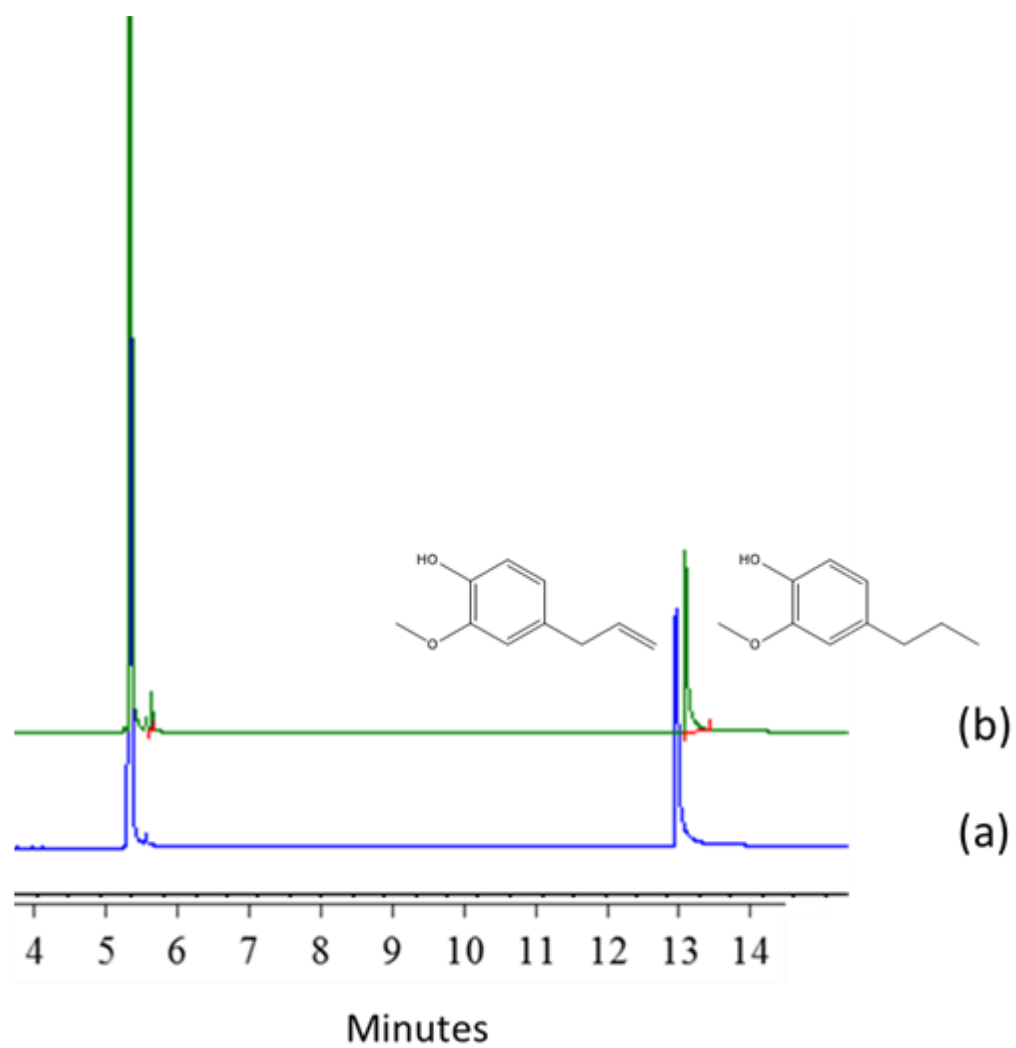
Figure 4B.13: Representative GC profile. Eugenol, 4.0 mmol; Ru/Al$_2$O$_3$-Acidic, IPA, 30 mL; N$_2$ pressure, 0.7 MPa at room temperature; 2 h; 1000 rpm.

(a) Before reaction; (b) After reaction;

4B.3.2.11. Recycle study of the catalyst

The reusability of Ru/Al$_2$O$_3$-Acidic catalyst was achieved by conducting multiple catalytic runs with spent catalyst. During the recycle study, the spent catalyst was recovered by centrifugation after the reaction. Next catalytic run was conducted with recovered wet catalyst without any pre-treatment. In addition, the catalyst activity was checked by maintaining constant S/C ratio .After 3rd catalytic run, recovered wet catalyst was dried at 60 °C for 12 h and used for 4th run by maintaining S/C ratio.
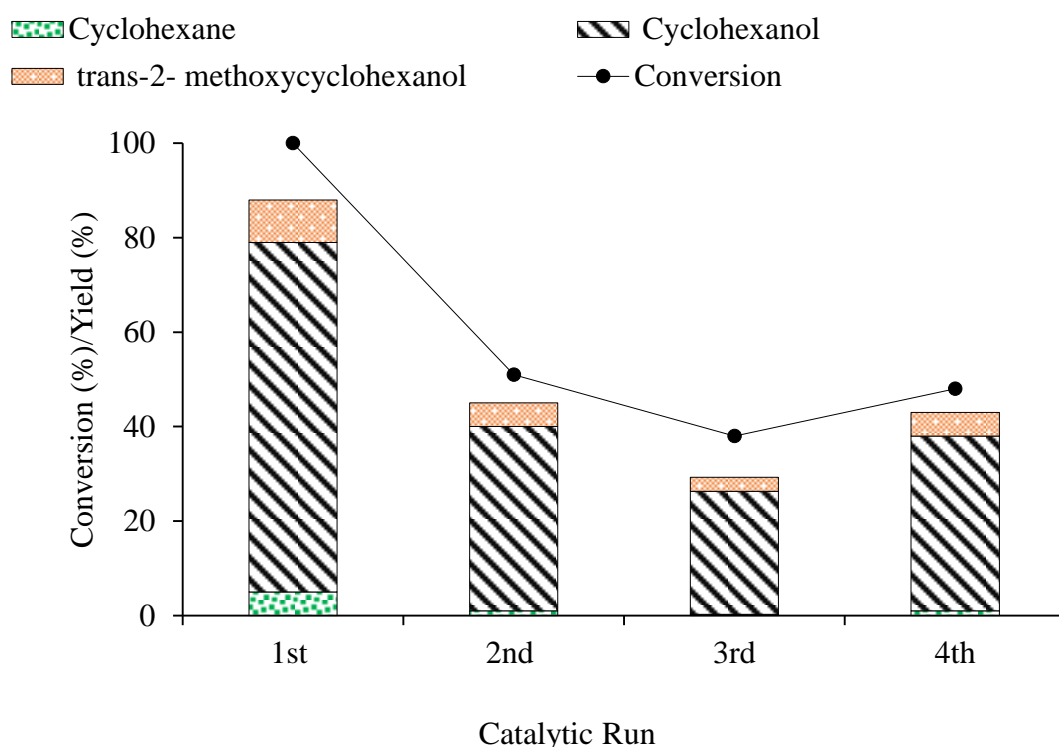
Figure 4B.14. Recycle study of catalyst

Reaction condition: Guaiacol/surface exposed Ru metal molar ratio, 35520; 2.13 wt% Guaiacol; IPA, N$_2$ pressure, 0.7 MPa at room temperature; 225 °C; 2 h; 1000 rpm. In the 2nd and 3rd run, Guaiacol/Ru molar ratio was not maintained as the catalyst was not dried. # In 4th run, wet recovered catalyst from 3rd run was dried at 60 °C for 12 h and Guaiacol/Ru molar ratio of 35520 was maintained.

Recycle study shown in Figure 4B.14 represents constant drop in the catalytic activity till 3rd run. This may be because of increase in substrate to catalyst ratio due to loss of active catalyst

during recovery of spent catalyst. Hence, the reaction was carried out by maintaining S/C ratio showing improved catalytic activity in the fourth run. It can be seen that obtained results were not appreciable in comparison to first catalytic run. This shows that some inherent property of catalyst is changed under the reaction conditions. To check this, spent catalyst was characterized.

4B.4. Characterization of the spent catalyst

It can be seen from the N_2 sorption data of spent Ru/Al$_2$O$_3$-Acidic catalyst that there is decrease in surface area of the catalyst (107 $m^2{\bullet}g^{-1}$). This phenomena is common and it happens due to adsorption of oxygenated compounds and coke over the catalytic surface. ICP-OES analysis result suggests leaching of Ru metal (6%) in spent catalyst. This may be a possible cause for decrease in the catalytic activity of the catalyst. CO chemisorption data of the spent catalyst shows increase in crystallite size of spent catalyst (2.6 nm) with 49% dispersion. The TPR profile of fresh and spent catalyst were matching with each other as shown in Figure 4B.15.. TEM profile shows deposition of coke on the catalytic surface (Figure 4B.16). From the spent catalyst analysis, it can be suggested that leaching of metal, increase in crystallite size, and deposition of coke is hampering the catalytic activity.
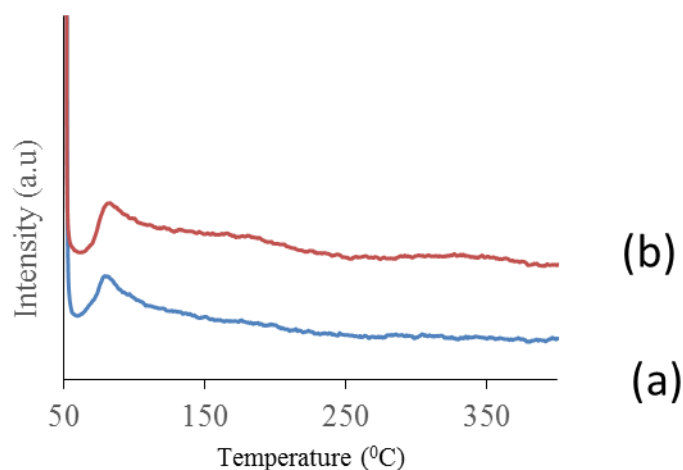
Figure 4B.15. TPR of spent catalyst (a) fresh catalyst (b) spent catalyst
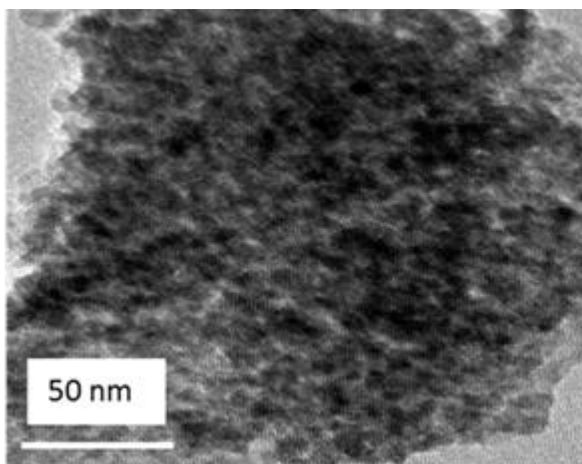
Figure 4B.16. TEM of spent catalyst

4B.5. Conclusion

CTH activity of various lignin derived monomers were tested with Ru metal base different supported catalyst. Support is playing an important role in achieving better CTH activity. Our distinctive observation is that catalyst reduced at lower temperature shows better CTH activity. In IPA medium with Ru/Al$_2$O$_3$-Acidic catalyst, 100% conversion of guaiacol, with 74% yield of cyclohexanol was achieved. Rate and activation energy of guaiacol conversion was calculated. Comparable Drift IR analysis was carried for supporting the path of suggested mechanism.

4B.6. References:

1.   Zakzeski, J.; Bruijnincx, P. C. A.; Jongerius, A. L.; Weckhuysen, B. M., The Catalytic Valorization of Lignin for the Production of Renewable Chemicals. *Chemical Reviews* 2010, *110* (6), 3552-3599.

2.   Zhao, C.; He, J.; Lemonidou, A. A.; Li, X.; Lercher, J. A., Aqueous-phase hydrodeoxygenation of bio-derived phenols to cycloalkanes. *Journal of Catalysis* 2011, *280* (1), 8-16.

3.   Chaudhary, R.; Dhepe, P. L., Solid base catalyzed depolymerization of lignin into low molecular weight products. *Green Chemistry* 2017, *19* (3), 778-788.

4. Deepa, A. K.; Dhepe, P. L., Solid acid catalyzed depolymerization of lignin into value added aromatic monomers. *RSC Advances* 2014, *4* (25), 12625.

5. Singh, S. K.; Dhepe, P. L., Isolation of lignin by organosolv process from different varieties of rice husk: Understanding their physical and chemical properties. *Bioresour Technol* 2016, *221*, 310-317.

6. Kumar, P.; Barrett, D. M.; Delwiche, M. J.; Stroeve, P., Methods for Pretreatment of Lignocellulosic Biomass for Efficient Hydrolysis and Biofuel Production. *Industrial & Engineering Chemistry Research* 2009, *48* (8), 3713-3729.

7. Dickerson, T.; Soria, J., Catalytic Fast Pyrolysis: A Review. *Energies* 2013, *6* (1), 514.

8. S. De, B. S. a. R. L., *Bioresour. Technol.* 2015, *178*, 108–118. 12.

9. N. Arun, R. V. S. a. A. K. D., *Renewable Sustainable Energy Rev.* 2015, *48*, 240–255.

10. A. M. Robinson, J. E. H. a. J. W. M., *ACS Catal.* 2016, *6*, 5026–5043.

11. X. Li, G. C., C. Liu, W. Ma, B. Yan and J. Zhang, *Renewable Sustainable Energy Rev.* 2017, *71*, 296–308.

12. Z. Lin, R. C., Z. Qu and J. G. Chen, *Green Chem.* 2018, *20*, 2679–2696.

13. Lai, Q.; Zhang, C.; Holles, J. H., Hydrodeoxygenation of guaiacol over Ni@Pd and Ni@Pt bimetallic overlayer catalysts. *Applied Catalysis A: General* 2016, *528*, 1-13.

14. Kim, T.-S.; Oh, S.; Kim, J.-Y.; Choi, I.-G.; Choi, J. W., Study on the hydrodeoxygenative upgrading of crude bio-oil produced from woody biomass by fast pyrolysis. *Energy* 2014, *68*, 437-443.

15. Michael Tuttle Musser, E. I. D. P. d. N., Cyclohexanol and Cyclohexanone. 2005, *10.1002/14356007.a08 217*.

16. Elkasabi, Y.; Liu, Q.; Choi, Y. S.; Strahan, G.; Boateng, A. A.; Regalbuto, J. R., Bio-oil hydrodeoxygenation catalysts produced using strong electrostatic adsorption. *Fuel* 2017, *207*, 510-521.

17. Boscagli, C.; Raffelt, K.; Grunwaldt, J.-D., Reactivity of platform molecules in pyrolysis oil and in water during hydrotreatment over nickel and ruthenium catalysts. *Biomass and Bioenergy* 2017, *106*, 63-73.

18.   Cai, Z.; Wang, F.; Zhang, X.; Ahishakiye, R.; Xie, Y.; Shen, Y., Selective hydrodeoxygenation of guaiacol to phenolics over activated carbon supported molybdenum catalysts. *Molecular Catalysis* 2017, *441*, 28-34.

19.   Boscagli, C. R., K.; Grunwaldt, J.-D., Reactivity of platform molecules in pyrolysis oil and in water during hydrotreatment over nickel and ruthenium catalysts. *Biomass and Bioenergy* 2017, , *106*, 63-73.

20.   Bui, V. N. L., D.; Afanasiev, P.; Geantet, C., Hydrodeoxygenation of guaiacol with CoMo catalysts. Part I: Promoting effect of cobalt on HDO selectivity and activity. *Applied Catalysis B: Environmental* 2011, *101 (3-4)*, 239-245.

21.   Cai, Z. W., F.; Zhang, X.; Ahishakiye, R.; Xie, Y.; Shen, Y., Selective hydrodeoxygenation of guaiacol to phenolics over activated carbon supported molybdenum catalysts. *Molecular Catalysis* 2017, *441*, 28-34.

22.   Dwiatmoko, A. A. K., I.; Zhou, L.; Choi, J.-W.; Suh, D. J.; Jae, J.; Ha, J.-M., Hydrodeoxygenation of guaiacol on tungstated zirconia supported Ru catalysts. *Applied Catalysis A: General* 2017, , *543*, 10-16.

23.   Hong, Y.-K. L., D.-W.; Eom, H.-J.; Lee, K.-Y., The catalytic activity of Pd/WOx/γ-Al2O3 for hydrodeoxygenation of guaiacol. *Applied Catalysis B: Environmental* 2014, , *150-151*, 438-445.

24.   Jung, K. B. L., J.; Ha, J.-M.; Lee, H.; Suh, D. J.; Jun, C.-H.; Jae, J. , Effective hydrodeoxygenation of lignin-derived phenols using bimetallic RuRe catalysts: Effect of carbon supports. *Catalysis Today* 2018, *303*, 191-199.

25.   Lee, H. K., H.; Yu, M. J.; Ko, C. H.; Jeon, J.-K.; Jae, J.; Park, S. H.; Jung, S.-C.; Park, Y.-K., Catalytic Hydrodeoxygenation of Bio-oil Model Compounds over Pt/HY Catalyst. *Scientific Reports* 2016, *6, 28765*.

26.   Leiva, K. G., R.; Sepulveda, C.; Laurenti, D.; Geantet, C.; Vrinat, M.; Garcia-Fierro, J. L.; Escalona, N., Conversion of guaiacol over supported ReOx catalysts: Support and metal loading effect. *Catalysis Today* 2017, *296* 228-238.

27.   Liu, S. W., H.; Smith, K. J.; Kim, C. S. , Hydrodeoxygenation of 2-Methoxyphenol over Ru, Pd, and Mo2C Catalysts Supported on Carbon. *Energy & Fuels* 2017, *31 (6)*, 6378-6388.

28.   Hong, Y.-K.; Lee, D.-W.; Eom, H.-J.; Lee, K.-Y., The catalytic activity of Pd/WOx/γ-Al2O3 for hydrodeoxygenation of guaiacol. *Applied Catalysis B: Environmental* 2014, *150-151*, 438-445.

29.   Dwiatmoko, A. A.; Kim, I.; Zhou, L.; Choi, J.-W.; Suh, D. J.; Jae, J.; Ha, J.-M., Hydrodeoxygenation of guaiacol on tungstated zirconia supported Ru catalysts. *Applied Catalysis A: General* 2017, *543*, 10-16.

30.   Deepa, A. K.; Dhepe, P. L., Function of Metals and Supports on the Hydrodeoxygenation of Phenolic Compounds. *ChemPlusChem* 2014, *79* (11), 1573-1583.

31.   Dheerendra Singh, P. L. D., Understanding the influence of alumina supported ruthenium catalysts synthesis and reactionparameters on the hydrodeoxygenation of ligninderived monomers,. *MolecularCatalysis,* 2020, *480*, 110525.

32.   Liu, S.; Wang, H.; Smith, K. J.; Kim, C. S., Hydrodeoxygenation of 2-Methoxyphenol over Ru, Pd, and Mo2C Catalysts Supported on Carbon. *Energy & Fuels* 2017, *31* (6), 6378-6388.

33.   Lee, H.; Kim, H.; Yu, M. J.; Ko, C. H.; Jeon, J.-K.; Jae, J.; Park, S. H.; Jung, S.-C.; Park, Y.-K., Catalytic Hydrodeoxygenation of Bio-oil Model Compounds over Pt/HY Catalyst. *Scientific Reports* 2016, *6*, 28765.

34.   Jung, K. B.; Lee, J.; Ha, J.-M.; Lee, H.; Suh, D. J.; Jun, C.-H.; Jae, J., Effective hydrodeoxygenation of lignin-derived phenols using bimetallic RuRe catalysts: Effect of carbon supports. *Catalysis Today* 2018, *303*, 191-199.

35.   Leiva, K.; Garcia, R.; Sepulveda, C.; Laurenti, D.; Geantet, C.; Vrinat, M.; Garcia-Fierro, J. L.; Escalona, N., Conversion of guaiacol over supported ReOx catalysts: Support and metal loading effect. *Catalysis Today* 2017, *296*, 228-238.

36.   Deepa, A. K. D., P. L., Function of Metals and Supports on the Hydrodeoxygenation of Phenolic Compounds, *ChemPlusChem* 2014, *79 (11)*, 1573-1583.

37.   Dheerendra Singh, P. L. D., Understanding the influence of alumina supported ruthenium catalysts synthesis and reactionparameters on the hydrodeoxygenation of ligninderived monomers. *MolecularCatalysis* 2020 *480*, 110525.

38.   Bui, V. N.; Laurenti, D.; Afanasiev, P.; Geantet, C., Hydrodeoxygenation of guaiacol with CoMo catalysts. Part I: Promoting effect of cobalt on HDO selectivity and activity. *Applied Catalysis B: Environmental* 2011, *101* (3-4), 239-245.

39.   Bui, V. N.; Laurenti, D.; Delichère, P.; Geantet, C., Hydrodeoxygenation of guaiacol: Part II: Support effect for CoMoS catalysts on HDO activity and selectivity. *Applied Catalysis B: Environmental* 2011, *101* (3), 246-255.

40.   Centeno, A.; Laurent, E.; Delmon, B., Influence of the Support of CoMo Sulfide Catalysts and of the Addition of Potassium and Platinum on the Catalytic Performances for the Hydrodeoxygenation of Carbonyl, Carboxyl, and Guaiacol-Type Molecules. *Journal of Catalysis* 1995, *154* (2), 288-298.

41.   Ruiz, P. E.; Frederick, B. G.; De Sisto, W. J.; Austin, R. N.; Radovic, L. R.; Leiva, K.; García, R.; Escalona, N.; Wheeler, M. C., Guaiacol hydrodeoxygenation on MoS2 catalysts: Influence of activated carbon supports. *Catalysis Communications* 2012, *27*, 44-48.

42.   Tyrone Ghampson, I.; Sepúlveda, C.; Garcia, R.; García Fierro, J. L.; Escalona, N.; DeSisto, W. J., Comparison of alumina- and SBA-15-supported molybdenum nitride catalysts for hydrodeoxygenation of guaiacol. *Applied Catalysis A: General* 2012, *435-436*, 51-60.

43.   Sepúlveda, C.; Leiva, K.; García, R.; Radovic, L. R.; Ghampson, I. T.; DeSisto, W. J.; Fierro, J. L. G.; Escalona, N., Hydrodeoxygenation of 2-methoxyphenol over Mo2N catalysts supported on activated carbons. *Catalysis Today* 2011, *172* (1), 232-239.

44.   Güvenatam, B.; Kurşun, O.; Heeres, E. H. J.; Pidko, E. A.; Hensen, E. J. M., Hydrodeoxygenation of mono- and dimeric lignin model compounds on noble metal catalysts. *Catalysis Today* 2014, *233*, 83-91.

45.   Ohta, H.; Kobayashi, H.; Hara, K.; Fukuoka, A., Hydrodeoxygenation of phenols as lignin models under acid-free conditions with carbon-supported platinum catalysts. *Chemical Communications* 2011, *47* (44), 12209-12211.

46.   Olcese, R. N.; Bettahar, M.; Petitjean, D.; Malaman, B.; Giovanella, F.; Dufour, A., Gas-phase hydrodeoxygenation of guaiacol over Fe/SiO2 catalyst. *Applied Catalysis B: Environmental* 2012, *115-116*, 63-73.

47.   Bykova, M. V.; Ermakov, D. Y.; Kaichev, V. V.; Bulavchenko, O. A.; Saraev, A. A.; Lebedev, M. Y.; Yakovlev, V. A., Ni-based sol–gel catalysts as promising systems for crude bio-oil upgrading: Guaiacol hydrodeoxygenation study. *Applied Catalysis B: Environmental* 2012, *113-114*, 296-307.

48.	Wang, X.; Rinaldi, R., Solvent Effects on the Hydrogenolysis of Diphenyl Ether with Raney Nickel and their Implications for the Conversion of Lignin. *ChemSusChem* 2012, *5* (8), 1455-1466.

49.	Zhou, M.; Ye, J.; Liu, P.; Xu, J.; Jiang, J., Water-Assisted Selective Hydrodeoxygenation of Guaiacol to Cyclohexanol over Supported Ni and Co Bimetallic Catalysts. *ACS Sustainable Chemistry & Engineering* 2017, *5* (10), 8824-8835.

50.	Abd Hamid, S. B.; Ambursa, M. M.; Sudarsanam, P.; Voon, L. H.; Bhargava, S. K., Effect of Ti loading on structure-activity properties of Cu-Ni/Ti-MCM-41 catalysts in hydrodeoxygenation of guaiacol. *Catalysis Communications* 2017, *94*, 18-22.

51.	Kim, M.; Ha, J.-M.; Lee, K.-Y.; Jae, J., Catalytic transfer hydrogenation/hydrogenolysis of guaiacol to cyclohexane over bimetallic RuRe/C catalysts. *Catalysis Communications* 2016, *86*, 113-118.

52.	JunHu, S. Z., RuiXiaob, Xiaoxiang Jianga, YunjunWanga, YahuiSuna, PingLu,;, Catalytic transfer hydrogenolysis of lignin into monophenols over platinum-rhenium supported on titanium dioxide using isopropanol as in situ hydrogen source. *Bioresource Technology* 2019, *279,* , 228-233.

53.	Gilkey, M. J.; Xu, B., Heterogeneous Catalytic Transfer Hydrogenation as an Effective Pathway in Biomass Upgrading. *ACS Catalysis* 2016, *6* (3), 1420-1436.

54.	Song, Q. W., F.; Cai, J.; Wang, Y.; Zhang, J.; Yu, W.; Xu, *J. Energy Environ. Sci.* 2013, , *6* 994−1007.

55.	Barta, K. M., T. D.; Fettig, M. L.; Scott, S. L.; Iretskii, A. V.; Ford, P. C. , *Green Chem.* 2010, *12*, 1640−1647.

56.	Singh, A. K. J., S.; Kim, J. Y.; Sharma, S.; Basavaraju, K. C.; Kim, M.-G.; Kim, K.-R.; Lee, J. S.; Lee, H. H.; Kim, D.-P. , *ACS Catal.* 2015, *5*, 6964−6972.

57.	X. Wang, R. R., 2013. *Angew. Chem. Int. Ed. 52* 11499-11503.

58.	X. Wang, R. R., *Energy Environment Science* 2012 *5* 8244-8260.

59.	H. Wu, J. S., C. Xie, C. Wu, C. Chen, B. Han, , *ACS sustainable Chemistry and Engineering,* 2018, *6* 2872-2877.

60.	*Green Chem.* 2019, *21* 3715–3743.

61.	Environment, G. E., 2018, *3* 328-334.

62.	*ACS Catal.* 2016, *6*, 1420−1436.

63. Tauster, S. J., Strong Metal-Support Interactions. *Account of chemical research* 1987.

64. S. J. Tauster, S. C. F., and R. L. Garten, Strong Metal-Support Interactions.Group 8 Noble Metals Supported on TiO2; *Journal of the American Chemical Society* 1978.

Chapter 5A

Catalytic defunctionalization of lignin derived low molecular weight compound using AHF supported catalyst

5A.1. Introduction

It was demonstrated in the previous chapters (Chapter 4A and 4B) that Ru/Al$_2$O$_3$-Acidic could effectively catalyze defunctionalization/HDO of lignin-derived low molecular weight compounds. It was also seen that defunctionalization/HDO of lignin-derived low molecular weight compounds could be achieved using an external source of hydrogen (Chapter 4A) as well as in-situ generated hydrogen (Chapter 4B). Efficient defunctionalization/HDO activity was achieved using Ru/Al$_2$O$_3$-Acidic at 225 ^{o}C, 1 MPa H$_2$, in cyclohexane solvent, and at 225 ^{o}C, 0.7 MPa N$_2$, in isopropyl alcohol. In both the cases, defunctionalization produces cyclohexanol as a major product and achieved up to 80% yield. Although Ru/Al$_2$O$_3$–Acidic is active for the defunctionalization/HDO process, Ru is a costly metal (approx. USD 250 oz^{-1}), and use of it will make the process economically infeasible. So, it was decided to carry out defunctionalization/HDO reaction with non-precious metals, which will reduce the cost of defunctionlization/HDO process. The use of non-precious metals for the process is already known in the literature. It was reported that sulphided cobalt (Co), sulphided nickel (Ni), and combination of both the metals with molybdenum over Al$_2$O$_3$ and zeolite support are active for the HDO of low molecular weight compounds [1-5]. However, reported system is associated with some issues like zeolite support undergoes deactivation due to coke deposition or dealumination by hydrolysis when conducted at high temperatures (300-600 °C)[6, 7]. Sulphided metal catalytic system leads to contamination of sulfur in products and also deactivation of the catalyst by coke deposition on the catalyst surface,[5, 8]. The defunctionalization of guaiacol is also reported with Ni-Mo/TiO$_2$ at 350 ^{o}C, 6.8 MPa H$_2$ to obtained phenol (38%) and cresol (28%) as products [9]. Aqueous phase defunctionalization/HDO of guaiacol in the presence of Raney Ni and Nafion/SiO$_2$ at 300 °C under 4 MPa H$_2$ produced 71% yield of cyclohexane with 100% conversion [10]. As can be seen from the reported literature, Nickel (Ni) and Cobalt (Co) are the active non-precious metals used in the defunctionalization process. It is observed from the previous chapters (Chapter 4A and Chapter 4B) that Al$_2$O$_3$ support gives better activity than any other supports, so it was decided to conduct defunctionalization of low molecular weight compounds using alumina supported non-precious metal (Co, Ni) catalysts. However, in this work, alumina support was prepared using a unique technique. Non-precious metal/Support catalyst was used for HDO of guaiacol as shown in Scheme 5A.1.
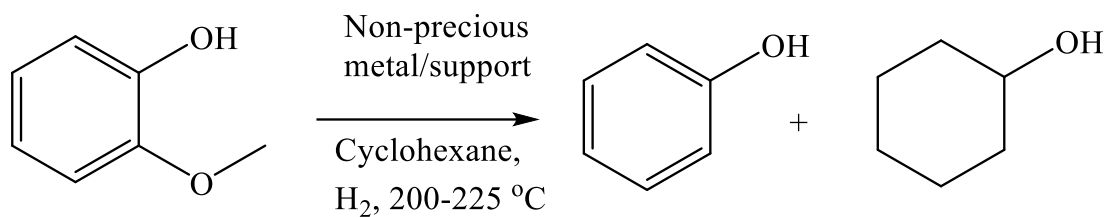
Scheme 5A.1. Hydrodeoxygenation/defunctionalization of lignin-derived low molecular weight compounds (guaiacol)

5A.2. Experiment section

5A.2.1. Materials

For the details on all the materials used in this study, please refer Chapter 4, section 4A.2.1.

5A.2.2. Catalyst synthesis

Co and Ni metals were supported on aluminium hollow fiber (AHF) with 5wt% loading. For the details on the catalyst synthesis kindly refer Chapter 2B, Section 2B.4.1-2B.4.3.

5A.2.3. Catalytic runs

Reactions were carried out in batch mode reactor and for more details on the catalytic runs, kindly refer Chapter 4, section 4A.2.3.

5A.2.4. Recycle experiment

Spent catalyst was recovered after earlier reaction and was used for further reaction. The details on the recycle experiment can be found in Chapter 4, section 4A.2.4.

5A.2.5. Analysis of reaction mixture

Reaction mixture was analysed using GC and GC-MS techniques and for the details about the methodologies used and instruments used for the analysis of reaction mixture, please refer Chapter 4, section 4A.2.5.

TOF was calculated using following formula

$$TOF = \frac{\text{Moles of substrate reacted}}{\text{Moles of metal X Time (s)}}$$

5A.3. Results and discussion

5A.3.1. Catalyst characterization

Synthesized catalysts were characterized using different physico-chemical techniques. For details on catalyst characterization, kindly refer Chapter 2B, Section 2B.5, Subsection 2B.5.1-2B.5.8.

5A.3.2. Catalyst activity

Hydrodeoxygenation (HDO) reactions were carried out in high-pressure high-temperature batch mode reactors and the analysis of the reaction mixture was done on GC and GC-MS (for details, please refer experiment section).

5A.3.2.1. Effect of support on the HDO of Guaiacol
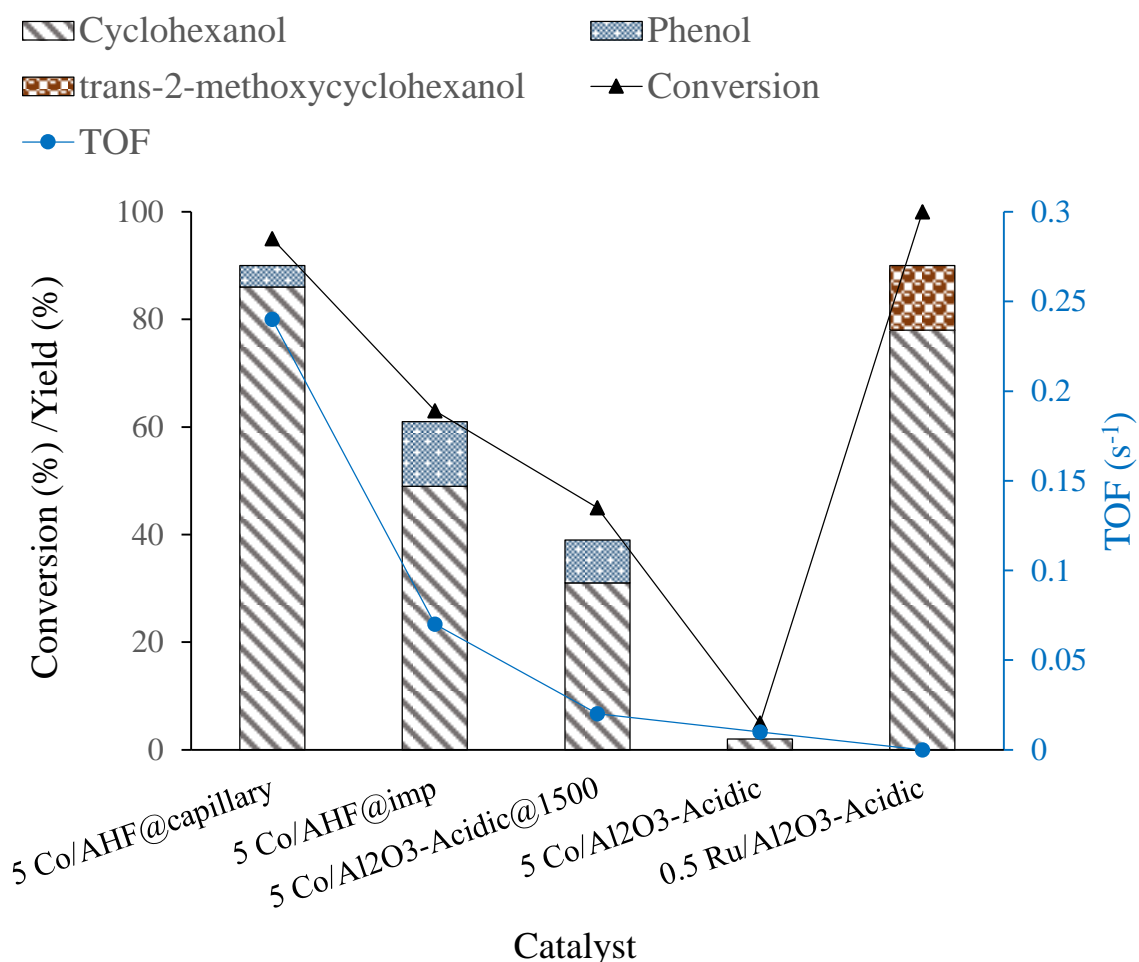
Figure 5A.1. Effect of support on the hydrodeoxygenation of guaiacol

Reaction condition: Guaiacol/Co molar ratio, 13; 2.15 wt% Guaiacol in cyclohexane; H_2, 1 MPa @RT; 225 °C; 4 h; 1000 rpm.

Initially, HDO experiment was conducted with 5 Co/Al_2O_3-Acidic catalyst, using guaiacol, 0.5 g; catalyst, 0.375 g; Cyclohexane, 30 mL; H_2 pressure, 1 MPa at RT; 225 °C; 4 h; 1000 rpm since in earlier study with Ru/Al_2O_3-Acidic catalyst under these conditions maximum HDO activity was observed (Chapter 4A). However, as can be seen from Figure 5A.1, only 5% conversion of guaiacol was seen with 2% cyclohexanol yield under this condition. Further modification in Al_2O_3-Acidic support was carried out by calcining it at 1500 °C (30 -500 °C, 8 °C•min^{-1}; 0.5 h; 500-900 °C, 8 °C•min^{-1}, 1 h; 900-1500 °C, 4 °C•min^{-1}, 4 h;). As seen, with this modified catalyst (5 Co/Al_2O_3-Acidic@1500), increased guaiacol conversion from 5% to 45% and improvement in the yield of cyclohexanol (31%) and formation of phenol with 8% yield was observed. It was decided to further modify Al_2O_3-Acidic support to make alumina hollow fiber (AHF), on account of the improved activity of calcined Al_2O_3-Acidic at 1500°C. AHF sintered at 1500 °C was crushed, and cobalt (Co) was impregnated over it (5 Co/AHF@imp). An improvement in guaiacol conversion to 63% with 49% yield of cyclohexanol and 12% yield of phenol was observed with this modification.

Further catalytic experiment was conducted with catalyst, 5 Co/AHF@capillary where impregnation of metal was achieved using capillary action in the long fiber (20-22 cm). The drastic change in the activity of hydrodeoxygenation was found with this catalyst as guaiacol conversion was increased up to 95% and increase in yield of cyclohexanol (86%) was observed along with 4% yield of phenol. A dramatic change in the catalytic activity was observed with same metal loading with different support conditions. To investigate this, details about the physico-chemical properties of synthesized catalysts were checked. TPR results suggest that cobalt (Co) impregnated on Al_2O_3-Acidic support may present in higher oxidation state since no peak for hydrogen consumption was seen (Chapter 2B, Figure 2B.14). When the support was changed from Al_2O_3-Acidic to Al_2O_3-Acidic@1500 calcined at 1500°C and AHF, a clear peak for hydrogen consumption can be observed. This observation suggests that if the metal is present in higher oxidation state then it may not be active for the HDO reaction, but if it is present in the reduced state then, it is active for HDO reaction. XPS analysis was performed to

confirmed the oxidation state of metal and found that with AHF support Co is present in the reduced state as well as higher oxidation state, while Ni is present in the metallic state (Chapter 2B, Figure 2B.15). Another reason of higher catalytic activity of AHF was better metal dispersion, which can be seen from TEM images of the synthesized catalyst (Chapter 2B, Figure 2B.13).

5A.3.2.2. Effect of metal on the HDO of Guaiacol
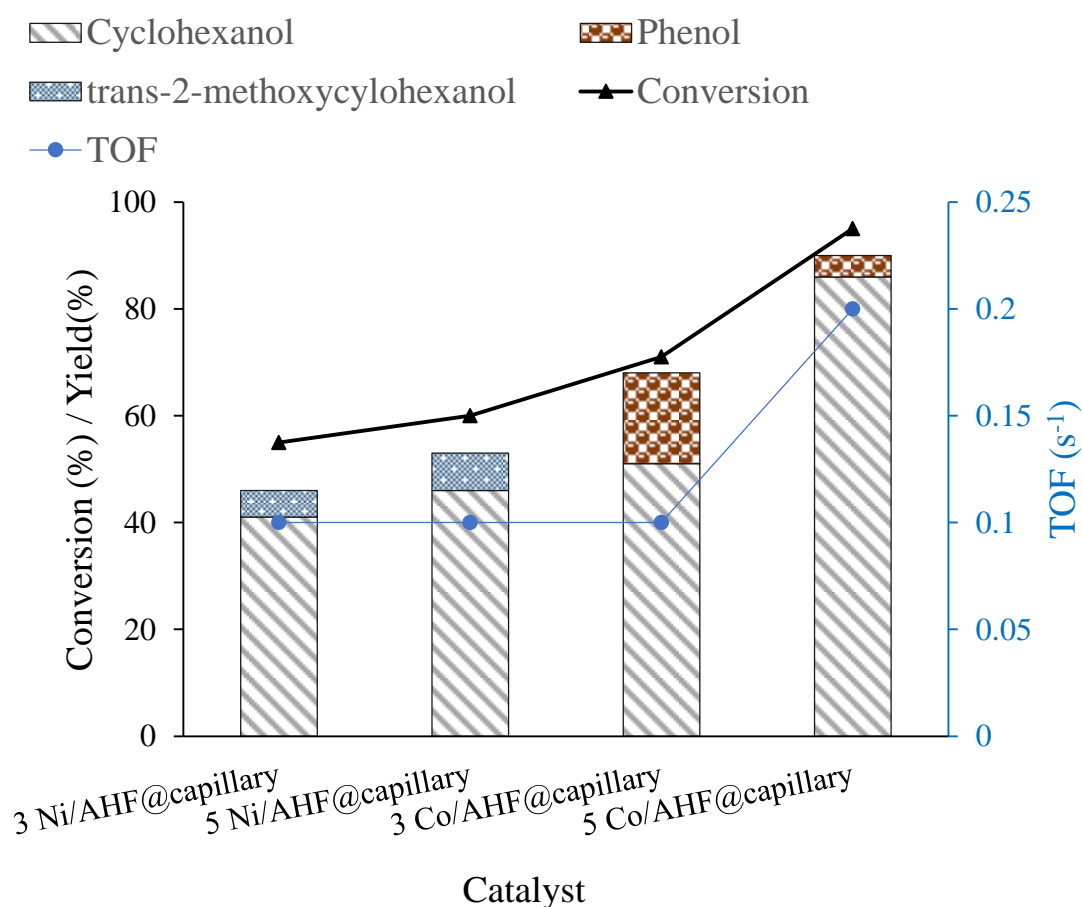
Figure 5A.2. Effect of metal on the hydrodeoxygenation of guaiacol

Reaction condition: Guaiacol/M (5 Co or 5 Ni) molar ratio, 13; Guaiacol/metal (3 Co, 3 Ni) molar ratio, 21; 2.15 wt% Guaiacol in cyclohexane; H_2, 1 MPa @RT; 225 °C; 4 h; 1000 rpm.

It was found from the earlier support study that catalyst with AHF as support is more active in the HDO of guaiacol. Further, the effect of metal was studied with comparing different metal loadings of Ni and Co impregnated over AHF using capillary action. It can be seen from Figure 5A.2 that when Ni metal was used for HDO instead of Co, it typically showed lower activity. From the figure, it is apparent that Ni followed different reaction path than that of Co metal although major product formed was same, cyclohexanol. To describe this further, a careful look at obtained results (Figure 5A.2) suggests that in Ni catalyzed HDO, first; ring hydrogenation of guaiacol occurred to form intermediate product, trans-2-methoxycyclohexanol. This product after cleavage of C-OMe bond produced cyclohexanol as a major product. While Co impregnated catalyst was following different HDO reaction pathway and as seen, with Co catalyst, first phenol was formed by the cleavage of C-OMe bond, and further hydrogenation of phenol occurred to yield final product, cyclohexanol. A possible cause of this behaviour could be explained based on the reduction potential of Ni and Co. Reduction potential of Ni (-0.25 V) is higher compared to Co (-0.27V). Due to the higher reduction potential of Ni, over this metal, molecular hydrogen easily splits and thus more hydrogenation active species are available to carry out ring hydrogenation as first step. On the other hand due to lower reduction potential of Co, cleavage of O-Me is preferred over ring hydrogenation as first step. Initially, HDO reactions were performed using 5% lading of (Co, Ni) metal. As seen from the Figure 5A.2, with 5% loading of Co metal, a very good HDO activity (95% conversion, 86 % cyclohexanol yield, 4% phenol yield) was achieved as compared to Ni metal (71% conversion, 51% cyclohexanol yield, 17% trans-2-methoxycyclohexanol yield). The difference in the activity could be due to reluctant behaviour of Ni, which required high temperature for the activation as compared to Co. This observation is based on TPR study, where reduction of Co is possible at lower temperature (240-280 °C), while reduction of Ni required high temperature (260-360 °C). When metal loading was reduced to 3%, guaiacol conversion was decreased to 71% (Co) with a decrease in the yield of cyclohexanol to 51%. However, increase in phenol yield to 17% was seen. Similar trend can be seen with 3% loading of Ni metal, in which conversion of guaiacol was decreased to 55% and the yield of both cyclohexanol (41%) and trans-2-methoxy cyclohexanol (5%) was decreased. It might be possible that due to decrease in the active catalytic centres present in the catalyst due to decrease in the metal loading. To understand this, TOF calculation was done to correlate the catalytic activity of the catalyst and

it was seen that 5 Co/Al$_2$O$_3$@capilllary showed the highest TOF (0.2 s^{-1}) with the highest HDO activity. Order of TOF is as follows:

3 Ni/Al$_2$O$_3$@capillary (0.1 s^{-1}) ≈ 5 Ni/Al$_2$O$_3$@capillary (0.1 s^{-1}) ≈ 3Co/Al$_2$O$_3$@capllary (0.1 s^{-1}) < 5 Co/Al$_2$O$_3$@ capillary (0.2 s^{-1})

Based on this data, it is rather difficult to predict why Co showed better activity than Ni and with a change in loading of metal also did not change the TOF drastically. In view of this, it is important to carry out further investigations in this work.

5A.3.2.3. Effect of temperature on the HDO of Guaiacol
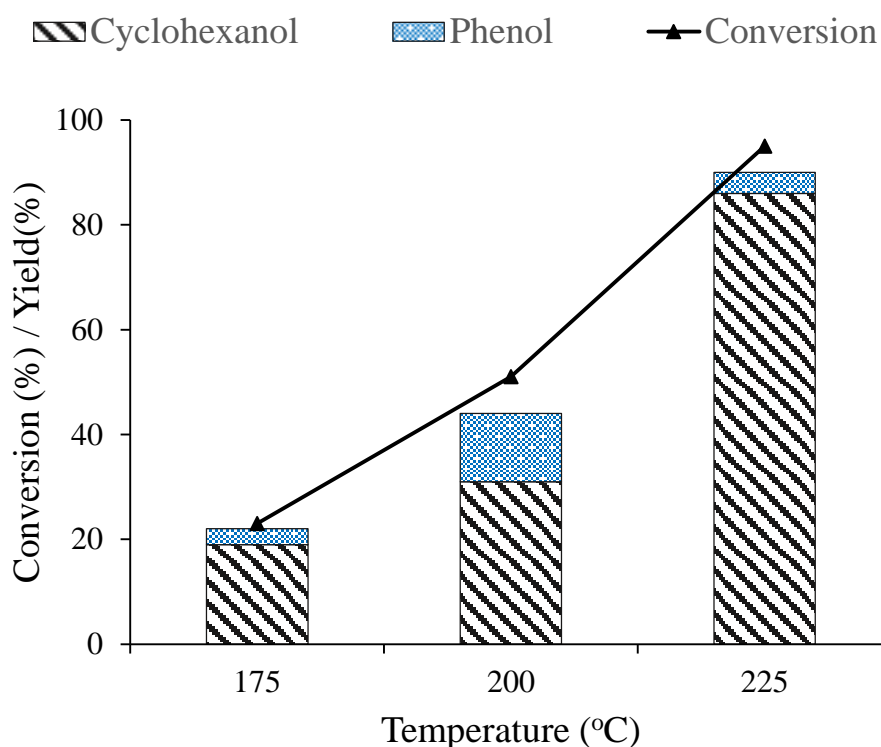
Figure 5A.3. Effect of temperature on the hydrodeoxygenation of guaiacol

Reaction condition: Guaiacol/Co molar ratio, 13; 5 Co/Al$_2$O$_3$@capilllary, 0.375g; 2.15 wt% Guaiacol in cyclohexane; H$_2$, 1 MPa @RT; 4 h; 1000 rpm.

To check the effect of temperature in HDO activity, the reaction was conducted at various temperatures and the results are represented in Figure 5A.3. Results showed very less

conversion of guaiacol (23%) with 19% cyclohexanol and 3% phenol yield at 175 °C. On increasing the reaction temperature to 200 °C, guaiacol conversion was increased to 51% and the formation of 31% cyclohexanol and 13% phenol was found. Further increase in the temperature to 225 °C, showed 95% conversion of guaiacol with 86% yield of cyclohexanol and 4 % phenol. On increasing temperature HDO activity increases due to increase of collision between substrate and catalyst, at higher temperature mostly guaiacol exists in vapour state.

5A.3.2.4. Effect of catalyst weight on the HDO of Guaiacol
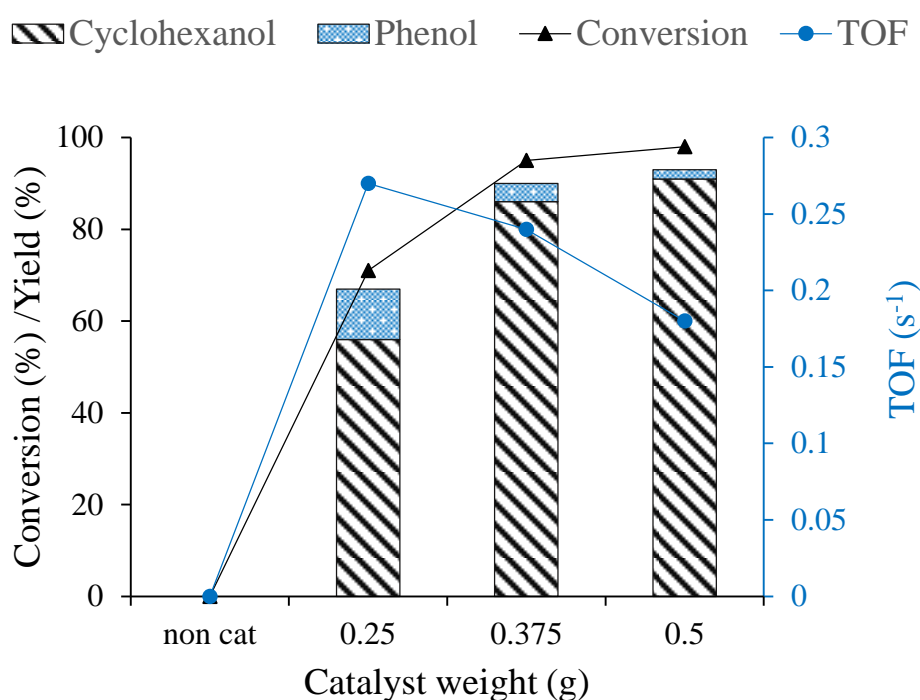
Figure 5A.4. Effect of catalyst weight on the hydrodeoxygenation of guaiacol

Reaction condition: 5 Co/Al$_2$O$_3$@capilllary; 2.15 wt% Guaiacol in cyclohexane; H$_2$, 1 MPa @RT; 225 °C; 4 h; 1000 rpm.

In order to optimize the catalyst loading for better HDO activity, reactions were carried out with different catalyst loadings (0.25, 0.375, 0.5 g) under the same reaction conditions (Figure 5A.4). It was observed that the non-catalytic HDO is not possible, however, as the loading of

the catalyst increased from 0.25 to 0.5 g, the conversion of guaiacol increased from 71 to 98%, with increase in cyclohexanol yield from 56 to 91% and decrease in phenol yield from 11 to 2%. This improvement in results with increased catalyst loading shows that active sites of catalyst increases leading to improvement in results. A careful look at the results suggests that Co catalyzed HDO proceeds via formation of intermediate product, phenol. Further, phenol gets converted into cyclohexanol. Conversion of phenol into cyclohexanol is slower process because in all the catalytic run, intermediate phenol was not completely converted. Based on this fact, it can be explained that conversion of phenol to cyclohexanol is rate-determining step for the cobalt catalysed reactions.

5A.3.2.5. Effect of time on the HDO of Guaiacol
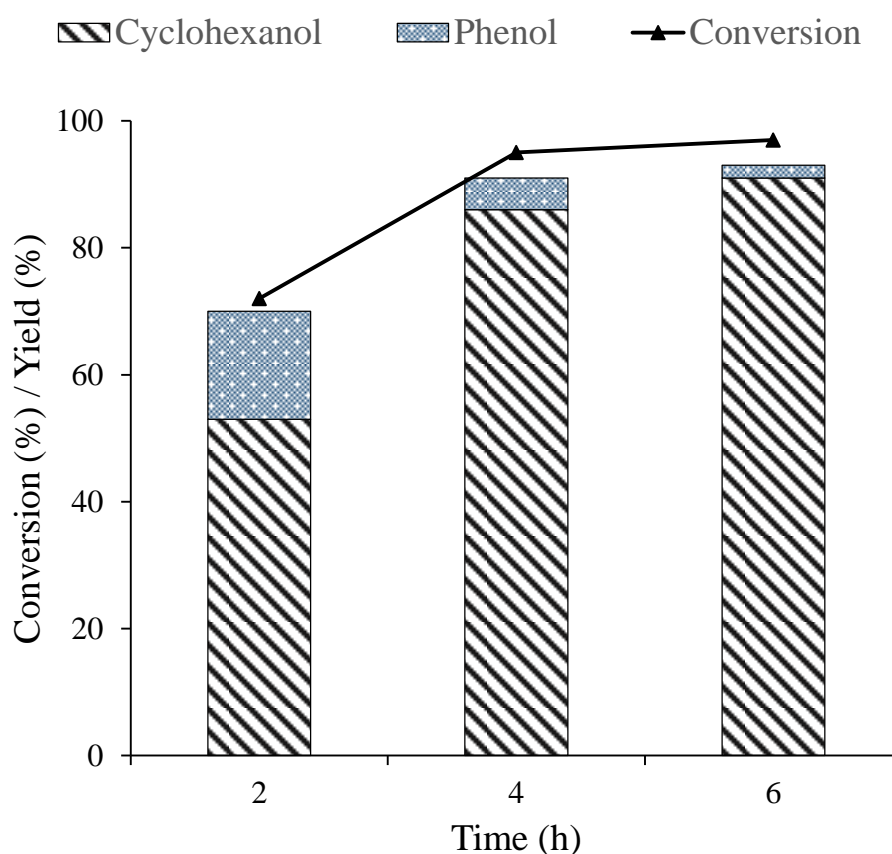
Figure 5A.5. Effect of time on the hydrodeoxygenation of guaiacol

Reaction condition: Guaiacol/Co molar ratio, 13; 5 Co/Al$_2$O$_3$@capilllary, 0.375g; 2.15 wt% Guaiacol in cyclohexane; H$_2$, 1 MPa@ RT; 225 °C; 1000 rpm.

It was clear from the study that 95% conversion of guaiacol is possible within 4 h. Figure 5A.5, showed 86% yield of cyclohexanol and formation of 5 % Phenol. For the complete conversion of guaiacol and improving the yield of cyclohexanol, the reaction was carried out for longer time 6 h, and as seen from the Figure 5A.5, guaiacol conversion increased to 97% and improve in the yield of cyclohexanol (91%) with (2%) phenol formation was obtained. Still, guaiacol was not completely converted, This fact could be due saturation achieved on catalyst surface in longer time run. HDO activity was increased much when the reaction was conducted for longer time. It was decided to check catalytic activity for shorter time. HDO reaction was conducted for 2 h, and decrease in guaiacol conversion to 72% with 53% yield of cyclohexanol, and 17% phenol formation was seen. This result is much lower compared to 4 h run. It might be possible due to decrease in the substrate to catalyst interaction.

5A.3.2.6. Effect of pressure on the HDO of Guaiacol
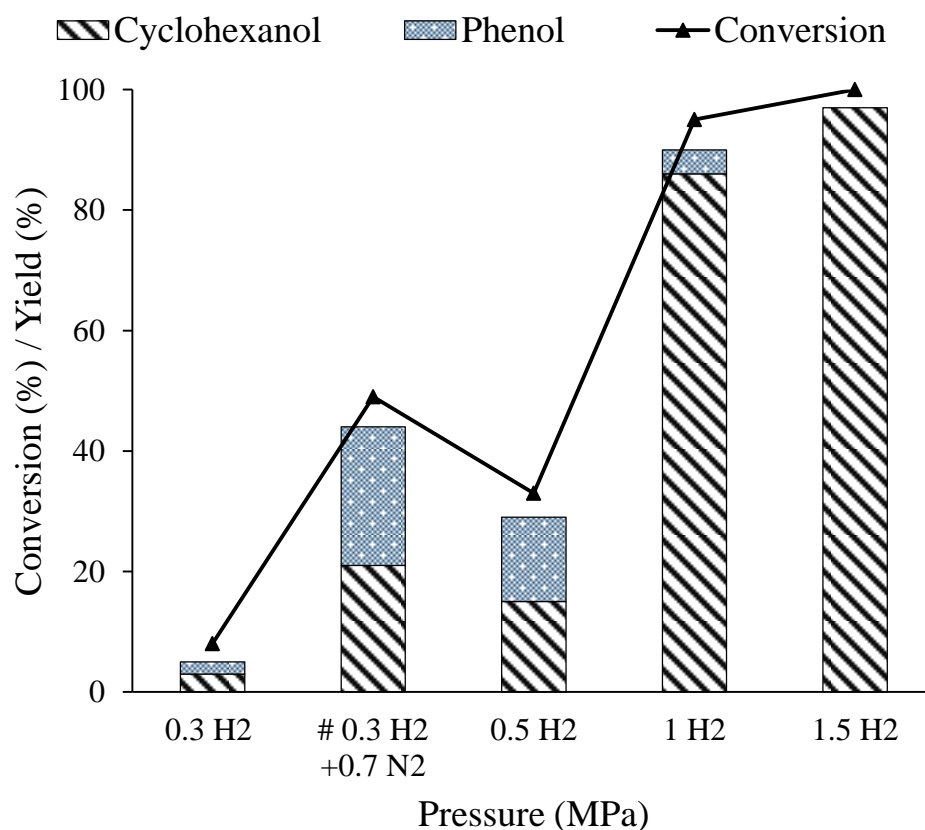
Figure 5A.6. Effect of pressure on the hydrodeoxygenation of guaiacol

Reaction condition: Guaiacol/Co molar ratio, 13; 5 Co/Al$_2$O$_3$@capilllary, 0.375g; 2.15 wt% Guaiacol in cyclohexane; 1000 rpm. # 0.3 MPa H$_2$ + 0.7 MPa N$_2$; 225 °C; 1000 rpm.

Initially, the HDO experiment was conducted at 1 MPa H$_2$ pressure @RT (Figure 5A.6), and 95% conversion of guaiacol and 86% yield of cyclohexanol was obtained. For the complete conversion of guaiacol, the experiment was also done with 1.5 MPa H$_2$ pressure @RT and found that high pressure was encouraging the guaiacol conversion (100 %), and intermediate phenol was also converted into the final product cyclohexanol (97%). HDO experiment was also carried out at lower pressure i.e., 0.5 MPa and 0.3 MPa. In both the cases decreased in the conversion of guaiacol and yield of cyclohexanol was found. To check whether H$_2$ partial pressure or total partial pressure is helping in the high HDO activity. One experiment was conducted with 0.3 MPa H$_2$ + 0.7 MPa N$_2$, maintaining the 10 MPa @RT total pressure, and

found that guaiacol conversion is high (49%) with the formation of 21% cyclohexanol and 23% phenol compared to HDO reaction conducted at 0.3 MPa H_2 and 0.5 MPa H_2, where guaiacol conversion was 8% and 33%, respectively. These results showed that not only high pressure of H_2 but total partial pressure generated at the final temperature was encouraging the hydrodeoxygenation results.

5A.3.2.7. Recycle study
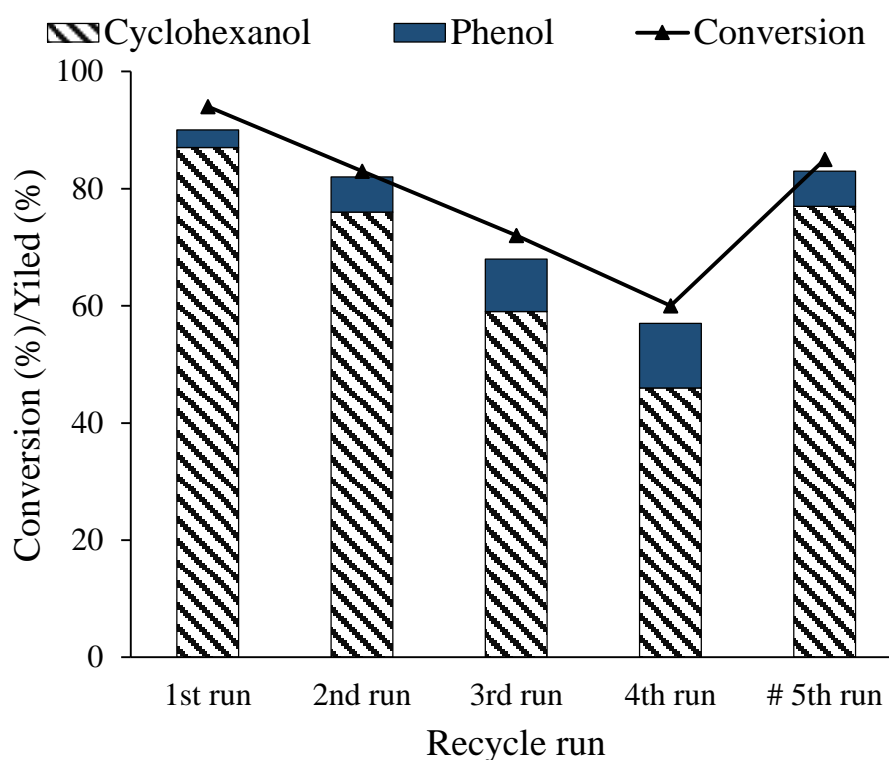
Figure 5A.7. Recycle study on the hydrodeoxygenation of guaiacol

Reaction condition: Guaiacol/Co molar ratio, 13; 5 Co/Al$_2$O$_3$@capilllary, 0.375g; 2.15 wt% Guaiacol; cyclohexane, H_2 pressure, 1 MPa at room temperature; 225 °C; 4 h; 1000 rpm. In the 2nd,3rd run, and 4th run Guaiacol/Co molar ratio was not maintained as catalyst was not dried. # In 5th run, wet recovered catalyst from 4th run was dried at 60 °C for 12 h, and Guaiacol/Co molar ratio of 13 was maintained.

The reusability study of the catalyst was done with the spent 5 Co/AHF@capillary catalyst (Figure 5A.7). After completion of the reaction, the reaction mixture was centrifuged, and the recovered catalyst was dried at RT and used for next run till 4th run. The recycle study shows decrease in the activity of the catalyst. This could be due to the loss of catalyst concentration in the multiple runs. Careful look of the recycle study data also confirms intermediate product, phenol formation. Yield of phenol was increasing in consecutive runs and thus overall activity of hydrogenation was decreasing. These results also suggest that for the conversion of intermediate phenol, required active catalytic centers, which were not available for the reaction. This also confirmed that phenol to cyclohexanol (Hydrogenation) is the rate-determining step of the Co catalyzed HDO reaction. To prove this aspect, 5th run was conducted by maintaining the substrate to catalyst ratio and can be seen that the conversion of guaiacol was increased to 85% with 77% yield of cyclohexanol.

5A.3.2.8. Recycle study: Characterization of spent catalyst

As seen from Figure 5A.8, TPR profiles of fresh and spent 5 Co/Al_2O_3@capillary catalysts are almost same. However, it was seen that in spent catalyst slightly higher hydrogen was used compared to fresh catalyst. This might be because of hydrogen used for the removal of coke/carbon deposited on the spent catalyst. This suggestion is in line with the ~90% mass balance (based on GC) obtained in all the reactions as seen from above discussions. Moreover, higher hydrogen consumption at temperatures of 150-350 ^{o}C indicates that the coke deposited on the catalyst surface was amorphous in nature and was easily removable. TEM image presented in Figure 5A.9, showed no change in their morphology.
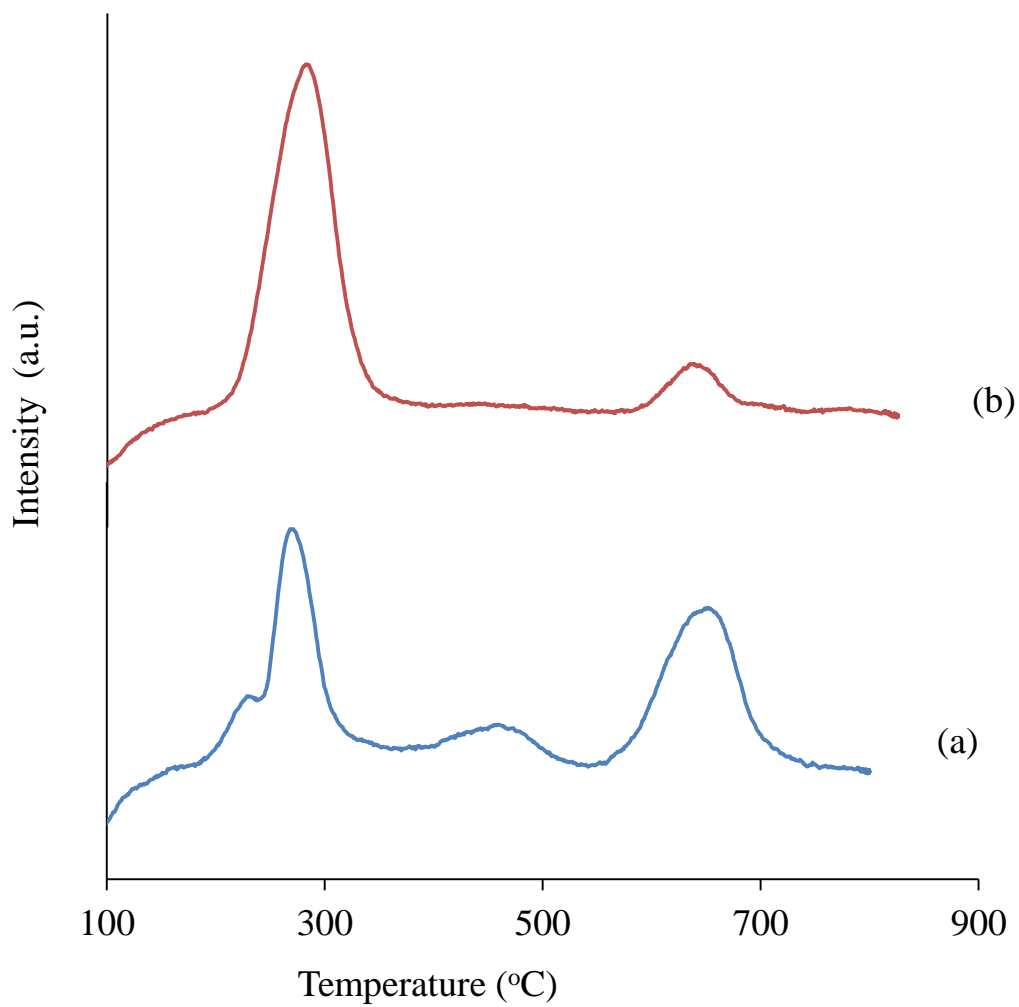
Figure 5A.8. TPR profiles of 5 Co/AHF@capillary catalyst (a) Fresh; (b) Spent
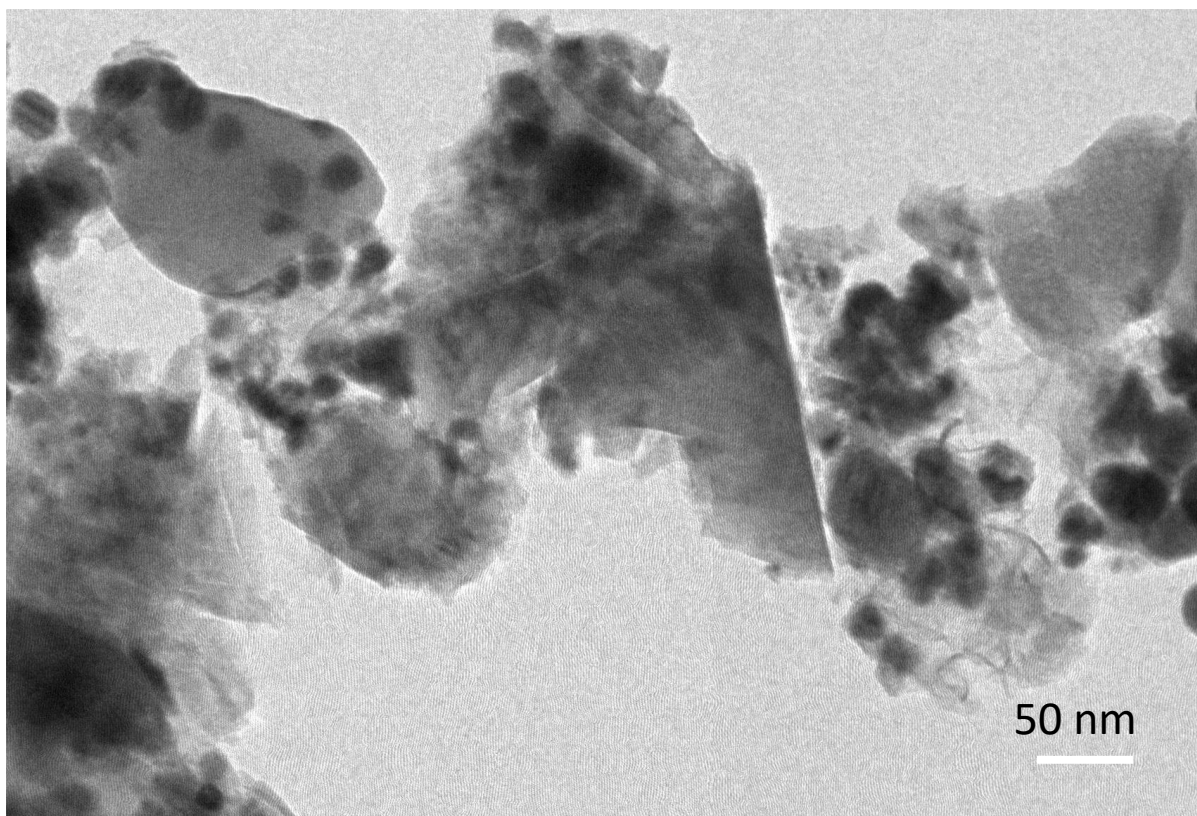
Figure 5A.9. TEM image of spent catalyst, 5 Co/AHF@capillary;

5A.4. Conclusion

Hydrodeoxygenation of low molecular weight compounds was achieved under milder condition (225 °C, 1 MPa H_2) using non-precious metal Co and Ni. Modification in the (Al_2O_3) support was helping in achieving better HDO activity and gave 86% yield of cyclohexanol. Intermediate phenol formation is the rate-determining step. Modified catalytic synthesis procedure (capillary action) was used, which is helping to get uniform distribution of metal on the support confirmed by the TEM images.

5A.5. References:

1. Zhao, C.; Lercher, J. A., Upgrading pyrolysis oil over Ni/HZSM-5 by cascade reactions. *Angewandte Chemie (International ed. in English)* **2012,***51* (24), 5935-40.

2. Bui, V. N.; Laurenti, D.; Afanasiev, P.; Geantet, C., Hydrodeoxygenation of guaiacol with CoMo catalysts. Part I: Promoting effect of cobalt on HDO selectivity and activity. *Applied Catalysis B: Environmental* **2011,***101* (3), 239-245.

3. Bui, V. N.; Laurenti, D.; Delichère, P.; Geantet, C., Hydrodeoxygenation of guaiacol: Part II: Support effect for CoMoS catalysts on HDO activity and selectivity. *Applied Catalysis B: Environmental* **2011,***101* (3), 246-255.

4. Lin, Y.-C.; Li, C.-L.; Wan, H.-P.; Lee, H.-T.; Liu, C.-F., Catalytic Hydrodeoxygenation of Guaiacol on Rh-Based and Sulfided CoMo and NiMo Catalysts. *Energy & Fuels* **2011,***25* (3), 890-896.

5. Zhu, X.; Lobban, L. L.; Mallinson, R. G.; Resasco, D. E., Bifunctional transalkylation and hydrodeoxygenation of anisole over a Pt/HBeta catalyst. *Journal of Catalysis* **2011,***281* (1), 21-29.

6. Gayubo, A. G.; Aguayo, A. T.; Atutxa, A.; Aguado, R.; Olazar, M.; Bilbao, J., Transformation of Oxygenate Components of Biomass Pyrolysis Oil on a HZSM-5 Zeolite. II. Aldehydes, Ketones, and Acids. *Industrial & Engineering Chemistry Research* **2004,***43* (11), 2619-2626.

7. Adjaye, J. D.; Bakhshi, N. N., Catalytic conversion of a biomass-derived oil to fuels and chemicals I: Model compound studies and reaction pathways. *Biomass and Bioenergy* **1995,***8* (3), 131-149.

8. Huber, G. W.; Iborra, S.; Corma, A., Synthesis of Transportation Fuels from Biomass: Chemistry, Catalysts, and Engineering. *Chemical Reviews* **2006,***106* (9), 4044-4098.

9. Aqsha, A.; Katta, L.; Mahinpey, N., Catalytic Hydrodeoxygenation of Guaiacol as Lignin Model Component Using Ni-Mo/TiO$_2$ and Ni-V/TiO$_2$ Catalysts. *Catalysis Letters* **2015,***145* (6), 1351-1363.

10. Zhao, C.; Kou, Y.; Lemonidou, A. A.; Li, X.; Lercher, J. A., Hydrodeoxygenation of bio-derived phenols to hydrocarbons using RANEY[registered sign] Ni and Nafion/SiO2 catalysts. *Chemical Communications* **2010,***46* (3), 412-414.

Chapter 5B

Alumina Hollow Fiber (AHF) supported Co catalyzed continuous defunctionalization of guaiacol into cyclohexanol

5B.1. Introduction

As seen from the previous chapters (Chapter 4A, 4B), Ru/Al$_2$O$_3$-Acidic catalyst could effectively catalyze defunctionalization/hydrodeoxygenation (HDO) of guaiacol in batch mode reactor. It was also demonstrated in Chapter 5A, that 5 Co/AHF@capillary catalyst is an efficient catalytic system for the HDO of guaiacol. Previously, all catalytic experiments were conducted in batch mode reactor. For the demonstration of the mainstream process on the industrial scale, it is desirable to develop the process in continuous flow. Most of the industrial plants prefer to use continuous production plant rather than batch mode plant. Continuous mode production is more economically feasible because it reduces the production cost. The motivation of this work is that, there are number of reports on HDO of guaiacol in batch process and barely few for continuous production [1-6]. As it was discussed earlier in Chapter 1, cyclohexanol produced via defunctionalization of guaiacol is an important intermediate product, which can be utilized in the production of adipic acid. The major part of this thesis also covers the effective defunctionalization of guaiacol into cyclohexanol operated at milder reaction condition (225 °C; 1 MPa H$_2$; cyclohexane, solvent). The catalytic activity of 5 Co/AHF@capillary was also employed for the defunctionalization of guaiacol in batch mode reactor at 225 °C, 1 MPa H$_2$, cyclohexane solvent and showed 95% conversion of guaiacol with 86% yield of cyclohexanol. As discussed, continuous flow system is more preferable to be used on industrial scale than batch system. It was decided to check the catalytic activity of 5 Co/AHF@capillary catalyst for the HDO of guaiacol in a continuous flow reactor. It was also seen, in Chapter 2B that, AHF synthesized is found in the cylindrical form and catalytic activity of 5 Co/AHF@capillary was examined after crushing it into powder form (Chapter 5A). Major issues associated with the powder form of the catalyst is pressure drop, limitation of mass flow, heat transfer, and diffusion limitation. At the industry level, it is preferable to use extrudate, which reduces those limitations, which are associated with the powder form of the catalyst. Use of 5 Co/AHF@capillary as synthesized may contribute to reduce those problems. Thus, it was decided to develop the reactor system to load the 5 Co/AHF@capillary catalyst as synthesized. 5 Co/AHF@capillary catalyst was placed into the newly designed catalyst holding

system and loaded into the continuous flow reactor. The reaction scheme for the HDO of guaiacol is shown in Scheme 5B.1.
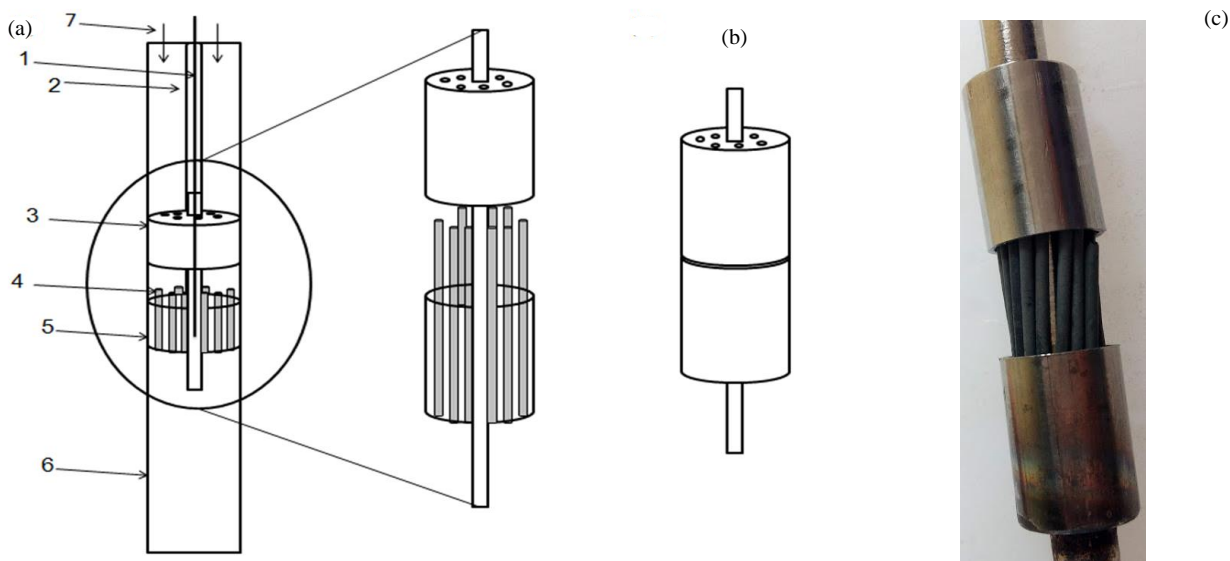
Figure 5B.1. (a) Model reactor set up with the loaded catalyst; catalyst loaded module; (1) Thermocouple (2) Thermowell (3) Topside cap with holes (4) Co/AHF@capillary catalyst (5) Bottom container with holes at the bottom, (6) Flow reactor; (b) Model Co/AHF@capillary (c) Real image of the reactor set up with loaded 5 Co/AHF@capillary;
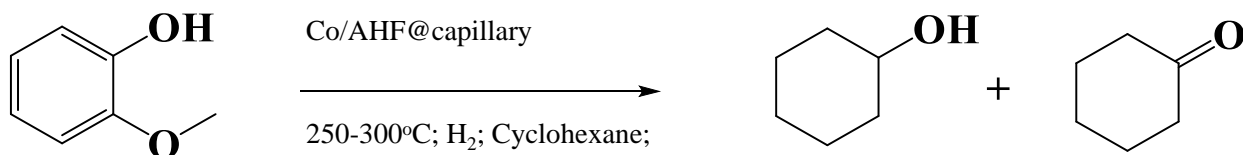
Scheme 5B.1. Hydrodeoxygenation/defunctionalization of lignin-derived low molecular weight compounds (guaiacol)

5B.2. Experiment section

5B.2.1. Materials

For the details on all the materials used in this study, please refer to Chapter 4, Section 4A.2.1.

5B.2.2. Catalyst synthesis

Co metal was supported on aluminum hollow fiber (AHF) with 5 wt% loading. For the details on the catalyst synthesis kindly refer to Chapter 2B, Section 2B.4.1-2B.4.3.

5B.2.3. Catalytic runs

HDO experiments were conducted in continuous flow stainless steel cylindrical reactor in downflow, reactor placed in the two-zone furnace (13 mm id Geomechanique, France). Experiments were carried out between 250-300 $^{\circ}$C and 1.5-3.5 MPa H_2 pressure. Catalyst bed temperature measure by Cr-Al thermocouple. Prior to the reaction catalyst were activated in the presence of H_2 (25 mL•min^{-1}) at 300 $^{\circ}$C for 6h. The reactant was allowed to pass through the reactor using a high-precision syringe pump (ISCO Model 500D) at required flow rate. The product mixture was cooled using chilled water condenser and collected in a gas-liquid separator.

5B.2.4. Durability of the 5 Co/AHF@capillary catalyst

5 Co/AHF@capillary catalyst durability was also tested for longer time. HDO experiment was conducted at an optimized reaction condition.

5B.2.5. Analysis of reaction mixture

The reaction mixture was analyzed using GC and GC-MS techniques and for the details about the methodologies used and instruments used for the analysis of reaction mixture, please refer to Chapter 4, Section 4A.2.5.

5B.3. Results and discussion

5B.3.1. Catalyst characterization

Synthesized catalysts were characterized using different physico-chemical techniques. For details on catalyst characterization, kindly refer to Chapter 2B, Section 2B.5, Subsection 2B.5.1- 2B.5.8

5B.3.2. Catalyst activity

Hydrodeoxygenation (HDO) reactions were carried out in fixed bed reactor, the analysis of the reaction mixture was done on GC and GC-MS (for details, please refer experiment section).

5B.3.2.1. Effect of temperature on the HDO of Guaiacol
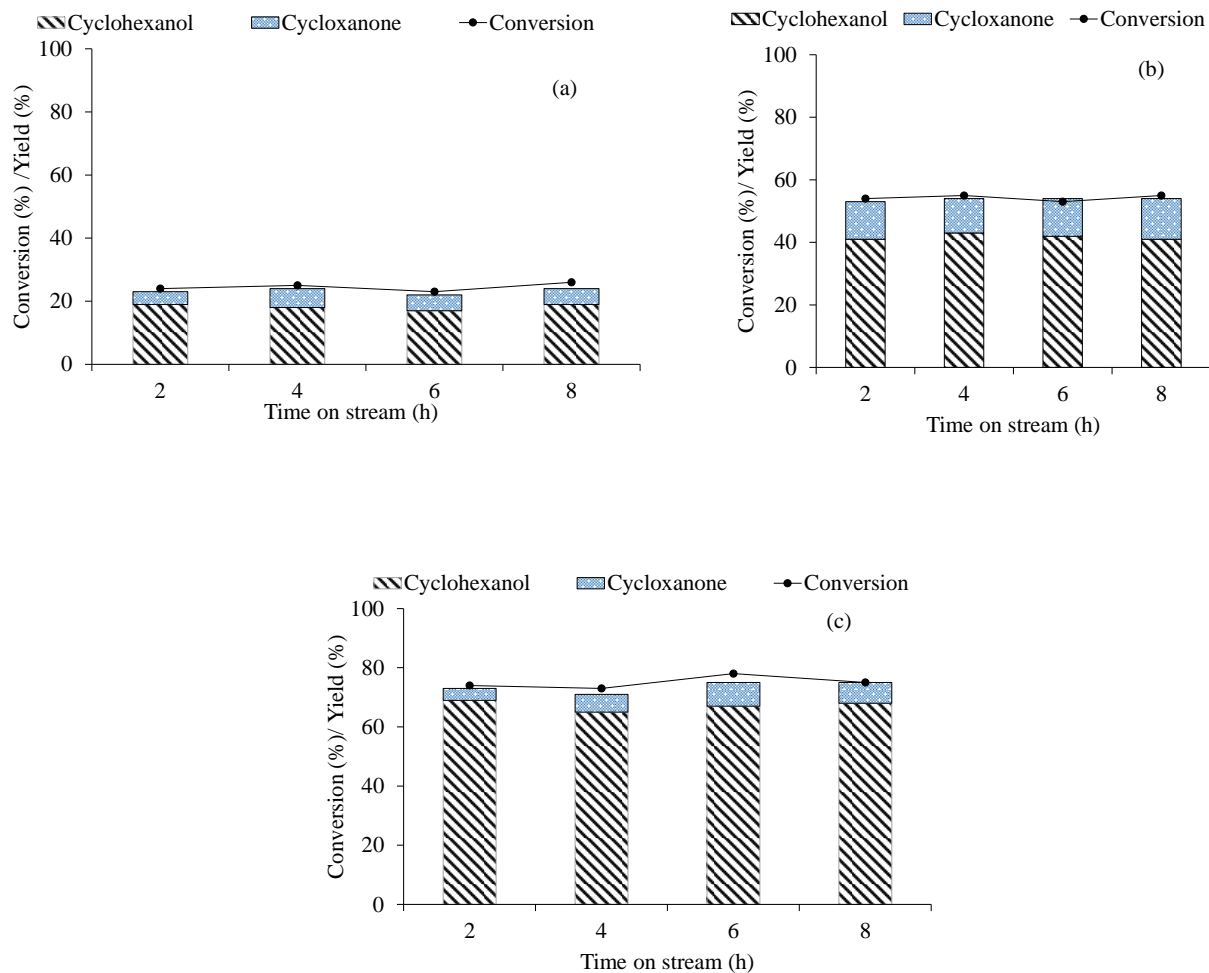
Figure 5B.2. Effect of Temperature on the hydrodeoxygenation of guaiacol

Reaction condition: WHSV•h^{-1}:13.3, (20 mL•h^{-1}•1.5g^{-1} catalyst) ; (a) 250 °C; (b) 275 °C (c) 300 °C; 5 Co/ AHF@capillay; 2.5 MPa H$_2$; 25mL•min^{-1} H$_2$ flow

As seen from Figure 5B.2, HDO reactions were conducted in the temperature range from 250-300 °C. When the reaction was carried out at 250 °C, 25% conversion of guaiacol was possible with

18% cyclohexanol yield and 6% cyclohexanone yield. On increasing temperature to 275 $^{\circ}$C, guaiacol conversion increases to 55% with 43% cyclohexanol yield and 11% cyclohexanone yield. Further, reaction temperature was increased to 300 $^{\circ}$C and found that guaiacol conversion increases to 73% and formation of 65% cyclohexanol and 6% cyclohexanone were found. On increasing temperature, conversion of guaiacol is increases due to the increase of the kinetic energy of guaiacol molecule, mostly guaiacol molecule will exist in gaseous form (B.P 205 $^{\circ}$C), and adsorption and desorption phenomena is also increases with temperature.

5B.3.2.2. Effect of H₂ pressure in the HDO of Guaiacol
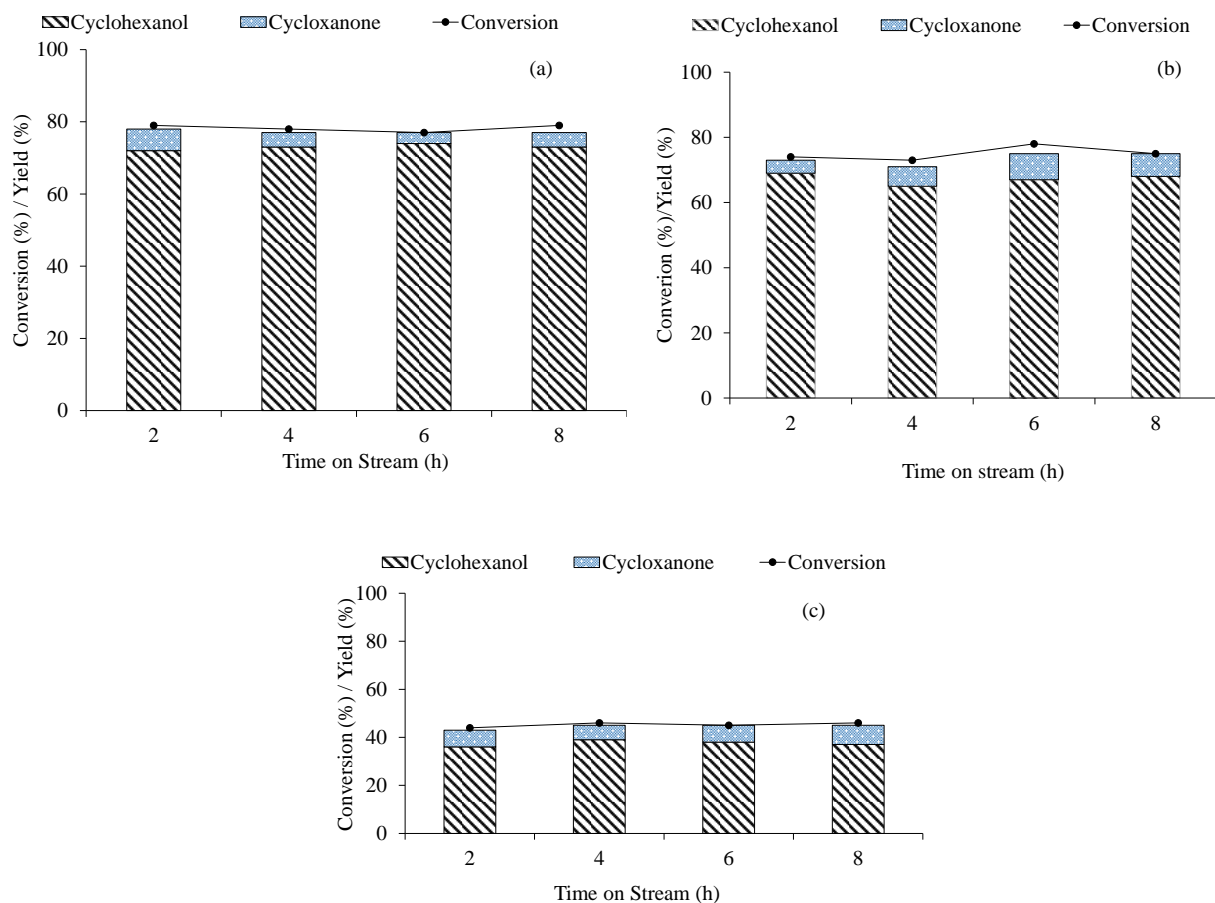
Figure 5B.3. Effect of pressure on the hydrodeoxygenation of guaiacol

Reaction condition: WHSV•h^{-1}:13.3, (20 mL•h^{-1}•1.5g^{-1} catalyst); 300 ºC; 5 Co/ AHF@capillay, (a) 1.5 MPa H$_2$; (b) 2.5 MPa H$_2$; (c) 3.5 MPa H$_2$; 25mL•min^{-1} H$_2$ flow;

It was seen from the temperature study in Figure 5B.2 that at 300ºC; 2.5 MPa H$_2$ pressure, maximum 73% guaiacol conversion with 65% cyclohexanol yield, and formation of 6% cyclohexanone was obtained. Further, to study the effect of pressure on the reaction, reaction was carried out at different pressures of H$_2$ viz, 1.5 MPa, 2.5 MPaand 3.5 MPa and the results are represented in Figure 5B.3. When HDO reaction was performed at lower H$_2$ pressure, 1.5 MPa

H$_2$, guaiacol conversion decreases to 72% with 53% cyclohexanol yield and 17% yield of cyclohexanone. A careful look of these results suggests that lower pressure is not affecting guaiacol conversion that much but intermediate cyclohexanone yield is more (17%) compared to 2.5 MPa H$_2$ i.e. 6%. It is suggesting that the HDO reaction might be proceeding via cyclohexanone intermediate. Further on increasing pressure to 3.5 MPa, an increase in conversion of guaiacol to 86% with 81% yield of cyclohexanol with 4 % yield of cyclohexanone was found. It is obvious because at high-pressure solubility of H$_2$ increases which helped in high HDO activity.

5B.3.2.3. Effect of WHSV on the HDO of Guaiacol

Effect of WHSV on HDO of guaiacol was studied by varying the liquid flow of reaction and the results are represented in Figure 5B.4. Initially, the reaction was conducted at WHSV of 13.3 and found that the conversion of guaiacol was 73% with 65% yield of cyclohexanol with 6% cyclohexanone yield. Further, the reaction was conducted at lower flow rate with WHSV of 6.6 and conversion of guaiacol was almost similar i.e., 79% with 72% cyclohexanol yield of and 6% cyclohexanone. The difference in the activity is due to the increase of residential time of substrate on the catalytic surface due to lower WHSV 6.6. Later, WHSV was increased to 20 and conversion of guaiacol decreased to 44% with the formation of cyclohexanol to 36% and 7% cyclohexanone formation. This is again obvious behavior due to decrease in residential time of substrate on the catalyst surface.
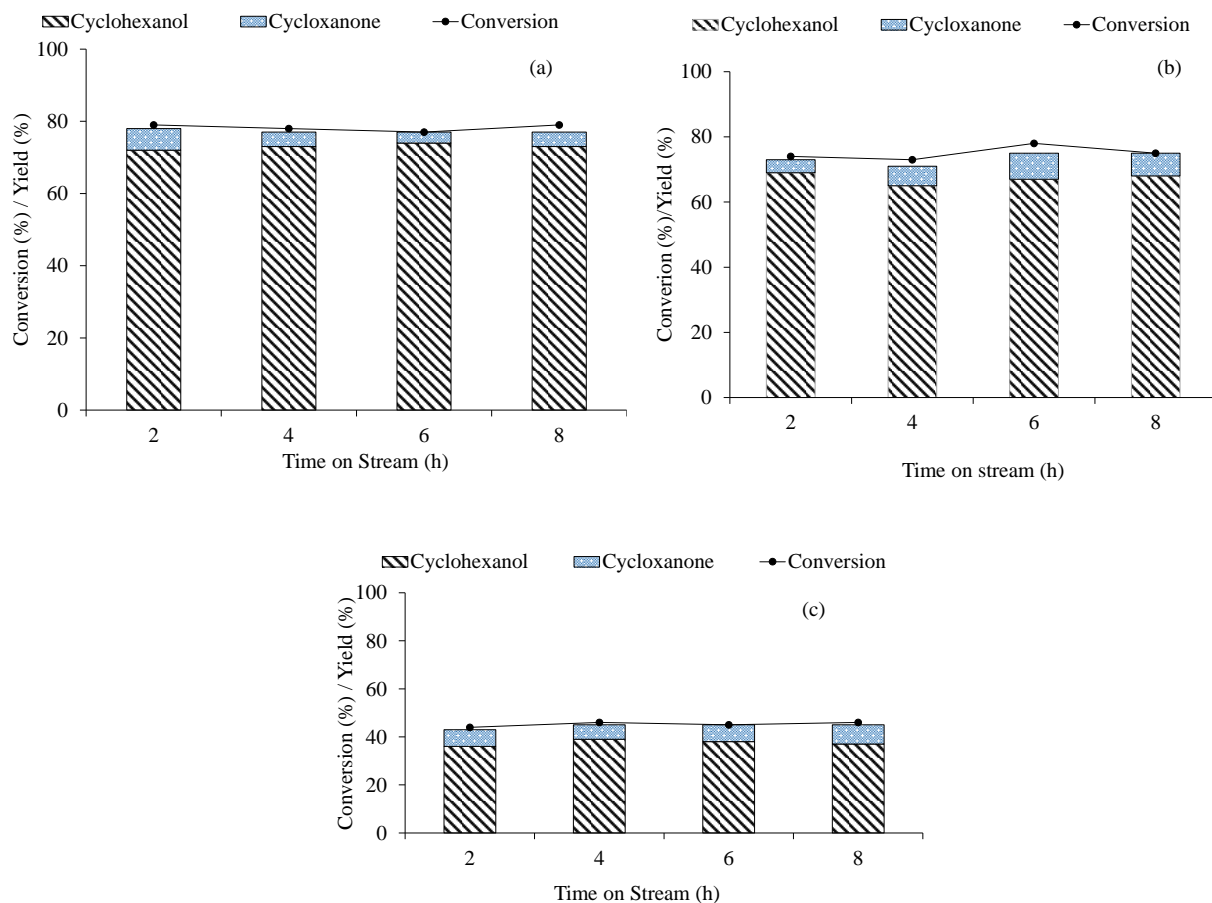
Figure 5B.4. Effect of WHSV on the hydrodeoxygenation of guaiacol

Reaction condition: WHSV•h⁻¹: (a) 6.6; (b) 13.3; (c) 20; 300 ºC; 5 Co/ AHF@capillay, 2.5 MPa H_2; 25mL•min⁻¹ H_2 flow;

5B.3.2.4. Effect of gas flow on the HDO of guaiacol

Effect of gas flow was also investigated for the HDO of guaiacol and the results are represented in Figure 5B.5. Initially reaction was conducted at 25mL•min⁻¹ H_2 flow and found that 73% conversion of guaiacol is possible with 65% yield of cyclohexanol and 6% yield of cyclohexanone. Further, the gas flow rate decreased to 18 mL•min⁻¹ and found that the conversion of guaiacol increases to 83% with the 74% yield of cyclohexanol and 5% yield of cyclohexanone. The decrease in gas flow also increases the contact time of the substrate on the catalyst surface. Further, the

reaction was conducted under higher gas flow of 35 mL•min^{-1} and guaiacol conversion was seen to be decreasing to 56% with 45% yield of cyclohexanol and 9% yield of cyclohexanone.The decrease in the activity is due to the decrease in the residential time of the substrate on the catalyst surface.
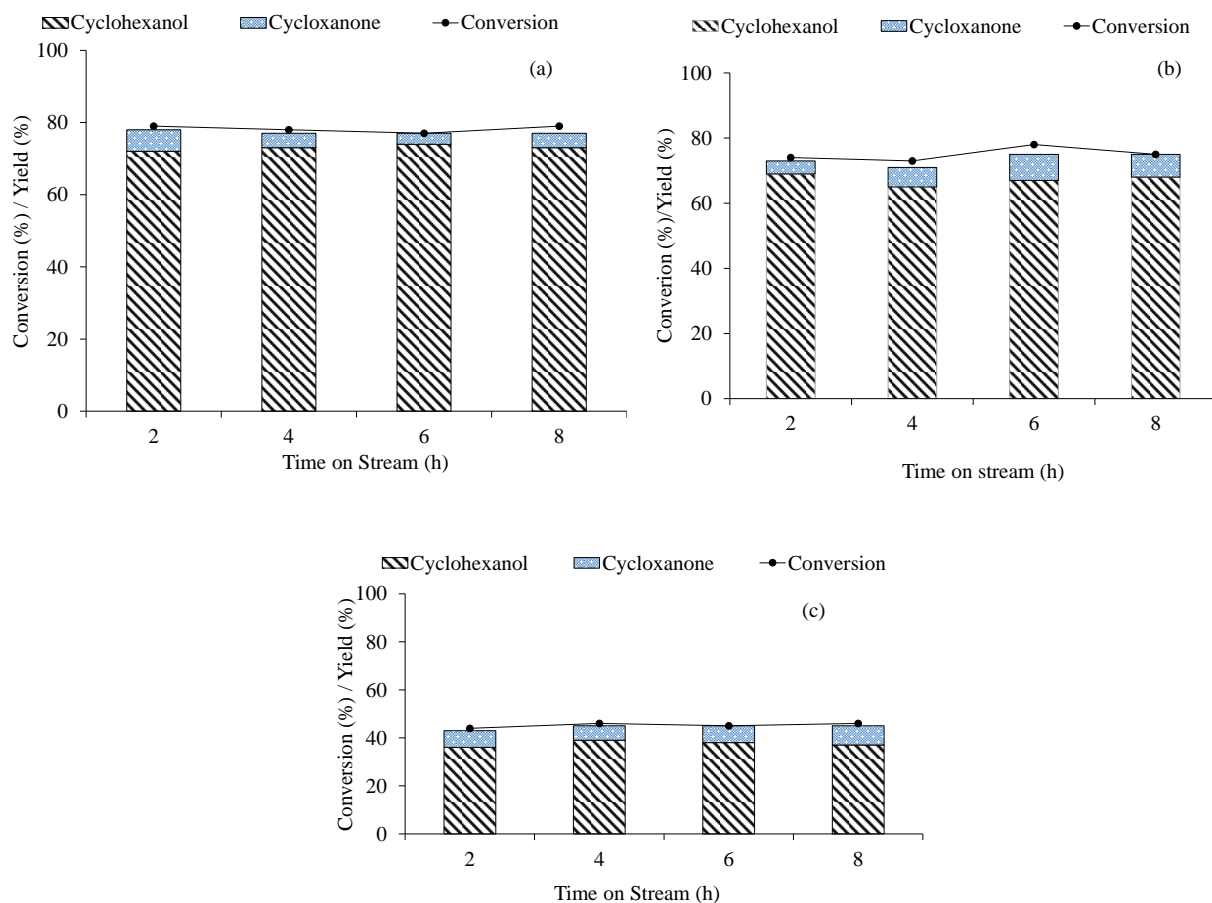
Figure 5B.5. Effect of gas flow on the hydrodeoxygenation of guaiacol

Reaction condition: Reaction condition:WHSV•h^{-1}: 13.3; 300 °C; 5 Co/ AHF@capillay, 2.5 MPa H$_2$; (a) 15mL•min^{-1} H$_2$ flow; (b)25mL•min^{-1} H$_2$ flow; (c) 35mL•min^{-1} H$_2$ flow

5B.3.2.5. Long-term on–stream stability of 5 Co/AHF@capillary
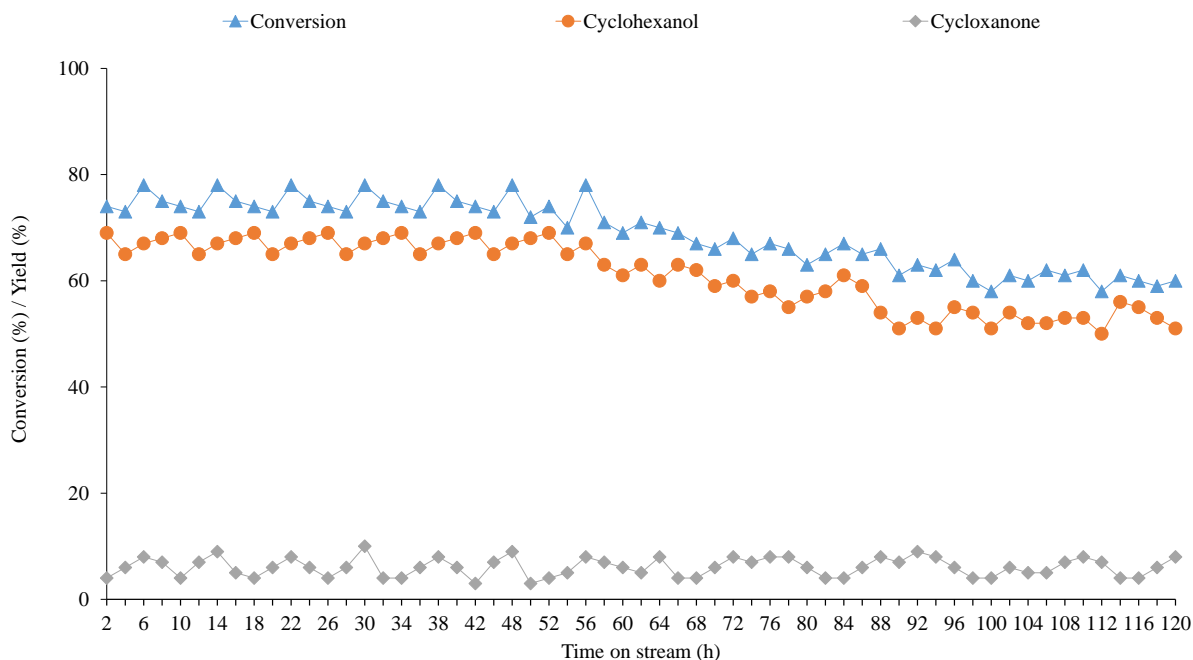
Figure 5B.6. Time on stream

Reaction condition: WHSV•h^{-1}: 13.3; 300 ^{o}C; 5 Co/ AHF@capillay, 2.5 MPa H$_2$; 25mL•min^{-1} H$_2$ flow

The durability test of the catalyst, 5 Co/AHF@capillarycatalyst was conducted under optimized reaction conditions (300 ^{o}C, 2.5 MPa H$_2$, 25 mL•min^{-1} H$_2$, WHSV, 13.3). It can be seen from Figure 5B.6 that guaiacol conversion is almost constant up to 73% with 65% yield of cyclohexanol for the 50 h run. Further on increasing the timing of reaction, slight decrease in HDO activity was seen and it reaches to 61% guaiacol conversion with 56% cyclohexanol yield. Decrease in activity is observed due to the deposition of coke on the catalyst surface.

5B.4. Conclusion

Hydrodeoxygenation of guaiacol was achieved in flow mode reactor under milder condition (300 $^{\circ}$C, 2.5 MPa H$_2$, 25ml•min^{-1}) using non-precious 5 Co/AHF@capillary. Modification in the (Al$_2$O$_3$) support was helping in achieving better HDO activity and gave 73% yield of cyclohexanol. Use of model reactor setup used for the loading of the 5 Co/AHF@capillary as synthesized was helpful for the better HDO activity. Use of cylindrical form of the catalyst is minimizing the limitation of catalyst.

5B.5. References:

1.   A.K. Deepa, P. L. D., Function of Metals and Supports on the Hydrodeoxygenation of Phenolic Compounds, . *ChemPlusChem,* **2014,***79* ( ), 1573-1583.

2.   Deepa, A. K., Dhepe, P. L., *RSC Adv* **2014,***4*, 12625-12629.

3.   S. Liu, H. W., K.J. Smith, C.S. Kim Hydrodeoxygenation of 2-Methoxyphenol over Ru, Pd, and Mo2C Catalysts Supported on Carbon, *Energy & Fuels* **2017,***31* 6378-6388.

4.   Sandip K. Singha, P. L. D., Ionic liquids catalyzed lignin liquefaction:mechanistic studies using TPO-MS, FT-IR, RAMAN and 1D, 2D-HSQC/NOSEY NMR. *Green Chemistry* **2016,***18*, 4098-4108.

5.   Shaomin Liu , K. L., R. Hughes, Preparation of porous aluminium oxide (Al2O3) hollow fibremembranes by a combined phase-inversion and sintering method. *ceramics international,* **2003,***29* 875–881.

6.   Y.K. Hong, D. W. L., H.J. Eom, K.Y. Lee, The catalytic activity of Pd/WOx/γ-Al2O3 for hydrodeoxygenation of guaiacol. *Appl. Catal. B: Environ.* **2014** *150-151* 438-445.

Chapter 6

**Functionalization of lignin derived monomers:
Altering the O/C ratio of lignin derived monomers
without sacrificing atom efficiency by alkylation**

6.1. Introduction

As discussed earlier, base catalyzed lignin depolymerization was achieved and further defunctionalization of lignin derived low molecular weight compounds was carried out to alter the O/C ratio in the depolymerized products. Depolymerization of lignin produces variety of aromatic and low molecular weight compounds such as vanillin, methyl vanillate, eugenol, acetosyringone, guaiacone, homovanillic acid, vinyl guaiacol, butyl hydroxyl etc.[1-7]. These oxygenates having high O/C ratio (0.3-0.5) makes them unstable, corrosive and also restricts their use as fuel. In order to enhance their fuel quality and stability. It is advisable to reduce O/C ratio and improve C/H ratio. As discussed earlier, defunctionalization/hydrodeoxygenation (HDO) process is generally preferred to reduce the O/C ratio [8-14] but, uses high amount of hydrogen during reaction also yields ring hydrogenation products thereby diminishing its aromatic structure and compromise the atom efficiency. However, few of the reports are shown to produce aromatics (arenes) by precise cleavage of β-O-4 bonds using small amount of hydrogen and maintain the aromatic structure. Defunctionalization of lignin derived monomers was achieved using supported metal catalysts, Chapter 4) such as precious metal (Ru; Chapter 4) and non-precious metals (Co, Ni; Chapter 5). Defunctionalization pathways required bifunctional catalyst, in which metal is used to activate molecular hydrogen (either external hydrogen source or in-situ generated hydrogen) along with support to have interaction with substrate molecules. Since, most of the reports and also this thesis (Chapter 4 and 5) discusses defunctionalization. It was thought to replace molecular H_2 (expensive), and metal for altering O/C ratio. To achieve this, solid acid catalyzed functionalization of low molecular weight compounds is conducted. In this chapter, solid acids catalyzed functionalization /alkylation of lignin derived variety of monomers such as guaiacol, veretrole, phenol, anisole, and catechol using numerous alcohols as alkylating agents is reported. Another route to reduce the O/C ratio and improve H/C ratio is addition of C and H atoms in the structures of these monomers, which can be achieved by carrying out systematic and controlled alkylation of these monomers [15]. By doing so, an already established market for these compounds (additives in gasoline, lubricants, and in several other consumer products) can be tapped [16-19]. By meticulously designing the catalysts and reaction parameters, it is possible to achieve either O-alkylation or C-alkylation [19-22]. Typically, alkylating agents used for alkylation are either olefins or alcohols, which are readily available [23-25]. Alkylation of phenols is an electrophilic aromatic substitution and when it is done in the presence of alcohols

the electrophile can be the protonated alcohol (an alkoxonium species) or a carbenium ion resulting from alcohol dehydration. In the O-alkylation, products are formed by electrophilic attack on.

The phenolic OH and in case of C-alkylation, products are formed when electrophile attack occurs on the aromatic ring. It has also been proposed that C-alkylation products could be formed through intramolecular rearrangement of the kinetically favoured O-alkylation product, i.e., via an aryl alkyl ether intermediate product [19, 20, 22].

In the literature few of the studies are reported for the alkylation of phenol, and substituted phenols using different solid acid catalysts such as zeolites, modified zeolites, phosphated materials and sulphated materials [26-30]. The effects of acid-base properties of catalysts are also investigated in the alkylation of phenol with methanol over modified MgO catalyst [26]. Immobilised ionic liquids too are used as acid catalysts for the alkylation of phenol with dodecane [27].Though, literature establishes the fact that alcohols act as alkylating agents but a systematic comparative study with different substrates and alcohols combination over different catalysts is not performed and hence my approach was to investigate this aspect of the reaction. For doing so, various solid acid catalysts like H-USY, SiO_2-Al_2O_3, K10 clay, Al-pillared clay were evaluated for the functionalization of substrates like guaiacol, which is one of the characteristic compound obtained after lignin depolymerisation, and other compounds such as veratrole, catechol, anisole, phenol and toluene were used (Scheme 6.1). The alkylating agents used in this study are, methanol, ethanol, n-butanol, s-butanol, t-butanol, pentanol, hexanol, and octanol.
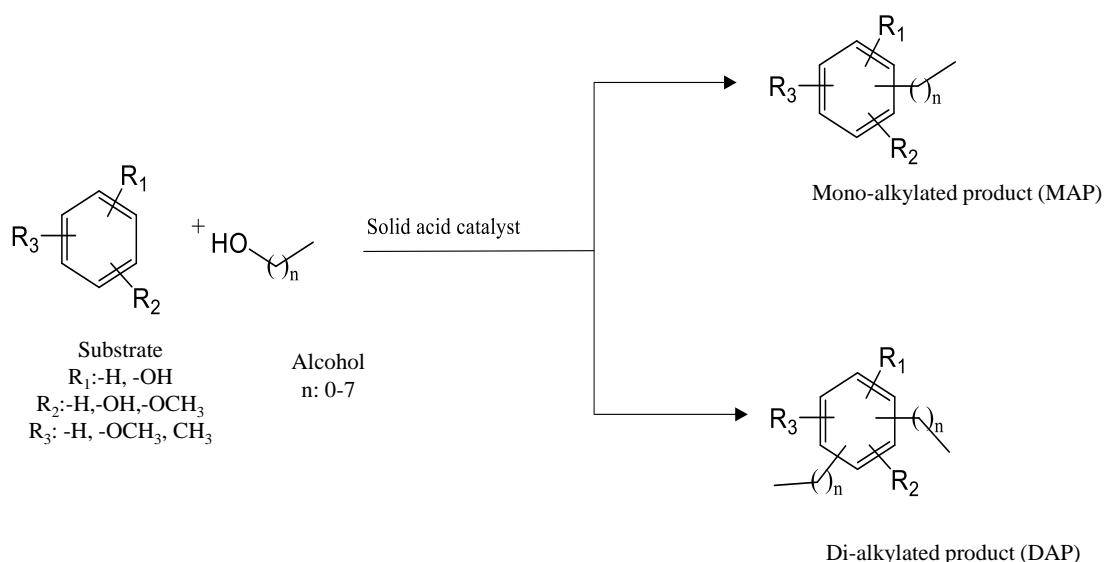
Scheme 6.1. Alkylation of lignin derived monomers with alcohols as alkylating agent.

6.2. Experiment section

6.2.1. Materials

Zeolite, H-USY (Si/Al = 15), was obtained from Zeolyst International. Prior to use, zeolite was calcined at 400 °C for 16 h in an air flow. SiO_2−Al_2O_3 (Si/Al =5.3), K10 clay and Al pillared clay were purchased from Aldrich, USA. Various aromatic monomers (guaiacol, veratrole, catechol, anisole, phenol and toluene) were purchased from Aldrich, Alfa Aesar, and TCI Chemicals and used as received. Solvents such as methanol (99.9%), ethanol (99.7%), butanol (99.9%), isopropanol (99.9%), isobutanol (99.9%), pentanol (99.9%), hexanol (99.9%), octanol (99.9%), hexane (99%), cyclohexane (99%), and hexadecane (99%) were purchased from LOBA Chemicals, India. All the chemicals were used as received without any treatment.

6.2.2. Catalytic runs

Batch mode reactions were performed in high temperature high pressure 100 mL stainless steel Parr make reactor. In a typical reaction, the reactor was charged with 30 mL cyclohexane, 0.5 g catalyst, 4 mmol guaiacol and 10 mmol hexanol (alcohol). N_2 gas was flushed in reactor to remove any residual air. After pressurization with N_2 gas up to required pressure (0.7-1.5 MPa) reactor was heated slowly to reach desired temperature (200-260 °C). Until reaction

temperature is reached the stirring speed was maintained at 200 rpm. After attaining the reaction temperature, the stirring speed was increased to 1000 rpm and this time was noted down as a starting time of the reaction.

6.2.3. Analysis of the reaction mixture

After completion of reaction, the reactor was cooled to room temperature and the reaction mixture was collected, filtered through 0.22 µm syringe filter and used for the analysis. Gas chromatography (Agilent GC 7890B) was equipped with HP-5 capillary column (0.25 µm x 0.32 mm x 30 m) and FID detector. The GC-MS (Agilent 7890B GC and Agilent MS5977A MSD) equipped with DB-5MS column (0.25 µm X 0.25 mm X 30 m) was used for the analysis. NIST library was used for the identification of products. The details on the calculations are given in ESI.

6.3. Results and Discussion

6.3.1. Catalyst Characterization

All the catalysts were characterized to correlate their activity with their morphologies. For the details of characterization technique used Refer (Chapter 2B). XRD analysis of solid acid catalyst was carried to confirm their morphology (Chapter 2B, Figure 2B.17). Later, N_2-physisorption analysis was performed to understand the pore diameter and surface area of the catalysts and the results are presented in Chapter 2B, (Table 2B.11). Inductive coupled plasma optical emission spectroscopy (ICP-OES) analysis was done to calculate Si/Al ratio of the solid catalyst (Chapter 2B, Table 2B.12). For the measurement of acidity of the catalysts, TPD analysis with probe molecule, NH_3 was performed (Chapters 2B, Table 2B.11) and Chapter 2B, Figure 2B.18.

6.3.2. Catalytic activity

Alkylation reactions were performed in the autoclaves and the analysis of reaction mixture was done using GC and GC-MS.

6.3.2.1. Effect of different solid acid catalyst

It is known that the alkylation reactions are performed over acidic catalysts and hence alkylation of lignin derived aromatic monomer, guaiacol with hexanol as alkylating agent were

performed over various acidic catalysts. When the reactions were carried out for 2 h at 250 °C under inert atmosphere, H-USY (Si/Al=15) catalyst showed maximum conversion (100%) with the formation of mono alkylated product (MAP) as major category of product (72%) with dialkylated product (DAP) formation of 28% (Table 6.1; Figure 6.1). It is important to note here that based on the GC-MS library, fragmentation pattern of the products matches well with the C-alkylation products rather than O-alkylation and thus it is suggested that only C-alkylation products are formed during the reaction. With amorphous SiO_2-Al_2O_3 (Si/Al = 5.3), 85% conversion with 58.3% MAP formation and 30.9% DAP formation was achieved. Another two catalysts, Al-pillared clay and K-10 clay showed 81 and 60% conversion with 23.3 and 23.7% DAP formation, respectively. Since the aim of the work is to decrease the O/C ratio, it is desired to achieve higher DAP products. The MAP/DAP ratio calculation showed that SiO_2-Al_2O_3 (1.88) and K-10 (1.86) catalysts performed better in achieving lowest ratio. In case of MAP products, O/C ratio is 0.153 and for DAP products, it is 0.105 in comparison to guaiacol, which has O/C ratio of 0.285. As seen from the results, highest DAP formation was observed with SiO_2-Al_2O_3 catalyst and it is known that with higher acidity, higher extent of alkylation is possible. As seen from Table 6.2, SiO_2-Al_2O_3 has a total acidity of 0.61 mmol•g^{-1} which is higher than H-USY (0.28 mmol•g^{-1}) and clay K-10 (0.36 mmol•g^{-1}) catalysts. Although, Al-pillared clay has a higher total acidity of 0.65 mmol•g^{-1} but still the catalyst showed lower activity than SiO_2-Al_2O_3 catalyst. This might be a function of availability of the acidic sites for the interaction with the substrate as in case of SiO_2-Al_2O_3 catalyst, surface area is higher (374 m^2•g^{-1}) than

Al-pillared clay (170 m^2•g^{-1}). Although, fresh H-USY catalyst had higher surface area (631 m^2•g^{-1}) due to its channel structure, but it was observed that during the reaction, its structure has collapsed and the surface area has decreased drastically to 275 m^2•g^{-1} compared to decrease in surface area observed in spent SiO_2-Al_2O_3 (268 m^2•g^{-1}) catalyst (Fresh, 374 m^2•g^{-1}) (Chapter 2B; Table 2B.12). In view of this, it is inferred that most of the acid sites present in H-USY are buried under the collapsed structure during the reaction and thus are not available for the interaction with substrate (mostly MAP) molecules. This also explains the fact that though on H-USY, complete conversion of guaiacol was achieved as an initial activity to yield MAP but subsequently due to lack of acid sites to react over, formation of DAP was restricted. To confirm these postulations, along with nitrogen sorption studies to understand the change of surface area; XRD Figure 6.2 and TGA analyses Figure 6.3 of spent H-USY catalyst were also performed and the characterization results clearly elaborate that the catalyst has undergone

structural degradation with coke formation was also seen. Another reason for higher MAP formation with H-USY catalyst is due to shape selectivity as H-USY has pore diameter of (0.71 x 0.77 nm) Figure 6.4, and it would be possible to arise hindrance for the formation of DAP product as is evident from higher MAP (72%) formation than DAP (28%). In view of the highest desired activity achieved over SiO_2-Al_2O_3 catalyst, further reactions were carried out with this catalyst.

Table 6.1. Effect of different solid acid catalysts on the alkylation of guaiacol.

Entry	Solid acid	Conv. of guaiacol (%)	Product distribution (%)			MAP/DAP[c]
			DHE[d]	MAP[a]	DAP[b]	
1	H-USY	100	0	72.0	28.0	2.57
2	SiO_2-Al_2O_3	85	10.8	58.3	30.9	1.88
3	Al-pillared clay	81	28.8	47.9	23.3	2.05
4	ClayK-10	60	32.1	44.2	23.7	1.86
5	Without catalyst	0	0	0	0	0

Reaction condition: Guaiacol, 4 mmol; hexanol, 10 mmol; catalyst, 0.5 g; cyclohexane, 30 mL; 250 °C; N_2, 0.7 MPa at room temperature; 2 h; 1000 rpm. (a) MAP (Monoalkylated product), (b) DAP (Dialkylated product), (c) MAP/DAP (Monoalkylated/Dialkylated), (d) DHE (Di hexyl ether)
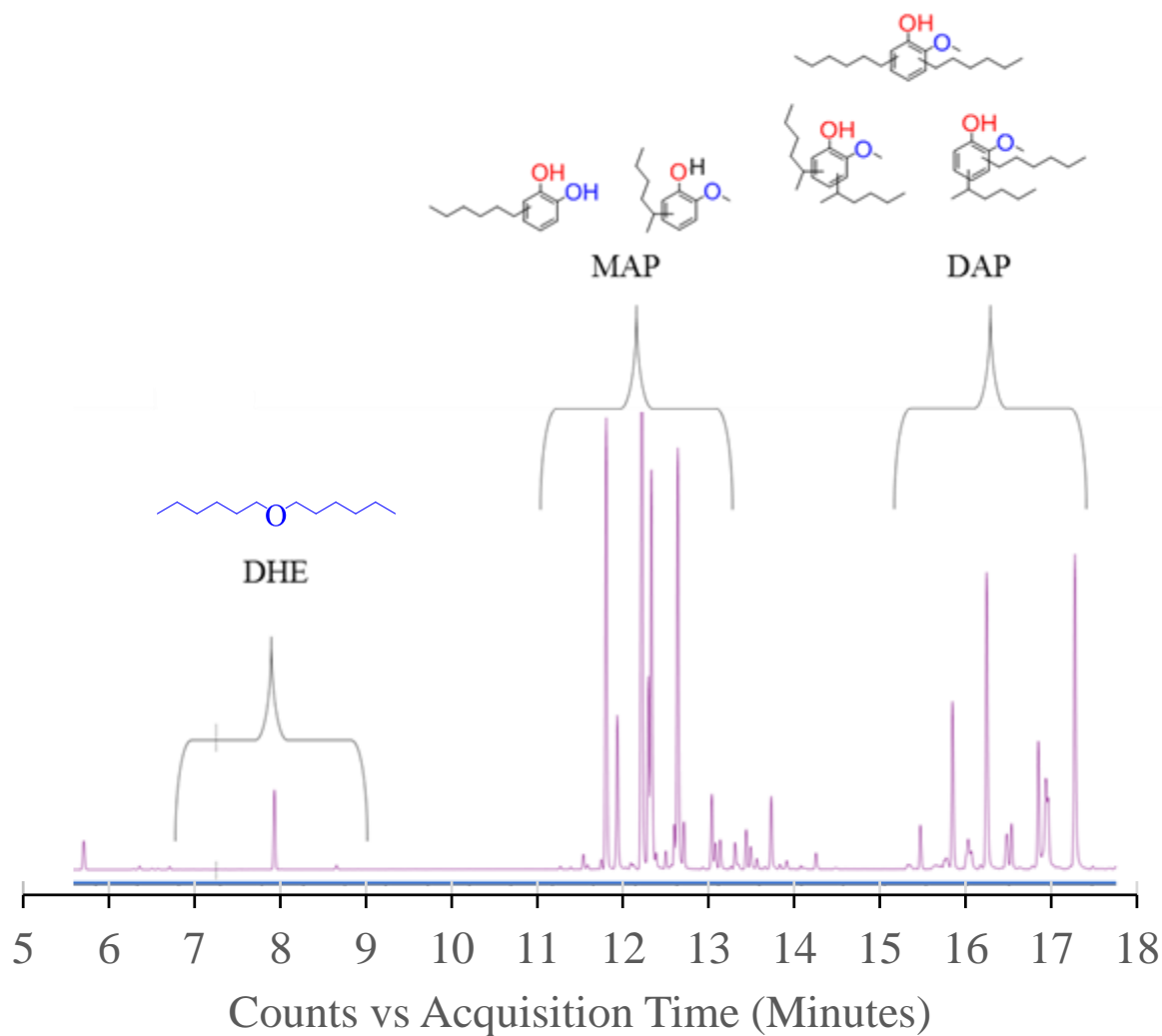
Figure 6.1. Typical GC-MS profile of the reaction mixture

Reaction condition: Guaiacol, 4 mmol; hexanol, 10 mmol; catalyst, 0.5 g; cyclohexane, 30 mL; N_2, 0.7 MPa at room temperature; 2 h; 1000 rpm.

Table 6.2. NH$_3$-TPD study of fresh and spent catalysts

Entry	Catalyst	Total acidity (mmol•g^{-1}) Fresh catalyst	Total acidity (mmol•g^{-1}) spent catalyst
1	SiO$_2$-Al$_2$O$_3$	0.61	0.49
2	Clay K-10	0.36	0.34
3	Al-pillared clay	0.65	0.60
4	H-USY	0.28	0.23
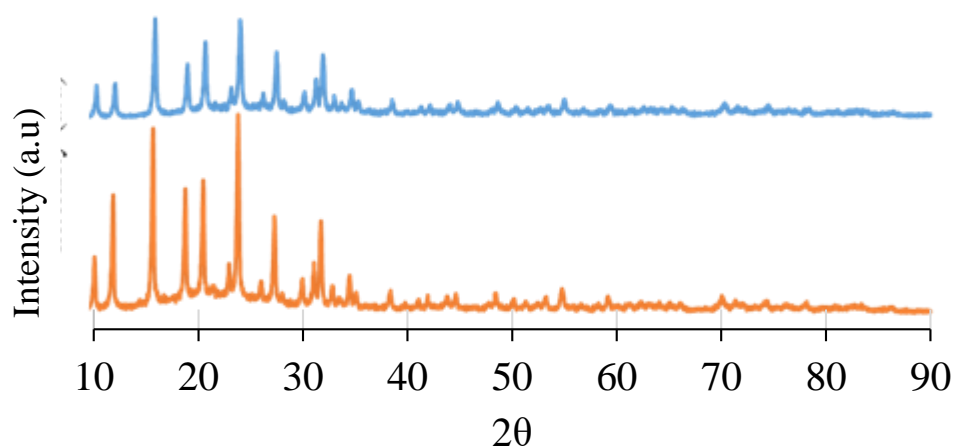
Figure 6.2. XRD pattern of (a) Fresh and (b) Spent H-USY catalyst
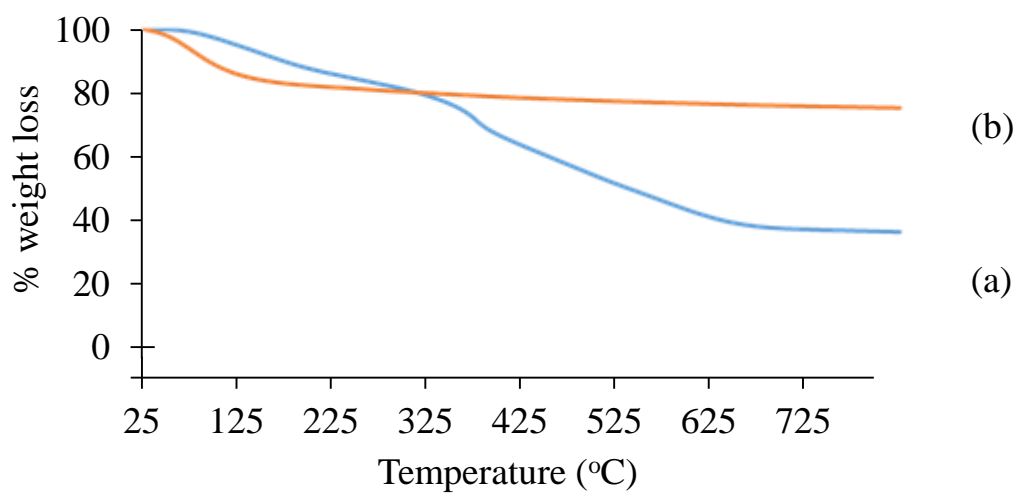
Figure 6.3. TGA patterns of (a) Spent and (b) Fresh H-USY catalyst
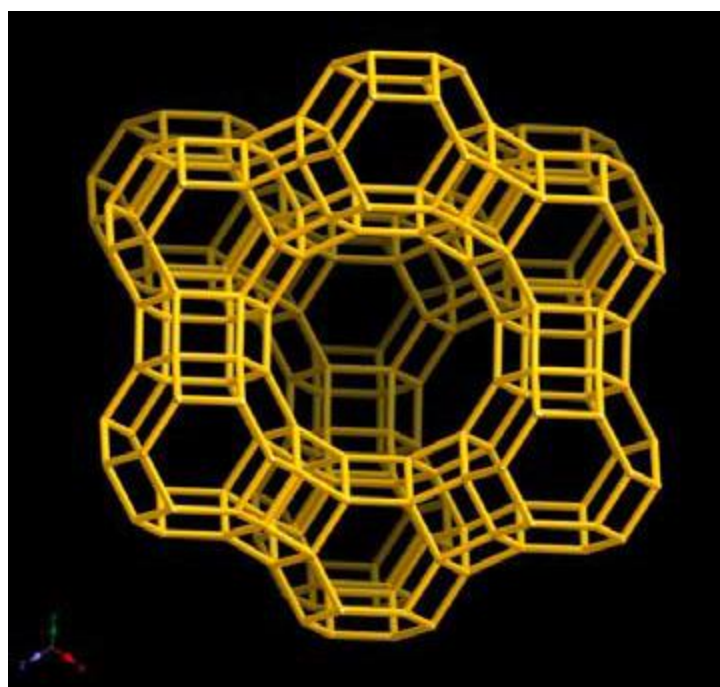
Figure 6.4. Crystal structure of H-USY Zeolite

6.3.2.2. Effect of temperature on the alkylation of guaiacol using hexanol as alkylating agent

Since over SiO_2-Al_2O_3 as a catalyst, 30.9% of DAP formation was observed at 250 °C with lower conversion (85%), reaction was performed at higher temperature to enhance the conversion and yield of DAP. As summarized in Table 6.3, when reaction was carried out at 260 °C, catalyst gave 95% conversion with contribution to DAP formation was 29.2%. Besides DAP, formation of MAP with higher concentration (70.7%) compared to 250 °C (58.3%) was also seen. With an increase in reaction temperature from 250 °C to 260 °C, conversion of guaiacol has increased and that of intermediate product, DHE (0.1%) was decreased to yield higher MAP but, it did not translate in to enhancement in the formation of DAP. Subsequently, reactions were performed at lower temperatures of 220 °C and 240 °C and higher DAP formation of 36.1% was seen at 220 °C under lower conversion of 55%. These results illustrate that for the dialkylation lower temperatures are preferred. However, when temperature was further decreased to 200 °C, guaiacol remained unconverted. From the GC profile Figure 6.5, it is evident that product formation intensifies with increase in temperature until 250 °C at which conversion was 85%. However, at 260 °C, even if 95% conversion was observed, concentration of product peaks was decreased compared to 250 °C, since guaiacol and alkylated products start forming undesired degradation products at higher temperatures, which could not be analysed by GC. In view of these results, 250 °C is considered as an optimum temperature to achieve respectable activity.

Table 6.3. Effect of temperature on the alkylation of guaiacol.

Entry	T (°C)	t (h)	N_2 pressure (MPa)	Conv. of guaiacol (%)	Product distribution (%)			MAP/DAP[c]
					DHE[d]	MAP[a]	DAP[b]	
1	220	2	0.7	55	5.0	58.9	36.1	1.63
2	240	2	0.7	82	11.6	58.5	29.9	1.95

3	250	2	0.7	85	10.8	58.3	30.9	1.88
4	260	2	0.7	95	0.1	70.7	29.2	2.42

Reaction condition: Guaiacol, 4 mmol; hexanol, 10 mmol; SiO_2-Al_2O_3, 0.5 g; cyclohexane, 30 mL; 1000 rpm. (a) MAP (Monoalkylated product), (b) DAP (Dialkylated product), (c) MAP/DAP (Monoalkylated/Dialkylated), (d) DHE (Di hexyl ether)
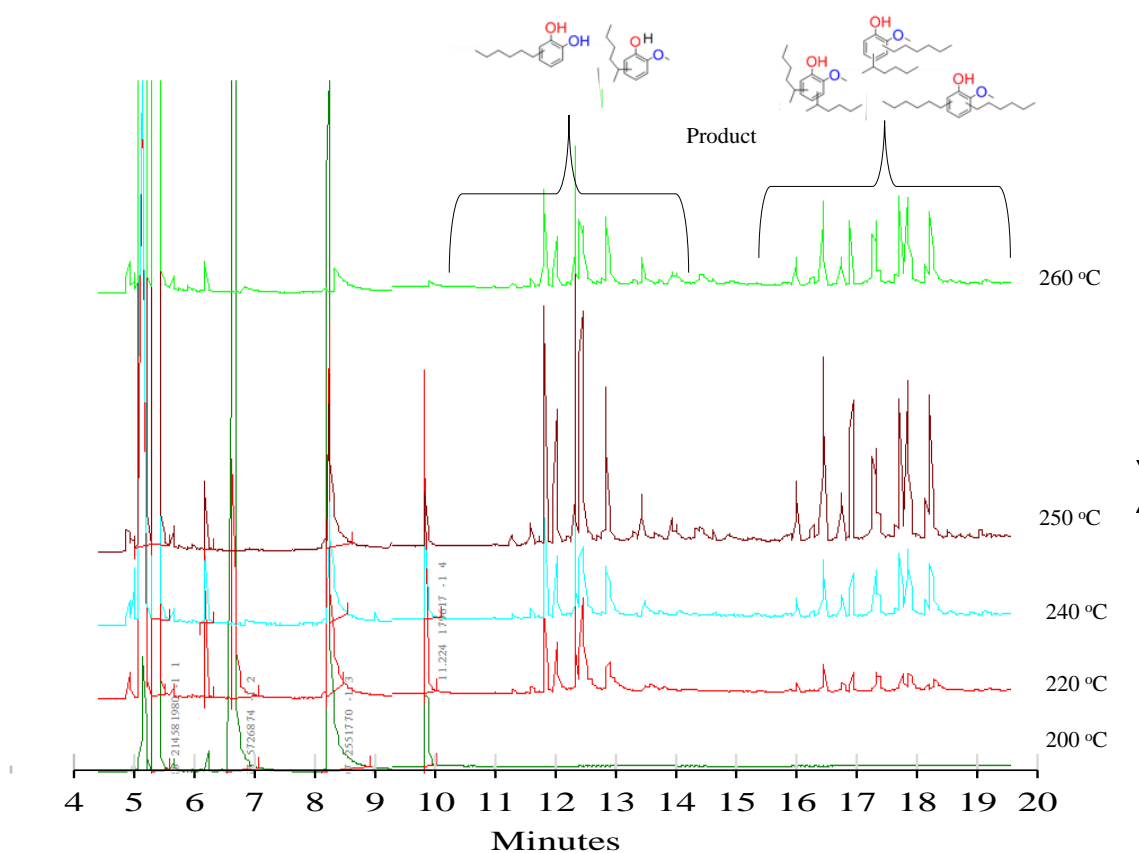
Figure 6.5. Effect of temperature on the product distribution.

Reaction conditions: Guaiacol, 4 mmol; hexanol, 10 mmol; SiO_2-Al_2O_3, 0.5 g; cyclohexane, 30 mL; N_2, 0.7 MPa at room temperature; 2 h; 1000 rpm.

6.3.2.3. Effect of pressure on the alkylation of guaiacol using hexanol as alkylating agent

Until now maximum yield of DAP (30.9%) is observed at 250 °C under 0.7 MPa nitrogen pressure charged at room temperature. Under this condition, total pressure of 3 MPa was seen. To improve the yield further, effect of partial pressure of hexanol and dihexyl ether was studied by varying the nitrogen pressure. Guaiacol has a boiling point of 204-206 °C, hexanol has a boiling point of 157 °C and DHE boils at 222 °C. In view of this, under the reaction condition of 250 °C, all the three compounds are partially in the vapor phase and that presence of nitrogen will affect the equilibrium of these compounds present in vapour phase and liquid phase. As seen from the Table 6.4 in the absence of external nitrogen charged in the reactor, same level of conversion of guaiacol (85%) as with 0.7 MPa nitrogen charged reaction was observed. However, higher DAP (39.1%) and lower DHE (4.4%) was seen as compared to reaction with 0.7 MPa nitrogen pressure. In this reaction MAP/DAP ratio of 1.44 was observed which was lower than reaction carried out in presence of nitrogen. These results indicate that if this reaction is carried out in the vapour phase, higher DAP formation can be achieved. Nevertheless, detailed study on this aspect is required to establish this fact. When nitrogen pressure was increased to 1.5 MPa, lower conversion (77%) was seen.

Table 6.4. Effect of pressure on the alkylation of guaiacol.

Entry	T (°C)	t (h)	N$_2$ pressure (MPa)	Conv. of guaiacol (%)	Product distribution (%)			MAP/DAP[c]
					DHE[d]	MAP[a]	DAP[b]	
1	250	2	0	85	4.4	56.5	39.1	1.44
2	250	2	0.7	85	10.8	58.3	30.9	1.88
3	250	2	1.5	77	14.9	53.2	31.9	1.66

Reaction condition: Guaiacol, 4 mmol; hexanol, 10 mmol; SiO$_2$-Al$_2$O$_3$, 0.5 g; cyclohexane, 30 mL;1000 rpm. (a) MAP (Monoalkylated product), (b) DAP (Dialkylated product), (c) MAP/DAP (Monoalkylated/Dialkylated), (d) DHE (Di hexyl ether)

6.3.2.4. Effect of time on the alkylation of guaiacol using hexanol as alkylating agent

To check the effect of reaction time on the alkylation of guaiacol, reactions were carried out for 1, 2 and 4 h. It was obvious to see that with an increase in time from 1 h to 2 h, conversion of guaiacol and intermediate, DHE to alkylated products has happened. However, results show that an increase in time from 2 h to 4 h does not change the distribution of products (Table 6.5). This indicates that the reaction might be attaining equilibrium.

Table 6.5. Effect of time on the alkylation of guaiacol.

Entry	T (°C)	t (h)	N₂ pressure (MPa)	Conv. of guaiacol (%)	Product distribution (%)			MAP/DAP[c]
					DHE[d]	MAP[a]	DAP[b]	
1	250	1	0.7	68	35.8	38.5	25.7	1.49
2	250	2	0.7	85	10.8	58.3	30.9	1.88
3	250	4	0.7	95	12.4	58.9	28.7	2.05

Reaction condition: Guaiacol, 4 mmol; hexanol, 10 mmol; SiO_2-Al_2O_3, 0.5 g; cyclohexane, 30 mL; 1000 rpm. (a) MAP (Monoalkylated product), (b) DAP (Dialkylated product), (c) MAP/DAP (Monoalkylated/Dialkylated), (d) DHE (Di hexyl ether)

6.3.2.5. Effect of concentration of catalyst and adsorption study of substrates

In order to optimize the catalyst loading reactions were carried out with different catalyst loading (0.25, 0.375, 0.5, 0.750 g) at 250 °C under 0.7 MPa N_2 atmosphere (Figure 6.6.). It is observed that in the absence of catalyst, reaction does not proceed (Table 6.1). When reaction was carried out with 0.25 g of catalyst, conversion of guaiacol reached up to 68% with the appearance of mono and dialkylated product (Figure 6.7). Subsequently, concentration of the catalyst was increased up to 0.75 g and marginal increase in the conversion was observed after each increase in the concentration. At 0.75 g catalyst concentration maximum conversion (93%) was seen but in this reaction, lower concentration of the product was seen (Figure 6.7.) with decrease of DHE formation. The decrease in the product(s) could be due to possible adsorption of product(s) on the catalyst surface or degradation of product(s) to undetected product(s) as catalyst concentration has drastically increased. Hence adsorption study of

guaiacol and hexanol was performed for 2 and 6 h. As shown in Figures 6.8. and 6.9. The adsorption of guaiacol enhances with an increase in time and catalyst concentration and found to be 33% in 6 h over 0.75 g catalyst. The quantification of the adsorption of guaiacol is given in Table 6.6 and as seen, with increase in catalyst concentration in the reaction system, higher adsorption of guaiacol is seen. Similarly, hexanol adsorption study showed 14% adsorption within 6 h over 0.75 g catalyst concentration (Figures 6.10 and 6.11). The quantification of the adsorption of hexanol is given in Table 6.7, From the quantification data it can be suggested that guaiacol has a preference for adsorption on the catalyst surface as except on 0.75 g catalyst, higher amount of guaiacol is adsorbed on 0.25 and 0.50 g catalysts compared to hexanol. Further to prove that guaiacol and hexanol were adsorbed on the catalyst surface TGA analysis of the catalyst samples after 6 h of adsorption study was performed. From the TGA profiles (Figures 6.12 and 6.13), it is proven that with an increase in catalyst concentration, adsorption of reactant increases. Thus, these studies prove that with increase in catalyst weight during the reaction, higher adsorption of the substrate and products is possible which may lead to degradation of products or substrates. This is turn shows decreased activity of the catalyst with higher concentration.
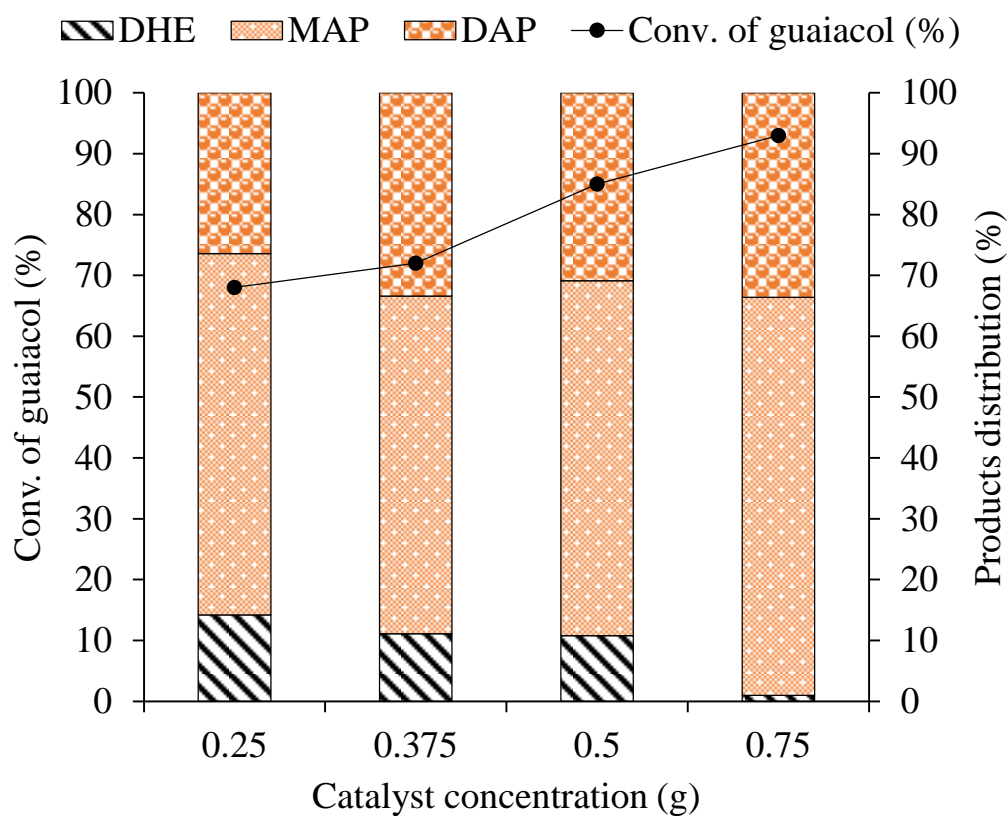
Figure 6.6. Effect of catalyst concentration on the alkylation of guaiacol.
Reaction condition: Guaiacol, 4 mmol; hexanol, 10 mmol; SiO_2-Al_2O_3; cyclohexane, 30 mL; 250 °C; N_2, 0.7 MPa at room temperature; 2 h; 1000 rpm.; MAP (Monoalkylated product), DAP (Dialkylated product), DHE (Di hexyl ether).
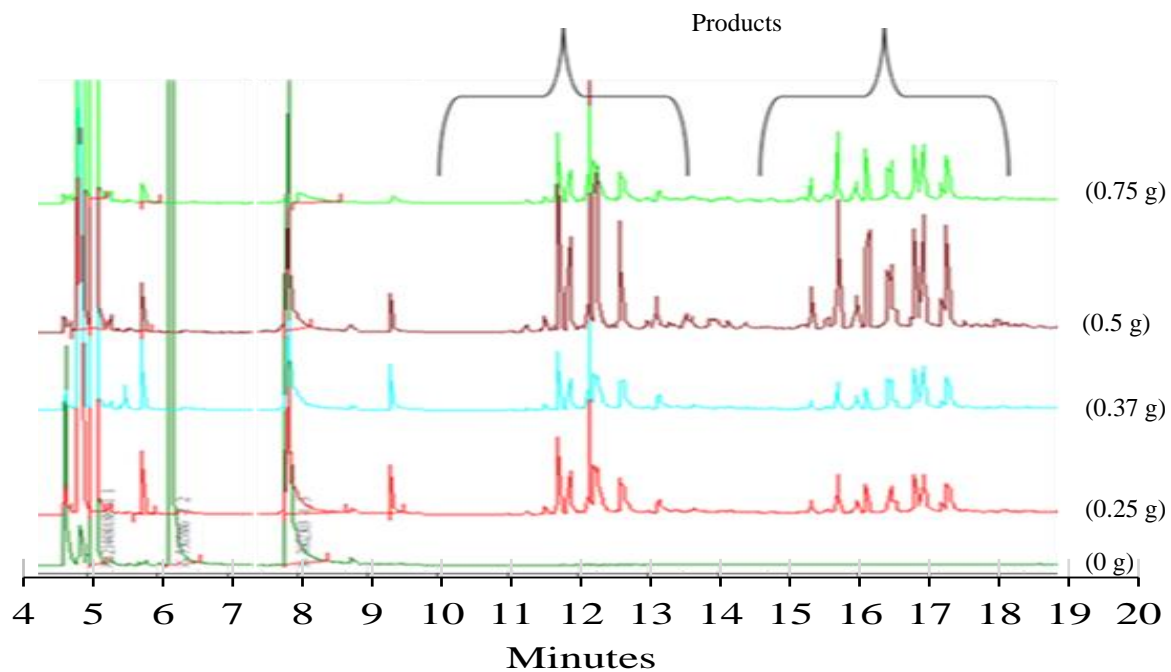
Figure 6.7. Effect of catalyst concentration on the alkylation of guaiacol.

Reaction conditions: Guaiacol, 4 mmol; Hexanol, 10 mmol; SiO_2-Al_2O_3; cyclohexane, 30 mL; 250 °C; N_2, 0.7 MPa at room temperature; 2 h; 1000 rpm.
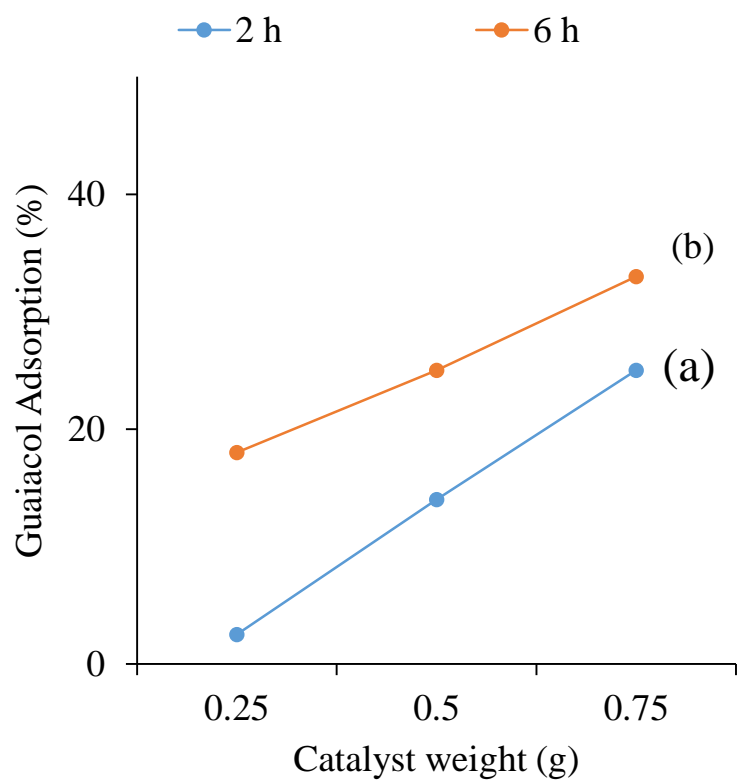
Figure 6.8. Guaiacol adsorption on the SiO_2-Al_2O_3 catalyst.

Reaction condition: Guaiacol, 4 mmol; SiO_2-Al_2O_3, cyclohexane, 30 mL. (a) 2 h; (b) 6 h
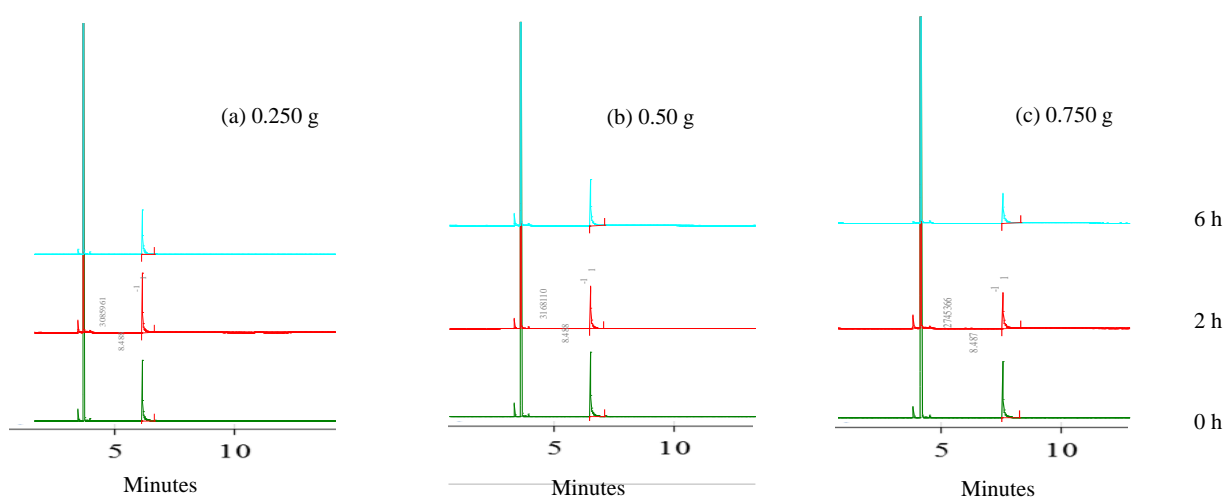
Figure 6.9. GC profile of guaiacol adsorption study done over SiO_2-Al_2O_3 catalyst

.

Reaction condition: Guaiacol, 4 mmol; SiO_2-Al_2O_3, cyclohexane, 30 mL. Samples after 6 h adsorption study; stirred @RT.
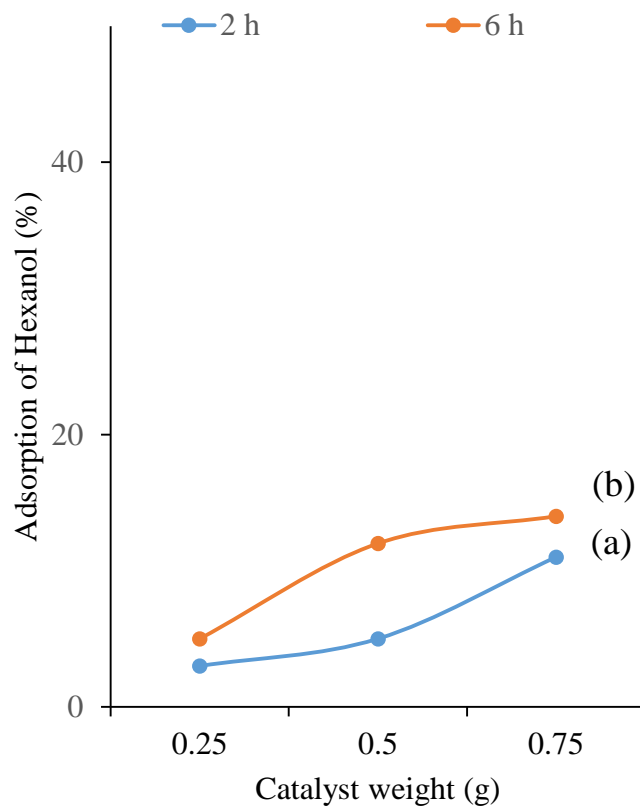
Figure 6.10. Hexanol adsorption on the SiO_2-Al_2O_3 catalyst.

Reaction condition: Hexanol, 10 mmol; SiO_2-Al_2O_3, cyclohexane, 30 mL. (a) 2 h; (b) 6 h; stirred @RT
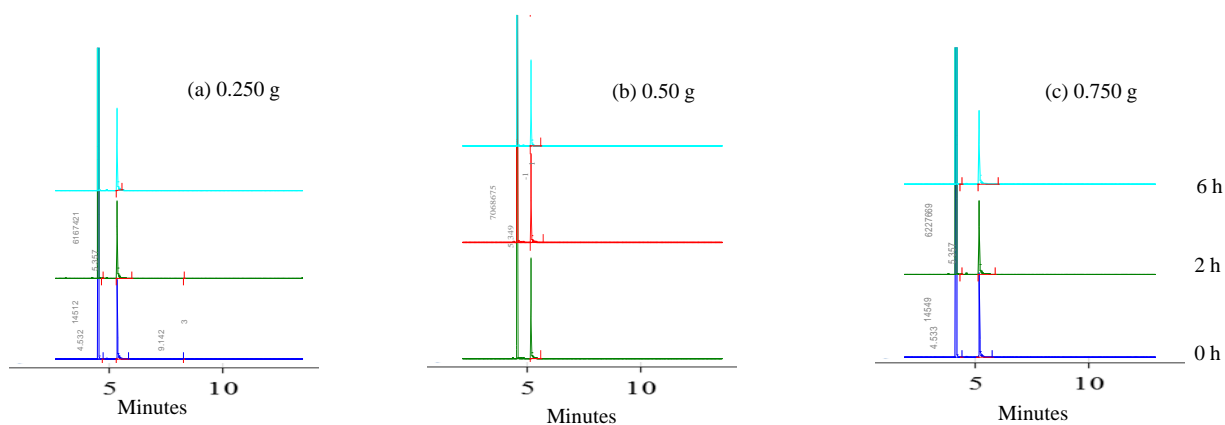
Figure 6.11. GC profile of hexanol adsorption study done over SiO$_2$-Al$_2$O$_3$ catalyst.
Reaction condition: Hexanol, 10 mmol; SiO$_2$-Al$_2$O$_3$, cyclohexane, 30 mL. Samples after 6 h adsorption study;@ stirred RT;
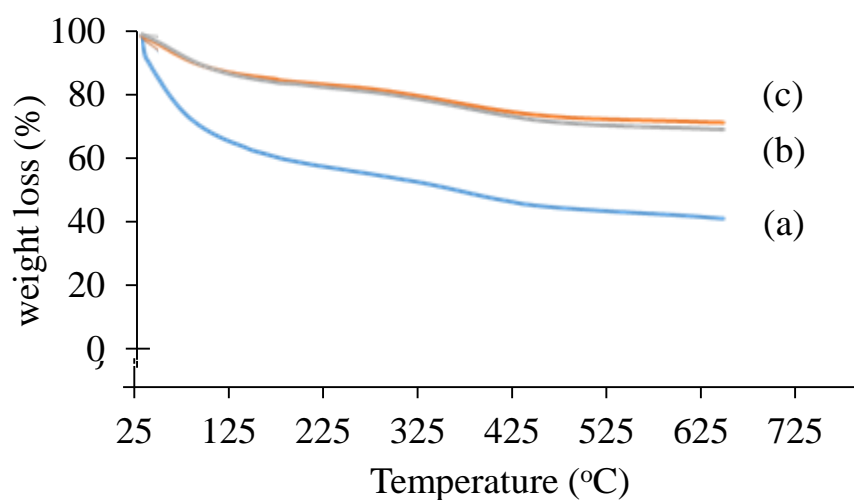
Figure 6.12. TGA profiles of catalysts after adsorption of guaiacol.
Reaction condition: Guaiacol, 4 mmol g; cyclohexane, 30 mL; SiO$_2$-Al$_2$O$_3$ (a) 0.750 g; (b) 0.5 g; (C) 0.25g. Samples after 6 h adsorption study.@ stirred RT;
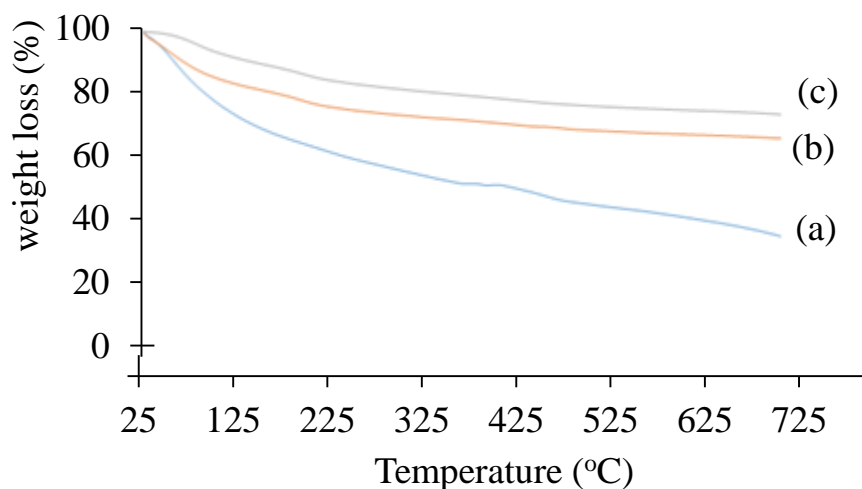
Figure 6.13. TGA profiles of catalysts after adsorption of hexanol.

Reaction condition: Hexanol, 10 mmol g; cyclohexane, 30 mL; SiO_2-Al_2O_3, (a) 0.750 g; (b) 0.5 g; (C) 0.25g. Samples after 6 h adsorption study.

Table 6.6. CHNS analysis of spent and fresh catalyst after adsorption of guaiacol.

Catalysts		SiO_2-Al_2O_3			
		Fresh	**0.250 g**	**0.50 g**	**0.750 g**
Elemental analysis of fresh catalyst (mg)	C	1.0	-	-	-
	H	0.2	-	-	-
Elemental analysis after adsorption of guaiacol on catalyst (mg)	C	-	93.0	148.0	240.0
	H	-	0.9	1.6	3.3

Table 6.7. CHNS analysis of fresh and spent catalysts after adsorption of hexanol.

Catalysts		SiO$_2$-Al$_2$O$_3$			
		Fresh	**0.250 g**	**0.50 g**	**0.750 g**
Elemental analysis of fresh catalyst (mg)	C	4.0	-	-	-
	H	0.9	-	-	-
Elemental analysis after adsorption of hexanol on catalyst (mg)	C	-	117.1	247.2	183.0
	H	-	4.6	9.0	6.0

6.3.2.6. Effect of different solvents

Typically reactions are carried out in cyclohexane as a solvent but to check the effect of different solvents on the reaction, reactions were also carried out in hexane and hexadecane solvents. Since hexane is lower boiling solvent (68 °C), compared to cyclohexane (81 °C), total pressure of 3.5 MPa at 250 °C was observed with hexane as compared to 3 MPa observed with cyclohexane as a solvent. In comparison to this, with hexadecane (B.P., 286.8 °C) as a solvent, 1.2 MPa pressure was observed at 250 °C. From the Figure 6.14., it is seen that the order of conversion of guaiacol is hexadecane < hexane < cyclohexane. Cyclohexane showed better performance with maximum conversion and highest DAP concentration (30.9%). The possible reasons for this difference in activity could be either change in overall pressure during the reaction or the difference in the solubility of guaiacol and hexanol in different solvents. As reported above, with increase in boiling point of the solvent, overall pressure in the reactor was decreased from 3.5 MPa to 3 MPa to 1.23 MPa. This may severely affect substrate-catalyst interaction. However, as per above reported pressure study (Table 6.4.), no much difference in the activity with change in pressure is seen. Hence the solubility of guaiacol and hexanol was checked in all the three solvents and it was observed that both guaiacol and hexanol showed

highest solubility in cyclohexane (Table 6.8.). In view of this, it is anticipated that solubility plays a major role in deciding the activity of the catalyst.
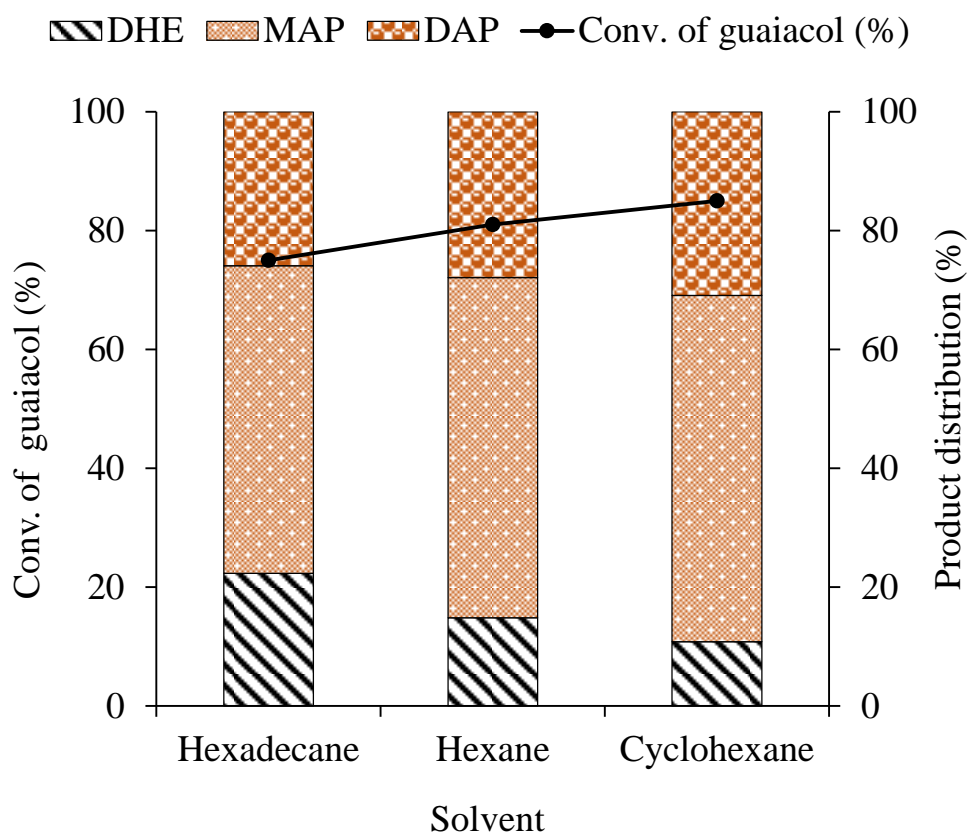
Figure 6.14. Effect of solvent on the alkylation of guaiacol

Reaction condition: Guaiacol, 4 mmol; hexanol, 10 mmol; SiO_2-Al_2O_3, 0.5 g; solvent, 30 mL; 250 ºC; N_2, 0.7 MPa at room temperature; 2 h; 1000 rpm. MAP (Monoalkylated product), DAP (Dialkylated product), DHE (Di hexyl ether).

Table 6.8. Solubility of hexanol and guaiacol in different solvents.

Solubility	Cyclohexane (%)	Hexane (%)	Hexadecane (%)
Guaiacol	100	95	80
Hexanol	100	98	88

6.3.2.7. Effect of guaiacol to hexanol molar ratio

Reactions were carried out with varying guaiacol/hexanol molar ratio to understand the role of alkylating agent on the catalytic activity and also to increase DAP formation, if possible. Lower conversion (74 %) of guaiacol was obtained when reaction was carried with 0.80 ratio. This could be due to lower concentration of alkylating agent. However, before reaction, it was thought that since guaiacol adsorbs preferentially over the catalyst (Figure 6.8), lower amount of hexanol may improve the overall activity as guaiacol may interact efficiently with the active sites. To improve the results, ratio was changed to 0.50 and 0.40 and under these ratios, conversion of guaiacol was increased to 80 % and 85 %, respectively. Further decrease in ratio to 0.34 though showed similar conversion (86%) but the yield of DAP was decreased in comparison with 0.40 ratio. A careful look of the data suggests that with a decrease in ratio to 0.34, higher amount of DHE was seen. This was obvious because, concentration of hexanol has increased. Moreover, it is shown in the adsorption (Figure 6.8) study that guaiacol adsorbs preferably on the catalyst surface. It is considered that excess of hexanol may alter the adsorption pattern of substrate on catalyst and thus may poison the catalyst site which eventually would restrict the interaction of guaiacol with the catalyst to yield further alkylated products.

6.3.2.8. Substrate and alcohol study

Since SiO_2-Al_2O_3 catalyst showed good activity for the alkylation of guaiacol (Figure 6.5), alkylation of other aromatic monomers such as, veratrole (B.P 207 ^{o}C), catechol (B.P 240 ^{o}C), anisole (B.P 153 ^{o}C), phenol (B.P 181 ^{o}C), and toluene (B.P 110.6 ^{o}C), was carried out under similar conditions. From the substrate study, it was found that the substituted phenolic compounds enriched with the electron are more flexible for the alkylation. To prove this, activity was compared with nonphenolic compound i.e. toluene showed clear evident that if

heteroatom is not present, catalytic activity is very low. As seen from Figure 6.15., various MAP and DAP products were observed with following trend of conversion (Figure 6.16.).

Toluene (15%) < Anisole (67%) <Catechol (75%)< Guaiacol (85%) < Veratrole (91%) < Phenol (91%)

To check the effect of alkylating agents on the reaction, different alcohols were used and the formation of various products are shown in Figure 6.17, Reactions were carried out at 250 °C for 2 h with guaiacol as a substrate and by keeping guaiacol to alcohol molar ratio constant at 0.4. It was observed that except methanol which is having higher polarity (5.1) showed lower conversion of guaiacol and on the other alcohols showed higher conversions (Figure 6.17.). It is also seen that with branched alcohols, formation of MAP products is predominant due to bulky structure of alcohols.
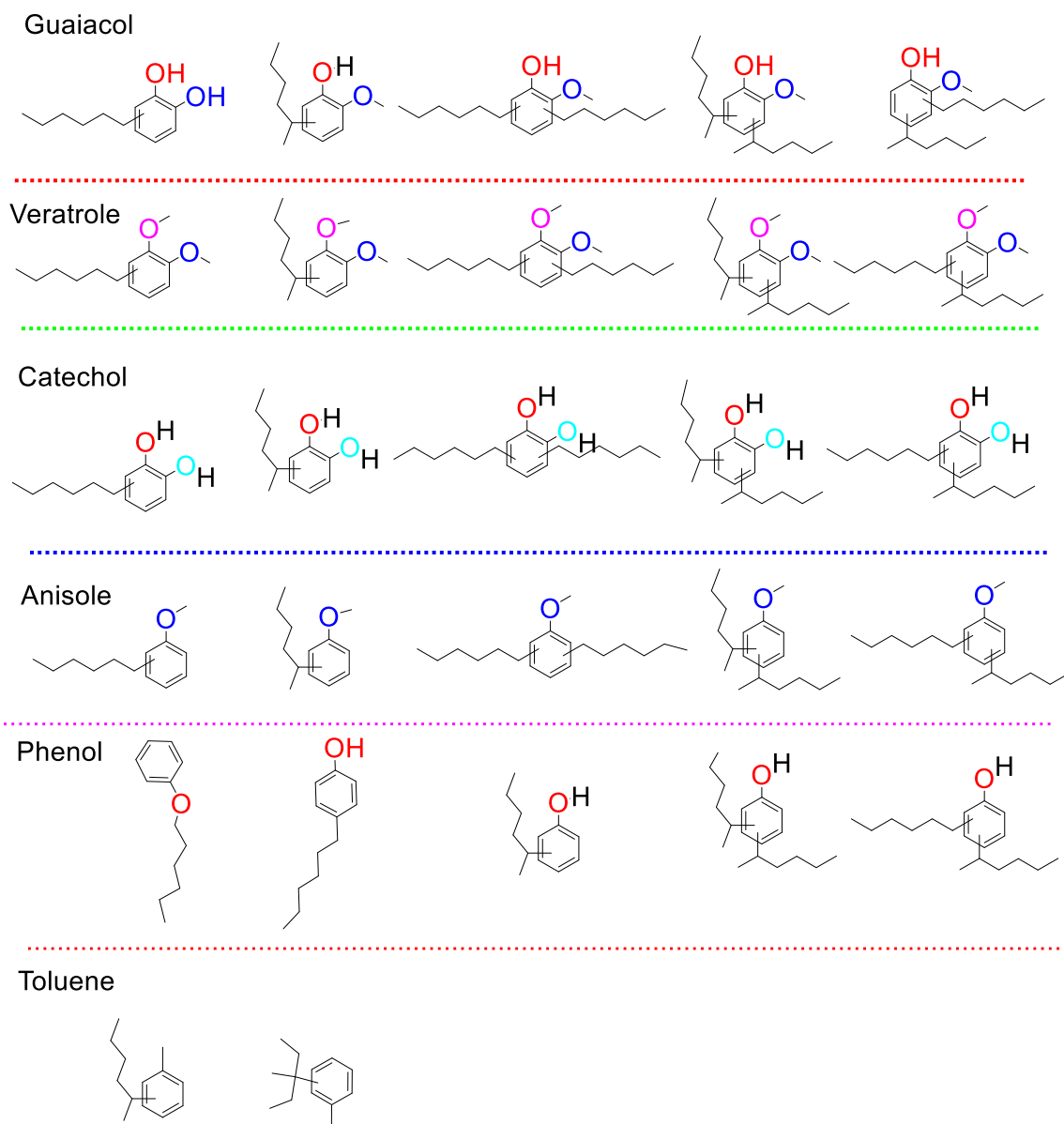
Figure 6.15. Products identified from GC-MS using various substrates.

Reaction conditions: Substrate, 4 mmol; hexanol, 10 mmol; SiO_2-Al_2O_3; 0.5g; cyclohexane, 30 mL; 250 ºC; N_2, 0.7 MPa at room temperature; 2 h; 1000 rpm.
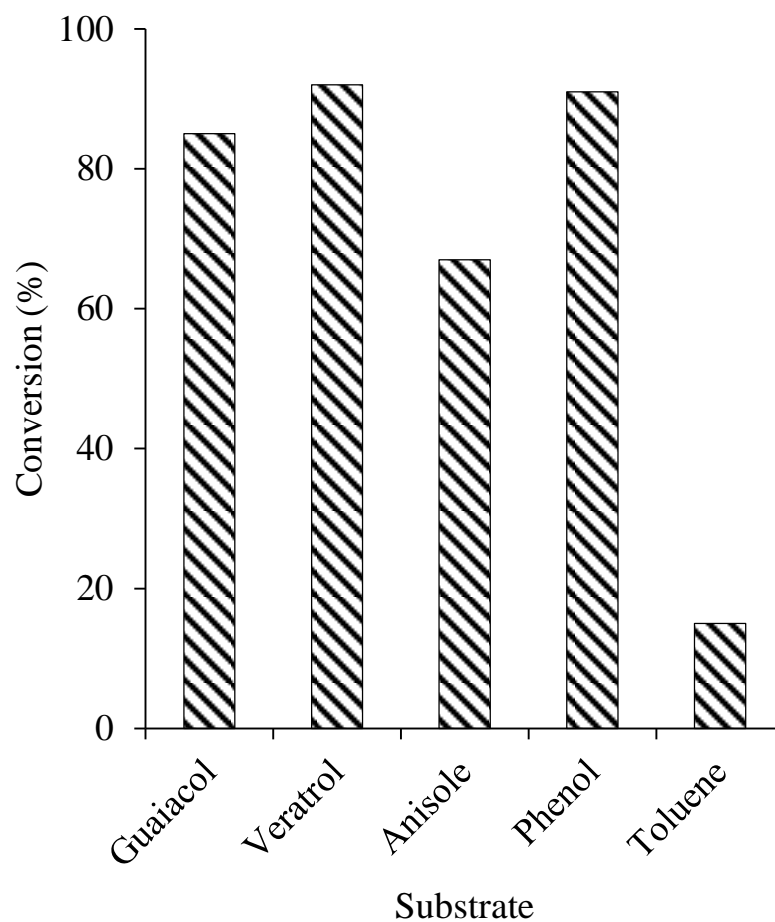
Figure 6.16. Conversion of substrates.

Reaction condition: Substrate, 4 mmol; alcohol, 10 mmol; SiO_2-Al_2O_3, 0.5 g; cyclohexane, 30 mL; 250 ℃; N_2, 0.7 MPa at room temperature; 2 h; 1000 rpm.
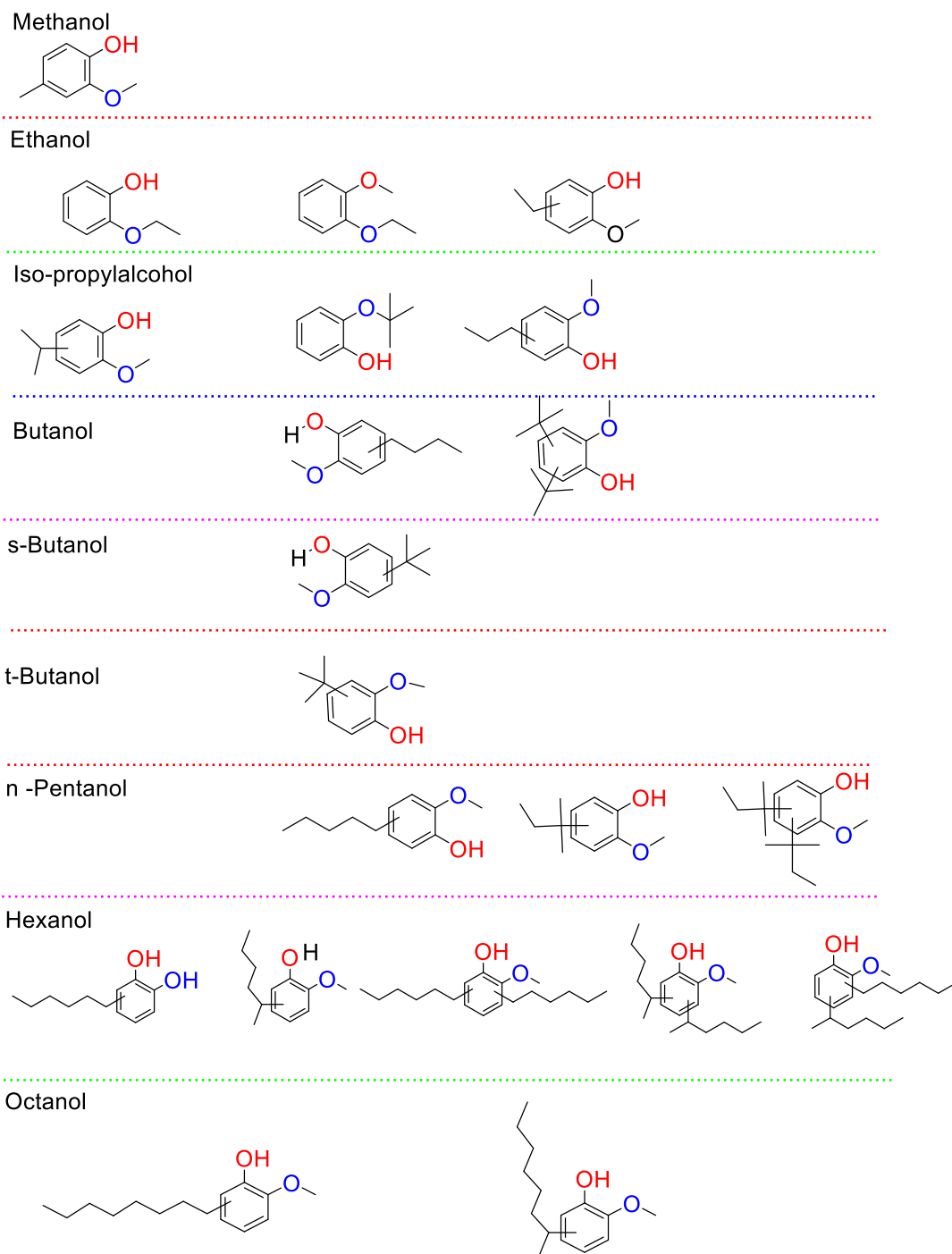
Figure 6.17. Products identified from GC-MS using various alkylating agents.

Reaction conditions: Guaiacol, 4 mmol; alcohol, 10 mmol; SiO_2-Al_2O_3, 0.5g; cyclohexane, 30 mL; 250 °C; N_2, 0.7 MPa at room temperature; 2 h; 1000 rpm.
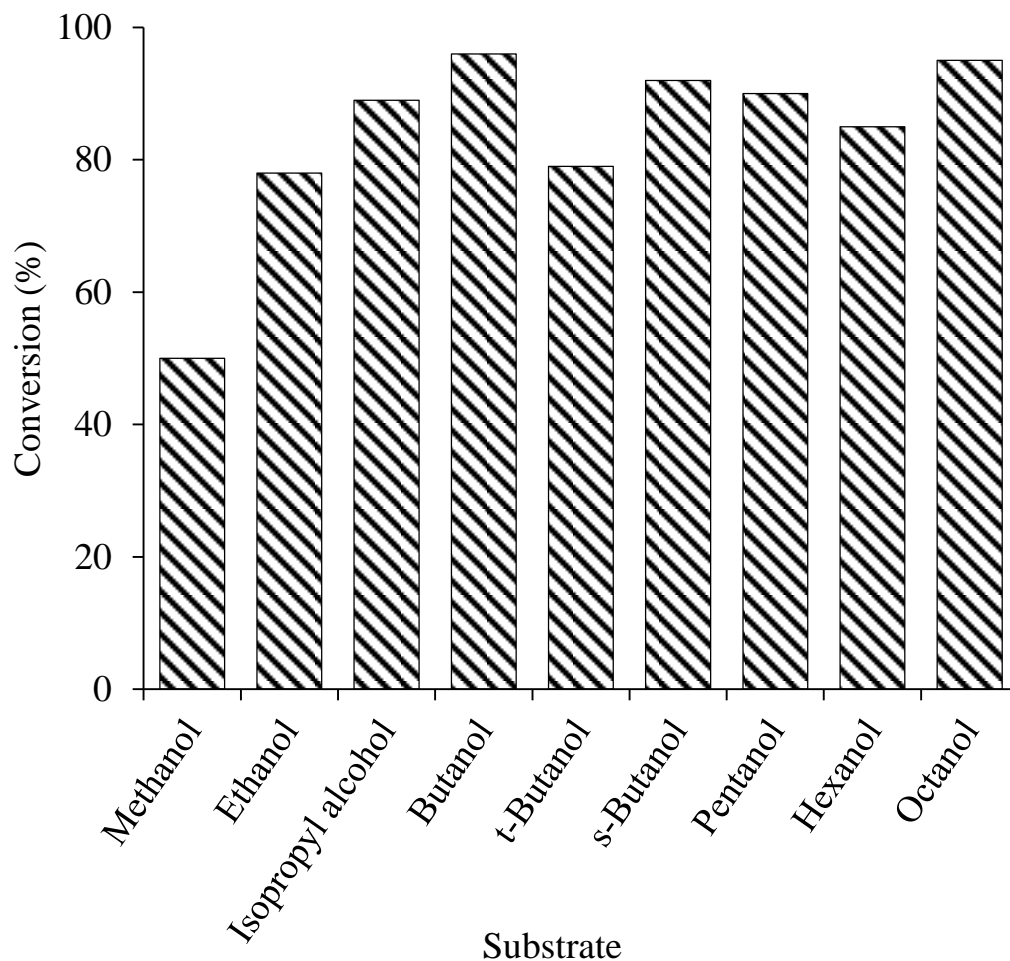
Figure 6.18. Conversion of guaiacol with different alkylating agents.

Reaction condition: Guaiacol, 4 mmol; alcohol, 10 mmol; SiO_2-Al_2O_3, 0.5 g; cyclohexane, 30 mL; 250 °C; N_2, 0.7 MPa at room temperature; 2 h; 1000 rpm.

6.3.2.9. Recycle study of catalyst

The reusability of SiO$_2$-Al$_2$O$_3$ catalyst was checked by carrying out multiple catalytic runs with spent catalyst. During the recycle study the recovery of spent catalyst was done by centrifugation. The recovered wet catalyst was used in the next catalytic run without any pre-treatment. Recycle study suggested marginal drop in the catalyst activity as guaiacol conversion was decreased from 85 % to 70 % and further to 60 % in consecutive runs (Table 6.9.). This was due to increase in substrate to catalyst ratio due to loss of catalyst during recovery of spent catalyst. A look at the table explains that after recycling of the catalyst formation of DAP is decreasing this may be due to the fact that few of the acid sites are buried under coke/carbon formed during the reaction. This might be another explanation for decrease in the activity in consecutive runs.

Table 6.9.. Recycle study of catalyst

Entry	Run No	Catalyst (g)	Conv. of guaiacol (%)	Product distribution (%)			MAP/DAP[c]
				DHE[d]	MAP[a]	DAP[b]	
1	1	0.50	85	10.8	58.3	30.9	1.88
2	2	0.44	70	8.1	64.0	27.9	2.29
3	3	0.36	64	7.3	68.5	24.2	2.83

Reaction condition : Guaiacol, 4 mmol; hexanol, 10 mmol; SiO$_2$-Al$_2$O$_3$; 0.5 g; cyclohexane, 30 mL; 250 °C; N,, 0.7 MPa at room temperature; 2 h; 1000 rpm. (a) MAP (Monoalkylated product), (b) DAP (Dialkylated product), (c) MAP/DAP (Monoalkylated/Dialkylated), (d) DHE (Di hexyl ether)

6.3.2.10. Characterization of spent catalyst

The N_2 sorption data (Table 6.10.) of spent SiO_2-Al_2O_3 catalyst showed slight decrease in the surface area of spent catalyst (268 $m^2 \cdot g^{-1}$). This is due to adsorption of coke or product on the catalyst surface as is proven from the adsorption study (Figure 6.8). A drastic decrease in the surface area of H-USY catalyst reveals that the catalyst is unstable under the reaction conditions. Based on the ICP-OES analysis of fresh and spent catalyst, it is suggested that SiO_2-Al_2O_3 catalyst is stable as almost same Si/Al ratio was observed in both the samples (Table 6.11). Since in case of H-USY also almost similar Si/Al ratio was seen in fresh and spent catalysts, it indicates that although the structure has collapsed (nitrogen sorption study) however, there is no leaching of Si or Al in the solution. The TPD profile (Figure 6.19) shows slight decrease in acidity of spent catalysts (Table 6.12). The CHNS elemental analysis of spent catalysts confirm the adsorption of carbon compounds on the catalytic surface (Table 6.13). This might be the reason for the decrease in the acidic sites in spent catalysts as the treatment given to the catalysts before TPD analysis was not sufficient to remove all the carbon present on the catalyst surface.

Table 6.10. Summary on nitrogen sorption data of fresh and spent catalysts.

Catalyst		BET surface area ($m^2 \cdot g^{-1}$)	Pore volume (V) ($cm^3 \cdot g^{-1}$)	Pore radius (nm)
SiO_2-Al_2O_3 (Si/Al=5.3)	Fresh	374	0.35	3.81
	Spent	268	0.27	1.86
Clay K-10	Fresh	192	0.21	1.89
	Spent	143	0.18	1.89
Al-pillared clay	Fresh	170	0.16	1.84
	Spent	64	0.092	1.90
H-USY (Si/Al=15)	Fresh	631	0.41	nd
	Spent	275	0.20	nd

Table 6.11. Summary on ICP-OES analysis of fresh and spent catalyst.

Catalyst	Total acidity (mmol•g^{-1}) Fresh catalyst	Total acidity (mmol•g^{-1}) Spent catalyst
SiO$_2$-Al$_2$O$_3$ (Si/Al=5.3)	0.61	0.49
Clay K-10	0.36	0.34
Al-pillared clay	0.65	0.60
H-USY (Si/Al=15)	0.28	0.23
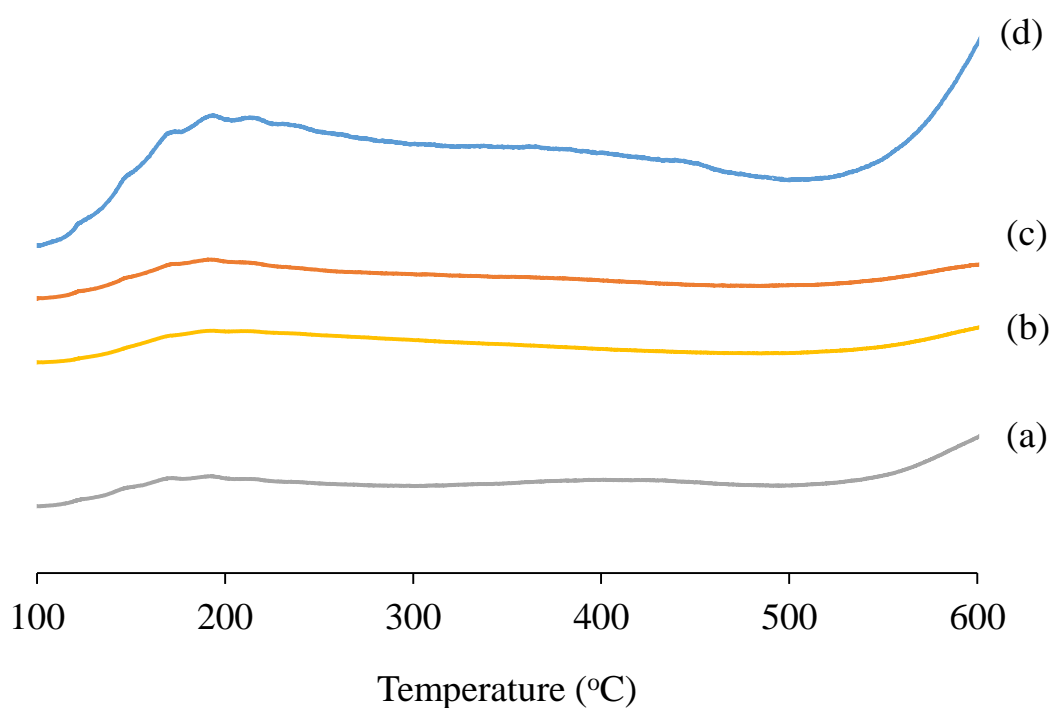
Figure 6.19. NH$_3$-TPD of spent catalysts (a) Cay K-10, (b) Al-pillared clay (c) H-USY (Si/Al= 15), (d) SiO$_2$-Al$_2$O$_3$ (Si/Al= 5.3).

Table 6.12. NH$_3$-TPD study of fresh and spent catalysts.

Catalyst	Theoretical Si/Al ratio	Experimental Si/Al ratio of fresh catalyst	Experimental Si/Al ratio spent catalyst
SiO$_2$-Al$_2$O$_3$ (Si/Al=5.3)	5.30	5.20	5.22
Clay K-10	Nd	Nd	Nd
Al-pillared clay	Nd	Nd	Nd
H-USY (Si/Al=15)	15.0	14.90	14.70

Table 6.13. CHNS elemental analysis of fresh and spent catalyst.

Catalysts		SiO$_2$-Al$_2$O$_3$	Clay (K-10)	Al pillared clay	H-HUSY
Elemental analysis of fresh catalyst (%)	C	0.3	Nd	Nd	Nd
	H	0.8	Nd	Nd	Nd
Elemental analysis of spent catalyst (%)	C	8.0	8.9	16.4	21.5
	H	1.2	1.2	2.2	2.0

6.3.2.11. Conclusions

In the current work, various solid acid catalysts were evaluated in the alkylation of lignin derived aromatic monomers. Amongst all the solid acid catalysts, SiO_2-Al_2O_3 catalyst showed best efficiency to yield DAP products thereby decreasing the O/C ratio. After careful study on the reaction parameters it was observed that lower MAP/DAP ratio of 1.88 could be achieved when reactions were carried out at 250 °C under N_2 atmosphere for 2 h. Use of various substrates and alkylating agents suggested that use of higher alcohols, which are preferable to reduce O/C ratio are efficient in showing better activity. Use of branched alkylating agents restrict yielding DAP products due to steric hindrance and thus higher amount of MAP products could be observed.

6.4. References:

1.   Chaudhary, R.; Dhepe, P. L., Solid base catalyzed depolymerization of lignin into low molecular weight products. *Green Chemistry* **2017,** *19* (3), 778-788.

2.   Chaudhary, R.; Dhepe, P. L., Depolymerization of lignin using solid base catalyst. *Energy & Fuels* **2019**.

3.   Deepa, A. K.; Dhepe, P. L., Lignin Depolymerization into Aromatic Monomers over Solid Acid Catalysts. *ACS Catalysis* **2014,** *5* (1), 365-379.

4.   Deepa, A. K.; Dhepe, P. L., Solid acid catalyzed depolymerization of lignin into value added aromatic monomers. *RSC Advances* **2014,** *4* (25).

5.   Singh, S. K.; Banerjee, S.; Vanka, K.; Dhepe, P. L., Understanding interactions between lignin and ionic liquids with experimental and theoretical studies during catalytic depolymerisation. *Catalysis Today* **2018,** *309*, 98-108.

6.   Singh, S. K.; Dhepe, P. L., Ionic liquids catalyzed lignin liquefaction: mechanistic studies using TPO-MS, FT-IR, RAMAN and 1D, 2D-HSQC/NOSEY NMR. *Green Chemistry* **2016,** *18* (14), 4098-4108.

7.   Singh, S. K. D., Paresh L. , Effect of structural properties of organosolv lignins isolated from different rice husks on their liquefaction using acidic ionic liquids. *J Clean Technologies Environmental Policy* **2018,** *20* (4), 739-750.

8. Mortensen, P. M. G., J. D. Jensen, P. A. Knudsen, K. G. Jensen, A. D., A review of catalytic upgrading of bio-oil to engine fuels. *Applied Catalysis A: General* **2011,** *407* (1), 1-19.

9. Yakovlev, V. A. K., S. A. Sherstyuk, O. V. Dundich, V. O. Ermakov, D. Yu Novopashina, V. M. Lebedev, M. Yu Bulavchenko, O. Parmon, V. N., Development of new catalytic systems for upgraded bio-fuels production from bio-crude-oil and biodiesel. *Catalysis Today* **2009,** *144* (3), 362-366.

10. Mortensen, P. M. G., Jan-Dierk Jensen, Peter A. Jensen, Anker D. , Screening of Catalysts for Hydrodeoxygenation of Phenol as a Model Compound for Bio-oil. *ACS Catalysis* **2013,** *3* (8), 1774-1785.

11. Mortensen, P. M. G., Diego de Carvalho, Hudson W. P. Damsgaard, Christian D. Grunwaldt, Jan-Dierk Jensen, Peter A. Wagner, Jakob B. Jensen, Anker D., Stability and resistance of nickel catalysts for hydrodeoxygenation: carbon deposition and effects of sulfur, potassium, and chlorine in the feed. *Catalysis Science & Technology* **2014,** *4* (10), 3672-3686.

12. Ambursa, M. M. S., Putla Voon, Lee Hwei Hamid, Sharifah Bee Abd Bhargava, Suresh K., Bimetallic Cu-Ni catalysts supported on MCM-41 and Ti-MCM-41 porous materials for hydrodeoxygenation of lignin model compound into transportation fuels. *Fuel Processing Technology* **2017,** *162*, 87-97.

13. Figueirêdo, M. B. J., Z. Deuss, P. J. Venderbosch, R. H. Heeres, H. J., Hydrotreatment of pyrolytic lignins to aromatics and phenolics using heterogeneous catalysts. *Fuel Processing Technology* **2019,** *189*, 28-38.

14. Remón, J. O., Elba Foguet, Carlos Pinilla, José Luis Suelves, Isabel, Towards a sustainable bio-fuels production from lignocellulosic bio-oils: Influence of operating conditions on the hydrodeoxygenation of guaiacol over a Mo2C/CNF catalyst. *Fuel Processing Technology* **2019,** *191*, 111-120.

15. Zhao, C. S., Wenji Lercher, Johannes A., Aqueous Phase Hydroalkylation and Hydrodeoxygenation of Phenol by Dual Functional Catalysts Comprised of Pd/C and H/La-BEA. *ACS Catalysis* **2012,** *2* (12), 2714-2723.

16. Velu, S. S., C. S., Selective C-alkylation of phenol with methanol over catalysts derived from copper-aluminium hydrotalcite-like compounds. *Applied Catalysis A: General* **1996,** *145* (1), 141-153.

17. Schmidt, R. J., Industrial catalytic processes phenol production. *Applied Catalysis A: General* **2005,** *280* (1), 89-103.

18. Cui, K. Y., Le Ma, Zewei Yan, Fei Wu, Kai Sang, Yushuai Chen, Hong Li, Yongdan Selective conversion of guaiacol to substituted alkylphenols in supercritical ethanol over MoO3. *Applied Catalysis B: Environmental* **2017,** *219*, 592-602.

19. Zhao, Z. S., Hui Wan, Chuan Hu, Mary Y. Liu, Yuanshuai Mei, Donghai Camaioni, Donald M. Hu, Jian Zhi Lercher, Johannes A., Mechanism of Phenol Alkylation in Zeolite H-BEA Using In Situ Solid-State NMR Spectroscopy. *Journal of the American Chemical Society* **2017,** *139* (27), 9178-9185.

20. Dewar, M. J. S. P., Acid-catalysed rearrangements of alkyl aryl ethers. Part II. Rearrangements in the presence of sulphuric–acetic acid mixtures. *Journal of the Chemical Society* **1959,** (0), 4086-4090.

21. Ma, Q. C., Deb Faglioni, Francesco Muller, Rick P. Goddard, William A. Harris, Thomas Campbell, Curt Tang, Yongchun Alkylation of Phenol: A Mechanistic View. *The Journal of Physical Chemistry A* **2006,** *110* (6), 2246-2252.

22. Bregolato, M. B., V. Busco, C. Ugliengo, P. Bordiga, S. Cavani, F. Ballarini, N. Maselli, L. Passeri, S. Rossetti, I. Forni, L., Methylation of phenol over high-silica beta zeolite: Effect of zeolite acidity and crystal size on catalyst behaviour. *Journal of Catalysis* **2007,** *245* (2), 285-300.

23. Lee, S. C. L., Si Woo Kim, Ki Seok Lee, Tae Jin Kim, Dong Hyun Kim, Jae Chang, O-alkylation of phenol derivatives over basic zeolites. *Catalysis Today* **1998,** *44* (1), 253-258.

24. Hu, C. Z., Yunfeng Xu, Lin Peng, Ge, Continuous syntheses of octyl phenol or nonane phenol on supported heteropoly acid catalysts. *Applied Catalysis A: General* **1999,** *177* (2), 237-244.

25. Sato, S. T., Ryoji Sodesawa, Toshiaki Matsumoto, Kotaro Kamimura, Yoichiro, Ortho-Selective Alkylation of Phenol with 1-Propanol Catalyzed by CeO2–MgO. *Journal of Catalysis* **1999,** *184* (1), 180-188.

26. Choi, W. C. K., Jong Seob Lee, Tae Hong Woo, Seong Ihl, Balancing acidity and basicity for highly selective and stable modified MgO catalysts in the alkylation of phenol with methanol. *Catalysis Today* **2000,** *63* (2), 229-236.

27.   DeCastro, C. S., E. Valkenberg, M. H. Hölderich, W. F. , Immobilised Ionic Liquids as Lewis Acid Catalysts for the Alkylation of Aromatic Compounds with Dodecene. *Journal of Catalysis* **2000,** *196* (1), 86-94.

28.   Hajipour, A. R. K., Hirbod, Hexagonal zirconium phosphate nanoparticles as an efficient and recyclable catalyst for selective solvent-free alkylation of phenol with cyclohexanol. *Applied Catalysis A: General* **2014,** *482*, 99-107.

29.   Anand, R., Gore, K. & Rao, B.   Alkylation of Phenol with Cyclohexanol and Cyclohexene Using HY and Modified HY Zeolites. *Catalysis Letters* **2002,** *81*, 33.

30.   Resasco, M. Á. G. B. D. E., Reaction pathways in the liquid phase alkylation of biomass-derived phenolic compounds. *AIChE J.* **2015,** *61,* 598.

Chapter 7

Summary and conclusion

Lignocellulosic biomass has been identified as an important source for the synthesis of carbon-based valuable chemical. Lignin is considered as an important constituent of ligno cellulosic biomass. Large quantity of lignin is produced in Bio-ethanol, paper and pulp industry. Lignin can be used in various ways for the production of valuable chemicals. Considering these points, Homogenous base-catalyzed depolymerization of lignin was successfully performed. Product distribution of homogeneous base-catalyzed depolymerization is not very clear in the reported literature. So the current study is focused on the identification of mechanistic path of the base-catalyzed depolymerization and distribution of the product. Although the depolymerized products are important, due to the formation of the mixture of aromatic monomers, it is very difficult to separate from each other. This Thesis is also focused on the value-addition of depolymerized products. The Ph.D. thesis is distributed in seven Chapters and significant results and conclusions from each Chapter are summarized in this chapter.

Chapter 1.

Chapter 1, discusses the over all significance of lignocellulosic biomass and its constituents like cellulose, hemicellulose, and lignin. Various processes have been developed for the isolation of lignin but commercially lignin is produced via (Kraft, Soda, Sulfite, Organosolv method). Several processes are also present for the conversion of lignin into value-added chemicals (Pyrolysis, hydrolysis, gasification, etc.). Lignin chemistry have some drawbacks like use of high temperature, pressure, precious metal. These conditions are also responsible for the formation of byproducts such as char, tar, and gaseous products. Homogeneous base-catalyzed depolymerization is well known, but the distribution of products and mechanistic insight into the depolymerization is still challenging.

In the current work, depolymerization of lignin into low molecular weight compound was completed using homogeneous base catalyst. Further, defunctionalization of lignin-derived monomers was achieved using supported metal catalyst. Another strategy (Alkylation) was used for the up-gradation of lignin-derived low molecular weight compounds.

Base/H_2O/250ºC/N_2

Lignin   Low molecular weight aromatic compounds
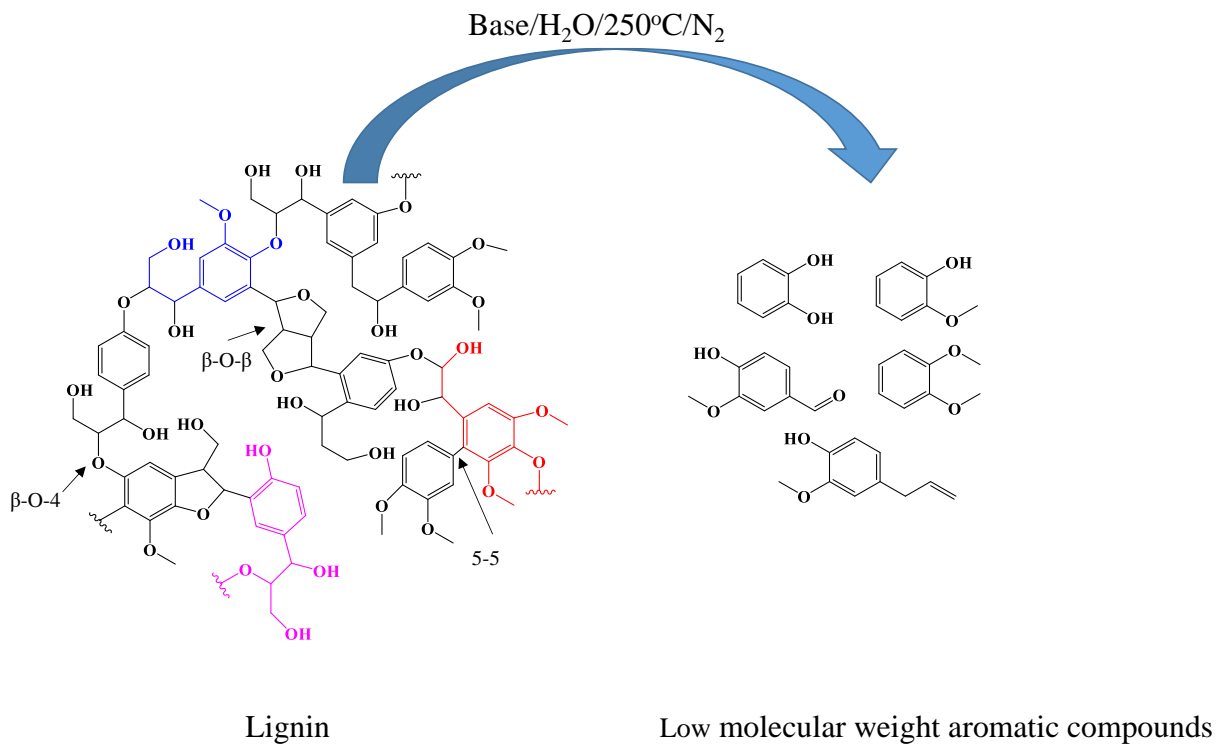
Figure 7.1. Base catalyzed lignin depolymerization

Chapter 2. This chapter divided into two subpart

Chapter 2A.

This chapter deals with characterization details of the various types of commercials lignin (Lignin, Alkaline; Lignin, Alkali, Lignin, Dealkaline, Na-lignosulfonate lignin, Industrial N-lignin, Industrial K-lignin) used for the Ph.D. work. All the procured lignin samples were characterized using the various technique.

‡ CHNS analysis of all lignin samples were performed and suggested that lignin is composed of 32-66% C and 4-8% H, along with sulfur impurity 0.7-3.7%. Based on the results general

MMF formula of lignin was calculated. HHV and DBV were also calculated for all lignin samples. Contamination of S in lignin also suggesting the isolation process used for lignin, i.e. Kraft process, where NaOH and Na_2S are used for the isolation of lignin. ICP-OES and SEM-EDAX analysis confirmed the presence of Na and S content in the lignin sample, also confirmed the isolation procedure used ie. Kraft process.

- ATR and ^{13}C NMR analysis of lignin samples confirm the various types of functional groups present in the lignin sample such as hydroxyl, methoxy, carbonyl, etc.
- TGA-DTA analysis of the lignin sample suggests thermal degradation of it and It showed residual content between 10-57% under N_2 medium.
- XRD analysis of the lignin sample was carried out and suggests that mostly lignin is amorphous in nature.
- The solubility of lignin was checked in the various solvent and based on the results, Alkaline water was selected for the catalytic depolymerization.

Chapter 2B.

In Chapter 2B, details on the synthesis and characterization of solid acid and supported metal catalysts are discussed. Solid acid was used for the functionalization of lignin-derived low molecular weight compound and supported metal catalyst used for the defunctionalization of lignin-derived low molecular weight compound.

- XRD analysis was performed for the confirmation of the phase of support and metal used. For the synthesis of supported metal catalysts, γ-Al_2O_3 (Acidic, Basic, Neutral) and SiO_2-Al_2O_3 and SiO_2.
- ICP-OES analysis of supported metal catalysts was carried out to compare the loading of metal.
- NH_3 and CO_2-TPD analysis of supported metal catalyst and the solid acid catalyst was carried out to calculate corresponding acidity and basicity.

- BET and CO-chemisorption analysis were carried out to calculate the corresponding surface area, crystallite size, and metal dispersion. The activity of the catalyst was compared with obtained results.

- XPS- analysis of supported metal catalyst was conducted to confirm the oxidation state of metal and activity compared with obtained results.

Chapter 3.

Chapter 3, deals catalytic depolymerization of lignin using various homogeneous bases. The study was focused on the distribution of depolymerized products.

Various homogenous bases were employed for the depolymerization of lignin into low molecular weight compounds. Under the optimum reaction condition for the depolymerization of lignin (Lignin/NaOH, 3.6 (wt./wt.); Alkaline water, (50 mL); 250 ºC, 1000 rpm, 1h) showed upto 31% DEE soluble products.

Among all used catalytic systems, NaOH was found more capable for the depolymerization of lignin into low molecular weight compound.
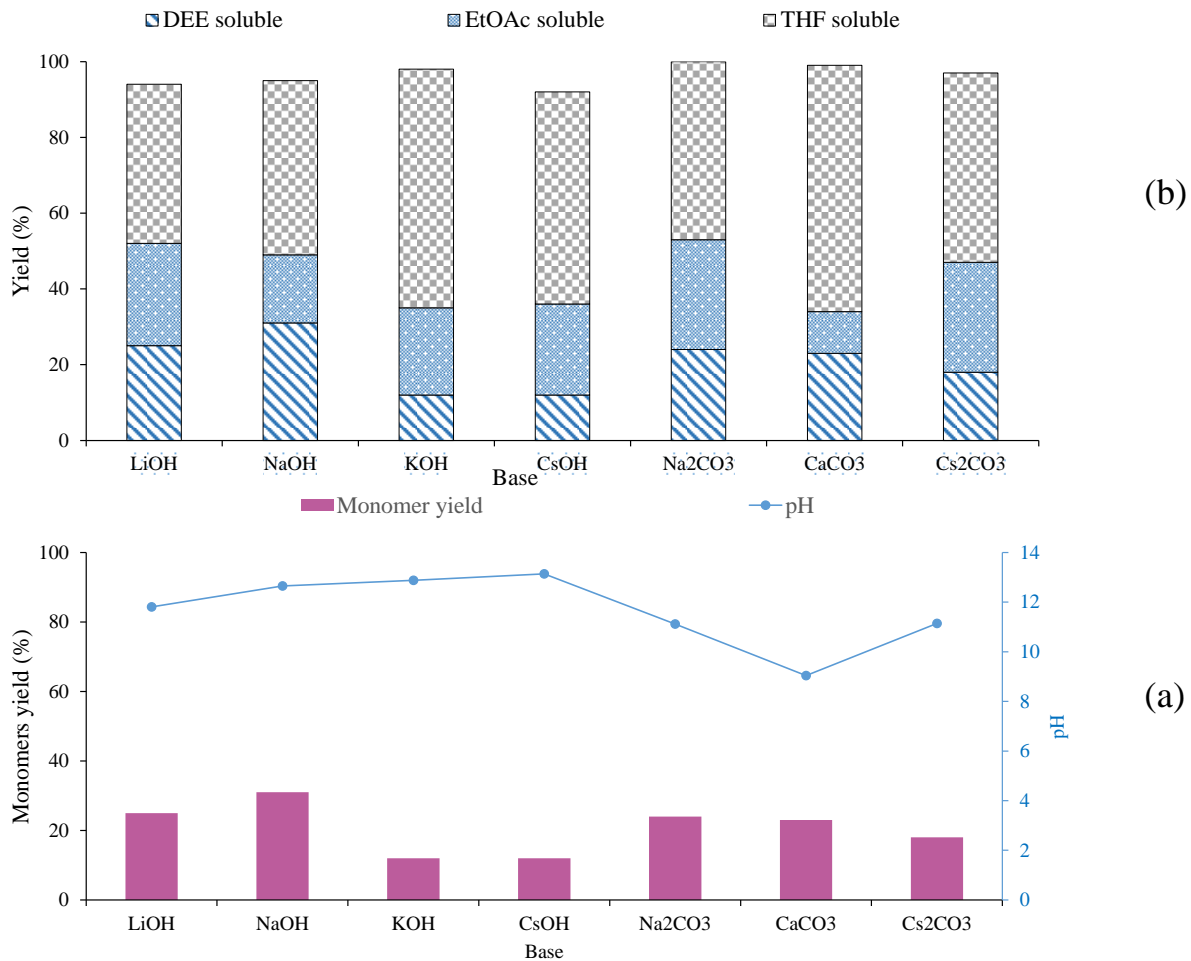
Figure 7.2. Depolymerization of lignin using various Bases

Reaction condition: Lignin, Alkaline 0.5 g; Base, 3.4 mmol; H_2O, 50 mL; 250 °C; 1 h; N_2, 2 MPa @ RT; 1000 rpm. DEE:diethyl ether, EtOAc:ethyl acetate, THF:tetrahydrofuran; (a) DEE soluble products yield; (b) DEE, EtOAc and THF soluble products yield.

The controlled experiment was designed for the solubility of lignin and depolymerized products and it was seen that lignin is soluble in neutralized reaction mixture but the depolymerized product is not soluble. Further investigation and understanding of the results suggest that lignin

depolymerizes into low molecular weight compounds but the decrease in solubilty due to repolymerization happened during depolymerization reaction.

To prove this aspect, another controlled study was done with model compound of lignin and found that depolymerized products having an alkyl chain are not soluble in neutralized reaction mixture. Both the experiment suggest that after depolymerization decrease in solubility of depolymerized products is due to repolymerization.

Identification and quantification of depolymerized products was done using various techniques like GC, GC-MS, LC, LC-MS, MALDI-TOF, ATR.

Chapter 4. This chapter is divided into sub-chapters

Chapter 4A.

This Chapter is focused on the use of a supported metal catalyst on the defunctionalization of lignin-derived low molecular weight compounds. To complete this objective, various Ru based supported metal catalysts were synthesized using the wet impregnation method and employed for catalytic defunctionalization lignin-derived monomers. Veretrol, Anisole, Phenol, Eugenol and Guaiacol substrates were used for the defunctionalization using a supported metal catalyst with very low loading of Ru metal (0.5%). Detailed study was conducted using Guaiacol substrate due to its similarities with the lignin substrate.

Defunctionaliztion of lignin-derived low molecular weight compound was achieved at 225 $^{\circ}$C, with 1MPa H_2@RT in cyclohexane solvent in 4h. At optimum condition, 100% conversion of guaiacol with 78% cyclohexanol formation was achieved.

Adsorption study of substrate suggests that the defunctionalization of lignin-derived monomers is possible in only non-polar solvent at given condition, due to successive adsorption and desorption happening between substrate and solvent in the polar solvent.

	Ru/Al2O3-Basic	Ru/Al2O3-Neutral	Ru/Al2O3-Acidic (commercial)	Ru/Al2O3-Acidic	Ru/SiO2	Ru/SiO2-Al2O3
Acidity (mmol.g⁻¹)	-	0.16	0.47	0.46	-	0.76

Figure 7.3. Effect of support on the hydrodeoxygenation of Guaiacol.

Reaction condition: Guaiacol/Ru molar ratio, 165; 2.15 wt% Guaiacol in cyclohexane; H_2, 1 MPa at room temperature; 225 °C; 4 h; 1000 rpm.

Chapter 4B.

Chapter 4B, discusses the catalytic transfer hydrogenation of lignin-derived low molecular weight compound using Ru based catalyst. At optimized condition, the defunctionalization of lignin-derived low molecular weight compound was achieved at 225ºC, with 0.7 MPa N_2@RT in IPA solvent within 2h, and resulted 100% conversion of guaiacol with 72% yield of cyclohexanol.

Results also suggest that defunctionalization using CTH pathways is easier to proceed compared to external H$_2$ source.
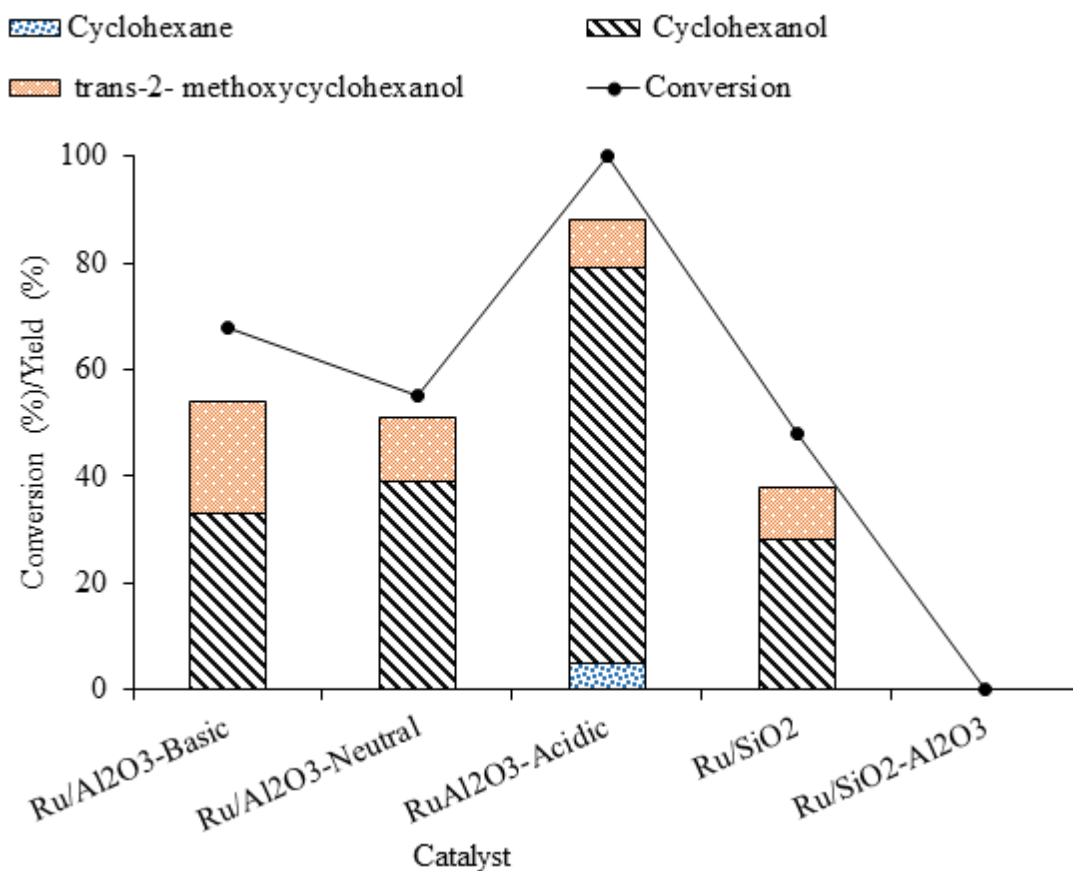
Figure 7.4. Effect of support on the CTH of Guaiacol.

Reaction condition: Guaiacol/surface exposed Ru metal molar ratio, 35520; 2.13 wt% Guaiacol in IPA; N$_2$, 0.7 MPa at room temperature; 225 °C; 2 h; 1000 rpm.

Chapter 5. This chapter is also divided into two sub-chapter

Chapter 5A.

This Chapter is devoted to the defunctionalization of lignin-derived monomers using non-precious metal (Co, Ni). Under optimized condition, the defunctionalization of lignin-derived low molecular weight compound was achieved at 225°C, with 1 MPa H_2@RT in Cyclohexane solvent in 4h, with a 95% conversion of guaiacol with 86 % yield of cyclohexanol. Modified alumina support (AHF) was found to be more active for the defunctionalization of lignin-derived monomers.
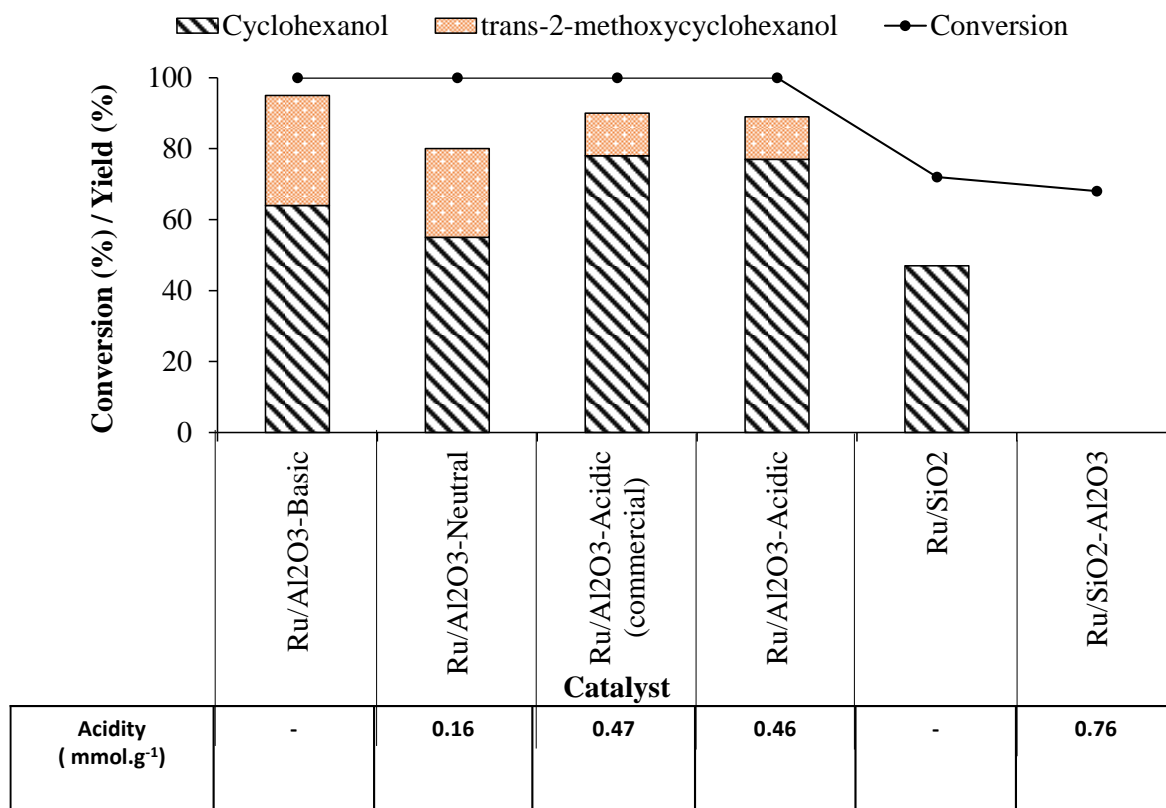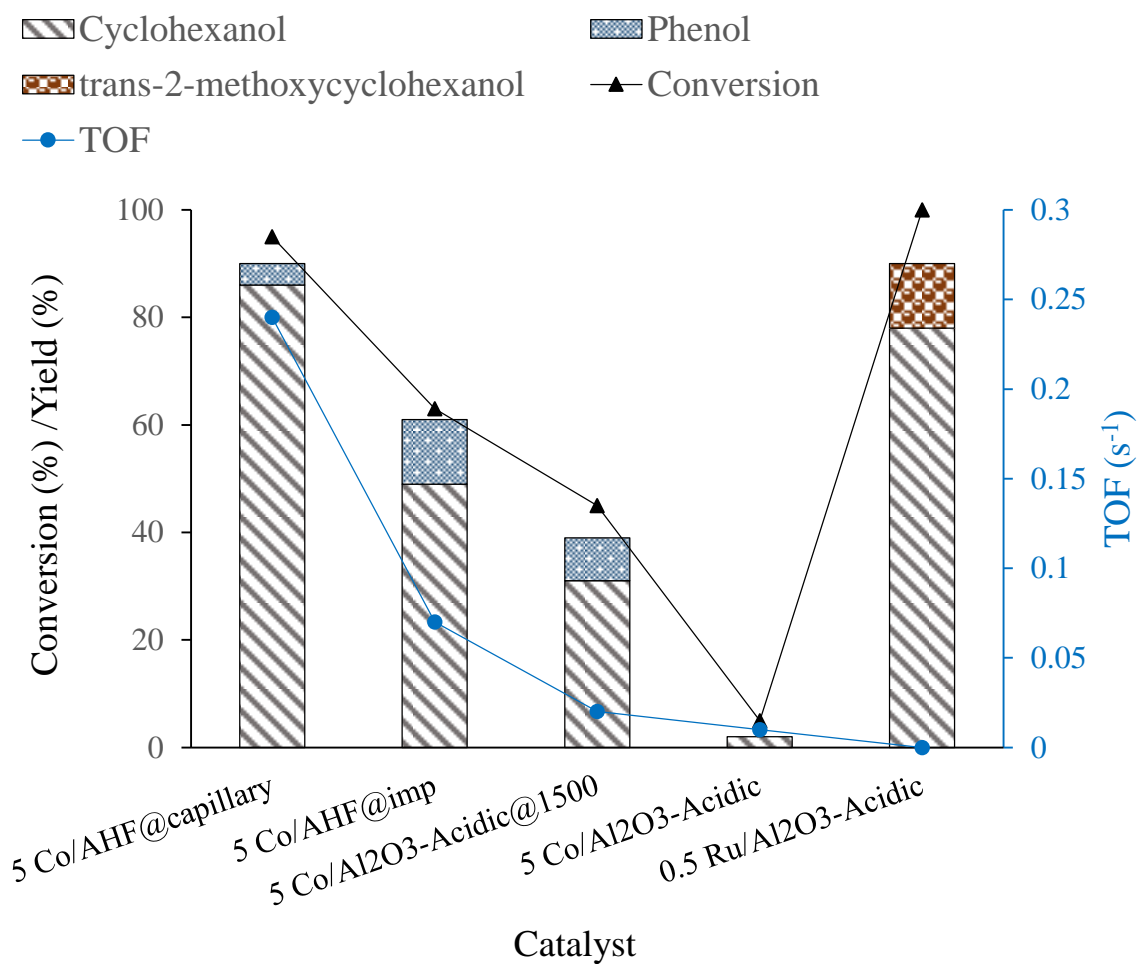

Figure 7.5. Effect of support on the hydrodeoxygenation of Guaiacol

Reaction condition: Guaiacol/Co molar ratio, 13; 2.15 wt% Guaiacol in cyclohexane; H$_2$, 1 MPa @RT; 225 °C; 4 h; 1000 rpm.

Chapter 5B

Catalytic defunctionalization of guaiacol was also achieved in a continuous flow reactor. Results suggests that 5 Co/AHF@capillary, is a very active catalyst system for the defunctionalization of lignin-derived monomers.
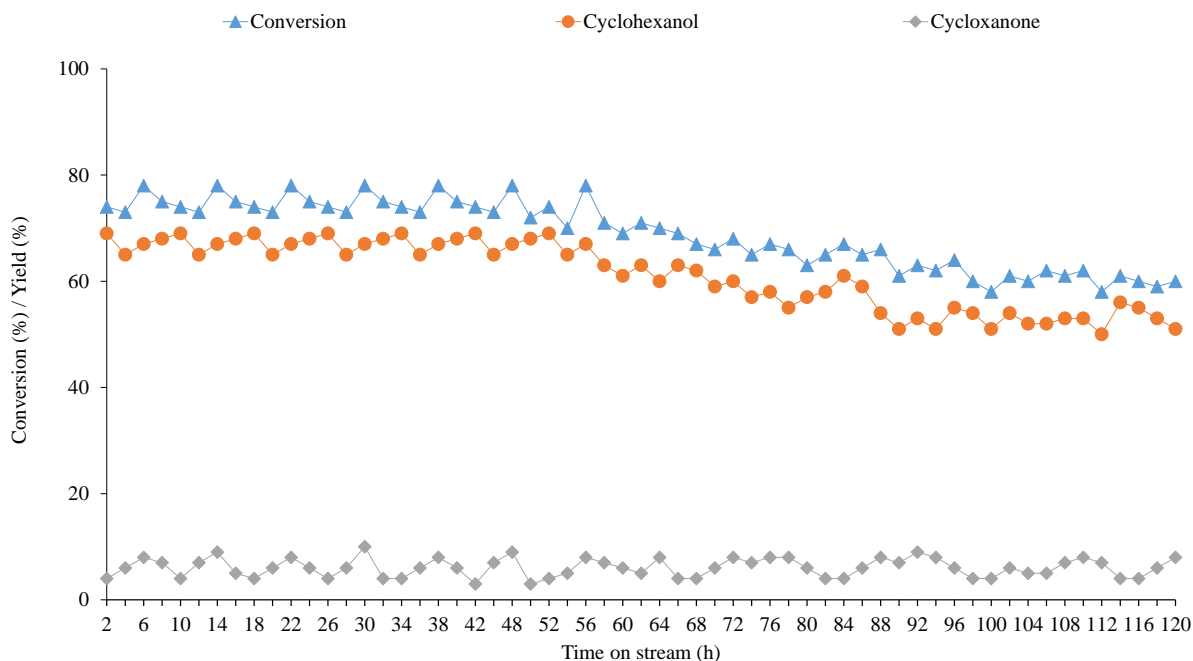
Figure 7.6. Time on stream

Reaction condition: WHSV•h^{-1}: 13.3; 300°C; 5 Co/ AHF@capillay, 2.5 MPa H$_2$; 25mL•min^{-1} H$_2$

Chapter 6.

Chapter 6, deals with the catalytic functionalization of lignin-derived monomers using solid acid catalysts. Among all used solid acid catalyst, SiO_2-Al_2O_3 was found to be more active for the functionalization of lignin-derived monomers.
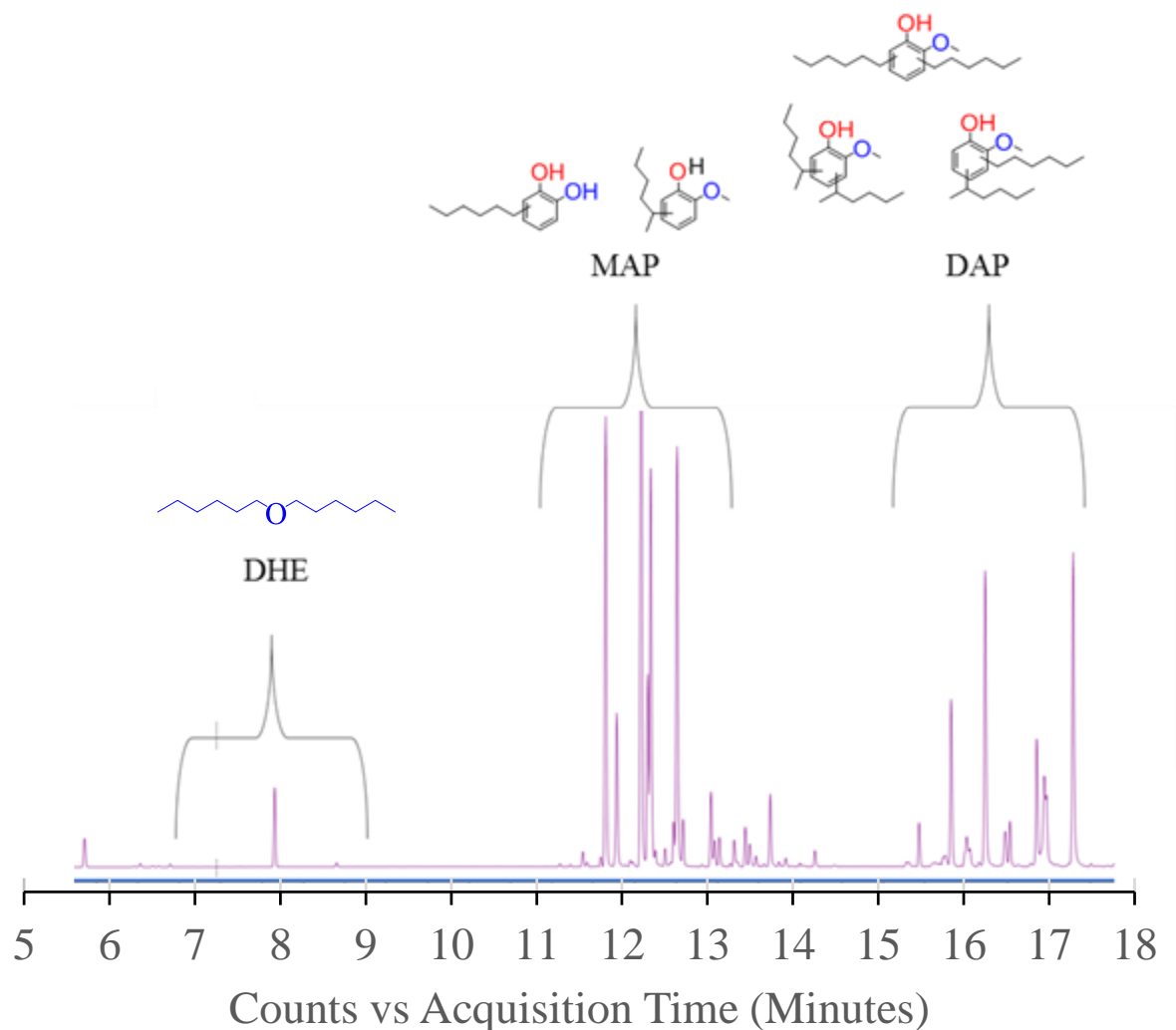
Figure 7.7. Typical GC-MS profile of the reaction mixture

Reaction condition: Guaiacol, 4 mmol; hexanol, 10 mmol; catalyst, 0.5 g; cyclohexane, 30 mL; N_2, 0.7 MPa at room temperature; 2 h; 1000 rpm.

Chapter 7.

Chapter 7. concludes the thesis, a detailed on lignin chemistry was performed using a homogeneous base which included the following focused studies

- ⚕ Catalytic depolymerization of lignin.
- ⚕ Defunctionlilzation of lignin-derived monomers using a supported metal catalyst.
- ⚕ Functionalization of lignin-derived monomers using the Solid acid catalyst.

List of Publication

- Dheerendra Singh, Paresh L. Dhepe*, "Understanding the influence of alumina supported Ruthenium catalysts synthesis and reaction parameters on the hydrodeoxygenation of lignin derived monomers", Molecular Catalysis (Accepted in July 2019).

- Dheerendra Singh, Paresh L. Dhepe*, "Altering the O/C ratio of lignin derived monomers without sacrificing atom efficiency", Chemistry Select (December 2019)

- Dheerendra Singh, Paresh L. Dhepe*, "Pathway for the transfer hydrogenation of lignin derived monomers: Mechanistic and kinetic study over the alumina supported Ruthenium catalysts**", (To be communicated).

Work Presented

- Delivered oral presentation in CATSYM23 entitled "Effect of supports & metals on the up-gradation of lignin derived phenolic compounds" held in Bengaluru, 17-19th January 2018.
- Presented a poster on the occasion of National Science Day in CSIR-NCL, Pune on 28th February 2019.
- Delivered oral presentation in research student annual conference (NCL-RF) in CSIR-NCL, Pune on 29th November 2019.
- Presented a poster in CSIR-Inter Institutional student conference on sustainable chemistry for health, Environment and Materials (Su-CHEM Yuva 2019) held at Hyderabad on 24-26th July, 2019.

Notes

dherenupdths

PRIMARY SOURCES

1   M. G. Dohade, P. L. Dhepe. "Efficient hydrogenation of concentrated aqueous furfural solutions into furfuryl alcohol under ambient conditions in presence of PtCo bimetallic catalyst", Green Chemistry, 2017
Crossref
   418 words — 1%

2   Richa Chaudhary, Paresh L. Dhepe. "Solid base catalyzed depolymerization of lignin into low molecular weight products", Green Chemistry, 2017
Crossref
   286 words — 1%

3   Zhe Cai, Fumin Wang, Xubin Zhang, Rosine Ahishakiye, Yi Xie, Yu Shen. "Selective hydrodeoxygenation of guaiacol to phenolics over activated carbon supported molybdenum catalysts", Molecular Catalysis, 2017
Crossref
   164 words — < 1%

4   sicr.ro
Internet
   164 words — < 1%

5   Changzhi Li, Xiaochen Zhao, Aiqin Wang, George W. Huber, Tao Zhang. "Catalytic Transformation of Lignin for the Production of Chemicals and Fuels", Chemical Reviews, 2015
Crossref
   164 words — < 1%

6   Rui Dang, Xiangrong Ma, Jiao Luo, Yuanyuan Zhang, Jiawei Fu, Chunyan Li, Ning Yang. "Hydrodeoxygenation of 2-methoxy phenol: Effects of catalysts and process parameters on conversion and products selectivity", Journal of the Energy Institute, 2020
Crossref
   128 words — < 1%

7   Zhenchao Zhao, Hui Shi, Chuan Wan, Mary Y. Hu, 126 words — < 1%
    Yuanshuai Liu, Donghai Mei, Donald M. Camaioni,
    Jian Zhi Hu, Johannes A. Lercher. "Mechanism of
    Phenol Alkylation in Zeolite H-BEA Using In Situ Solid-State NMR
    Spectroscopy", Journal of the American Chemical Society, 2017
    Crossref

8   link.springer.com   103 words — < 1%
    Internet

9   Alexandre C. Dimian, Costin Sorin Bildea, Anton A.   98 words — < 1%
    Kiss. "Sustainable Process Technology", Elsevier
    BV, 2019
    Crossref

10 Manisha G. Dohade, Paresh L. Dhepe. "One pot   86 words — < 1%
    conversion of furfural to 2-methylfuran in the
    presence of PtCo bimetallic catalyst", Clean Technologies and
    Environmental Policy, 2017
    Crossref

11 www.innovationservices.philips.com   80 words — < 1%
    Internet

12 Behling, R., S. Valange, and G. Chatel.
    "Heterogeneous catalytic oxidation for lignin
    valorization into valuable chemicals: what results? 80 words — < 1%
    What limitations? What trends?", Green Chemistry,
    2016.
    Crossref

13 Manisha Dohade, Paresh L. Dhepe. "Efficient   79 words — < 1%
    method for cyclopentanone synthesis from furfural:
    understanding the role of solvents and solubility in a bimetallic
    catalytic system", Catalysis Science & Technology, 2018
    Crossref

14 Deuss, Peter J., and Katalin Barta. "From models to 77 words — < 1%
    lignin: Transition metal catalysis for selective bond
    cleavage reactions", Coordination Chemistry Reviews, 2016.
    Crossref

15 Srikanth Dama, Seema R. Ghodke, Richa Bobade, Hanmant R. Gurav, Satyanarayana Chilukuri. "Active and durable alkaline earth metal substituted perovskite catalysts for dry reforming of methane", Applied Catalysis B: Environmental, 2018
Crossref

72 words — < 1%

16 baadalsg.inflibnet.ac.in
Internet

68 words — < 1%

17 Ayillath K. Deepa, Paresh L. Dhepe. "Function of Metals and Supports on the Hydrodeoxygenation of Phenolic Compounds", ChemPlusChem, 2014
Crossref

56 words — < 1%

18 www.spectraresearch.com
Internet

51 words — < 1%

19 Manisha G. Dohade, Paresh L. Dhepe. "EFFICIENT CONVERSION OF SUGARS TO SUGAR ALCOHOLS IN PRESENCE OF RU/C CATALYST UNDER MILD REACTION CONDITION", Catalysis in Green Chemistry and Engineering, 2018
Crossref

49 words — < 1%

20 www.rsc.org
Internet

48 words — < 1%

21 www.intechopen.com
Internet

48 words — < 1%

22 shodhganga.inflibnet.ac.in
Internet

46 words — < 1%

23 Deepa, A. K., and Paresh Laxmikant Dhepe. "Lignin depolymerization into aromatic monomers over solid acid catalysts", ACS Catalysis
Crossref

41 words — < 1%

24 Richa Chaudhary, Paresh L. Dhepe. "Depolymerization of Lignin Using a Solid Base Catalyst", Energy & Fuels, 2019

31 words — < 1%

Crossref

25 www.deepdyve.com
    Internet

31 words — < 1%

26 oro.open.ac.uk
    Internet

28 words — < 1%

27 uzspace.uzulu.ac.za
    Internet

27 words — < 1%

28 Reddy, A.S.. "Selective ortho-methylation of phenol with methanol over copper manganese mixed-oxide spinel catalysts", Journal of Catalysis, 20061025
    Crossref

26 words — < 1%

29 Matthew J. Gilkey, Bingjun Xu. "Heterogeneous Catalytic Transfer Hydrogenation as an Effective Pathway in Biomass Upgrading", ACS Catalysis, 2016
    Crossref

25 words — < 1%

30 www.freepatentsonline.com
    Internet

25 words — < 1%

31 etheses.whiterose.ac.uk
    Internet

23 words — < 1%

32 onlinelibrary.wiley.com
    Internet

21 words — < 1%

33 Sandip K. Singh, Paresh L. Dhepe. "Novel Synthesis of Immobilized Brønsted- Acidic Ionic Liquid: Application in Lignin Depolymerization", ChemistrySelect, 2018
    Crossref

20 words — < 1%

34 Vijaykumar S. Marakatti, Nidhi Arora, Sandhya Rai, Saurav Ch. Sarma, Sebastian C. Peter. " Understanding the Role of Atomic Ordering in the Crystal Structures of Ni Sn toward Efficient Vapor Phase Furfural Hydrogenation ", ACS Sustainable Chemistry & Engineering, 2018

20 words — < 1%

Crossref

35 "Production of Biofuels and Chemicals from Lignin", Springer Science and Business Media LLC, 2016
Crossref
20 words — < 1%

36 Hajipour, Abdol Reza, and Hirbod Karimi. "Hexagonal zirconium phosphate nanoparticles as an efficient and recyclable catalyst for selective solvent-free alkylation of phenol with cyclohexanol", Applied Catalysis A General, 2014.
Crossref
20 words — < 1%

37 Sandip K. Singh, Paresh L. Dhepe. "Effect of structural properties of organosolv lignins isolated from different rice husks on their liquefaction using acidic ionic liquids", Clean Technologies and Environmental Policy, 2017
Crossref
18 words — < 1%

38 Matyas Kosa, Haoxi Ben, Hans Theliander, Arthur J. Ragauskas. "Pyrolysis oils from CO2 precipitated Kraft lignin", Green Chemistry, 2011
Crossref
18 words — < 1%

39 Venkataraman Vishwanathan. "Alkylation of catechol with methanol to guaiacol over sulphate-modified zirconia solid acid catalysts", Reaction Kinetics and Catalysis Letters, 12/2007
Crossref
16 words — < 1%

40 Miguel Ángel González-Borja, Daniel E. Resasco. "Reaction pathways in the liquid phase alkylation of biomass-derived phenolic compounds", AIChE Journal, 2015
Crossref
15 words — < 1%

41 Jingbo Mao, Jinxia Zhou, Zhi Xia, Zhiguang Wang, Zhanwei Xu, Wenjuan Xu, Peifang Yan, Kairui Liu, Xinwen Guo, Z. Conrad Zhang. " Anatase TiO Activated by Gold Nanoparticles for Selective Hydrodeoxygenation of Guaiacol to Phenolics ", ACS Catalysis, 2016
Crossref
13 words — < 1%

42 www.ncbi.nlm.nih.gov

	Internet	13 words — < 1%
43	Toledano, A.. "Comparative study of lignin fractionation by ultrafiltration and selective precipitation", Chemical Engineering Journal, 20100215 Crossref	13 words — < 1%
44	ijens.org Internet	13 words — < 1%
45	"Waste Management and Resource Efficiency", Springer Science and Business Media LLC, 2019 Crossref	13 words — < 1%
46	www.hindawi.com Internet	13 words — < 1%
47	Sandip K. Singh, Paresh L. Dhepe. "Lignin Conversion Using Catalytic Ionic Liquids: Understanding the Role of Cations, Anions, and Hammett Acidity Functions", Industrial & Engineering Chemistry Research, 2019 Crossref	13 words — < 1%
48	dyuthi.cusat.ac.in Internet	12 words — < 1%
49	Sawant, D.P.. "Alkylation of benzene with @a-olefins over zirconia supported 12-silicotungstic acid", Journal of Molecular Catalysis. A, Chemical, 20050802 Crossref	12 words — < 1%
50	www.mater-rep.com Internet	12 words — < 1%
51	www.dovepress.com Internet	12 words — < 1%
52	etd.lib.metu.edu.tr Internet	12 words — < 1%

53 Jeong, J.H.. "Ru-doped Ni catalysts effective for the steam reforming of methane without the pre-reduction treatment with H"2", Applied Catalysis A, General, 20060411
Crossref

12 words — < 1%

54 Gregory Chatel, Robin D. Rogers. "Review: Oxidation of Lignin Using Ionic Liquids—An Innovative Strategy To Produce Renewable Chemicals", ACS Sustainable Chemistry & Engineering, 2013
Crossref

12 words — < 1%

55 Roman Klimkiewicz, Hanna Grabowska, Włodzimierz Miśta, Kazimierz Przybylski. "Mg–Zn and Mn–Zn Ferrites Derived from Coil Core Materials as New Phenol Methylation Catalysts", Industrial & Engineering Chemistry Research, 2012
Crossref

12 words — < 1%

56 hdl.handle.net
Internet

11 words — < 1%

57 Ogawa, M.. "Simple and effective method for producing [^1^1C]phosgene using an environmental CCl"4 gas detection tube", Nuclear Medicine and Biology, 201001
Crossref

11 words — < 1%

58 Roberto A. Rossi. "Recent Advances in the S_{RN}1 Reaction of Organic Halides", PATAI S Chemistry of Functional Groups, 12/15/2009
Crossref

11 words — < 1%

59 "Progress in Automation, Robotics and Measuring Techniques", Springer Science and Business Media LLC, 2015
Crossref

11 words — < 1%

60 "Hemicellulose: Isolation and Its Application in Pharmacy", Handbook of Sustainable Polymers, 2015.
Crossref

11 words — < 1%

61 B. K. Reck, T. E. Graedel. "Challenges in Metal Recycling", Science, 2012
Crossref

11 words — < 1%

62 Fujita, S.I.. "Mesoporous smectites incorporated with alkali metal cations as solid base catalysts", Applied Catalysis A, General, 20061004
Crossref

10 words — < 1%

63 Anil K. Suresh. "Metallic Nanocrystallites and their Interaction with Microbial Systems", Springer Science and Business Media LLC, 2012
Crossref

10 words — < 1%

64 Jie Zhang, Chuang Li, Xiao Chen, Weixiang Guan, Changhai Liang. "Insights into the reaction pathway of hydrodeoxygenation of dibenzofuran over MgO supported noble-metals catalysts", Catalysis Today, 2019
Crossref

10 words — < 1%

65 Rajendra Srivastava. "Assessment of the Catalytic Activities of Novel Brönsted Acidic Ionic Liquid Catalysts", Catalysis Letters, 2010
Crossref

10 words — < 1%

66 Noraini Hamzah, Norasikin Mohamad Nordin, Ainol Hayah Ahmad Nadzri, Yah Awg Nik, Mohamad B. Kassim, Mohd Ambar Yarmo. "Enhanced activity of Ru/TiO2 catalyst using bisupport, bentonite-TiO2 for hydrogenolysis of glycerol in aqueous media", Applied Catalysis A: General, 2012
Crossref

10 words — < 1%

67 S. Ramesh, B.S. Jai Prakash, Y.S. Bhat. "Highly active and selective C-alkylation of p-cresol with cyclohexanol using p-TSA treated clays under solvent free microwave irradiation", Applied Catalysis A: General, 2012
Crossref

10 words — < 1%

68 pt.scribd.com
Internet

10 words — < 1%

69 Bernhard Gollas, Joanne M Elliott, Philip N Bartlett.

"Electrodeposition and properties of nanostructured platinum films studied by quartz crystal impedance measurements at 10 MHz", Electrochimica Acta, 2000
Crossref

10 words — < 1%

70 Seale, Mary-Margaret, Dimitry Zemlyanov, Christy L. Cooper, Emily Haglund, Tarl W. Prow, Lisa M. Reece, James F. Leary, and Dan V. Nicolau. "<title>Multifunctional nanoparticles for drug/gene delivery in nanomedicine</title>", Nanoscale Imaging Spectroscopy Sensing and Actuation for Biomedical Applications IV, 2007.
Crossref

10 words — < 1%

71 Shimin Kang, Xianglan Li, Juan Fan, Jie Chang. "Hydrothermal conversion of lignin: A review", Renewable and Sustainable Energy Reviews, 2013
Crossref

10 words — < 1%

72 Guo, Yanzhu, Jinghui Zhou, Jialong Wen, Guangwei Sun, and Yijia Sun. "Structural transformations of triploid of Populus tomentosa Carr. lignin during auto-catalyzed ethanol organosolv pretreatment", Industrial Crops and Products, 2015.
Crossref

10 words — < 1%

73 Feng, S H, J S Chen, and Z Shi. "COMPLETE DISASSEMBLY OF LIGNIN IN PHENOL-WATER SOLVENT", Hydrothermal Reactions and Techniques, 2003.
Crossref

10 words — < 1%

74 Hai Wang, Melvin Tucker, Yun Ji. "Recent Development in Chemical Depolymerization of Lignin: A Review", Journal of Applied Chemistry, 2013
Crossref

10 words — < 1%

75 ulir.ul.ie
Internet

10 words — < 1%

76 Samudrala Shanthi Priya, Vanama Pavan Kumar, Mannepalli Lakshmi Kantam, Suresh K. Bhargava

10 words — < 1%

et al. "High Efficiency Conversion of Glycerol to 1,3-Propanediol Using a Novel Platinum–Tungsten Catalyst Supported on SBA-15", Industrial & Engineering Chemistry Research, 2015

Crossref